NBS SPECIAL PUBLICATION 653

U.S. DEPARTMENT OF COMMERCE/National Bureau of Standards

Laser-Cooled and Trapped Atoms

NATIONAL BUREAU OF STANDARDS

The National Bureau of Standards[1] was established by an act of Congress on March 3, 1901. The Bureau's overall goal is to strengthen and advance the Nation's science and technology and facilitate their effective application for public benefit. To this end, the Bureau conducts research and provides: (1) a basis for the Nation's physical measurement system, (2) scientific and technological services for industry and government, (3) a technical basis for equity in trade, and (4) technical services to promote public safety. The Bureau's technical work is performed by the National Measurement Laboratory, the National Engineering Laboratory, and the Institute for Computer Sciences and Technology.

THE NATIONAL MEASUREMENT LABORATORY provides the national system of physical and chemical and materials measurement; coordinates the system with measurement systems of other nations and furnishes essential services leading to accurate and uniform physical and chemical measurement throughout the Nation's scientific community, industry, and commerce; conducts materials research leading to improved methods of measurement, standards, and data on the properties of materials needed by industry, commerce, educational institutions, and Government; provides advisory and research services to other Government agencies; develops, produces, and distributes Standard Reference Materials; and provides calibration services. The Laboratory consists of the following centers:

Absolute Physical Quantities[2] — Radiation Research — Chemical Physics — Analytical Chemistry — Materials Science

THE NATIONAL ENGINEERING LABORATORY provides technology and technical services to the public and private sectors to address national needs and to solve national problems; conducts research in engineering and applied science in support of these efforts; builds and maintains competence in the necessary disciplines required to carry out this research and technical service; develops engineering data and measurement capabilities; provides engineering measurement traceability services; develops test methods and proposes engineering standards and code changes; develops and proposes new engineering practices; and develops and improves mechanisms to transfer results of its research to the ultimate user. The Laboratory consists of the following centers:

Applied Mathematics — Electronics and Electrical Engineering[2] — Manufacturing Engineering — Building Technology — Fire Research — Chemical Engineering[2]

THE INSTITUTE FOR COMPUTER SCIENCES AND TECHNOLOGY conducts research and provides scientific and technical services to aid Federal agencies in the selection, acquisition, application, and use of computer technology to improve effectiveness and economy in Government operations in accordance with Public Law 89-306 (40 U.S.C. 759), relevant Executive Orders, and other directives; carries out this mission by managing the Federal Information Processing Standards Program, developing Federal ADP standards guidelines, and managing Federal participation in ADP voluntary standardization activities; provides scientific and technological advisory services and assistance to Federal agencies; and provides the technical foundation for computer-related policies of the Federal Government. The Institute consists of the following centers:

Programming Science and Technology — Computer Systems Engineering.

[1]Headquarters and Laboratories at Gaithersburg, MD, unless otherwise noted; mailing address Washington, DC 20234.
[2]Some divisions within the center are located at Boulder, CO 80303.

Laser-Cooled and Trapped Atoms

Proceedings of the Workshop on Spectroscopic Applications of Slow Atomic Beams NBS Gaithersburg, MD, 14-15 April 1983

NBS special publication

William D. Phillips, Editor

Electrical Measurements and Standards Division
Center for Absolute Physical Quantities
National Measurement Laboratory
National Bureau of Standards
Washington, DC 20234

Sponsored by:

Office of Naval Research
Arlington, VA 22217
and
National Bureau of Standards
Washington, DC 20234

U.S. DEPARTMENT OF COMMERCE, Malcolm Baldrige, Secretary
NATIONAL BUREAU OF STANDARDS, Ernest Ambler, Director

Issued June 1983

Library of Congress Catalog Card Number: 83-600541

National Bureau of Standards Special Publication 653
Natl. Bur. Stand. (U.S.), Spec. Publ. 653, 172 pages (June 1983)
CODEN: XNBSAV

U.S. GOVERNMENT PRINTING OFFICE
WASHINGTON: 1983

For sale by the Superintendent of Documents, U.S. Government Printing Office, Washington, DC 20402
Price
(Add 25 percent for other than U.S. mailing)

PREFACE

My personal interest in the field of laser-cooled and trapped atoms dates from Ashkin's 1978 paper on laser trapping and cooling of atoms [1]. While atom traps had been proposed as early as 1968 by Letokhov [2] and 1970 by Ashkin [3] and a good bit of theoretical work had been done, the 1978 proposal caused a renewed interest in the field both because the proposal seemed so promising and because of the beautiful demonstration of laser cooling in ion traps by Wineland et al. [4] and Neuhauser et al. [5].

Since 1978 there has been extensive theoretical work on the motion of atoms in laser fields as well as discussions of other kinds of traps for neutral atoms. Bjorkholm et al. demonstrated the dipole forces which could make optical trapping possible [6]. An experimental realization of an optical trap, however, proved to be more elusive. A basic problem was that the atoms had to be cooled considerably before they could be loaded into the very shallow optical traps.

The earliest attempts to cool an atomic beam, by Letokhov and colleagues at the Institute of Spectroscopy in Moscow, were hampered by optical pumping [7]. The Moscow group overcame the optical pumping problem and reported a clear demonstration of laser deceleration in 1981 [8]. In 1982 the group at the National Bureau of Standards in Gaithersburg reported a different method which eliminated optical pumping and in addition compensated for the changing Doppler shift of the decelerated atoms [9]. More recently the NBS group succeeded in cooling a beam of atoms to energies comparable to the depth of proposed optical traps [10]. By this time it had become obvious that the production of slow atomic beams was an interesting development in itself, apart from the possibility that such atoms might eventually find their way into an optical trap.

In the light of all these developments, Bob Junker of the Office of Naval Research suggested that the time was ripe for an assessment of where the field of slow neutral atoms stood and where it was headed. From these discussions came the idea for a small gathering of scientists in a workshop atmosphere to discuss slow atoms and particularly to speculate on the possibilities for future work, especially work which might lead to applications in high resolution spectroscopy or time and frequency standards.

The resulting workshop, under the joint sponsorship of the Office of Naval Research and the National Bureau of Standards, did not stray too far from the original goal. It included a review of the present status and direction of frequency standards work, the theory of atom-field interaction and traps, and experiments on laser cooling of beams. A number of proposals for traps for neutral atoms were presented as well as new ideas for cooling atoms in traps, beams, and gases.

Thirty-four invited scientists attended the workshop, and contributed 21 papers to these proceedings [11]. They represented universities, government and private laboratories across the country, and included some foreign visitors at U.S. institutions. While this attendance exceeded the "small gathering" initially envisioned, the discussions were as lively and informal as we had hoped they would be. Discussions often lasted as long as presentations, and the Workshop was enriched by a number of impromptu presentations.

It is to be hoped that the May 2 deadline for final submission of manuscripts has allowed authors to consider the discussions and ideas which grew from the Workshop. I would like to mention two instances of this: G. L. Greene has kindly included his impromptu remarks concerning magnetic trapping of ultra-cold neutrons in these proceedings, and J. P. Gordon has presented a new general proof concerning the possibility of radiative confinement of atoms in traps which rely only on the scattering force.

I would like to thank some of the many people who helped to make this Workshop a success: Kathy Stang of the NBS National Measurement Laboratory offices who guided the coordination of the Workshop from the beginning and who, with Naomi Crockett, handled the registration; Sara Torrence and Kathleen Kilmer of the NBS Public Information Division who made so many of the arrangements needed for a smooth operation; Brenda Main and Lesa Childress of the NBS Electrical Measurements and Standards Division Office, who handled the considerable secretarial effort which goes into such a meeting; Barry Taylor and John Prodan who, in addition to participating in the meeting provided invaluable assistance in planning and arranging; Sam Stein who coordinated the efforts of the NBS Time and Frequency Division in providing the overviews of the status of time and frequency standards; Bob Junker and the Office of Naval Research for proposing this Workshop and providing important guidance as well as the major financial support for the Workshop and for this publication; finally, all the participants in the workshop who through a very long day and a half of talks and discussions maintained the high level of interest and enthusiasm which made the Workshop such a rewarding experience.

[1] A. Ashkin, Phys. Rev. Lett. 40, 729 (1978).

[2] V. S. Letokhov, Pis'ma Zh. Eksp. Teor. Fiz. 7, 348 (1968) [JETP Lett. 7, 272 (1968)].

[3] A. Ashkin, Phys. Rev. Lett. 25, 1321 (1970).

[4] D. J. Wineland et al., Phys. Rev. Lett. 40, 1639 (1978).

[5] W. Neuhauser et al., Phys. Rev. Lett., 41, 233 (1978).

[6] J. E. Bjorkholm et al., Phys. Rev. Lett. 41, 1361 (1978).

[7] V. I. Balykin, V. S. Letokhov, and V. I. Mishin, JETP Lett. 29, 561 (1979). [Pis'ma Zh. Eksp. Teor. Fiz. 29, 614 (1979)]; Sov. Phys. JETP, 51, 692 (1980) [Zh. Eksp. Teor. Fiz. 87, 1376 (1980)]; V. I. Balykin, Opt. Commun. 33, 31 (1980).

[8] S. V. Andreev et al., Pis'ma Zh. Eksp. Theor. Fiz. 34, 463 (1981) [JETP Lett. 34, 442 (1981)].

[9] W. D. Phillips and H. Metcalf, Phys. Rev. Lett. 48, 596 (1982).

[10] J. V. Prodan, W. D. Phillips, and H. Metcalf, Phys. Rev. Lett. 49, 1149 (1982).

[11] The opinions expressed by non-NBS authors in these proceedings are their own and their appearance in this publication does not represent an endorsement by the Bureau of Standards or the U.S. Government. Any mention of commercial products in this publication does not imply a recommendation or endorsement by the National Bureau of Standards.

William D. Phillips
Gaithersburg, Maryland
May 1983

TABLE OF CONTENTS

Laser-Cooled and Trapped Atoms, (Proceedings of the Workshop on Spectroscopic Applications of Slow Atomic Beams, held at NBS, Gaithersburg, MD, 14-15 April 1983) Ed. by W. D. Phillips, Natl. Bur. Stand. (U.S.) Spec. Publ. 653 (1983).

NEUTRAL ATOMIC BEAM COOLING EXPERIMENTS AT NBS

William D. Phillips, John V. Prodan* and Harold J. Metcalf**

Electrical Measurements and Standards Division
National Bureau of Standards
Washington, DC 20234

We have decelerated and cooled a neutral atomic sodium beam using a near resonant, counterpropagating laser beam. A spatially varying magnetic field compensates for the changing Doppler shift as the atoms decelerate, keeping the atoms in resonance with the laser. We have observed final velocities as low as 40 m/s, or about 25 times slower than the initial thermal velocity. By compressing the atomic velocity distribution we have increased the atomic density per unit velocity by as much as a factor of 30 over that of the thermal distribution.

Key words: frequency standards, high resolution spectroscopy, laser cooling, laser trapping, slow atomic beam.

1. Introduction

The techniques and results for resonant deceleration of neutral atoms have been presented in some detail elsewhere [1,2]. In this paper we review those techniques and results, discuss more recent results, describe the problems associated with neutral atom cooling, and discuss some possibilities for applications.

Laser deceleration of an atomic beam is accomplished by directing a resonant laser beam against the propagation direction of an atomic beam. The atoms absorb photons from the laser beam, receiving repeated momentum kicks in the direction of the laser beam. Since the reradiation pattern is symmetric with respect to reflection in any plane, no net average momentum transfer results from the reradiation, and the atoms slow down. (Of course, the reradiation contributes to a random walk of the atomic momentum about its average value.) The velocity change per photon is $\Delta v = h\nu/Mc$, where ν is the photon frequency and M is the atom's mass. For Na atoms making transitions at 589 nm ($3S \rightarrow 3P$) this is a velocity change of 3 cm/s per photon.

The maximum acceleration can be calculated by noting that when the transition is heavily saturated, the atom spends half its time in the excited state and while excited it radiates at a rate determined by the natural lifetime :

$$a_{max} = \frac{h\nu}{Mc} \frac{1}{2\tau} \simeq 10^6 \text{ m/s}^2 \quad . \tag{1}$$

for the case of Na where τ = 16 ns. Na atoms with a typical thermal velocity of 1000 m/s can, with this acceleration, be stopped in 1 ms over a 0.5 m distance, after scattering over 30,000 photons.

The situation for atom beam deceleration should be contrasted to the case of cooling ions in a trap [3]. In that case, the laser must be tuned on the red side of the transition frequency to cool. A blue tuning will heat the ions. For the atomic beam, counterpropagation of the cooling beam guarantees deceleration, regardless of the tuning. The tuning only affects the rate of deceleration. This rate, however, should be maximized since in contrast to the case of an ion trap the atoms are in the apparatus for only a short time.

Because of the large number of photons needed for deceleration the relative size of the transverse spread in momentum, caused by the random reradiation, is small. This spread is given approximately by the square root of the number of photons radiated, and for Na is about 1/2% of the initial velocity.

*NBS-NRC Postdoctoral Fellow
**Permanent Address: Dept. of Physics, SUNY, Stony Brook, NY

The disadvantage of this large number is that during the many optical cycles involved, undesired optical pumping effects are likely to occur. Hyperfine interaction splits the Na $3S_{1/2}$ state by 1772 MHz into F=1 and F=2 components. Since the natural linewidth is only 10 MHz, if the laser induces a transition from $3S_{1/2}$, F=2 to a 3P state which decays to $3S_{1/2}$, F=1, that atom will not be reexcited at a reasonable rate, because it is so far out of resonance with the laser. This kind optical pumping is likely to occur after about 100 optical cycles, so the amount of deceleration would ordinarily be severely limited. Another process limiting deceleration is the changing Doppler shift as the atoms decelerate. 200 photons will shift the velocity by 6 m/s, which corresponds to a Doppler shift of 10 MHz, the natural linewidth. This process would soon take the atoms out of resonance, effectively ending the deceleration process.

We have solved the optical pumping problem by using a magnetic field applied along the direction of the laser-atomic beam axis and a circularly polarized laser. The details are given in Ref. [1], but in essence this creates an effective two-level system between the F=2, M_F=2 component of the ground state and the F=3, M_F=3 component of the excited $3P_{3/2}$ state. With a field greater than 0.05 T the probability of transitions outside these two levels is small enough to be negligible.

The magnetic field also allows us to solve the Doppler shift problem. By winding a solenoid with more turns at one end than the other, we can create a spatially varying magnetic field. The Zeeman shift of the transition frequency (14 GHz/T) is then also spatially varying and can be chosen to compensate for the varying Doppler shift. If we assume that the atoms will decelerate at a constant rate a, the velocity as a function of distance traveled will be

$$v(z) = \sqrt{v_0^2 - 2az} \quad . \tag{2}$$

Equating the Doppler shift corresponding to this velocity to the Zeeman shift induced by the field yields a field whose spatial dependence is

$$B(z) = B_b + B_0 \sqrt{1 - 2az/v_0^2} \quad . \tag{3}$$

The bias field B_b is chosen to keep the field high enough to avoid optical pumping. B_0 is the field which produces a Zeeman shift equal to the Doppler shift of an atom having velocity v_0.

A field with this shape will allow the deceleration to zero velocity of any atom with a velocity less than or equal to v_0. Lower velocities simply begin to decelerate at larger distances, when they first come into resonsnce.

2. Apparatus

We have constructed a multi-layer solenoid to reproduce the field given by Eq. (3). The length of the solenoid and strength of the field are chosen so that Na atoms at 1000 m/s can be stopped in about 1 m with an acceleration about half the theoretical maximum given by Eq. (1).

The solenoid is incorporated into an atomic beam apparatus shown schematically in Fig. 1. The atomic beam, from a 950 K Na source, collimated to 15 mrad full angle, enters the high field end of the solenoid, where the peak field is 0.16 T. When a given atom reaches a point in the solenoid where the combined Zeeman and Doppler shifts place it in resonance with the fixed frequency cooling laser, it absorbs photons and begins to decelerate. As long as the field does not change so rapidly that the rate of Zeeman shift change exceeds the possible rate of Doppler shift change, the atom will stay in resonance as it travels down the varying field of the solenoid.

The cooling laser beam is converging so as to approximately match the divergence of the atomic beam. In this way, the small component of transverse velocity which results from the imperfect collimation of the atomic beam is reduced along with the much larger longitudinal velocity.

The atomic velocity distribution is determined by observing fluorescence induced by a second, very weak probe laser which crosses the atomic beam at an angle of 11°. As the probe frequency is scanned, the induced fluorescence gives the atomic density as a function of velocity component along the probe. At 11° this corresponds to 98% of the longitudinal velocity of the atoms. Calibration of the probe laser scan is provided by directing a small portion of the probe beam perpendicular to the atomic beam. Since the atoms have nearly zero velocity component along this beam, the fluorescence it induces can be

used as a frequency marker for zero Doppler shift. The known hyperfine structure of Na, which is well resolved for the perpendicular excitation, provides a scale calibration for the probe scan.

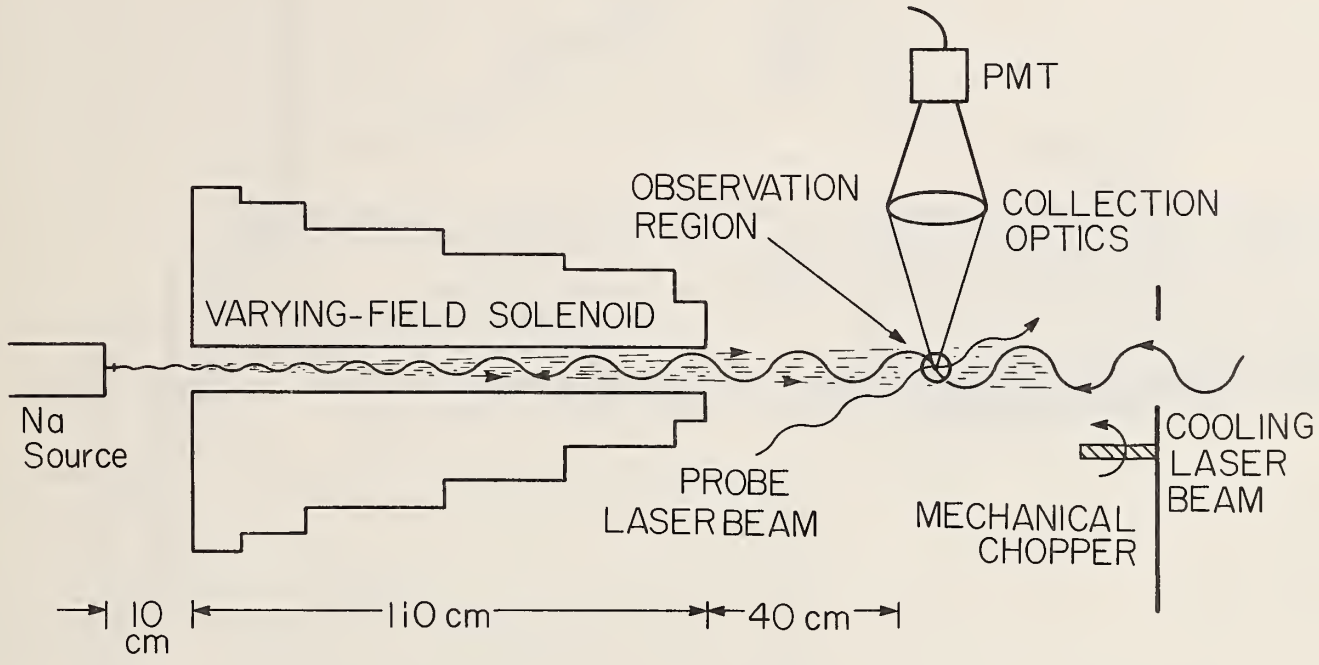

Fig. 1. Block diagram of experimental set-up.

In order to avoid confusion from the fluorescence induced by the much stronger cooling laser, we use a mechanical chopper to shut off the cooling beam just before observing fluorescence from the probe. A boxcar integrator is used to restrict the observation time to a short period after the cooling laser shuts off. The time for which the cooling laser is on is long compared with the atomic transit time through the apparatus so the detection technique gives the steady-state velocity distribution for continuous laser cooling.

3. Results

Figure 2 shows the effect of the cooling laser on the velocity distribution when only a uniform field is applied along the atomic beam. In this case, the amount of deceleration is limited by the uncompensated Doppler shift. Atoms are removed from that velocity group which is resonant with the laser and "pushed" to a lower velocity until they are too far out of resonance to absorb many more photons. The result of Fig. 2 is quite similar to the results reported by Andreev et al. [4]. In the latter experiment, two cooling laser frequencies, separated by the ground hyperfine splitting, are used to overcome optical pumping. In both cases, there is only about a 15% reduction from the velocity which is resonant with the laser.

Figure 3 shows the effect when the spatially varying field is added to the uniform field. In this case, where the Doppler shift is compensated by the Zeeman shift, a factor of two reduction in velocity is achieved. The density of atoms at the lower velocity is 30 times higher than at the peak of the thermal distribution, and the full width of the cooled velocity distribution is only 5% of the central velocity.

Since the total deceleration is limited by the total change in the magnetic field, to achieve lower velocities one simply tunes the laser to be initially resonant with slower atoms. Figure 4 shows the velocity distributions which result from a sequence of different laser tunings. As expected, when the tuning is to lower initial velocity, a lower final velocity is achieved. The final velocity actually changes more than the initial velocity, i.e., the total deceleration increases as the starting velocity

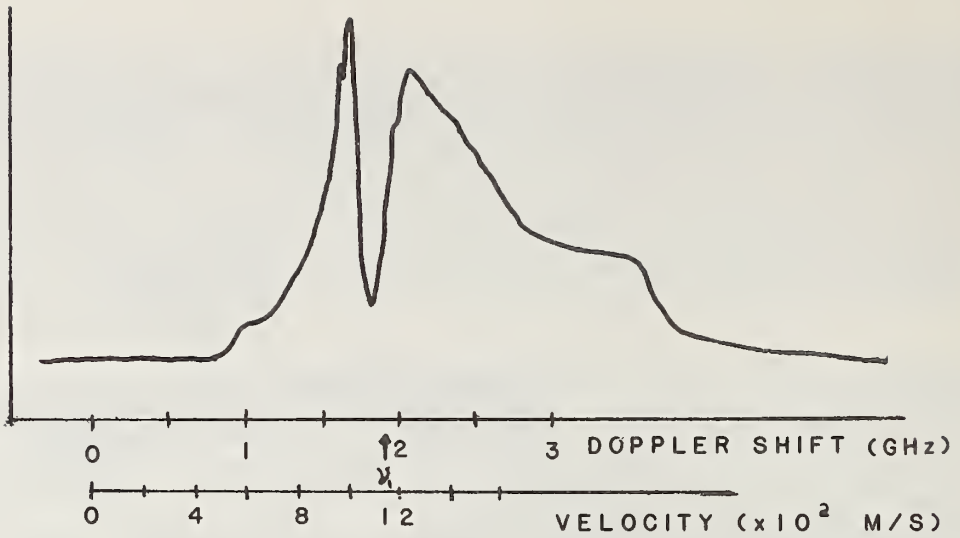

Fig. 2 Atomic velocity profile produced with the cooling laser at a frequency resonant with atoms (in a uniform magnetic field) whose initial Doppler shift is ν_1.

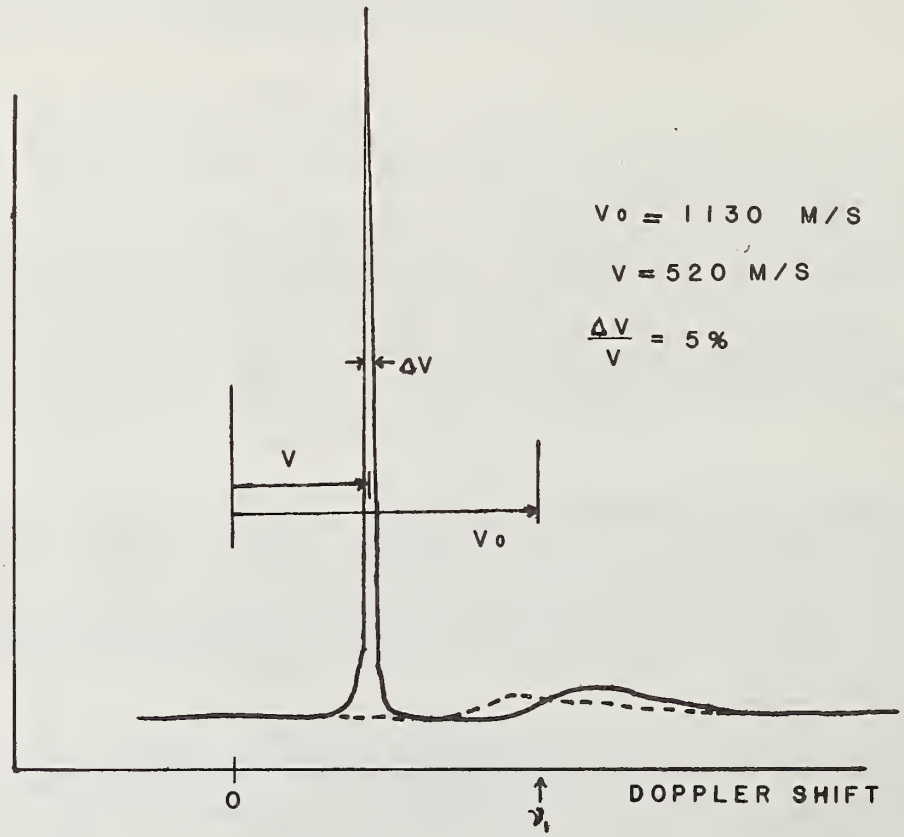

Fig. 3 Atomic velocity profile produced using the spatially varying magnetic field. The cooling laser is tuned to be in resonance (in the highest field) with atoms whose initial Doppler shift is ν_1. The dotted line represents the unmodified velocity profile.

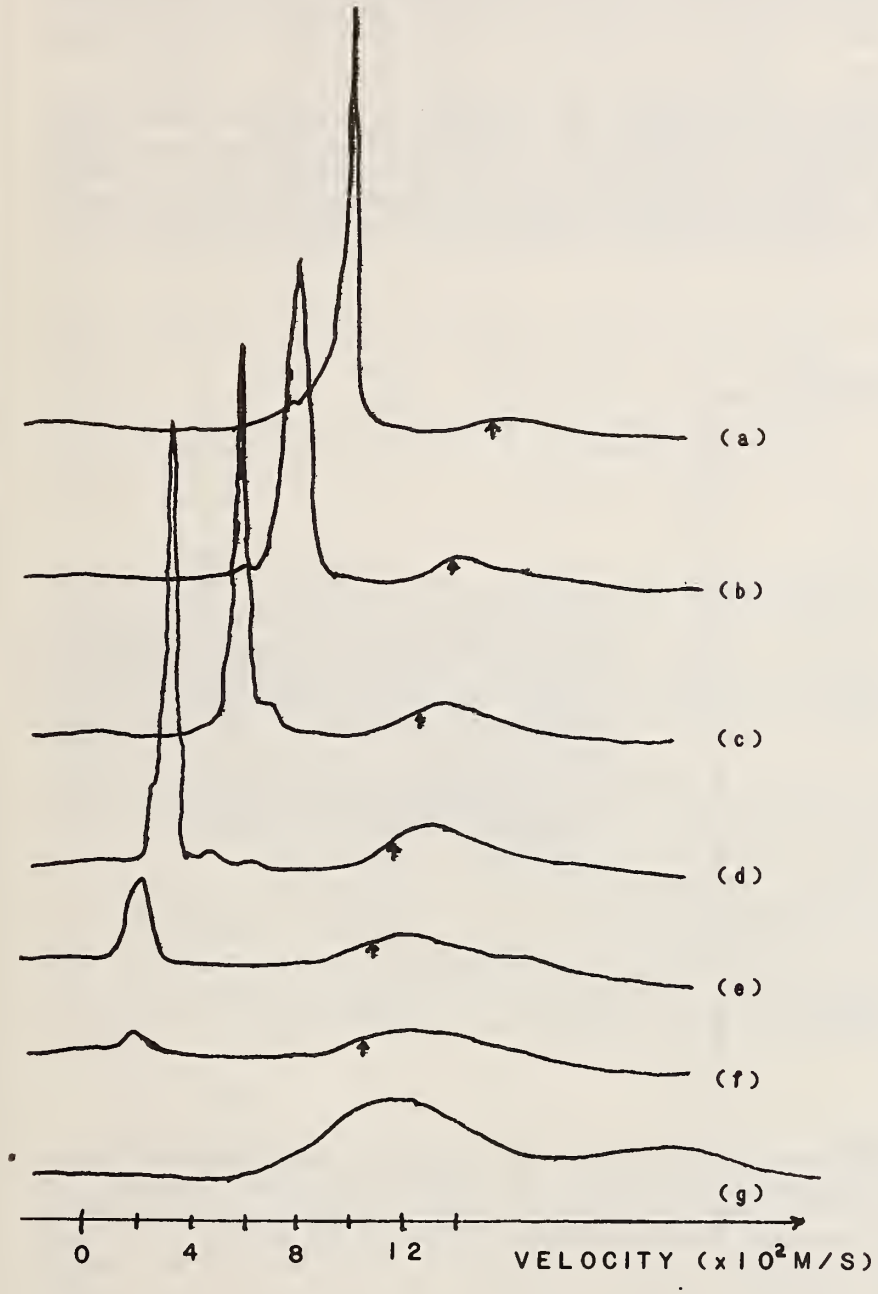

Fig. 4

Series of atomic velocity distributions using the spatially varying magnetic field and different tunings of the cooling laser. In each profile the position in the velocity distribution where the laser is tuned is marked by an arrow. The profile labeled (g) is the unmodified distribution produced by blocking the cooling laser.

is lowered. This is because the faster atoms see a more rapidly changing field near the end of the solenoid and they cannot decelerate fast enough to keep pace with the changing Zeeman shift. As a result, they "drop out" of the cooling process and do not experience the total deceleration implied by the available field change.

At a laser tuning such that the final atomic velocity is 200 m/s, about five times slower than the initial velocity, the amplitude of the slow atom peak decreases sharply and disappears entirely if the laser is tuned to a still slower velocity. This occurs because the deceleration of the atoms does not completely stop when the atoms leave the solenoid. Even though the magnetic field falls rapidly as the atoms exit the solenoid, when the velocity is below 200 m/s the atoms can still stay in resonance, or close enough to resonance that the cooling laser will actually stop them. This is not surprising considering that the stopping distance for saturated atoms at 200 m/s is only 2 cm.

To circumvent this problem, as well as to confirm the hypothesis given to explain it, we devised a modified detection scheme. Instead of observing the fluorescence immediately after the cooling laser shuts off (typical delay is 50 μs) we now wait a significant time before beginning the observation--on the order of several milliseconds. This allows the atoms which reach low velocities near the end of the magnet to drift in the dark, unaffected by any more deceleration, until they reach the observation region 40 cm away.

Figure 5a shows a sequence of velocity distributions obtained with various delay times. For longer delays, lower velocity atoms are observed. In fact, because the atoms are decelerated to near zero velocity over such a short distance near the end of the solenoid, the observed velocity is nearly inversely proportional to the delay time. Using the known delay times and the measured velocities, we can determine the location in the solenoid where the atoms originated. We find that the entire range

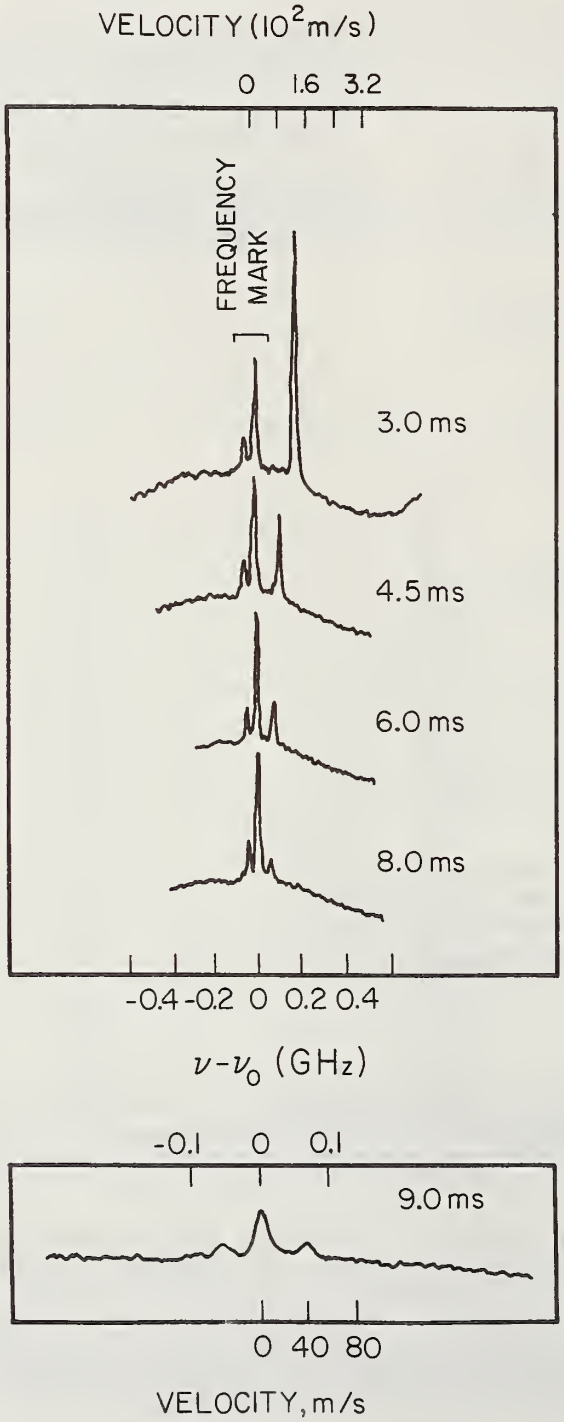

Fig. 5

(a) The velocity distribution of cooled atoms with various observational delay times. The broad background is from nonbeam N_a atoms. (b) Atoms observed at a velocity of 40 m/s and a delay of 9.0 ms. The left-most two peaks in all these distributions are frequency markers from which the residual Doppler shift (and hence atomic velocity) is measured.

of velocities in Fig. 5a come from a few centimeters near the end of the solenoid. Slower atoms come from regions of lower field, nearer the observation region, as expected.

The narrowness of the velocity distribution of slow atoms in Fig. 5a is in some sense artifical, since it is related to the narrowness of the gate time used for the observation. This is essentially a time-of-flight velocity selection, and longer gate time will usually result in a broader observed velocity distribution. Nevertheless, Fig. 3 shows a dramatic compression of the velocity, under steady-state conditions. Our working assumption, which is supported by the data, is that at any position in the solenoid, there exists in steady-state a narrow distribution of velocity whose central velocity corresponds to the magnetic field at that position. If we could extract atoms from a specific position we could obtain a continuous atomic beam with a narrow velocity distribution. Our delayed observation technique is a substitute for such an extraction.

Figure 5b shows the slowest velocity distribution we have obtained. Using a 9 ms delay we observed a central velocity of 40 m/s with a width of about 10 m/s. This is the true velocity width, since we found that it did not change as the gate time was increased. This is because at this very low velocity, so little atomic density exists at still lower velocity that admitting slower atoms, by extending the observation time, does not affect the results. After accounting for the width due to the natural, radiative width inherent in the detection (6 m/s) we infer an equivalent "temperature" of relative motion of 0.07 K. We estimate the atomic density within the natural linewidth to be on the order of 10^5 cm^{-3}.

One of the most striking features of Fig. 5 is the rapid decline in observed atomic density as $v^{2.5}$. For different tunings of the cooling laser we have observed dependences as strong as $v^{3.5}$. Simple considerations predict that the density at the observation point should vary as v^2 due to the angular divergence of the beam which increases as 1/v, and as v^{-1} due to the increase in density which comes as the velocity decreases but the flux stays the same. These effects combine to predict a density varying as v. This assumes that the gate time for observation is long enough to include the range of arrival times implied by the 6 m/s velocity width corresponding to the natural lifetime.

While we originally ascribed the rapid dependence we observe to the scattering of very slow atoms by background gas [2], improvements in the vacuum systems which allowed us to reduce the pressure by two orders of magnitude have shown that this is not the case. We do not now have a satisfactory explanation of the velocity dependence of the density. Work is continuing on this problem: we are doing a Monte Carlo simulation of the cooling process, analyzing the detection system in more detail and planning more experiments. We do believe that we understand certain aspects of the problem such as the dependence on cooling laser tuning (some tunings make it unlikely that any atoms will reach the very low velocities) and the dependence on observation time (too short observation windows restrict the observable velocity to a smaller range than the 6 m/s corresponding to the natural width), but we do not understand the persistence of a dependence on velocity which is always stronger than our simple model predicts.

4. Future Plans

Because we now believe that atoms are not being lost due to scattering, it seems reasonable to assume that whatever mechanism causes the density to decrease, it can be overcome by collecting the atoms efficiently and conducting them to the observation region. We intend to use a hexapole focussing magnet to achieve this. The hexapole acts as a positive lens to atoms. Its collection efficiency varies as v^{-4}, so we expect to be able to achieve significant improvements in the density of slow atoms.

An important unsolved problem for our cooling process is seen in Fig. 4. Curve (d) shows a large peak at about 300 m/s, with some smaller peaks at higher velocity. Under certain conditions we have observed four or more narrow, strong peaks of about equal intensity. They do not seem to be related in a simple way to known irregularities in the solenoid field, nor do they change significantly as those irregularities are varied. They depend strongly on tuning and power of the cooling laser. More cooling power always strengthens the slowest peak and weakens the faster ones. We do not have a suitable explanation for these peaks, although they would appear to be related to some process that causes atoms to drop out of the cooling process at specific velocities. Experiments in progress on cooling by scanning the cooling laser rather than using a varying field may help to shed some light on this question [5].

Extraction of atoms from the solenoid at a particular position corresponding to a particular velocity would be an important advance. We are considering using a mirror-coated micro-channel-plate as a

device which will pass the atomic beam into a dark region and still allow the cooling laser beam to overlap the atomic beam up to that point. If successful, such a scheme would allow production of a continuous beam of slow atoms, as opposed to the pulsed production which is imposed by our detection technique.

The ability to produce high intensity, nearly monoenergetic atomic beams such as in Fig. 3 raises the possibility of some interesting atomic beam experiments. One of these involves the use of transverse deflection of an atomic beam by light to study quantum statistics [6]. An experiment along these lines is discussed by Rubin and Lubell elsewhere in these proceedings [7].

An important application of slow atom techniques is in ultra-high resolution spectroscopy. This is discussed by W. Ertmer et al. elsewhere in these proceedings [8]. We simply note that if Ca atoms were decelerated even a very modest amount compared to what we have observed for Na, then the 2nd order Doppler effects which now limit the resolution of the Ca intercombination line at 657 nm [9] would be virtually eliminated.

One of the primary original motivations for this and other similar work has been the possibility of trapping neutral atoms in electromagnetic fields. Traps are discussed elsewhere [10,11,12,13], but a basic problem is that most such traps are so shallow in energy that very slow atoms are required. We have now produced atoms close to the energy of proposed traps.

A recent proposal for laser trapping by Minogin [14] is an extension to three dimensions of a one-dimensional radiation pressure trap proposed by Ashkin [10] Since the trap depends only on radiation pressure rather than the dipole force [10,11] it can be much larger than the tightly focussed dipole traps--on the order of 1 mm rather than several microns. This has two distinct advantages: first, with densities as high as 10^5 cm^{-3} which we have achieved for 40 m/s atoms, about 100 atoms could be expected to be in the trap if it were turned on at the proper time after the cooling laser shut off. This sort of operation would just be an extension of our delayed observation technique. Second, 1 mm is longer than the distance needed to bring saturated atoms at 40 m/s to rest. This gives a reasonable chance that some atoms will lose enough energy to remain in the trap. Two trapping frequencies would have to be used to avoid optical pumping, and with proper tuning of each, the trap would further cool the atoms. In principle, temperatures in the order of 10^{-3} K are possible.

This work was supported in part by the Office of Naval Research.

[1] W. D. Phillips and H. Metcalf, Phys. Rev. Lett. 48 596 (1982).

[2] J. V. Prodan, W. D. Phillips and H. Metcalf, Phys. Rev. Lett 49 1149 (1982).

[3] D. J. Wineland et al. Phys. Rev. Lett 40, 1639 (1978).

[4] S. V. Andreev et al. JETP Lett 34, 442 (1981) [Pis'ma Zh. Eksp. Teor. Fiz. 34, 463 (1981)].

[5] J. V. Prodan and W. D. Phillips, these proceedings

[6] R. J. Cook, Opt. Commun. 35, 347 (1980).

[7] K. Rubin and M. S. Lubell, these proceedings.

[8] W. Ertmer et al., these proceedings.

[9] Ch. Salomon et al., J. Phys. (Paris) 42, C8-3 (1981).

[10] A. Ashkin, Phys. Rev. Lett. 40, 729 (1978).

[11] J. P. Gordon and A. Ashkin, Phys. Rev. A 21, 1606 (1980).

[12] W. H. Wing, Phys. Rev. Lett. 45, 631 (1980).

[13] See also papers by W. H. Wing, W. C. Stwalley, D. E. Pritchard, J. P. Gordon, H. Metcalf and G. L. Greene in these proceedings.

[14] V. G. Minogin, Sov. J. Quantum Electron 12, 299 (1982) [Kvant. Elektron, (Moscow) 9, 505 (1982)], but see also J. Gordon, these proceedings for a criticism of such traps.

Laser-Cooled and Trapped Atoms, (Proceedings of the Workshop on Spectroscopic Applications of Slow Atomic Beams, held at NBS, Gaithersburg, MD, 14-15 April 1983) Ed. by W. D. Phillips, Natl. Bur. Stand. (U.S.) Spec. Publ. 653 (1983).

THE DESIGN OF ATOMIC FREQUENCY STANDARDS AND THEIR PERFORMANCE IN SPECIFIC APPLICATIONS

S. R. Stein

National Bureau of Standards
Boulder, Colorado 80303

ABSTRACT

The reduction of timing errors in atomic clocks is shown to be important for secure communications and navigation. An approach based upon control of all systematic frequency shifts and a reduction in both the first order Doppler shift and confinement effects is recommended. Ion storage is a promising technique because of its ability to achieve extremely long observation times, negligible confinement perturbations, and laser cooling. The applicability of atom cooling should be evaluated.

Key Words: Atomic Clocks, Frequency Standards, Navigation, Secure Communications

Introduction

The development of frequency standards and clocks has been one of the most visible applications of atomic and molecular spectroscopy. For this reason, it is natural for a workshop on slow beams to consider some of the requirements for improved frequency standards and what conclusions may be drawn about the scientific research necessary for their development. At least half the applications of atomic frequency standards are in high technology defense systems whose development now requires approximately a decade from planning to implementation. Although the role of atomic clocks is often critical, the clock is such a small part of such systems that plans rarely take into account required improvements in clock performance. The subject of this workshop directs our attention towards issues of timekeeping over long periods of time since much simpler techniques are adequate for short times.

There are three general types of atomic frequency standards which are commercially available today: the rubidium gas cell frequency standard, the cesium beam frequency standard, and the hydrogen maser. These three are only a small fraction of the instruments which have been demonstrated in the laboratory. Devices not developed commercially include active rubidium masers, cesium gas cell frequency standards, thallium atomic beam frequency standards, superconducting cavity stabilized oscillators, ammonia absorption frequency standards, calcium atomic beam frequency standards, methane stabilized lasers and many others. This paper will examine the ultimate performance limitations of today's state-of-the-art atomic frequency standards and the projected requirements for improvement. It will attempt to clarify

the most likely direction for research if we are to achieve these ends. Through analysis of these questions we hope to maximize the likelihood of producing additional important atomic frequency standards. Other performance characteristics such as acceleration sensitivity, size, weight and power are not considered.

The Role of Clocks in Navigation, Communications and Data Acquisition

For the sake of non-practitioners in the clock field, it may be worthwhile to start from the beginning and ask what essential function clocks serve. The answer is that they provide a uniform scale of the time coordinate between synchronization experiments. Without periodic resynchronizations, two independent clocks would necessarily differ from one and other by an amount which grows without any bound. Thus, for purposes of science and general commerce, the world would require only a single clock in a large communications network to disseminate the time of that clock. In fact, we are all quite used to operating in this fashion. Nearly every wall clock in the entire country is loosely locked to the time scale of the National Bureau of Standards by the actions of electrical utilities. Our wall clocks are only displays that register the number of cycles of the voltage delivered by the local power company.

But practically everyone wears a wristwatch in order to provide a memory of the last synchronization to Universal Time. Thus it is possible to have time information in locations not served by electric power or other means of resynchronization. Of course, depending upon his requirements, one will resynchronize his watch with the wall clock at appropriate intervals. Similarly, behind every application of an atomic frequency standard, one can discern some benefit for extending the interval of independent operation before resynchronization is required.

At first, this example may seem facetious, but it illustrates important aspects of the utilization of atomic frequency standards. In fact, the best wristwatches which are sold today are comparable in quality to the national time standards of only 150 years ago. Atomic frequency standards are employed when the application cannot or chooses not to provide frequent resynchronizations. Military systems often utilize atomic clocks to prevent jamming or increase the security. VLBI systems use remote clocks for time tagging the data acquisition process since the timing requirements are more stringent than any known means of remote time synchronization. NASA uses atomic clocks for deep space navigation for the same reasons. Commercial broadcasts and communications systems use atomic frequency standards to enhance system reliability. The benefits of using clocks - improved security, freedom from interference and redundancy - are intangibles but have great importance to modern society.

Performance of Atomic Frequency Standards

Since clocks are used to mark off uniform increments of time (phase), their performance is analyzed in terms of frequency variability. The generally accepted measure of this variability is the Allan variance, $\sigma_y^2(\tau)$, defined in reference [1]. This variance is a measure of the changes between successive frequency determinations. Figure 1 is the performance of the clocks in the NBS atomic time scale. It shows that there are two regions of averaging time for frequency measurements in which the performance of atomic frequency standard is qualitatively very different. The

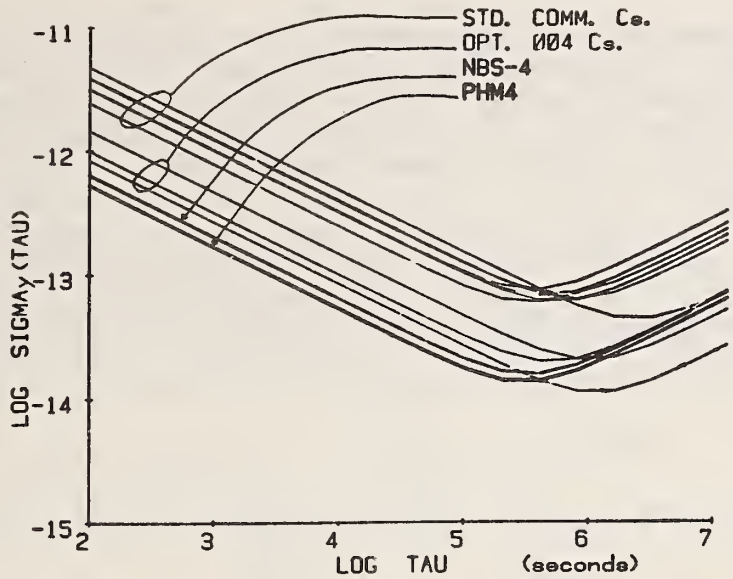

Figure 1: The estimated stability of the clocks in the NBS atomic time scale. NBS-4 is a laboratory cesium standard. PHM4 is a laboratory passive hydrogen standard. STD. COMM. Cs refers to the standard performance cesium standards from commercial manufacturers. OPT. 004 Cs is a high performance commercial option.

first performance region, called the short-term, is characterized by improving stability. In the second, long-term region, the performance ceases to improve and begins to get worse. Examination of the performance of passive and active frequency standards will illustrate the features of these two regions.

A passive frequency standard is one in which an external oscillator is used to probe an atomic absorption. Appropriate signal processing allows the formation of a discriminator signal and permits the probe oscillator to be locked to the atomic feature. In the short-term region, the frequency deviations are well understood and may be calculated quite accurately. The error between the frequency of the probe oscillator and the atomic resonance results from noise. For example, in the case of the cesium beam frequency standard the noise is due to a combination of the statistical fluctuations in the number of atoms that make the transition and shot noise of the detected signal. The result is white frequency noise which is described by [2]

$$\sigma_y(\tau) = \frac{0.2}{Q\,(S/N)^{1/2}\,\tau^{1/2}}$$

where Q is the atomic quality factor, $(S/N)^{1/2}$ is the voltage signal to noise ratio in a 1Hz BW and τ is the averaging time.

The short-term performance of a hydrogen maser is qualitatively different because the feedback to the atoms is high enough to permit power at the atomic transition frequency to be obtained from the ensemble of atoms. There is coherence between the individual atomic emitters so that white noise within the atomic linewidth perturbs the phase but not the frequency of the oscillation. Since the phase fluctuations are bounded, the frequency stability improves inversely with the averaging time [3].

$$\sigma_y(\tau) = \text{constant}/\tau$$

This feature of the hydrogen maser makes it the most stable atomic frequency standard in the region from approximately ten-seconds to a few hours. In the short-term, the frequency stability improves with the averaging time. Although such behavior should continue indefinitely, the standard eventually enters the long-term region in which the frequency stability begins to degrade due to imperfections in the control electronics. The atomic resonance frequency itself is subject to change resulting from variations in parameters such as magnetic field. In addition, there is always a difference between the frequency of the standard and the atomic line center and this differential is subject to change. As a result, the frequency of the standard displays an approximate random walk behavior and the frequency stability is given by the approximate formula

$$\sigma_y(\tau) \sim k\tau^{1/2}$$

where the value of k cannot be predicted from the design, but must be obtained emperically.

The frequency stability of an atomic clock will not deteriorate indefinitely as $\tau^{1/2}$ because frequency excursions beyond a certain size are exceedingly unlikely. For example, it would be unreasonable for the frequency to change by as much as a linewidth. In actuality, one knows with a fair degree of confidence that the frequency will change by much less than that over the life of the standard. Today, a manufacturer of cesium beam standards may specify a maximum lifetime frequency change of 3×10^{-12}. Thus the Allan variance is bounded by the limit

$$\sigma_y(\tau) \lesssim 3 \times 10^{-12} \quad \text{for} \quad \tau \gtrsim 100 \text{ s.}$$

Although there is no reason to expect that $\sigma_y(\tau)$ would remain constant at lower levels than implied by the above argument, such a model (flicker noise) has been improperly used for the long-term frequency stability of atomic frequency standards. New techniques of statistical analysis indicate that a random walk of frequency model is more conservative. Primary standards utilize techniques which quantitatively relate the frequency to the unperturbed atomic frequency. They are therefore said to have the property called accuracy, which is the ability to reproduce a specified frequency. NBS-6, the NBS primary frequency standard is estimated to be accurate to 8×10^{-14}. Thus NBS-6 could be used to assure that

$$\sigma_y(\tau) \lesssim 8 \times 10^{-14} \quad \text{for} \quad \tau \gtrsim 100 \text{ s.}$$

Time Dispersion: The Bottom Line

To compare the timekeeping capability of various clocks one must compute the rms error $x(\tau)$ which a clock accumulates in time τ. In order to simplify this very complicated problem we assume that the behavior of the clock is known and the frequency variations are described by

$$\sigma_y(\tau) \sim \left[b^2\tau^{-1} + c^2 + d^2\tau \right]^{1/2}$$

where b, c and d are the 1 second intercepts of the three dominant noise types - white frequency, "flicker" frequency, and random walk frequency. In practice, one must also take into account the uncertainties in clock parameters such as drift so this approach will yield slightly optimistic results. The time error of the clock has been shown to be [4]

$$X(\tau) \sim \left[b^2\tau + 1.4c^2\tau^2 + d^2\tau^3 \right]^{1/2}$$

Table 1 shows the time errors of two clocks. The performance of clock A is dominated by random walk frequency noise such that $\sigma_y(10^5 s) = 10^{-14}$. Clock B has an accuracy of 10^{-14} and the noise is conservatively estimated as $\sigma_y(\tau) = 10^{-14}$.

TABLE 1: Time Error in Nanoseconds

τ	Clock A $x(\tau)$	Clock B $x(\tau)$
10^5s	1	1
10^6s	32	12
10^7s	1000	120

Some Applications of Atomic Frequency Standards

Let us consider two applications which now or in the near future need improved frequency standards: secure diplomatic and military communications and military navigational systems. First, we consider the direct benefits of decreased time dispersion and extended update intervals. Later we will examine other important benefits of improving clock technology.

Secure communications are generally provided through the use of data encryption and steganography. (Encryption is the generation of a cypher text from a plain text message while steganography consists of techniques which hide the transmission of a message.) The encryption process is accomplished by a device called a crypto which uses an algorithm similar to the Data Encryption Standard published by the National Bureau of Standards and an encryption key. Decryption is accomplished by a second crypto using a decryption algorithm and key. Such systems require that the receiving crypto be synchronized to the transmitting crypto and this function is usually provided by the communication system itself.

. The level of security provided by such a system is generally sufficient for even the most sensitive commercial information. However, further levels of security are required for diplomatic and military communications. For these applications, it may also be desirable to employ some technique to hide the signal in order to protect against jamming or so that the signal may not be detected and decryption attempted. In fact, in some cases knowledge that a signal has been sent at all is more than one is willing to reveal. The most common methods of hiding communications signals are frequency hopping and pseudorandom noise spread spectrum modulation. Spread spectrum techniques hide the signal beneath a high level of simulated noise. For example, an audio voice channel may be mixed with an rf pseudorandom noise signal before transmission from the secure facility. Alternatively information at a rate of a few bits per minute may be phase modulated on a carrier in a band near 76

Hz [5]. In order to receive the signal it is necessary to integrate for substantial periods of time to synchronize the receiving crypto with the transmitting crypto and to extract the signal from the background noise. To make signal interception as difficult as possible, information required to synchronize the receiving crypto to the transmitting crypto is generally not transmitted with the message. The receiver contains a clock which maintains an imperfect memory of the original synchronization. After a period of time the synchronization degrades due to time dispersion between the two cryptos and the receiver must search over a larger and larger time interval for indication of successful signal decryption. A 20 MHz communications channel must be searched with tens of nanoseconds resolution. A 75 Hz channel requires only milliseconds resolution but long integration intervals are required to separate signal from noise. Once decryption commences, the crypto machines may be locked together. Thus the most difficult operational requirements for the frequency standard is the need to permit receivers which have been out of communication for substantial periods of time to quickly regain entry into the communications net. Communications systems now in the planning and development phases need frequency stability in the range of $\sigma_y(\tau) \sim 10^{-14}$ over long time intervals [6].

Satellite based military navigation systems place comparably stringent requirements on the satellite atomic frequency standards. For example, the desired performance of GPS satellite clocks is $\sigma_y(\tau) \lesssim 10^{-13}$ for time intervals between 1 and 10 days. This performance would result in a clock contribution to the navigation error of approximately 3 meters at one-day and 30-meters at 10-days. Today, it appears to be acceptable for the GPS system to operate for 10 days without updates from the ground. This policy may be based more on what is practical given today's technology than what is desirable for system operation. Longer periods of autonomous operation would serve to increase the security and survivability of the GPS system. It is important to bear in mind that the clock performance in the GPS system cannot be treated as an independent issue. The performance of the system during periods of autonomous operation is also degraded by the absence of updated ephemeris information. Improvements in both areas are necessary to extend the autonomous operation period at a given performance level. The availability of improved clocks would allow the study of the ephemeris in greater detail, thus speeding the solution of this overall problem. Improvement of clocks to the $\sigma_y(\tau) \lesssim 10^{-14}$ level would extend the autonomous operation period for the GPS system to 100 days with no degradation in current performance levels.

In addition to the actual timekeeping performance of atomic clocks, there are other aspects of performance which could be improved at the same time. There is considerable interest in reducing the turn-on time, and the sensitivity to radiation effects. The reliability and the lifetime of clocks need to be increased. Many or all of these are amenable to improvement.

Factors Limiting the Long-term Timekeeping Performance of Atomic Clocks

We have seen that for times of a day and longer, the performance of atomic frequency standards is limited by systematic offsets of the frequency from the ideal. By far the largest of the systematic offsets result from Doppler effects. In general, we may write the absorption frequency of an atom initially moving at velocity v with respect to a source at rest as

$$\omega \sim \omega_0 + \underset{\sim}{k} \cdot \underset{\sim}{v} - \frac{1}{2}\omega_0\left(\frac{v}{c}\right)^2 + \frac{\hbar\omega_0^2}{2Mc^2}$$

The measured frequency ω is equal to the nominal frequency ω_o with three corrections. The second term in the equation is an offset proportional to the velocity difference, v, between an atom and observer called the first order Doppler effect; k is the radiation wave vector. The third term is due to time dilation. Because of its quadratic behavior, this term is usually called second order Doppler effect. c is the speed of light. The fourth term takes into account the recoil of the atom. It will be neglected here since it is generally small except in the optical case.

The first order Doppler effect is generally the largest of all the systematic errors in the atomic frequency standard. A cesium atom from the vapor at 350K has a most probable velocity of approximately 200 meters per second. Thus the first order Doppler shift is approximately one part per million. Although at the present time there is little agreement on what limits the long-term performance of commercial atomic frequency standards, the situation is more clear in the case of laboratory standards which perform roughly a factor of 10 better than their commercial counterparts. It is fair to say that these devices are limited in performance either by residual first order Doppler shift or by whatever technique is used to cancel this shift.

There are several different Doppler cancellation approaches in common use. In the case of the hydrogen maser and the rubidium gas cell frequency standard, the atom is confined to a region of space smaller than one-half wavelength. Under these conditions the Doppler lineshape consists of a discrete, narrow line well resolved from the broad Doppler pedestal. The linewidth of this feature is determined by other mechanisms such as finite observation time or relaxation processes. In a hydrogen maser, the atoms are confined within a teflon coated vessel, whereas, in a rubidium frequency standard they are confined by collisions with a buffer gas. In either case, the atoms experience frequency perturbations which are extremely difficult to measure and control.

In a cesium beam frequency standard, collision effects are avoided by using a low density atomic beam which passes through a microwave cavity in a region where there are no reversals of the microwave phase. In a perfect, lossless microwave cavity, the first order Doppler shift would be perfectly nulled. However, the finite conductivity of the walls results in asymmetry of the counter propagating microwave fields and a residual first order Doppler shift which is proportional to the misalignment of the atomic beam from the orthogonality with microwave Poynting vector.

The second order Doppler effect is only on the order of 10^{-12} for room temperature atomic species, but is even more difficult to characterize. Furthermore, aging effects have been observed to change the velocity distribution by a significant amount. Figure 2 shows the velocity distribution of a cesium beam tube before and after a modification. The broken line was data taken after the standard had drifted in frequency $\delta\nu/\nu \sim 2 \times 10^{-12}$ over the course of one year. Note the non-Maxwellian nature of the density of atoms at high velocity. Since detector aging was the suspected cause, changes were made in the collector potentials and a subsequent velocity distribution measurement, indicated by the solid line, was more nearly normal. The frequency returned to its original value. Data such as this indicates that if all the more serious problems in atomic beam frequency standards were eliminated, variations in the second order Doppler effect would probably limit performance at the 10^{-14} level for a 350K beam temperature.

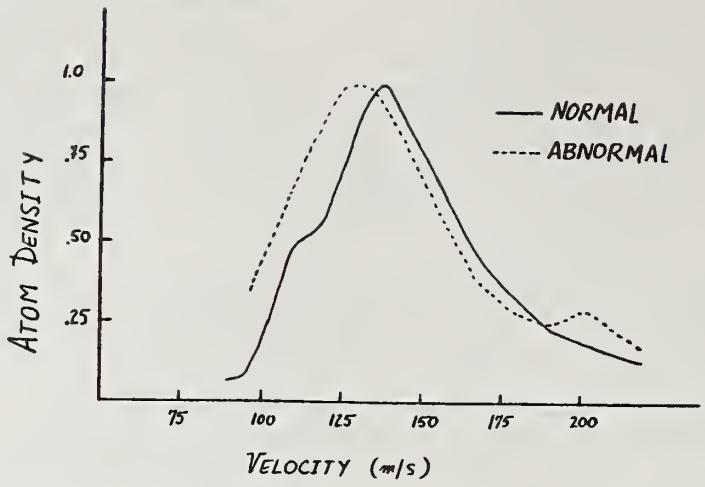

Figure 2: The change in detected atom velocity distribution due to aging of the detector in a commercial cesium beam tube. The accompanying frequency change was approximately $\Delta\nu/\nu = 2 \times 10^{-12}$.

The electronic control circuitry that determines the center of the resonance is subject to a very long list of problems that produce substantial frequency offsets. For analog control systems, the problems include harmonic distortion in the phase modulation, spurious lines in the microwave signal, variations in the mean microwave power and pulling by the microwave cavity. Digital control circuits reduce the problem associated with modulation and spurious signals but add additional difficulties related to maintaining symmetry of the squarewave modulation cycle. As a result of all of these problems, the best existing electronics has difficulty maintaining consistent operation even down to the 10^{-14} level.

Probable Direction for Breakthroughs in the Long-term Performance of Atomic Frequency Standards

The current generation of atomic frequency standards is extremely mature. Laboratory devices reach a performance floor of approximately 10^{-14} for times longer than one day. Performance deteriorates to worse than 10^{-13} for times of several months to one-year. Engineering improvements to existing commercial standards and some new commercial devices such as room temperature ion standards may very well achieve performance comparable to today's laboratory standards but significant improvements beyond what is achieved today in the laboratory are unlikely without some fundamental changes.

Major advances are likely to come through research and development focused in three directions. First, low velocity ions or atoms should be used in order to reduce the magnitude of the Doppler effects. Second, significantly higher atomic line-Q and longer observation times must be obtained. This would improve the ability to cancel the first order Doppler shift. Frequency offsets due to the electronic control circuitry would also be reduced at least in proportion to the increase in the Q. Finally, all variables which affect the operating frequency of the standard should be referenced directly back to the atomic frequency itself including such things as the Zeeman shift due to the finite magnetic field.

A reasonable objective for the next generation of advanced atomic frequency standards will be to achieve routine 10^{-15} performance for very long times. To accomplish this goal, the first order Doppler effect either needs to be reduced in absolute magnitude by a factor of 100 or nulling techniques must be improved by this same factor. The second order Doppler effect needs to be reduced to below the 10^{-15} level. For a trapped ion device, the first order Doppler effect is reduced to negligible proportions by confinement. Reduction of the second order effect requires a temperature of 300 mK. As explained earlier, traditional attempts to exploit this technique have resulted in significant frequency shifts due to the confinement mechanism. But the dc electric and magnetic fields used to confine ions result in uncertainties less than 10^{-15}, three orders of magnitude smaller than the best prior state-of-the-art. In the case of a neutral atomic beam, cooling to approximately 30 mK is needed to null the first order Doppler effect.

The ability to confine ions with negligible perturbations allows enormous enhancement of the atomic line-Q. Experiments performed on magnesium have demonstrated 10 millihertz linewidths at a transition frequency of 300 MHz or an atomic line-Q of 3×10^{10} [7]. Other experiments have demonstrated Q's as high as 2×10^{11} [8]. This is a factor of 10 to 100 improvement over the hydrogen maser, and a factor of 100 to 1000 improvement over the highest Q cesium atomic beams. Assuming that the same linewidth can be obtained using ^{201}Hg which has a hyperfine frequency of 26 GHz, the Q would be 10^{12}. Improvement in Q may also be obtained in a cold atomic beam. However, the effect of gravity on the beam inhibits obtaining very long interaction times and trapping is indicated. It is not known whether confinement effects can be made sufficiently small.

Frequency standards have reached the point where many of the parameters must be controlled to extremely high levels of precision. State-of-the-art control is required for temperature, the influences of external magnetic fields, and certain parameters of the electronic circuitry. In the past, this has been accomplished using a variety of sensors and references. In the future, it will be increasingly necessary to reference all critical variables directly to invariant atomic properties. For example, Zeeman frequency shifts can be measured by observing the magnetic field sensitive transitions. This philosophy may sound very much like the design principles of a primary frequency standard such as NBS-6. This is because the ability to guarantee from first principles that the frequency of a standard is within 10^{-15} of some arbitrary value assures that long term frequency stability must be better than 10^{-15} forever. Once such a standard is constructed, examination of the control signals over a long period of time will make it possible to design simpler devices which, although they have lost the property of frequency accuracy, retain adequate long term frequency stability for many applications. This design philosophy is exactly the one which led to the cesium beam standard and can probably be employed again to achieve dramatic results.

Building an accurate standard in order to achieve long term frequency stability can have significant additional advantages. Such a device should have greatly increased reliability due to its self-monitoring and correction capabilities. It would also have enhanced capability to withstand adverse environments such as extremes of temperature, radiation or EMP, since the atomic resonance itself is relatively unperturbed by these effects. The

accuracy approach would also improve the speed with which the standard could be brought into operation. Present day frequency standards suffer from retrace error. That is, the frequency after start up differs from the previous operating frequency. Sometimes the operating environment prevents the rapid evaluation of this new frequency. For example, when a cesium standard is started up on a GPS satellite, its frequency can be predicted to only 10^{-11}. The perturbations due to the atmospheric delays permit the new frequency to be measured to ~5×10^{-13} in 1 day and 1×10^{-13} after 5 days. An accurate frequency standard would evaluate its own frequency without the need to reference a standard on the ground. Its frequency would be known to 1×10^{-13} in hours.

In conclusion, we believe that it is now possible to make major improvements in the timekeeping ability of atomic clocks. Three approaches are recommended: The use of narrower atomic features, the reduction of Doppler effects and the evaluation of all systematic frequency offsets in terms of atomic properties. Laser cooling of stored ions is an extremely promising technique which should make it possible to achieve frequency accuracy and stability at the 10^{-15} level. Secure diplomatic and military communications, space and military navigation, and scientific investigations will be the prime beneficiaries.

REFERENCES

[1] J. A. Barnes, A. R. Chi, L. S. Cutler, D. J. Healey, D. B. Leeson, T. E. McGunigal, J. A. Mullen, W. I. Smith, R. L. Sydnor, R. F. C. Vessot and G. M. R. Winkler, IEEE Trans. Instrum. Meas. IM-20, 105 (1971).

[2] J. Vanier and L. G. Bernier, IEEE Trans. Instrum. Meas. IM-28, 188 (1979).

[3] L. S. Cutler and C. L. Searle, Proc. IEEE 54, 136 (1966).

[4] D. W. Allan and H. Hellwig, in Proceedings of the Position Location and Navigation Symposium, 29 (1978).

[5] Defense Electronics 14, 59 (1982).

[6] Private Communication, Department of the Navy (unclassified).

[7] W. M. Itano and D. J. Wineland, Phys. Rev. A24, 1364 (1981).

[8] R. Blatt, H. Schmatz and G. Werth, Phys. Rev. Lett. 48, 160 (1982).

Laser-Cooled and Trapped Atoms, (Proceedings of the Workshop on Spectroscopic Applications of Slow Atomic Beams, held at NBS, Gaithersburg, MD, 14-15 April 1983) Ed. by W. D. Phillips, Natl. Bur. Stand. (U.S.) Spec. Publ. 653 (1983).

FREQUENCY STANDARD RESEARCH USING STORED IONS

D. J. Wineland, Wayne M. Itano, J. C. Bergquist,
J. J. Bollinger, and H. Hemmati

National Bureau of Standards
Boulder, Colorado 80303

ABSTRACT

We summarize research undertaken to develop time and frequency standards based on stored ions. The ion storage method for high resolution spectroscopy is also briefly compared to the methods for stored neutrals and slow atomic beams.

Key Words: atomic clocks, atomic spectroscopy, frequency standards, high resolution spectroscopy, laser spectroscopy.

1. Introduction

The possibility of producing very cold atomic beams and stored neutrals is exciting. Certainly these experiments are interesting by themselves but they also point the way to some new experiments in high resolution spectroscopy and may result in new schemes for atomic frequency standards. The technique of stored ions also has great promise in these applications and therefore it is useful to compare these techniques so that potential problems can be addressed in the future. In the case of trapped ions, practical frequency standards techniques have already been demonstrated. Stabilities comparable to or better than some commercial standards have been achieved and the potential is clear to obtain long term stability and accuracy of 10^{-15} in a practical device. This paper is biased toward the stored ion technique but certain-

ly this method is not without difficult problems; moreover the potential problems with slow atomic beams and stored neutrals might be made small in the future.

1.1. Stored Ions vs Stored Neutrals or Atomic Beams

Probably the main attraction of the stored ion techniques for high resolution spectroscopy is that the ideal of an unperturbed species at rest in space is approached to a high degree. Specifically, charged particles such as electrons and atomic ions can be stored for long periods of time (essentially indefinitely) without the usual perturbations associated with confinement (for example the perturbations due to collisions with walls or buffer gasses in a traditional gas cell optical pumping experiment). This advantage would also appear to carry over when the stored ion technique is compared to the present schemes for stored neutrals. The current proposals for neutral trapping rely on strongly perturbing the internal structure of the atom (or molecule) to provide binding. This is especially clear for magnetostatic [1] and electrostatic [2] trapping where there is a direct trade off between the atom's kinetic energy and internal energy. In the case of laser traps this trade off is not quite as clear, but in traps using either induced dipole forces [3] or radiation pressure forces [4], rather strong ac Stark shifts accompany the trapping process. In all cases, these internal energy shifts associated with trapping may cause unwanted systematic frequency shifts in high resolution spectroscopy. This problem can be overcome if the trap is turned off while the "clock" transitions are driven, but even if maximum laser cooling is achieved on strongly allowed transitions, minimum velocities are on the order of 10 cm/s which would limit the time the trap could be off (therefore limiting Q) and would cause an additional heating mechanism. Of course, the confining fields of electromagnetic traps for ions can cause shifts but these appear to be controllable down to below 10^{-15} [5-7].

In principle, atoms in an atomic beam can be totally free of external fields; this is perhaps the principal advantage of the method. We note however, that typical residual fields due to contact potentials etc. in an atomic beam apparatus can be several mV/cm. These fields might cause observable systematic frequency shifts in certain experiments. A trapped ion on the

other hand seeks the region of zero electric field; for cooled ions the average magnitude of electric field can be below 1mV/cm [6]. Perhaps the chief limitation of the atomic beam method is caused by the net linear motion of atoms; even if Doppler cancellation schemes are used, residual first order Doppler shifts can be the limiting systematic effect. This is, for example, true for the cesium beam frequency standard, the most accurate frequency and time standard available. For the case of trapped ions, the same ions can be confined nearly indefinitely; therefore the net velocity averages to zero and first order Doppler shifts are nearly absent.

The primary disadvantage of the stored ion technique is that the number of trapped ions is typically small--approximately 10^6 ions or less for a trap of centimeter dimensions. Therefore one is usually restricted to use simple atomic systems where signal to noise can be maximized.

1.2 Scope of Paper

The remainder of the paper discusses stored ion experiments whose goal is very high resolution spectroscopy--i.e. stored ion frequency standards: present status and future goals.

2. Stored Ions and Frequency Standards

2.1. Microwave Frequency Standards

At present, the most accurate (reproducible) frequency standards are based on microwave transitions of atoms or molecules. The stability of a frequency standard increases with increased Q (transition frequency divided by linewidth) and increased signal to noise ratio. The reproducibility depends upon control of environmental factors. Standards based on narrow optical transitions have the advantage of higher Q for a given interaction time, for cases where the linewidth is limited by interaction time. However, the use of such a frequency standard to generate precise time, one of the chief applications of frequency standards, is very difficult with current technology. The main difficulty is dividing an optical frequency down to the RF region. Also, high-stability optical sources are not easy to produce.

An atomic frequency standard can be either active or passive in nature. In an active device, such as a self-oscillating hydrogen maser, excited atoms decay, emitting radiation with a stable frequency. In a passive device, such as a cesium atomic beam, the atomic resonance frequency is probed by radiation derived from an oscillator whose frequency is controlled in a feedback loop so that the frequency of the radiation matches that of the atoms. All of the proposed frequency standards based on stored ions to be discussed in this paper are passive devices.

Ions can be confined for long periods (as long as days) under ultrahigh vacuum conditions in ion traps by electric and magnetic fields. For frequency standard applications, stored ions have the combined advantages of long interaction times (hence narrow resonance lines), because both the storage and relaxation times can be long, and small perturbations to transition frequencies. Atoms in atomic beams also have small perturbations, but the interaction time is limited to the flight time through the apparatus ($\lesssim$ 0.01 s for room temperature atoms). Atoms can be stored without relaxation in buffer gases or coated cells for times up to about 1 s, but the transition frequencies are significantly perturbed by collisions. A possible disadvantage of ion traps is the low signal to noise ratio (S/N), due to the small number of ions that can be stored. However this disadvantage can be offset by obtaining very high Q, since the stability $\sigma_y(\tau)$ of an oscillator locked to an atomic transition scales as $(S/N \cdot Q)^{-1}$. For example, if an oscillator is locked to the 26 GHz hyperfine transition in $^{201}Hg^+$ and a linewidth of 0.01 Hz is obtained, then 100 stored ions can potentially give a stability $\sigma_y(\tau) = 6 \times 10^{-14}\tau^{-\frac{1}{2}}$ [8]. This would exceed any existing passive atomic frequency standard.

Several laboratories have worked on developing a frequency standard based on the 40.5 GHz ground state hyperfine splitting of $^{199}Hg^+$ ions stored in a trap of the rf quadrupole (Paul) type [9-13]. State selection and detection is by optical pumping. Resonance light from a lamp containing $^{202}Hg^+$ pumps ions from the F=1 level to the F=0 level. Resonant microwave radiation repopulates the F=1 level and is detected by an increase in the resonance fluorescence intensity. Resonance linewidths of about 1 Hz have been observed [12]. At present, the main accuracy limitation is the second-order Doppler (time

dilation) shift, which is relatively high (about 10^{-11}) because the average ion kinetic energy is a few eV. In a similar experiment on trapped $^{171}Yb^{+}$ ions, Blatt et al. [14] have observed a 0.06 Hz linewidth on a 12.6 GHz hyperfine transition, corresponding to a Q of 2×10^{11}, the highest yet obtained in microwave spectroscopy.

2.2 Laser Cooling and Microwave Frequency Standards

Perhaps the chief advantage of applying laser cooling to stored ions is the suppression of Doppler effects. Even without laser cooling, first order Doppler effects are highly suppressed because of the long term storage. However, without laser cooling, second order Doppler shifts can be relatively large (approximately 2×10^{-13} for room temperature Hg^{+} ions) and since the velocity distributions are non-Maxwellian -- these shifts are difficult to precisely characterize.

With laser cooling, temperatures < 1K are easily obtained. The lowest temperatures (approximately 0.01 K) have been obtained for single ions [15-17]. However for a microwave frequency standard, many ions are required in order to keep the signal to noise ratio high enough to maintain desired stability [6,8]. So far the only reported experiments with the goal of a laser cooled microwave frequency standard are those of NBS [18,19]. These experiments are based on the storage of many ions (10^2-10^5) in a Penning trap where residual heating mechanisms [20] are apparently much less than in the rf trap. The Penning trap [20] requires static electric and magnetic fields for trapping. Since the required magnetic fields are rather large ($\sim$ 1T), one uses extremum points in the clock transition frequency vs. magnetic field; for these conditions, stabilities below 10^{-15} should be obtained [8,18,19]. Linewidths of approximately 0.01 Hz have been obtained on 300 MHz nuclear spin flip hyperfine transitions in $^{25}Mg^{+}$ [21] and an oscillator has been locked to a similar transition in $^{9}Be^{+}$, giving a stability approaching 10^{-13}. Operation on a 26 GHz transition in $^{201}Hg^{+}$ is anticipated; inaccuracy of < 10^{-15} and stabilities better than 10^{-16} appear possible [8].

2.3. Optical Frequency Standards

The potential accuracy and stability of optical frequency standards, where a single isolated ion can be used to advantage (i.e. signal to noise ratio is sacrificed in favor of very high Q), are extremely high. Anticipated accuracies of 10^{-18} do not seem unreasonable provided that sufficiently narrow band lasers ($\lesssim$ 10 Hz) are eventually obtained.

Optical frequency standards have the basic advantage of higher Q for fixed coherent interaction time. Dehmelt has proposed optical frequency standards based on forbidden transitions of single, laser cooled group III A ions (Tl^+, In^+, Ga^+, Al^+, or B^+) stored in small rf traps [7]. Penning traps or Penning/rf trap combinations might also be used [22]. The $6^2S_{1/2}$ - $6^2P_{1/2}$ - $5^2D_{3/2}$ Raman transition in Ba^+ could be used as a reference to generate a stable infrared difference frequency in a nonlinear crystal [7,23]. Also in Ba^+, the $5^2D_{5/2}$ to $5^2D_{3/2}$ 12 μm transition [24] and the quadrupole-allowed $6^2S_{1/2}$ to $5^2D_{5/2}$ 1.8 μm transition [25] have been proposed as standards. Other high Q optical transitions in Sr^+ [26] Pb^+, I^+, and Bi^+ [27] have been suggested for stored ion frequency standards. The two-photon [28,8] or single photon quadrupole [18] $5d^{10}6s\ ^2S_{1/2}$ to $5d^96s^2\ ^2D_{5/2}$ transition in Hg^+ has also been suggested. Two-photon transitions have the advantage of being first-order Doppler free even for a cloud of many ions, where it is impossible to satisfy the Dicke criterion at optical wavelengths. They have the disadvantage that the large fields required to drive the transition cause ac Stark shifts.

3. References

[1] W. Paul and U. Trinks, Inst. Phys. Conf. Ser. No. 42, 18 (1978).

[2] W. H. Wing, Phys. Rev. Lett. 45, 631 (1980).

[3] See for example: A. Ashkin, Science 210, 1081 (1980); V. S. Letokhov and V. G. Minogin, Phys. Rep. 73, 1 (1981); and references therein.

[4] V. G. Minogin and J. Javanainen, Optics Commun. 43, 119 (1982).

[5] Wayne M. Itano, L. L. Lewis, and D. J. Wineland, Phys. Rev. A 25, 1233 (1982).

[6] D. J. Wineland, in "Precision Measurements and Fundamental Constants II" (B. N. Taylor and W. D. Phillips eds.) National Bur. Stds. (U. S.), Spec. Publ. 617, in press.

[7] H. Dehmelt, I.E.E.E. Trans. Instrum. Meas. IM31, 83 (1982).

[8] D. J. Wineland, W. M. Itano, J. C. Bergquist, and F. L. Walls, Proc. 35th Annual Symposium on Frequency Control, U. S. Army Electronics Command, Fort Monmouth, NJ, 1981 (Electronic Industries Assoc., 2001 Eye St., N. W., Washington, D. C., 20006, 1981) pp. 602-611.

[9] F. G. Major and G. Werth, Phys. Rev. Lett. 30, 1155 (1973).

[10] M. D. McGuire, R. Petsch, and G. Werth, Phys. Rev. A 17, 1999 (1978).

[11] M. Jardino, M. Desaintfuscien, R. Barillet, J. Viennet, P. Petit, and C. Audoin, Appl. Phys. 24, 107 (1981).

[12] L. S. Cutler, R. P. Gifford, and M. D. McGuire, Proc. 13th Annual Precise Time and Time Interval Applications and Planning Meeting, Washington, D.C., 1981 (NASA Conf. Publ. 2220, NASA Scientific and Tech. Info. Branch, 1982) pp. 563-578.

[13] L. Maleki, Proc. 13th Annual Precise Time and Time Interval Applications and Planning Meeting, Washington, D. C., 1981 (NASA Conf. Publ. 2220, NASA Scientific and Tech. Info. Branch, 1982) pp. 593-607.

[14] R. Blatt, H. Schnatz, and G. Werth, Phys. Rev. Lett. 48, 1601 (1982).

[15] W. Neuhauser, M. Hohenstatt, P. Toschek, H. Dehmelt, Phys. Rev. A 22, 1137 (1980).

[16] D. J. Wineland and Wayne M. Itano, Phys. Lett. 82A, 75 (1981).

[17] W. Nagourney, G. Janik, and H. Dehmelt, Proc. Nat. Acad. Sci., USA, 80 643 (1983).

[18] D. J. Wineland, J. C. Bergquist, R. E. Drullinger, H. Hemmati, W. M. Itano, and F. L. Walls, J. de Physique 42, C8-307 (1981).

[19] Wayne M. Itano, D. J. Wineland, H. Hemmati, J. C. Bergquist, and J. J. Bollinger. To be published in I.E.E.E., Trans. Nuc. Sci., NS30, No. 2, Apr. 1983.

[20] D. J. Wineland, Wayne M. Itano, and R. S. Van Dyck, Jr., in Advances in Atomic and Molecular Physics, Eds. Bederson and Bates (Academic, New York) Vol. 19. To be published.

[21] Wayne M. Itano and D. J. Wineland, Phys. Rev. A24, 1364 (1981).

[22] D. J. Wineland and W. M. Itano, Bull. Am. Phys. Soc. 27, 864 (1982).

[23] W. Neuhauser, M. Hohenstatt, P. Toschek, H. Dehmelt, Proc. 5th Int. Conf. on Spectral Lineshapes, West Berlin (1980).

[24] H. Dehmelt, W. Nagourney, G. Janik, Bull. Am. Phys. Soc. 27 402 (1982).

[25] H. G. Dehmelt, J. de Physique 42, C8-299 (1981).

[26] H. G. Dehmelt and H. Walther, Bull. Am. Phys. Soc. 20, 61 (1975).

[27] F. Strumia, Proc. 32nd Ann. Symp. Freq. Control, Fort Monmouth, New Jersey, Electronic Industries Assoc., 2001 Eye St., N. W. Washington, D. C., p. 444 (1978).

[28] P. L. Bender, J. L. Hall, R. H. Garstang, F. M. J. Pichanick, W. W. Smith, R. L. Barger, and J. B. West, Bull. Am. Phys. Soc. 21, 599 (1976).

Laser-Cooled and Trapped Atoms, (Proceedings of the Workshop on Spectroscopic Applications of Slow Atomic Beams, held at NBS, Gaithersburg, MD, 14-15 April 1983) Ed. by W. D. Phillips, Natl. Bur. Stand. (U. S.) Spec. Publ. 653 (1983).

Optical Frequency Synthesis Spectroscopy

K. M. Evenson, D. A. Jennings, F. R. Petersen, J. S. Wells, and R. E. Drullinger
Time and Frequency Division
National Bureau of Standards

ABSTRACT

In order to measure the super narrow spectral features of cooled atoms and ions, in the optical region, optical frequency synthesis (OFS) techniques rather than wavelength techniques must be used. It is anticipated that many of these resonances will be in the optical region of the spectrum, and this paper will address the state-of-the-art of the measurements of frequencies in that region. Two recent optical frequency measurements of iodine transitions in the visible will be described as well as recent improvements in fabricating the point-contact diode used in these measurements.

Key words: optical spectroscopy, optical frequency synthesis (OFS), iodine

Introduction

One of man's most accurate and precise endeavors is that of frequency measurement; therefore, it is not surprising that a significant part of his understanding of the physical world is through the application of these measurement techniques. Specifically, the extension of both frequency measurement and other radio frequency techniques to the optical region has made a significant impact on the fields of metrology and spectroscopy.

Optical frequency synthesis (OFS) [1] is an extension of radio and microwave frequency measurement techniques into the infrared and visible region of the electromagnetic spectrum. This advance has been made possible by the development of a source of radiation (the laser), sub-Doppler frequency stabilization techniques, and the broadband harmonic generating capability of metal-insulator-metal (MIM) diodes. OFS is a "bootstrap" method whereby harmonic combinations of spectrally pure and measurable lower frequency laser oscillators are used to generate higher laser frequencies. This technique has now been used to extend "direct" or "absolute" frequency measurements from the far infrared into the visible spectrum. Most importantly, direct frequency measurements are now being made in this region of the spectrum for the first time. It is in this region that the most accurate wavelength measurements traditionally have been made and the meter has been defined. Now we have two different methods for making excellent comparisons of radiations in the visible, one utilizing wavelength metrologic techniques and the other utilizing frequency metrology (OFS). At the current state of the art, wavelength comparisons are subject to inaccuracies of the order of a few parts in 10^{11} because of diffraction, imperfections in the optical components, etc. However, frequency comparisons can be made which are limited only by the quality of the oscillators and can be referred to a primary standard that is four orders of magnitude better than the primary length standard!

The metrologic significance of laser frequency measurement was first most clearly demonstrated in 1972 when both the frequency and wavelength of the methane stabilized He-Ne laser at 3.39 μm (88 THz) were accurately measured. The product of these is a value of the speed of light [2] 100 times more accurate than the value accepted at that time, a value limited only by the krypton primary length standard itself. The possibility of improving length metrology with the use of laser radiation, and also fixing the speed of light gave impetus to the Consultative Committee for the Definition of the Meter (CCDM) to propose a redefinition of the meter based on the second. In 1982 the CCDM proposed: "The meter is the length of the path travelled by light in vacuum during a time interval 1/299 792 458 of a second" [3]. With this definition, the meter could be realized using the wavelength of any laser which is stabilized to a narrow atomic or molecular absorption feature for which the frequency is known. The wavelength, λ, would be determined from the relation $\lambda = c/\nu$, where c is the fixed value of the speed of light, and ν is the measured frequency of the stabilized laser. To realize this definition, it is necessary to accurately measure the frequency of certain absorption lines in the visible spectral region.

The first such measurements were performed at NBS in the spring of 1982. Two iodine lines which are suitable for realizing the new meter were accurately measured with optical frequency synthesis techniques. The first of these lines [4], a visible yellow iodine absorption line at 520 THz (576 nm), was measured using nonlinear crystals as frequency doublers above 130 THz (2.3 μm) and the MIM diode for harmonic generation at lower frequencies. This accomplishment was quickly followed by the measurement [5] of the red He-Ne iodine stabilized laser at 473 THz (633 nm), where the final frequency was synthesized by resonant enhanced four wave mixing of three known frequencies in a helium-neon plasma.

Additionally, because of the importance of the MIM diode to this technology, we shall describe some experiments which revealed improved coupling techniques and some surprising results concerning the sharpness of the diode tip which resulted in more stable diodes.

The OFS measurements of iodine

We describe the measurement of the frequency of the o hyperfine component of the visible $^{127}I_2$ 17-1 P(62) transition at 520 THz (576 nm) and the i hyperfine component of the $^{127}I_2$ 11-5 R(127) - stabilized He-Ne laser [6] at 473 THz (633nm) to 1.6 parts in 10^{10}. The frequencies were measured in three steps. First, a CO_2 laser line was compared with the CH_4-stabilized He-Ne laser at 88 THz (3.39 μm) [7], which presently is the most accurately known of all laser frequencies. Then, various CO_2 lasers referred to this CH_4 referenced laser were used in separate measurements of the 520 THz and 473 THz I_2 transitions. Since the 520 THz iodine line was used to measure the 473 THz frequency, the 520 THz frequency measurement will be discussed first.

The OFS technique here consists of a "chain" of lasers linking lower frequency lasers to higher ones with harmonic generation and heterodyning techniques as is shown in Fig. 1. In a MIM diode, three harmonics of one 26 THz CO_2 laser radiation plus two harmonics of another are heterodyned with the 130 THz color center laser radiation to produce a rf beat which is measured. Part of the color center laser radiation is subsequently frequency doubled and locked to the 260 THz He-Ne laser radia-

tion. The He-Ne laser radiation is in turn frequency doubled and frequency locked to a 520 THz cw dye laser. The 520 THz cw dye ring laser at the top of the chain was servo-locked to the o hyperfine component of the $^{127}I_2$, 17-1 P(62) transition observed in saturated fluorescence. The line had a full width at half maximum of 1 MHz for an iodine pressure of 4 Pa. The center of the transition could be determined to within 40 kHz.

The He-Ne 260 THz laser employed an 8 m discharge tube and generated 100 mW of single mode output power. The He and Ne gas mixture was adjusted to optimize single mode output power. A resonant reflector with a thin lossy metallic film positioned 9 cm from the high reflectivity end mirror provided tuning and mode selection. Approximately 90 mW of the output power was focused into a temperature tuned lithium niobate frequency-doubling crystal (T = 185°C) to generate 50 μw of power at 520 THz. This visible radiation was collinearly mixed with a portion of the cw dye laser output on a Si photodiode to produce a rf beat used to lock the two lasers together.

The cw color center laser operating at 2.3 μm was used as a frequency transfer oscillator for connecting the He-Ne laser frequency to the accurately known CO_2 laser frequency. The color center laser used $(F_2^+)_A$ centers in lithium-doped KCl [8], and provided broadly tunable laser output from 2 to 2.5 μm. When pumped with 4 W from a cw 1.33 μm Nd:YAG laser, the color center laser produced over 100 mW of output power at 2.3 μm. The laser was operated in a ring configuration to insure efficient single mode operation and was actively stabilized to a stable optical resonator with a resulting linewidth of less than 20 kHz.

The 2.3 μm radiation was focused into a temperature phase matched lithium niobate frequency-doubling crystal (T = 530°C) and generated approximately 10 μW of 1.15 μm radiation. This second harmonic output was combined collinearly on a beamsplitter with 10 mW from the He-Ne laser, and both beams were focused onto a high speed Ge photodiode. The resulting beat frequency was displayed on a rf spectrum analyzer and measured with an adjustable marker oscillator which was frequency counted.

The remainder of the non-doubled 2.3 μm radiation was focused onto a W-Ni point contact MIM diode. Coincident on the diode were the beams from two $^{13}C^{16}O_2$ lasers operating on the adjacent lines $P_I(50)$ and $P_I(52)$. The $P_I(50)$ laser was stabilized to the saturated fluorescence signal from an external 5.3 Pa $^{13}C^{16}O_2$ absorption cell. The $P_I(52)$ laser was phase locked to the $P_I(50)$ laser via a stabilized 62 GHz klystron. These two CO_2 lines were selected such that twice the frequency of one CO_2 laser plus three times the frequency of the other CO_2 laser nearly equalled the necessary color center laser frequency (130 THz). The free running CO_2 lasers each had approximately a 3 kHz linewidth; however, the average frequency difference of the two lasers was held stable to within 1 Hz in a 1 second averaging period.

The frequency of the $P_I(50)$ laser was determined by comparing it against a CH_4-stabilized He-Ne laser operating at 88 THz. International intercomparisons have shown frequency reproducibility of this device to be about $\pm 3 \times 10^{-11}$, and a number of absolute measurements of its frequency have been reported [3]. We took the average value of the 4 most recent measurements of this frequency as the basis for measurements described in this paper: the CH_4-stabilized He-Ne laser frequency was taken to be 88 376 181.609 MHz ± 0.009 MHz.

The result of the frequency chain measurement of the o hyperfine component of the $^{127}I_2$ 17-1 P(62) transition was

$$\nu_{I_2} = 520\ 206\ 808.547\ \text{MHz} \pm 0.081\ \text{MHz}.$$

This value is in agreement with previous, less accurate measurements [9]. The estimated frequency error represents a line center uncertainty of 1.6 parts in 10^{10}. Most of this uncertainty arises from the dispersion of the measured frequencies of the CH_4 standard, with the rest of the error appearing from effects such as reproducibility of the I_2 lock point, uncompensated pressure shifts, and counting and interpolation errors at each stage of the chain. Table 1 shows the error budget for this measurement.

The 633 nm He-Ne laser frequency was measured in a significantly different manner. Several years ago Klementyev et al. proposed a method of synthesizing 473 THz radiation using sum frequency mixing in Ne [10]. In this scheme, shown in Fig. 2, 473 THz radiation is generated by the nonlinear resonant mixing of radiation at the three measurable transition frequencies: 88 THz (3.39 μm), 125 THz (2.39 μm), and 260 THz (1.15 μm). The sum frequency at 473 THz is radiated by coherent polarization on the $3s_2$-$2p_4$ transition in Ne which results from the nonlinear interaction of the three fields resonant with three cascade transitions connecting the same two atomic levels. In our experiment, we used a separate laser for each of the frequencies, and mixed them in a low pressure He-Ne discharge tube. The experimental arrangement is shown in Fig. 3. Summed in the tube were radiations at 88 THz from a CH_4-stabilized He-Ne laser (amplified to 8 mW), 125 THz from a 2.39 μm color center laser (50 mW) frequency-referenced to CO_2, and 260 THz from a 1.15 μm He-Ne laser (200 mW) referenced to I_2 at 520 THz. Approximately 5×10^{-8} W was generated at 473 THz. Mixing could be verified by blocking any one of the three input beams, which immediately caused the generated 473 THz red light to disappear or by frequency shifting any of the three source lasers which caused a corresponding shift in the synthesized frequency.

The 473 THz radiation from the summing tube was combined on a beamsplitter with 40 μW of radiation from a ^{3}He-^{20}Ne 473 THz laser stabilized on either the g or i hyperfine component of the $^{127}I_2$, 11-5, R(127) transition. From this beat and knowledge of the three infrared laser frequencies, the frequency of the i-component adjusted to the operating conditions recommended by the CCDM was determined to be

$$\nu_{I_2} = 473\ 612\ 214.830\ \text{MHz} \pm 0.070\ \text{MHz}$$

The estimated frequency error represents a line center uncertainty of 1.6 parts in 10^{10}. Again, most of this uncertainty arises from lack of knowledge of the CH_4 standard frequency, with the rest due to uncertainty in the reproducibility of the lock points of both the I_2-stabilized He-Ne laser (1×10^{-10}), and of the I_2-stabilized second harmonic of the 1.15 μm laser. The error budget for the measurement is shown in Table II.

Both visible frequency measurements described above represent an improvement in accuracy by almost 3 orders of magnitude over previous frequency measurements to the visible [9]. However, the

uncertainty reported here does not yet approach the limits of this measurement technique, but is rather limited by the quality of the laser sources [11]. Our measurements were limited mainly by the frequency reproducibility of the lasers. Using the currently proposed redefinition of the meter, either of these lines could serve as a length standard with an improvement of about a factor of 10 compared to the present official length standard based on the ^{86}Kr discharge lamp. However, we have the techniques at this time to improve these or similar measurements by many orders of magnitude.

The speed of visible light

In order to check the accuracy of the value of the speed of light used in the new definition of the meter, a value of c using visible radiation is obtained by multiplying the value of the frequency of the red iodine absorption by the most accurately available wavelength value. The wavelength for this transition is obtained from four published values which are 632 991 399.0 ±0.8 fm [12], 632 991 399.8 ± 0.9 fm [13], 632 991 400.0 ±12. fm [14], and 632 993 398.0 ±3 fm [15]. The weighted average of these measurements is 632 991 399.4 ±0.6 fm. The value for the speed of light is, of course, the product of the frequency and wavelength and is c = 299 792 458.6 ±0.3 m/s, with a one sigma uncertainty.

This value of c, the most accurate ever measured for visible light, is in good agreement with the defined value of c proposed by the CCDM [14] and will, thus, maintain "continuity" in the meter with the new definition.

The MIM Diode

Metal-Insulator-Metal diodes in a point contact configuration, used at room temperature, are the most successful and versatile devices for absolute measurements of laser frequencies from the far infrared to the visible [16]. Field induced electron tunneling is the most widely accepted explanation for their extremely broadband response [17-19]. However, there is also some evidence for more than one phenomenon occurring in the diodes which contribute to the video detection at visible wavelengths [20]. Most experiments and theories have indicated that the contact area should be as small as possible in order to decrease the capacitance and hence minimize the time of response. Consequently, tip radii in the 40-90 nm range have been generally used. This feature seriously affects the mechanical stability of the diodes, sometimes preventing their use as routine laboratory devices. Also, delicate and short lived contacts can make quantitative and systematic investigation of the physical mechanisms involved in detection and harmonic generation difficult.

Encouraged by a chance measurement at infrared frequencies in which video signals were almost unaffected with the use of a dull point, we performed more quantitative tests on the diode. Most of the interest in point contact MIM diodes lies in their high speed of response used in generating laser harmonics. In this experiment, that property was tested by the generation of third harmonic signals. Radiations from a 3.39 μm He-Ne laser at 88 THz and from a $R_I(30)$ CO_2 laser emission at 29 THz were focused on the diode with conical antenna coupling. Microwave power at 48 GHz from a phase-locked klystron also radiated the diode to produce a beat signal of a few tens of megahertz. After amplification in a broadband amplifier, the beat note with a signal-to-noise (S/N) ratio up to 25-30 dB in a

30 kHz bandwidth could be observed on a spectrum analyzer. The power focused on the diode was 30 mW from each of the lasers. The microwave power was in general adjusted to be close to the saturation power for the diode. The S/N ratio of the heterodyne signal was measured as a function of the resistance (adjusted mechanically) for each diode. The video sensitivity at 10 μm, 3.39 μm, and 48 GHz was also recorded. Typically the rectified signals increased almost linearly with the resistance up to about 1 kΩ and then showed some saturation (the signal at 2 kΩ about 50% higher than the one at 1 kΩ). The shape of the video response vs the impedance was the same at 3.39 μm and 10 μm, but with a decrease of about two orders of magnitude in the detected signal strength at the shorter wavelength. With a resistance of 500 Ω, typical dc signals were 20 mV at 10 μm and 200 μV at 3.39 μm. The parabolic mirror used for focusing was machined for operation at wavelengths greater than 10 μm; therefore, a good share of the decrease was probably due to the optics. The measured dc signals were almost the same for all the tip radii between 50 and 760 nm with resistances below 1 kΩ. A small decrease (about 10% of the sensitivity at higher resistance could be observed for the less sharp diodes. The beat S/N ratio was optimum for resistance values between 300 and 500 Ω with a gradual decrease of the signal at increasing resistance and a rapid decrease at lower values. Typical results are shown in Fig. 4. Diodes with four significantly different tip radii were used. No significant decreases in the S/N were observed from "sharp" to "dull" points. This is very surprising for the capacitance should be determined by the area of the contact, i.e., the square of the tip radius. For a radius of some tens of nanometers, a frequency cut-off can be calculated of the order of 100 THz, and a radius of a few hundred nanometers should lead to a frequency cut-off two orders of magnitude lower. This is in complete disagreement with our experimental results. The "spreading resistance" in the base, proportional to the inverse of the contact radius, increases the RC time of response proportional to the radius [21], but it, by itself, does not explain the high speed operation of these blunter diodes. Our measurements were performed to help understand the operation of the diode; however, they seem to have had the opposite effect. For instance, the "effective contact area" may not simply be determined by the square of the radius of the tip. It is, moreover, not clear how the dielectric constant of the oxide in the contact changes and affects the capacitance under the high mechanical and thermal stresses present when the contact is made.

These results, besides stimulating questions about the theory of operation of the diode, have pointed out a practical design improvement. In particular, with the use of less sharp tip radii, the stability of the diode has been dramatically increased without a significant decrease in the sensitivity or speed of response. The same contact can be stable for hours to days in normal laboratory environmental conditions without readjustment. Also, the diode resistance can be more precisely adjusted and reset with a resolution of a few tens of ohms. This is particularly important for the maximization of the beat S/N ratio in harmonic generation and mixing experiments. This experimental result opens a new theoretical puzzle and new possibilities for practical applications of the point contact MIM diodes. For instance, in the far infrared, the sensitivity is comparable to that of a Golay cell, but the speed of response is twelve orders of magnitude faster!

Conclusion

The application of OFS techniques to the measurement of the super narrow resonances from cooled atoms and ions will introduce a new era in spectroscopy. Optical frequency synthesis spectroscopy has

already improved the accuracy of the spectral measurements of conventional spectra by two orders of magnitude compared with the use of wavelength techniques and promises further increases in accuracy. One possible application of the OFS technique could be the measurement of the Rydberg, which should be the first in a series of measurements promising unprecedented accuracy in our measurements of the fundamental constants. In this new era, measurements will be limited by ones ability to characterize the spectral features rather than the measurement techniques!

References

1. A frequency synthesizer in the radio or microwave region of the spectrum has phase coherence between the synthesized frequency and a reference or standard. Optical frequency synthesis implies phase coherence in a given mixing step but not necessarily between steps, i.e., there is not necessarily phase coherence between the optical frequency and the reference frequency.
2. K. M. Evenson, J. S. Wells, F. R. Petersen, B. L. Danielson, G. W. Day, R. L. Barger, and J. L. Hall, Phys. Rev. Lett. 29, 1346 (1972).
3. Comite Consultatif pour la Definition Du Metre, 7th Session, June 2-5, 1982 (Paris).
4. C. R. Pollock, D. A. Jennings, F. R. Petersen, J. S. Wells, R. E. Drullinger, E. C. Beaty, and K. M. Evenson, Opt. Lett. 8, 133 (1983).
5. D. A. Jennings, C. R. Pollock, F. R. Petersen, R. E. Drullinger, K. M. Evenson, J. S. Wells, J. L. Hall, and H. P. Layer, Opt. Lett. 8, 136 (1983).
6. H.P. Layer, IEEE Trans. on Inst. and Meas., Vol, IM-29, No. 4 (1980).
7. F.R. Petersen, (private communication)
8. I. Schneider and C.L. Marquardt, Opt. Lett. 5, pp. 214-15 (1980).
9. K.M. Baird, K.M. Evenson, G.R. Hanes, D.A. Jennings, and F.R. Petersen, Opt. Lett. 4, pp. 263-4 (1979).
10. V.M. Klementyev, Yu. A. Matyugin, V.P. Chebotayev, ZhETF Pisma 24, 8 (1976).
11. See reference 7, and H. P. Layer, W. R. C. Rowley, and B. R. Marx, Opt. Lett. 6, pp. 188 (1981).
12. W. R. C. Rowley and A. J. Wallard, J. Phys. E6, 647 (1973).
13. W. G. Schweitzer, Jr., E. G. Kessler, R. D. Deslattes, H. P. Layer, and J. R. Whetstone, Appl. Opt. 12, 2829 (1973).
14. Rapport: Comité Consultatif pour la Définition du Mètre, 5th Session, page M54 (1973) Bureau International des Poids et Measures, Sévres, France.
15. G. R. Hanes, K. M. Baird, and J. DeRemigis, Appl. Opt. 12, 1600 (1973).
16. K. M. Evenson, D. A. Jennings, and F. R. Petersen, J. Phys. (Paris) 42, C8-473 (1981).
17. S. M. Faris, T. K. Gustafson, and J. C. Wiesner, IEEE J. Quantum Electron. QE-9 737 (1973).
18. G. M. Elchinger, A. Sanchez, C. F. Davis, Jr., and A. Javan, J. Appl. Phys. 47, 591 (1976).
19. A. Sanchez, C. F. Davis, K. C. Liu, and A. Javan, J. Appl. Phys. 49, 5270 (1978).
20. H. U. Daniel, M. Steiner, and H. Walther, Appl. Phys. 25, 7 (1981).
21. D. J. E. Knight and P. T. Woods, J. Phys. E. Scient. Instr. 9, 898 (1976).

Table I. Error Budget for the 520 THz Visible Frequency Measurement

Component	Error
1. CO_2 laser uncertainty (3.4 kHz times effectively 20 harmonics)*	68 kHz
2. Electronic resettability of entire I_2 servo system	40 kHz
3. Uncertainty in first derivative offsets and pressure shifts	15 kHz
4. Statistical fluctuation in data	14 kHz
Total Uncertainty (summed Quadratically)	81 kHz

* This 3.4 kHz is due to an estimated 1×10^{-10} uncertainty in the CH_4-stabilized He-Ne frequency added in quadrature to the measurement uncertainties in the determination of the $P_I(50)$ frequency. (ref. 7)

Table II. Error Budget for the 473 THz Visible Frequency Measurement

Laser	Frequency in MHz	Measurement Uncertainty in kHz (independent of CH_4 uncertainty)	Correlated Uncertainty (due to CH_4 in kHz)
CH_4 88 THz	88 376 181.609	-	9
Color Center 125 THz	125 132 754.610	11	12
I_2/2 260 THz	260 103 404.273	25	30
		$\overline{27}.4$	$\overline{51}$
$^{127}I_2$ 11-5 R(127)g	473 612 340.492	47	
$^{127}I_2$ 11-5 R(127)i	473 612 214.789[a]	47	

Total Uncertainty $[(27.4)^2 + (51)^2 + (47)^2]^{\frac{1}{2}} = 74$ kHz

[a] The Comité Consultatif pour la Définition du Mètre [3] has recommended that the following conditions be realized when the $^{127}I_2$ molecule, transition 11-5, R(127), component i is used for intracavity stabilization of the 473-THz He-Ne laser: (1) I_2 cold-finger temperature of 15°C, (2) cavity standing-wave power of 40 mW, and (3) modulation peak-to-peak amplitude of 6 MHz. Therefore, the $^{127}I_2$ 11-5 R(127)i frequency adjusted for the recommended operating conditions is 473 612 214.830 ±0.074 MHz [5].

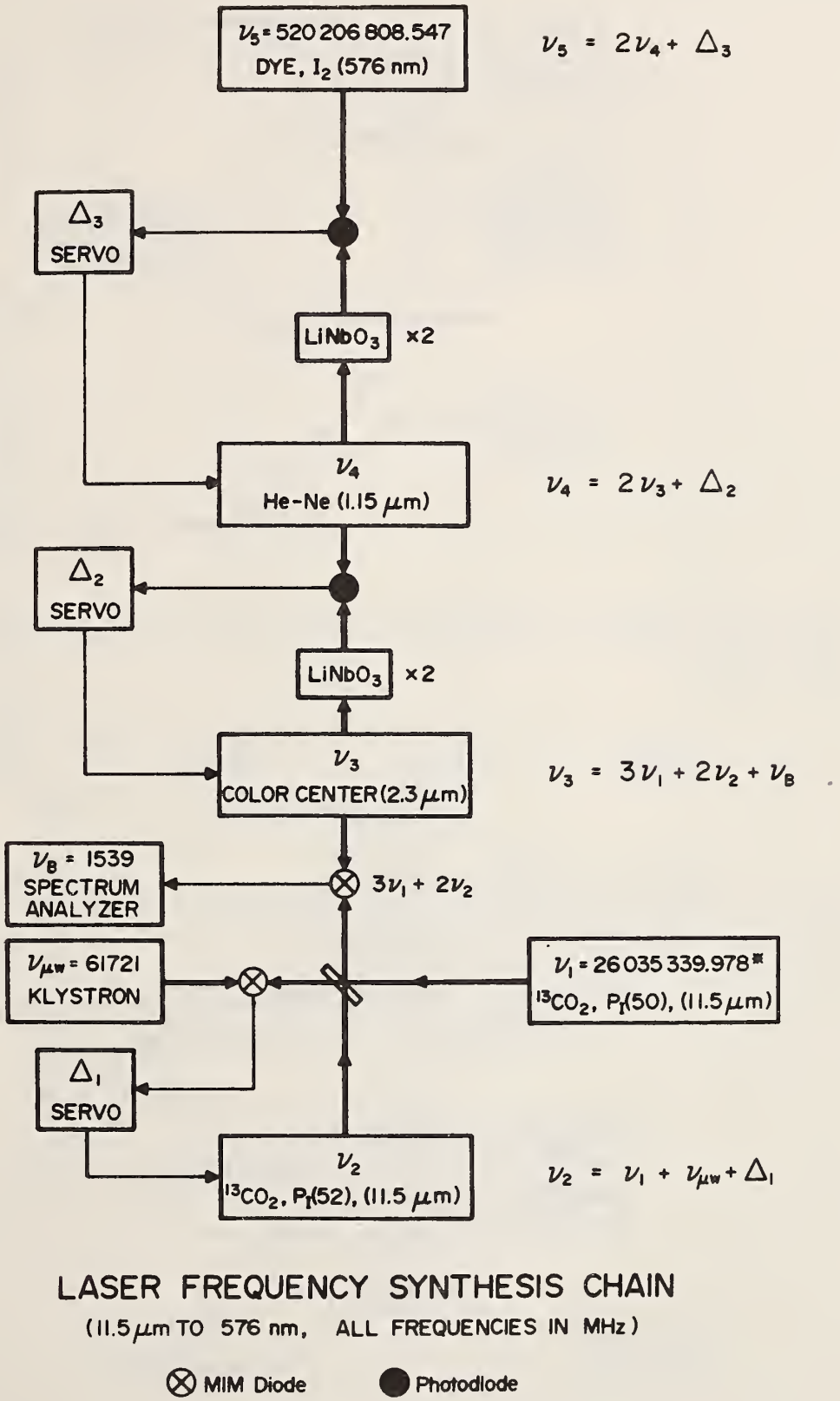

Fig. 1. The OFS chain for generating 520 THz radiation

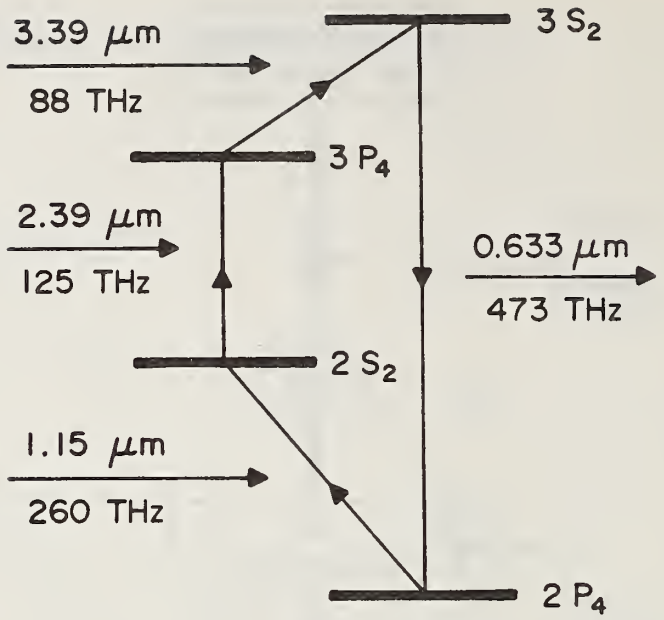

Fig. 2. Energy level diagram of Ne showing the pertinent cascade transitions used to synthesize 473 THz radiation.

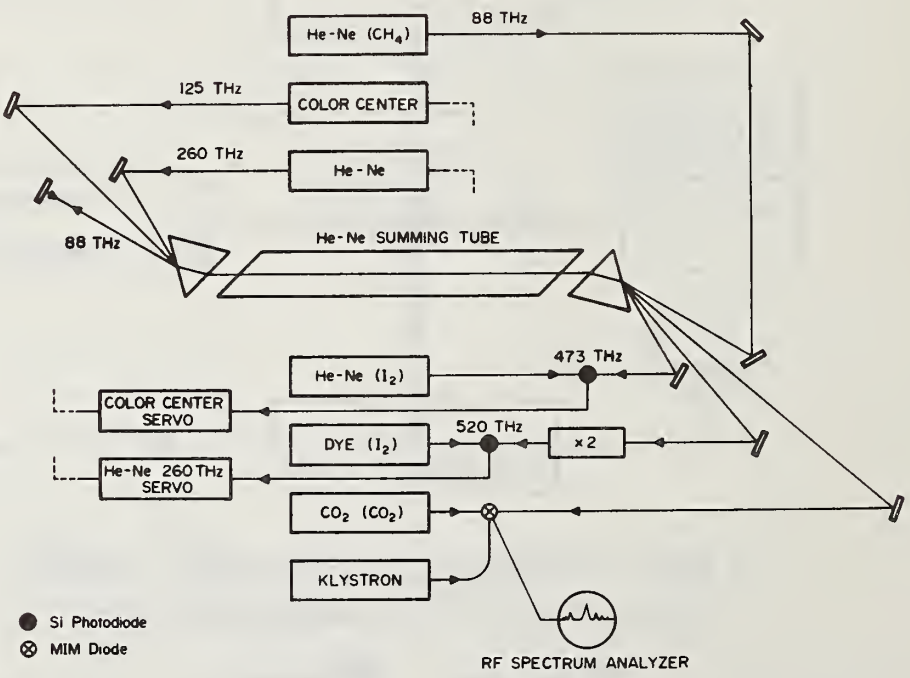

Fig. 3. Experimental apparatus for measuring the 473 THz laser frequency.

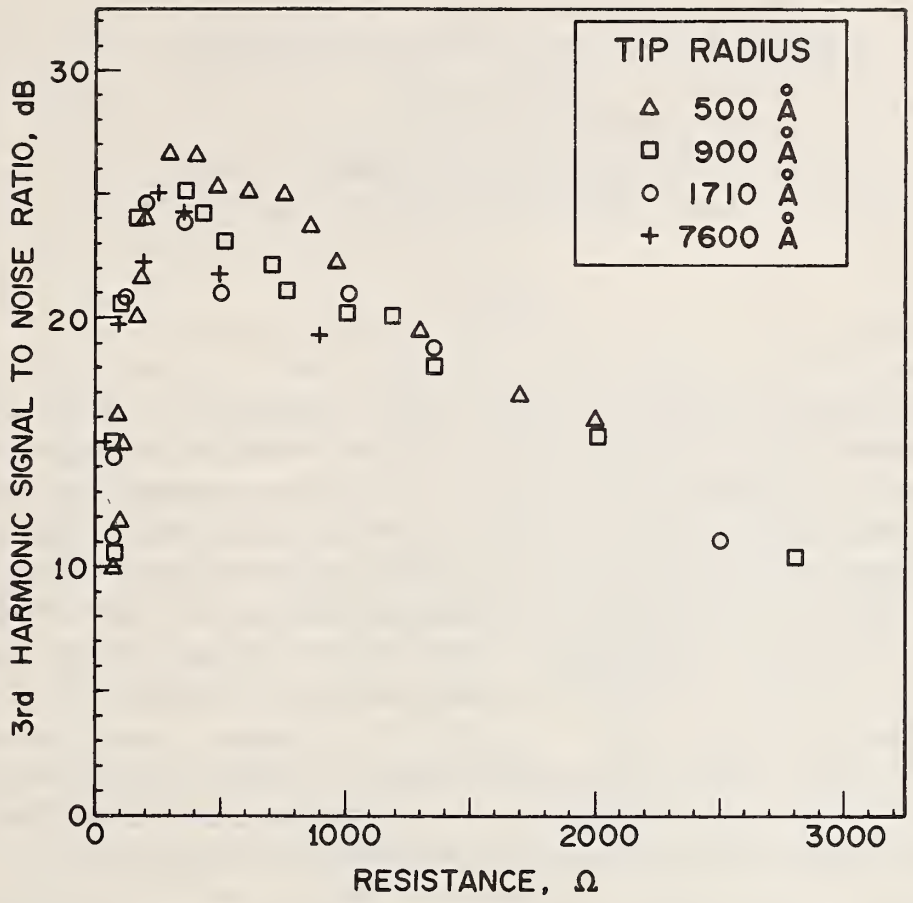

Fig. 4. Signal-to-noise ratios in a 30 kHz bandwidth for the observed beat signals in the third harmonic experiment as a function of the diode resistance. The beat was generated by the synthesis scheme $\nu_B = \nu_{3.39\ \mu m} - 3\nu_{R_I(30)} - 48.7$ GHz. Results for diodes with different tip radii of curvature are reported.

Laser-Cooled and Trapped Atoms, (Proceedings of the Workshop on Spectroscopic Applications of Slow Atomic Beams, held at NBS, Gaithersburg, MD, 14-15 April 1983) Ed. by W. D. Phillips, Natl. Bur. Stand. (U.S.) Spec. Publ. 653 (1983).

Limitations of Atomic Beam Frequency Standards

Lindon Lewis
Time and Frequency Division
National Bureau of Standards
Boulder, Colorado 80303

ABSTRACT

Atomic beam frequency standards may be placed into two categories: field standards and laboratory standards. While this distinction is somewhat artificial, because the two types of standards are interdependent, each category does have different requirements of accuracy, size, and cost. Despite this separation, generally the developments which produce the best laboratory standards eventually give rise to improved field standards. Existing field standards are limited in long term fractional frequency stability to $\sigma_y(\tau) \sim 3 \times 10^{-13}$, for $\tau \sim 6$ months. A laboratory standard such as NBS-6, the U. S. primary cesium standard, is limited in inaccuracy to $\Delta y \sim 8 \times 10^{-14}$. Proposed new cesium field standards are expected to yield long term stabilities of $\sigma_y(\tau) \sim 1 \times 10^{-14}$ ($\tau = 6$ months). Stored ion standards, prime candidates for new laboratory frequency standards, are expected to have better than $\Delta y = 1 \times 10^{-15}$ inaccuracy. As other approaches to atomic beam frequency standards are considered, they should attempt to compete favorably with these emerging technologies.

Key Words: atomic beams, atomic frequency standard, cooled atoms, optical pumping.

General Characteristics of Atomic Beam Standards

Atomic frequency standards may be divided into two categories--field standards and laboratory standards. The distinction is useful because the most highly desired characteristics in each category often preclude the realization of the properties most sought after in the other category. For example, a field standard must be durable, portable, reliable, and easily operated, with unsupervised operating periods of months to years. A laboratory standard, on the other hand, must attain the highest possible accuracy, even if the device requires considerable space, power, money, and the patience of five Ph.D. physicists. In discussing the limitations of existing standards, or in projecting the usefulness of proposed new standards,it is helpful to keep in mind the category of interest, as the criteria vary with application. At the same time, it is important to realize that this distinction is somewhat artificial, as field standards have historically descended from the laboratory standards. Generally, the knowledge and technologies which have been developed in order to adequately describe the frequency offsets and uncertainties in high accuracy laboratory standards have been sucessfully applied to the development of field standards. A good example of this relationship between research and application is the production of the commercial cesium beam standard, which followed the creation of the laboratory cesium standard. Because of this widespread use of cesium beams, this paper will discuss the limitations of atomic beam frequency standards in terms of the

cesium microwave resonance, although most of the comments may be applied to other devices as well.

All commercially available atomic beam frequency standards today use the 9.19263177 GHz hyperfine splitting of ground state Cs^{133} measured by the separated cavity Ramsey technique [1]. In addition, most national time metrology laboratories realize the definition of the second using a laboratory version of this same device. However, the reasons that the cesium microwave resonances has become the most popular timekeeping transition are partly technical [the atom is easily detected using an ionizing hot wire], and partly historical [once the second was defined in terms of the cesium HFS, other methods received less attention].

The main advantage of atomic beam standards over other types of atomic standards, such as rubidium cells and hydrogen masers, is that perturbations of the atoms are reduced by using only atoms which travel relatively freely through a vacuum chamber. In the rubidium and hydrogen standards, buffer gases and coated walls interact with the atoms to produce frequency shifts. These shifts cannot in general be calculated, and must instead be measured, which places limitations upon the accuracy and long term stability of the devices. On the other hand, confining the atoms with buffer gases or walls increases the interaction time of the atoms with the resonant microwave energy, producing narrower linewidths. In general, narrower linewidths result in some smaller systematic effects and better short term stability of the clock. The interaction time in an atomic beam, however, can only be increased either by lengthening the standard, or by reducing the atomic velocity.

All atomic beam frequency standards have the same generic features. There is a source of atoms, usually a multichannel collimator in the case of cesium clocks. The atoms are then prepared in a special energy state, generally by deflection in a strong inhomogeneous magnetic field. After state selection, the atoms pass through an interaction region which produces the clock transition, such as a Ramsey type of microwave cavity. The interaction time in this region determines the resonance linewidth. Finally, atoms which have made the clock transition are detected in a third region, traditionally another set of magnets which deflect atoms into a hot wire detector.

Table I summarizes several of the characteristics of such traditional cesium standards, both for commercially produced field standards, and for one laboratory cesium standard, NBS-6.

1982 Evaluation of NBS-6

Limitations to the stability and accuracy of both field and laboratory cesium standards can be described by referring to the results of the accuracy evaluation of NBS-6 completed in April 1982. A summary of this evaluation is given in Table II. Detailed discussions of the systematics in NBS-6 are given in references 2 and 3.

While several of the uncertainties given in this table appear at the 1 to 3 x 10^{-14} level, this is partly due to the fact that not much effort has been spent trying to reduce these uncertainties, due to the dominance of the cavity phase shift uncertainty ($\Delta y \sim 8 \times 10^{-14}$). The latter systematic is usually separated into two parts [4] an end-to-end microwave cavity phase shift, and a distributed cavity phase shift. In a primary standard, such as NBS-6, the frequency shift due to the former effect is cancelled to considerable accuracy (depending upon the clock stability and reproducibility

of velocity distributions) by reversal of the atomic beam direction. Roughly speaking, the average of the clock frequencies for the two directions is the correct value. This frequency offset is about 3.6×10^{-13} in NBS-6. To the degree that the atomic beam path is retraced upon beam reversal, the frequency shift due to distributed cavity phase shift (a consequence of residual 1st order Doppler) is also cancelled. In NBS-6, the size of this effect is about 1×10^{-13}/mm of spatial offset of the atomic beam [2]. Fractional frequency offsets Δy_ϕ due to microwave cavity phase shift $\Delta\phi$ are given by

$$\Delta y_\phi = \frac{\Delta\phi/2\pi}{(L/V_p)}\,\nu_o\,, \qquad (1)$$

where L is the interaction length, V_p is the effective atomic beam velocity, and ν_o is the resonance frequency. This expression shows explicitly that the effect of cavity phase shift can be reduced by increasing the interrogation time $\tau = (L/V_p)$.

If cavity phase shifts in commercial standards are comparable in size to those in NBS-6, then the expected frequency shifts due to distributed cavity phase shifts should be

$$\Delta y_\phi \sim \frac{Q(\text{laboratory std})}{Q(\text{field std})} \times 10^{-13} = 3 \times 10^{-12}.$$

This would suggest that cavity phase shifts may be a limiting systematic in field standards as well as in laboratory cesium standards.

Of the remaining systematics, those of most concern for improving standards' performance are second order Doppler and the various electronics servo limitations. For an atomic beam of effective velocity V_d, the clock fractional frequency is shifted by an amount

$$\Delta y_d = -\tfrac{1}{2}\,\frac{V_d^2}{c^2} \qquad (2)$$

Evaluation of this systematic requires knowledge of the atomic beam velocity distribution, as seen by the complete microwave resonance spectrometer. In the past this distribution has been determined by using pulsed interrogation techniques [5] and by unfolding the microwave spectrum at different microwave power levels [6]. While the uncertainty in this shift is quoted at the 1×10^{-14} level, it is anticipated that an order of magnitude reduction of the uncertainty may be had with exercise of considerable care in the measurement. This process is greatly helped if a narrower velocity distribution is used in the atomic beam.

The evaluation of NBS-6 requires that the electronic servo find the center of the microwave resonance to better than about one part in 10^5. Implicit is the assumption that the physical resonance itself is symmetric to this level. This assumption is supported by the fact that no significant frequency shift is observed when the amplitude of microwave phase modulation is changed. Further checks on frequency shifts due to imperfect electronics include measurement of integrator input offsets and frequency shifts with microwave power change. Again, the demands placed upon the servo are reduced with increase in microwave interaction time, since a narrower microwave resonance need not be split as finely.

One Approach to Improved Field Standards

One approach to considerably improved long term stability in field usable frequency standards involves the use of laser optical pumping in an "introspective" cesium beam standard. In an optically pumped cesium standard [7,8,9] the state selection region consists of an optical interaction region where atoms are converted into the desired energy level instead of rejected by inhomogeneous magnets. The laser pumping may be performed with either one or two lasers. In the first case, A laser beam tuned to the $^2S_{1/2}$, F=4 $\leftrightarrow$ $^2P_{3/2}$, F'=3 transition, (Figure I) crosses the upstream atomic beam. This laser pumps atoms into the F=3 ground state. In order to detect atoms in the F=4 ground state, a second laser is tuned downstream to the $^2S_{1/2}$, F=4 $\leftrightarrow$ $^2P_{3/2}$, F'=5 transition, which can produce many fluorescence photons for each atom in the F=4 ground state. With complete pumping upstream, no signal is observed in the detection region. As the microwave signal is tuned through the ground state HFS resonances, however, downstream fluorescence is increased, as shown in Figure II. (The apparent asymmetry between the (4,-1) $\leftrightarrow$ (3,-1) and (4,1) $\leftrightarrow$ (3,1) transitions in this curve is due to a synthesizer malfunction, and is not a true asymmetry). A preliminary version of such a standard is under construction now at NBS/Boulder. It is expected to have short term stability comparable to or better than that of conventional commerical cesium standards; laser diodes are used as the light sources [10].

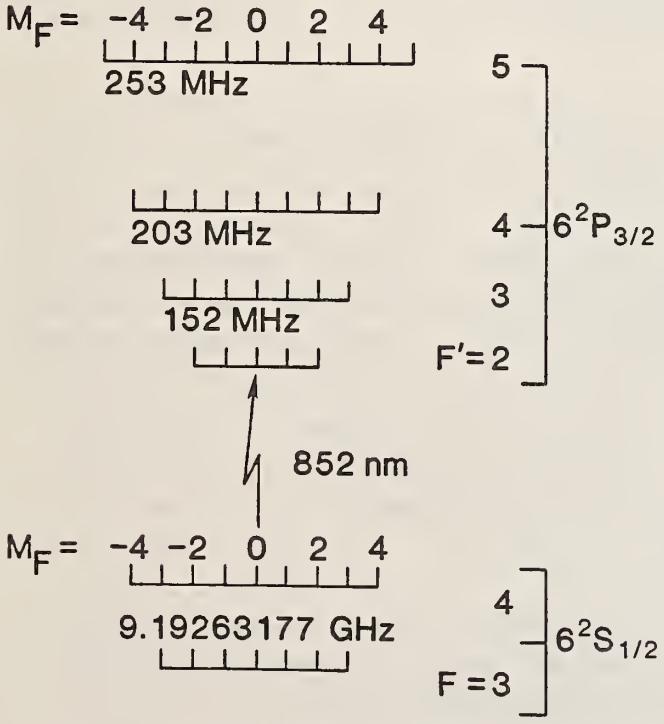

Figure I. Level diagram for Cs^{133}, showing hyperfine structure frequencies (not to scale).

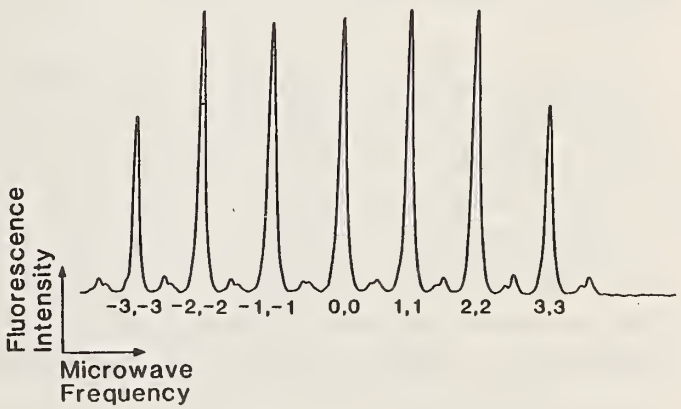

Figure II. One-laser optical pumping F=4 $\leftrightarrow$ F'=4, σ-polarization pump laser, and a F=4 $\leftrightarrow$ F'=5 detection laser.

A further refinement of this method is to use two lasers for optical pumping [11]. One laser may be tuned to the $^2S_{1/2}$, F=3 $\leftrightarrow$ $^2F_{3/2}$, F'=3 transition using π polarization. This pumps all magnetic midlevels of the F=3 ground state HFS into the F=4 HFS, with the exception of the m=0 sublevel. The second laser, tuned to the $^2S_{1/2}$, F=4 $\leftrightarrow$ $^2P_{3/2}$, F'=3 transition pumps atoms back to the F=3 HFS. After many cycles of this process, most atoms should reside in the F=3, m=0 sublevel. An example of this process is given in Figure III, where the pumping into m=0 is incomplete because of an insufficient number of pumping cycles. Further work on this technique is in progress.

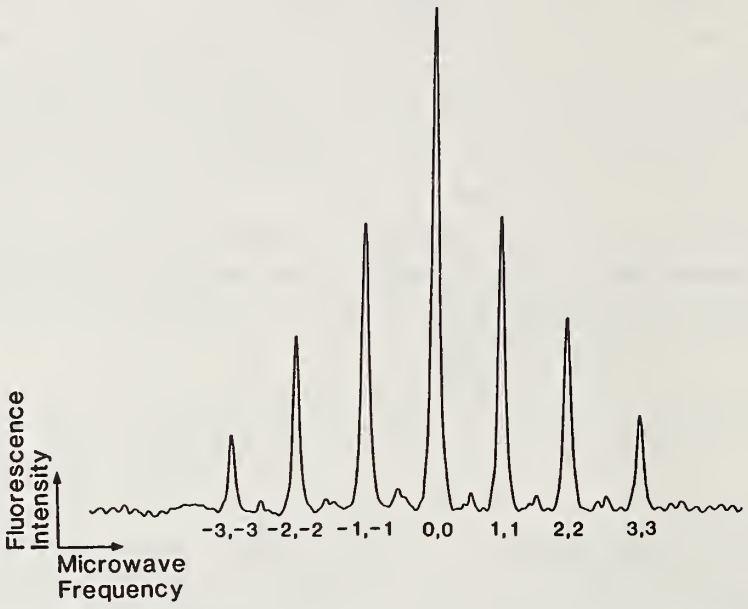

Figure III. Two-laser optical pumping, using both F=4 $\leftrightarrow$ F'=4, σ-polarization and F=3 $\leftrightarrow$ F'=3, π-polarization pump lasers, and a F=4 $\leftrightarrow$ F'=5 detection laser.

Optical pumping is expected to improve the performance of field standards by both reducing the size of systematics and by allowing more precise evaluation of their uncertainties. Since nearly all atoms are selected and detected, regardless of their spatial position or velocity, the effect of the distributed cavity place shift is simplified. A smaller cesium beam diameter is possible, resulting in a smaller microwave cavity window, which should give a smaller frequency offset [4]. In addition, since atoms which have been pumped into the F=3 HFS are invisible to the F=4 $\rightarrow$ F'=5 detection laser, it may be possible to operate simultaneously counterpropagating cesium beams, which would permit the evaluation of the cavity phase shift in a field standard.

Other benefits of optical pumping and fluorescence detection in a field standard include increased S/N, more symmetric microwave spectra (of the Zeeman split lines), and reduced liklihood of Majorana transitions, which may produce fairly substantial frequency shifts [12,13].

Further improvement in the performance of the proposed standard comes from use of on-board systematics evaluation. This "introspective" approach involves the measurement of sytematic effects by monitoring the atoms themselves. For example, the Zeeman splitting can be measured to give a value of the magnetic field which will shift the clock resonance a known amount. Other systematics to be measured in similar ways include second order Doppler and microwave power dependence.

It is expected that a thorough development of these principles will result in a cesium field standard with long term (six months) stability of 1×10^{-14}. Such a standard would find application in precision navigation and in highly secure communications sytems [14].

An Approach to Improved Laboratory Standards

Many of the systematics discussed above are reduced as the interaction time is increased. One approach to achieving longer interaction times is the use of stored ions [15]. Stored ions have allowed observation times of tens of seconds, with measured microwave Q's of more than 2×10^{11} [16], and projected microwave Q's of 3×10^{12}. These long observation times are obtained without the perturbations experienced in other confinement methods, such as buffer gases and coated walls. The systematic uncertainties are generally less than 1×10^{-15}. This suggests that a new type of primary standard with inaccuracy less than 1×10^{-15} may be constructed using stored ions.

Cooled Atomic Beams

The preceding description of existing and projected frequency standards may be used as a framework for discussion of the possible application of cooled beams to atomic frequency standards. In particular, the expected performance of new cesium beam and stored ions frequency standards places a lower limit on performance goals of any new technology, including cooled beams. In addition, many of the systematics discussed earlier will also be present in a cooled beam clock, as well as new sources of frequency offset.

While reduction of atomic beam velocity can increase the microwave Q in a cooled beam device, resulting in a reduction of certain systematics, larger Q in itself will not result in a more accurate frequency standard. The standard must be treated as a system, with a complete treatment of the interrelating parts in order to obtain an estimate of the system performance. For the purposes of this discussion, an abbreviated list of considerations will be given. Although the list is necessarily incomplete, it should serve as an example of the type of problems which must be solved if cooled neutral atoms are to be useful in frequency standards.

1. System goals. Inaccuracy of less than 1×10^{-15}, for a primary standard type of laboratory standard.
   Long term stability of $\sigma_y < 1 \times 10^{-14}$, for a field usable clock.
2. Lower atomic velocities. Considerable cooling of a sodium beam has been reported [17], with mean velocity of about 40 m/s and a velocity spread of about 10 m/s (down from a mean velocity of 1000 m/s), but this absolute value is not very different than that obtained in more traditional cesium beam standards. Becker [18] has reported a mean velocity of 93 m/s and a velocity width of 7 m/s for CS-1, the PTB primary cesium standard, which uses magnetic state selection, and no laser cooling. While this is not seen as a fundamental difficulty, very low atomic velocities have not yet been observed in a cooled beam.
3. Beam flux. As the technology is improved, and lower velocities are achieved, it is important that the reduction in atomic velocity is not achieved at an unacceptable cost in beam flux. The short term stability [19] of a clock is generally given by

$$\sigma_y(\tau) = K[Q(S/N)^{\frac{1}{2}}]^{-1}\tau^{-\frac{1}{2}} \qquad (3)$$

where S/N is the power signal-to-noise in a one hertz bandwidth, and K is a constant which depends upon the resonance lineshape. Generally, K lies between 0.1 and 1.0. For traditional cesium standards, $K \sim 0.2$. The quantity S/N is generally limited by the "shot noise" on the number of atoms in the atomic beam, which decreases relative to the signal as the beam flux is increased. The short term stability should be sufficient to permit measurement of clock performance within a reasonable period of time. In a field standard, this means $\sigma_y(\tau) < 1 \times 10^{-11}\tau^{-\frac{1}{2}}$. In a primary standard, $\sigma_y(\tau) < 1 \times 10^{-12}\tau^{-\frac{1}{2}}$.

4. Transverse heating. As an atomic beam is cooled, increased energy is associated with the atoms' transverse motion, resulting in a spreading of the beam. This effect might be reduced with the use of additional lasers or some other cooling mechanism. However, whatever method is chosen to prevent loss of beam flux through transverse heating, it must not introduce additional systematics, such as frequency shifts associated with the microwave cavity.
5. Cavity phase shift. In itself, this frequency shift is expected to be reduced in a slow atomic clock. (See Eq. 1). However, slow atoms are perturbed for a longer time by gravity and acceleration, resulting in larger deflection angles of the atomic beam. This can produce larger clock frequency shifts associated with the distributed cavity phase shift as discussed above.
6. Gravity. As longer and longer observation times are employed with free neutral atoms, gravity plays a more and more important role. Some effects are interactive, such as the cavity phase shift mentioned above. A more direct consequence is size and geometry, as a clock which uses very slow atoms must accomodate the falling atoms.
7. Light shifts. The use of lasers to perform the cooling of the atoms, and the concommitant fluorescence light can introduce substantial light shifts [20]. Methods would need to be developed to greatly reduce or eliminate this effect on the standard's performance.

References

[1] N. F. Ramsey, "Molecular Beams" (Oxford Univ. Press, 1956).

[2] D. J. Wineland et al., IEEEE Trans Instr. Meas. IM-25 (1976) 453.

[3] L. L. Lewis, F. L. Walls, and D. J. Glaze, J. de Phys (Paris) 42 (1981) C8-241.

[4] R. F. Lacey, 22nd Ann SFC (1968) 545.

[5] D. A. Howe, 30th Ann. SFC (1976) 451, H. Hellwig et al., Proc. 27th Ann. SFC (1973) 357.

[6] S. Jarvis, Jr., Metrologia 10 (1974) 87.

[7] L. L. Lewis, M. Feldman, and J. C. Bergquist, J. de Phys (Paris) 42 (1981) C8-271.

[8] G. Singh, P. DiLavore, and C. O. Alley, IEEE J. Quan. Elect. QE-7 (1971) 196.

[9] M. Arditi and J. L. Picqúe, J. Phys (Paris) 41 (1980) L-379.

[10] L. L. Lewis and M. Feldman, 35th Ann SFC (1981) 612.

[11] L. Cutler, private communication (1979).

[12] G. Becker, IEEE Trans. Instr. Meas. IM-27 (1978) 319.

[13] H. Hellwig, Proc. 5th Conf. on Atomic Measses and Fund. Constants, ed. by J. Sanders and A. Wapstra, Plenum Press (1976) 330, D. W. Allan et al., Proc. 31st SFC (1977) 555.

[14] S. R. Stein, paper included in this proceedings.

[15] D. J. Wineland, paper included in this proceedings.

[16] R. Blatt, H. Schnatz, and G. Werth, Phys. Rev. Lett. 48 (1982) 1601.

[17] J. V. Prodan, W. D. Phillips, and H. Metcalf, Phys. Rev. Lett. 49 (1982) 1149.

[18] G. Becker, Proc. of the 11th Ann PTTI (1979) 113.

[19] J. Vanier and L.-G. Bernier, IEEE Trans. Inst. and Meas. IM-30 (1981) 277.
[20] A. Brillet, Metrologia 17 (1981) 147.

Table I. Characteristics of Cesium Atomic Beam Frequency Standards

	Commercial Stds	NBS-6
Short term Stability	$1.5\times10^{-11}\ \tau^{-\frac{1}{2}}$	$5\times10^{-13}\ \tau^{-\frac{1}{2}}$
Long term Stability	3×10^{-13} (6 months) 3×10^{-12} (5 years)	1×10^{-14} (1 week)
Accuracy	7×10^{-12}	8×10^{-14}
Volume	$\sim .03\ m^3$	$\sim 5\ m^3$
Interaction Length	7.5 cm	375 cm
Microwave Q	1×10^{7}	2.8×10^{8}
Mean atomic velocity	100 m/s	190 m/s

Table II. NBS-6 Evaluation, April 1982.

Systematic	Value ($\times 10^{14}$)	Uncertainty ($\times 10^{14}$)
C-field	5335	3
Mag. field Inhomo.		0.2
Majorana		0.3
tail pulling		2
cavity pulling		0.1
RF spectrum		1.0
2nd order doppler	26	1.0
cavity phase shift	36	8.0
amplifier offset		1.0
2nd harmonic distortion		2.0
uncertainty in ϕ_C due to $\delta[\rho(v)]$		1.0
blackbody shift	1.7	0.0
		RSS 9.2
		random 1.0
		total (RSS) 9.3

Laser-Cooled and Trapped Atoms, (Proceedings of the Workshop on Spectroscopic Applications of Slow Atomic Beams, held at NBS, Gaithersburg, MD, 14-15 April 1983) Ed. by W. D. Phillips, Natl. Bur. Stand. (U. S.) Spec. Publ. 653 (1983).

Stabilization of a Microwave Oscillator Using a Resonance Raman Transition in a Sodium Beam

P.R. Hemmer and S. Ezekiel
Research Laboratory of Electronics
Massachusetts Institute of Technology, Cambridge, MA 02139

and C.C. Leiby, Jr.
Rome Air Development Center
Hansom Air Force Base, MA 02139

Preliminary results of stabilization of a 1772 MHz oscillator to a resonance Raman transition in an atomic beam of sodium are presented. Short term stability of 5.6×10^{-11} (τ = 100s) for a 15 cm interaction region separation has been achieved. Sources of frequency drift are briefly discussed.

Earlier experimental work [1] has shown that extremely narrow optical features can be obtained using a stimulated resonance Raman transition between two long-lived hyperfine ground sublevels in a sodium atomic beam. Such studies are of interest because they have possible applications both in spectroscopy and in the development of new time and frequency standards, especially in the microwave to millimeter regions of the spectrum. In this paper we present preliminary results of attempts to stabilize the frequency of a microwave oscillator using these narrow optical features.

Figure 1(a) shows schematically a stimulated resonance Raman transition between two long-lived states, 1 and 3, induced by two laser fields ω_1 and ω_2. In a well collimated atomic beam, the Raman transition linewidth for weak copropagating laser fields is determined by the decay rates of states 1 and 3, with a negligible contribution from state 2, i.e., the linewidth is set by the transit time, since states 1 and 3 are long lived[2]. To obtain a small transit time linewidth we use separated oscillatory field excitation [3,1] as illustrated in Figure 1(b), where L is the separation between the interaction regions. In the present experiment, states 1 and 3 correspond to the F = 1, m_F = 0 and F = 2, m_F = 0 hyperfine sublevels of the sodium $3\ ^2S_{1/2}$ ground state, separated by 1772 MHZ, and state 2 is the $3\ ^2P_{1/2}$ (F = 2, m_F = +1) excited state, having a 16 nsec. lifetime.

The laser field at frequency ω_1 is obtained from a single mode dye laser which is locked to the $1 \leftrightarrow 2$ transition. The laser field at frequency ω_2 is generated from that at ω_1 by an acoustooptic frequency shifter [1] driven with a microwave oscillator near 1772 MHZ. This greatly reduces the effects of laser jitter by correlating the jitters in the two laser frequencies so as to obtain a stable difference frequency $\omega_1 - \omega_2$.

Figure 2(a) shows a typical fringe lineshape corresponding to an interaction region separation of L = 15 cm. To obtain this trace the dc fluorescence collected from the second interaction region is monitored with a photomultiplier while the difference frequency $\omega_1 - \omega_2$ is scanned over the Raman transition.

To stabilize the frequency of the microwave oscillator to the central fringe in Figure 2(a) a discriminant is needed. This discriminant, which is shown in Figure 2(b), is obtained by frequency modulating the microwave source and demodulating the second region fluorescence signal with a lock-in amplifier. The output of the lock-in amplifier is then used in a feedback loop to hold the microwave oscillator frequency at the central zero of the discriminant [4]. The stability of this oscillator is then measured by comparing it with a commercial cesium clock.

Figure 3 shows a plot of the measured fractional frequency deviation of the microwave oscillator $\sigma_y(\tau)$, as a function of averaging time, τ. For τ = 100 seconds, the stability is 5.6×10^{-11}. The predicted [5] fractional frequency deviation, based on shot noise, appears as the dashed line superimposed on the data in Figure 3. As can be seen, the data is shot noise limited up to about τ = 500 seconds.

For τ greater than 500 seconds, the fractional frequency deviation no longer decreases with $\tau^{-1/2}$, indicating the presence of long term frequency drifts. Work is presently being performed to identify and study in detail the important sources of frequency error. These include:

(a) The relative misalignment of the laser beam at ω_1 and ω_2 away from copropagating.

(b) Phase shifts due to relative path length differences measured from the beam splitter in Figure 1(b) to each of the two interaction regions.

(c) Phase shifts which arise when the polarizations of the laser beams at ω_1 and ω_2 differ and there are birefringence optics present.

(d) Detunings of the pump laser, at ω_1, away from resonance with the $1 \leftrightarrow 2$ transition

(e) Laser intensity variations

(f) Optically induced atomic recoil

(g) Fluorescence from the interaction regions that propagates along the atomic beam [6].

(h) Effects of the sodium $3\ ^2P_{1/2}$ (F = 1) state which is 189 MHz below the $3\ ^2P_{1/2}$ (F = 2) state.

(i) Laser and atomic beam misalignments

(j) External magnetic fields

(k) Second order Doppler

We have already incorporated in our setup means for minimizing some of the effects mentioned above in order to obtain the data in Figure 3. A detailed discussion of error sources for the stimulated resonance Raman scheme will be the subject of a future publication [4].

Although the preliminary results presented here are for a sodium atomic beam, the techniques discussed are readily applicable to cesium. In fact, if cesium were substituted for sodium in our apparatus and everything else being equal, we would expect an improvement in stability by a factor of 16, i.e., $\sigma_y(\tau) = 3.5 \times 10^{-12}$ for $\tau = 100$ sec. This increase takes into consideration the larger hyperfine transition frequency of cesium, the greater atomic mass of cesium and the lower oven temperature needed to obtain the same atomic flux used in our present sodium apparatus. Moreover, if the interaction region separation were increased from our present 15 cm to 3.75 m, the separation of NBS-6, [7] we would obtain a $\sigma_y(\tau) \approx 2.5 \times 10^{-12}$ ($\tau = 100$s) for a Na beam and $\sigma_y(\tau) \approx 1.5 \times 10^{-13}$($\tau = 100$s) for a C_s beam.

Finally we are extremely interested in developing techniques for improving stability by slowing down the atomic beam. The recent radiation cooling experiments by Prodan, Phillips and Metcalf [8] at NBS are of much interest to us and are very applicable since their experiments were also conducted on sodium.

This research was supported by the Rome Air Development Center, Contract No. F19628-80-C-0077 and by the National Science Foundation.

References

[1] Thomas, J.E., Hemmer, P.R., Ezekiel, S., Leiby, Jr., C.C., Picard, R.H., and Willis, C.R. "Observation of Ramsey Fringes Using a Stimulated Resonance Raman Transition in a Sodium Atomic Beam." Phys. Rev. Lett. 48, 867, 1982.

[2] Thomas, J.E., Ezekiel, S., Leiby, Jr., C.C., Picard, R.H., and Willis, C.R. "Ultrahigh - resolutions spectroscopy and frequency standards in the microwave and far-infrared regions using optical lasers." Optics Lett. 6, 298, 1981.

[3] Ramsey, N.F. Molecular Beams. Oxford University Press, London, 1963.

[4] Hemmer, P.R., Ezekiel, S., Leiby, Jr., C.C. To be published.

[5] Lacey, R.F., Helgesson, A.L. and Holoway, J.H. "Short-term Stability of Passive Atomic Frequency Standards." Proc. IEEE 54, 170, 1966.

[6] Brillet, A. "Evaluation of the Light Shifts in an Optically Pumped Cesium Beam Frequency Standard." Metrologia 17, 147, 1981.

[7] Glaze, D.J., Hellwig, H., Allan, D.W., Jarvis, Jr., S. "NBS-4 and NBS-6: The NBS Primary Frequency Standards." Metrologia 13, 17, 1977.

[8] Prodan, J.V., Phillips, W.D., and Metcalf, H. "Laser Production of a Very Slow Monoenergetic Atomic Beam." Phys. Rev. Lett. 49, 1149, 1982.

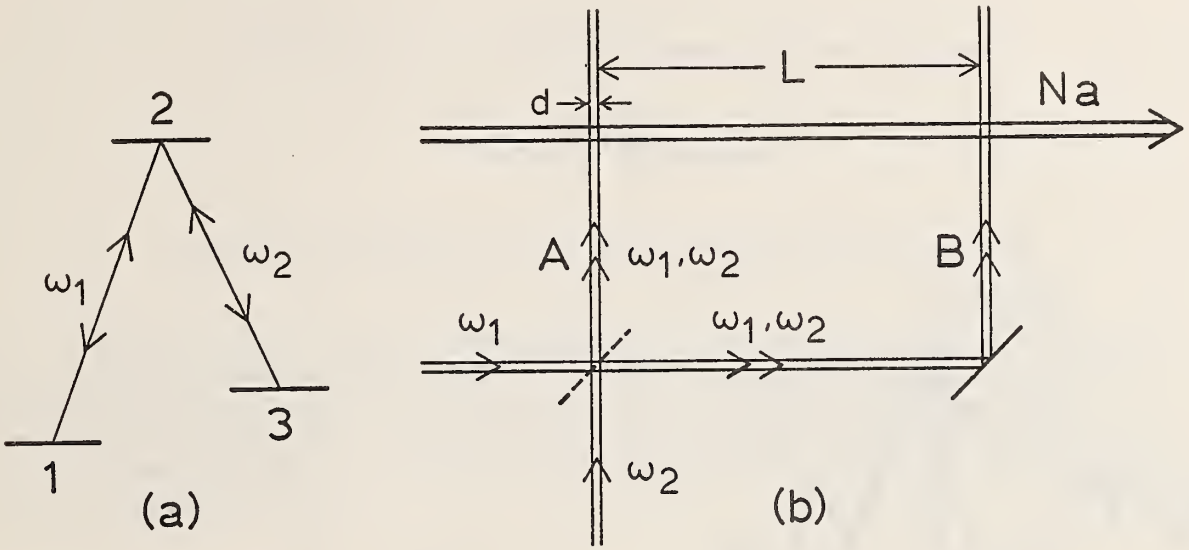

Figure 1. (a) Stimulated resonance Raman system. (b) schematic of setup for separated oscillatory field excitation using a stimulated resonance Raman transition.

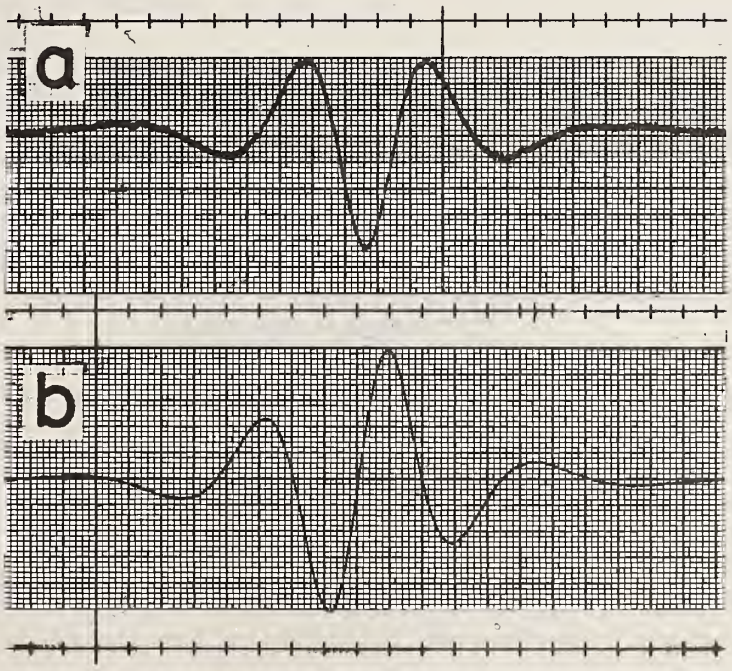

Figure 2. (a) Ramsey fringes corresponding to L = 15 cm. Scan rate 330 Hz/sec; τ = 10 msec; peak-to-valley amplitude ≈ 1pA; central fringe width FWHM approx. 2.16 kHz. (b) Discriminant obtained by frequency modulation. Scan rate 330 Hz/sec; τ = 100 msec.

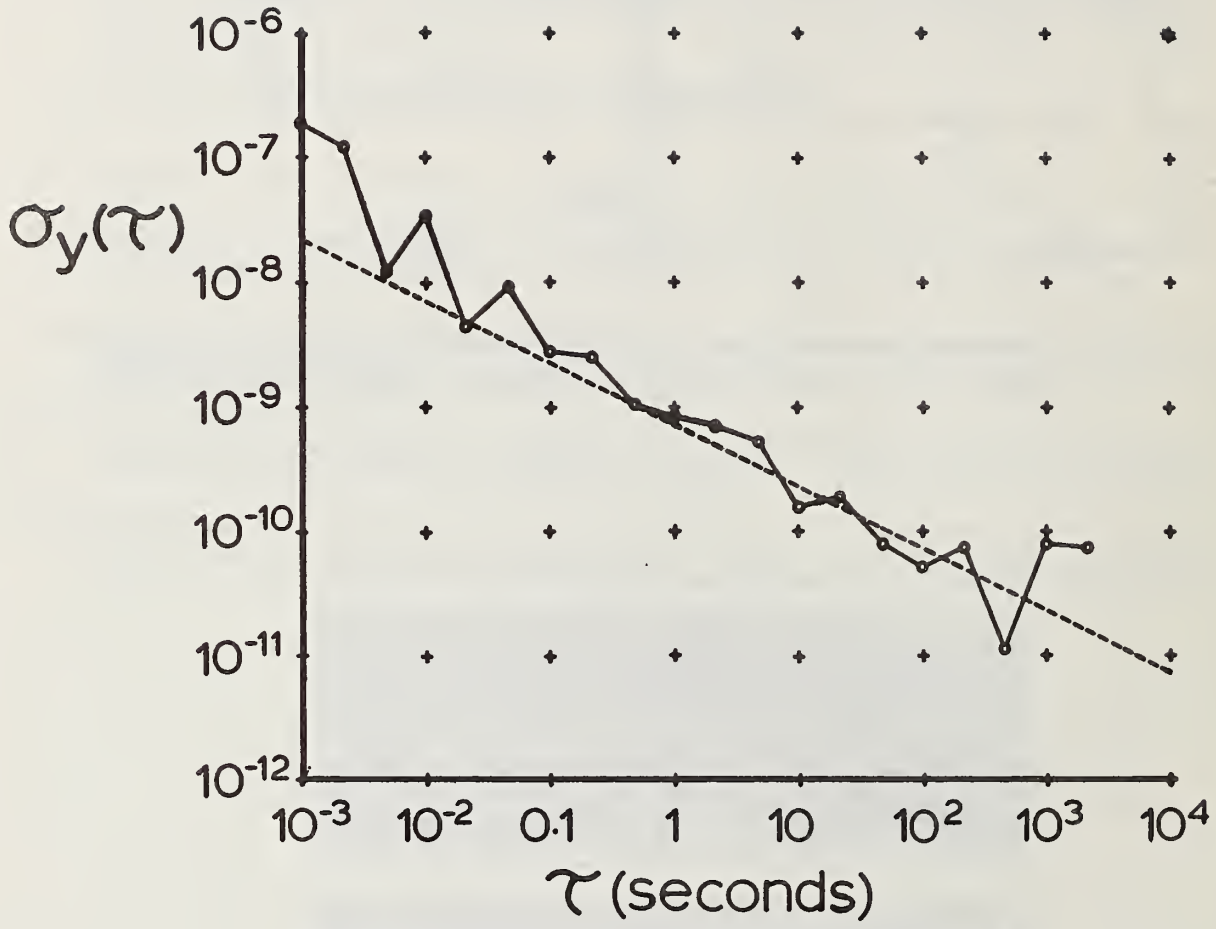

Figure 3. Fractional frequency stability vs. averaging time.

Laser-Cooled and Trapped Atoms, (Proceedings of the Workshop on Spectroscopic Applications of Slow Atomic Beams, held at NBS, Gaithersburg, MD, 14-15 April 1983) Ed. by W. D. Phillips, Natl. Bur. Stand. (U. S.) Spec. Publ. 653 (1983).

The Force on an Atom in a Laser and D.C. Field*

Marvin H. Mittleman

The City College of The City University of New York

The deflection of an atom depends upon the coupling of the field to the internal motion of the atom. This internal motion can be profoundly altered by a laser field so the deflection can depend upon the laser intensity and frequency. The force that an atom experiences in a combined D.C. and laser field is reviewed. The fluorescence of the atom is shown to play an important role.

1. Introduction

This note is a brief review of the theory of the force on an atom due to D.C. electric and/or magnetic fields (the external field) and a resonant laser field. It contains nothing new.[1,2] The laser is described here as a classical single mode electromagnetic field. Quantum corrections are not significant and multimode corrections can be included at the end of the calculation by a suitable averaging procedure. The laser-atom interaction is treated in dipole approximation as far as the internal motion of the atom is concerned. Corrections to this are usually negligible. However the center of mass motion of the atom will extend over many laser wavelengths so no such approximation is possible there.

The theory of the deflection of atoms by external fields is ancient. Only energy conservation is necessary to understand the effect: an atom in an external field will have its energy levels shifted by the field and it is usually sufficient to use perturbation theory, in one form or another, to obtain these shifts. Moreover, in the usual case, each of the levels will be shifted by a different amount. The total energy of the atom must be conserved since the external field is conservative. Therefore the energy shift of the internal state of the atom must be compensated by the change in the center of mass kinetic energy. Another way of saying this is that the energy level shift will act as a potential energy for the

---

*This work was supported by a contract from the U.S. Office of Naval Research, No. N00014-76C-0014.

center of mass motion. (This is analogous to the atom-atom scattering problem in which the electronic eigenvalue acts as an internuclear potential in the Born-Oppenheimer approximation.) The magnitude of the level shift will differ from level to level so the center of mass potential will also depend upon the level. In the absence of the laser, the change of the level shift with center of mass position will occur very slowly on the internal time scale of the atom so the atomic state will deform adiabatically and only a single level shift (usually that of the ground state) will enter. The laser will change this since it can strongly couple a pair of atomic states so that the atom will be in a superposition of these two states rather than in either one. Therefore the level shifts of both states will be relevant to the center of mass motion. The precise way that they enter will depend upon the way that the atom is resonant with the transition between the two states. This is governed by the ratio of two numbers. The first is the detuning frequency ($\hbar = 1$)

$$\Delta\omega = \omega_L - W_{10}(\vec{R}), \tag{1}$$

where ω_L is the laser frequency and $W_{10}(\vec{R}) = W_1(\vec{R}) - W_0(\vec{R})$ where $W_n(\vec{R})$ is the energy of the n-th electronic state of the atom which depends upon $\vec{R}$, the center of mass coordinate of the atom. The atomic states coupled by the laser have been labeled "1" and "0". The second number is the coupling matrix element of the two states

$$\Lambda(R) = \left(1 \left| \frac{e}{m} \frac{p\cdot E}{\omega_L} \right| 0\right) = |\Lambda| e^{i\Theta}, \tag{2}$$

where E is the amplitude of the electric field of the laser. A convenient ratio is, the detuning parameter, μ

$$\sinh \mu(R) = \frac{\Delta\omega}{\Lambda} . \tag{3}$$

For small values of μ the two states are significantly coupled whereas large values of μ give essentially one state or the other.

We have so far ignored the motion of the atom. The considerations described above are relevant in the rest frame of the atom. They can be transformed to the lab frame and the only significant change (for non-relativistic atoms) is that the laser frequency is Doppler shifted so that ω_L is replaced by $\bar{\omega}_L$ where

$$\bar{\omega}_L = \omega_L - \dot{R}\cdot k_L \tag{4}$$

and where $v = \dot{\vec{R}}$. Then the center of mass potential will depend upon the position and velocity of the atom. (In fact the dependence is much more complex in that this "potential" will depend upon the temporal history of the center of mass motion. This correction is negligible unless the atoms undergo accelerations comparable to the electronic accelerations in the atom. This is not realizable now.)

An objection can be raised to the reasoning just presented. It is that energy conservation was the underpinning of the logic but the laser is a time dependent field so energy conservation fails. The solution of the dilemma lies in Shirley's theorem[3] which states that the energy transferred to the particles must be an integer multiple of the laser frequency. (Energy is transferred in units of photons.) Then the energy of the particles is conserved modulo ω_L (not $\bar{\omega}_L$). But the potentials discussed above are continuous functions of their variables so energy conservation modulo ω_L is equivalent to absolute energy conservation and so the validity of the logic is restored.

At this point we must introduce the fluorescence of the atom. If the laser-atom coupling is effective ($|\mu| < 1$) the atom will spend a significant fraction of its time in the excited state. (The fraction will be 1/2 for $\mu = 0$.) In an experiment in which the atom is in the fields for many natural decay times ($\sim 10^{-8}$ sec), which is the usual case, the atom will fluoresce many times during its passage through the fields. This will modify the internal state of the atom and therefore the potential experienced by the center of mass. Fluorescence is a stochastic process and so the internal state of the atom will become an incoherent superposition of the atomic states after a few fluorescent emissions. We can restate this: in the absence of fluorescence, the atom starts in its ground state and moves, adiabatically, into the external and laser fields. The two internal atomic states in these fields can be written

$$\Phi_{\pm} = \frac{e^{-i\left(\frac{Mv^2}{2}t + M\vec{v}\cdot R\right)}}{(2\cosh\mu)^{\frac{1}{2}}} \{e^{\pm\mu/2} u_0 e^{\frac{i}{2}(\bar{\omega}_L t - k_L\cdot R)} \pm e^{\pm\mu/2 - i\theta} u_1 e^{-\frac{i}{2}(\bar{\omega}_L t - k\cdot R)}\} e^{-\frac{i}{2}(\bar{W}_0 + \bar{W}_1 \pm \varepsilon)t} \tag{5}$$

where u_0 and u_1 are the atomic states in the external field and the Rabi frequency is

$$\varepsilon = \sqrt{|\Lambda|^2 + \Delta\omega^2} \tag{6}$$

These states have been obtained by using the rotating wave approximation which is correct to terms of order $\Delta\omega/\bar{\omega}_L$ which is usually very small. The atomic ground state will deform adiabatically into either Φ_+ or Φ_-, depending upon the sign of $\Delta\omega$, but it will remain in this state. Fluorescence will however couple these states so the atom will go into an incoherent superposition of these two states after a few fluorescent times. The center of mass potential will then depend upon the details of the fluorescence.

It is easy to show that there can be many hundreds of fluorescent emissions during a typical experiment so that the treatment of the emission process by straightforward perturbation theory is out of the question. There are a variety of alternate treatments which can be used to deal with the problem. Perhaps the simplest is that due to Mollow[4] who showed that an approximate "constraint" can be written for the wave function of the fluorescent state. The method is sufficient to calculate some simple properties of the state which are all that is needed to describe the force acting on the center of mass of the atom. Since the atom is thrown into an incoherent superposition of the state Φ_+ and Φ_- it is clear that the force must depnd upon the probability of finding each of these states, $P_{\pm}$ and P_-. The Mollow technique gives these parameters. For times which are large compared to the natural decay time they are

$$P_{\pm} = e^{\pm 2\mu} / 2 \cos h\, 2\mu \,, \tag{7}$$

where we have also assumed that the Rabi frequency is large compared to the natural decay rate. (The assumption is easily removed.)

There is also a recoil force due to fluorescence. This may be understood in a simple way. The fluorescent process is one in which a laser photon is absorbed and then emitted as a fluorescent photon in (for example) a dipole pattern. In the rest frame of the atom there is no net momentum emitted into the fluorscent field so the process converts the momentum of the laser photon into momentum of the atom. (In the lab frame the fluorescent photons do carry away some momentum but this is a

small relativistic effect which is actually cancelled by the relativistic effect associated with the change of mass of the atom[5]). The force resulting from this recoil is

$$\hbar \vec{k}_L \dot{N}, \tag{8}$$

where $\dot{N}$ is the rate of emission of fluorscent photons. Again the Mollow technique yields

$$\dot{N} = \tfrac{1}{2}\gamma(\cosh 2\mu)^{-1}, \tag{9}$$

where γ is the natural decay rate of the excited state.

Finally there is one more contribution to the force on the atom which arises from the spatial inhomogeneity of the laser beam, the ponderomotive force. The laser enters the atomic Hamiltonian through the vector potential which we write as

$$\vec{A} = \frac{E(R)}{\bar{\omega}_L} \cos(\bar{\omega}_L t - k_L \cdot R). \tag{10}$$

The Hamiltonian contains the kinetic energy term

$$\frac{1}{2m}(p + eA)^2 = \frac{p^2}{2m} + \frac{e}{m} p \cdot A + \frac{e^2}{2m} A^2. \tag{11}$$

The last term may be written

$$\frac{e^2}{4m} \frac{E^2(R)}{\bar{\omega}_L^2} + \frac{e^2}{4m} \frac{E^2(R)}{\bar{\omega}_L^2} \cos 2(\bar{\omega}_L t - k_L \cdot R). \tag{12}$$

The second term of (12) has been assumed to be non-resonant with any atomic transition and so contributes terms similar to the counter rotating terms which have been dropped in obtaining (5). The first term of (12), which we call U_p, the

ponderomotive potential, does not couple to the electronic motion within the atom, it only acts as a potential for the center of mass motion.

We can now assemble the results to give the force

$$\vec{F} = -P_+ \nabla\left(\frac{W_0 + W_1 + \varepsilon}{2}\right) - P_- \nabla\left(\frac{W_0 + W_1 - \varepsilon}{2}\right) - \nabla U_p + h\vec{k}_L \dot{N} . \qquad (13)$$

If we interpret $\frac{1}{2}(W_0 + W_1 + \varepsilon)$ as the "energy" of the states $\Phi_{\pm}$ (5), the result (13) is readily understood.

This result applies for low intensity-near-resonant lasers since the shift of the energy levels of the atom due to the dynamic Stark effect has been neglected. This is usually a small effect but if it is large enough to affect the resonance condition it is significant. That is, if the dynamic Stark shift, ΔE_n^s, is comparable to $|\Lambda|$ it must be included. This can be done by using a complete set of atomic states which contain this shift, instead of the "bare" atomic states implied in the discussion here. The main change in the force due to this effect is the inclusion of the dynamic Stark shift terms in W_0 and W_1. (Care must be taken to prevent counting intermediate states more than once.) These terms are the same order of magnitude as the ponderomotive potential and must be included with it.[2]

The force can now be used in a classical equation of motion to describe the motion of the atoms but all the details will not be presented here. It should however be pointed out that the resonance condition is velocity dependent so that the laser can force the atom to change its velocity and thereby decouple itself from the laser. A judicious choice of the external field can compensate for this.

Finally, it should also be noted that the force (13) is the expectation value of an operator which has a non-vanishing variance. This will cause the velocity of the atom to spread. We shall not pursue this here.

2. References

[1] The material discussed here is from M. H. Mittleman, K. Rubin, R. H. Callender, and J. I. Gersten, Phys. Rev. A 16, 583(1977).

[2] The details of the mathematics of this discussion can be seen in "Introduction to the Theory of Laser-Atom Interactions," M. H. Mittleman, Plenum, New York, 1982.

[3] J. H. Shirley, Phys. Rev. B 138, 979(1965).

[4] B. R. Mollow, Phys. Rev. A 12, 1919(1975),

[5] This fact was pointed out to me by Dr. Richard Cook, private communication.

Laser-Cooled and Trapped Atoms, (Proceedings of the Workshop on Spectroscopic Applications of Slow Atomic Beams, held at NBS, Gaithersburg, MD, 14-15 April 1983) Ed. by W. D. Phillips, Natl. Bur. Stand. (U.S.) Spec. Publ. 653 (1983).

Magnetic Trapping of Decelerated Neutral Atoms

Harold J. Metcalf

State University of New York
Stony Brook, N.Y. 11794

A scheme is proposed for trapping atoms having finite magnetic moments using inhomogeneous magnetostatic fields. Fields of ~ 0.1 T can be used to contain atoms decelerated to $v \sim$ few m/s. Application to the N.B.S. decelerated atom project is discussed.

Key words: cooling, trapping, precision spectroscopy

1. Introduction

The use of electromagnetic forces to influence the motion of free, neutral atoms has been a subject of interest for many years. On the practical side, there are many spectroscopic and collision experiments that would benefit from the use of slow and/or cold atomic samples. On the theoretical side, the various limits to the control of atomic motion, as well as the approaches to them, present interesting and challenging problems. In this paper, we discuss some of the methods of confinement of neutral particles, with an emphasis on the use of inhomogeneous magnetic fields for those particles having magnetic moments. Then we describe the magnetic trap for slow sodium atoms proposed for use at the N.B.S. Since all of the trapping schemes described below share the common feature of being rather shallow compared with thermal energy at room temperature, deceleration and cooling are often inseparable from confinement.

The most popular mechanism for producing a force on free neutral atoms uses the electric field associated with light, particularly light at or near the resonant frequencies of atomic transitions. The influence of radiation force on free atoms using light from a resonance lamp was first observed in 1933 by Frisch [1] and in 1972 by Picqué and Vialle [2]. In that same year, Walther [3] and coworkers detected atomic deflection using a tunable dye laser beam. At least two applications for this phenomenon had been proposed two years earlier by Ashkin [4,5]. Although the phenomenon was regarded as a curiosity for many years, the advent of modern dye lasers has stimulated new interest in both influencing and controlling the motion of free atoms.

Interest in cooling (and trapping) grew rapidly as a result of work at Bell Laboratories [6] and at the U.S.S.R. Academy of Sciences [7]; the first experimental results were reported in 1978 [8]. Additional experimental results were reported by both the Russian group [9] and by us at the N.B.S. [10], but all this work was related to deceleration and cooling.

Trapping of atoms using resonance radiation has been proposed and discussed extensively by Letokhov and coworkers [11] and by Ashkin and coworkers [12]. These schemes exploit both the dipole force associated with the inhomogeneous electric field of both a non-uniform light beam and of the standing wave pattern from counter propagating beams, as well as the recoil associated with the transfer of momentum from the optical field to the atom (scattering). In the first case the dipole moments are produced by the light itself by mixing with or excitation to a state of opposite parity, resulting in an atomic superposition state having a non-zero dipole moment [13,14]. There have been a number of interesting geometries proposed for these optical traps, including a rather novel tetrahedral configuration [15] and an electromagnetic mirror [16]. The combined use of optical radiation for state preparation by excitation to Rydberg states, and electrostatic forces on the resulting highly polarizable atoms has been proposed for both trapping [14] and deceleration [17].

There has been considerably less work on the use of magnetic fields for steering and trapping. The deflection of particles having magnetic moments was first demonstrated by Stern and Gerlach [18] in a landmark experiment more than 60 years ago. It was not until the early 1950's that a generalized Stern-Gerlach approach to deflection appeared in the form of Paul's hexapole lens [19]. This idea has been exploited by both the atomic beam community [20] and the slow neutron people [21].

2. Magnetic Trap for Slow Neutral Atoms

The principle advantage to magnetic forces for slow atoms arises from the long time these atoms spend in any particular part of the field gradient. Even though the force is limited by the product of the magnetic moment (typically a Bohr magneton) and the field gradient (typically one or two Tesla/meter), the impulse delivered to the atoms is enhanced by the long interaction time. For example, the deflection in the Stern-Gerlach experiment is proportional to $1/v^2$.

In this section we describe the magnetic trap proposed for use at the N.B.S. In brief, the cylindrically symmetrical trap consists of two end mirrors separated by L composed of regions of sharply increasing magnetic fields for longitudinal confinement, and hexapole lens of focal length L/4 placed axially and halfway between them for transverse confinement. The optical cavity analog of this trap is shown below.

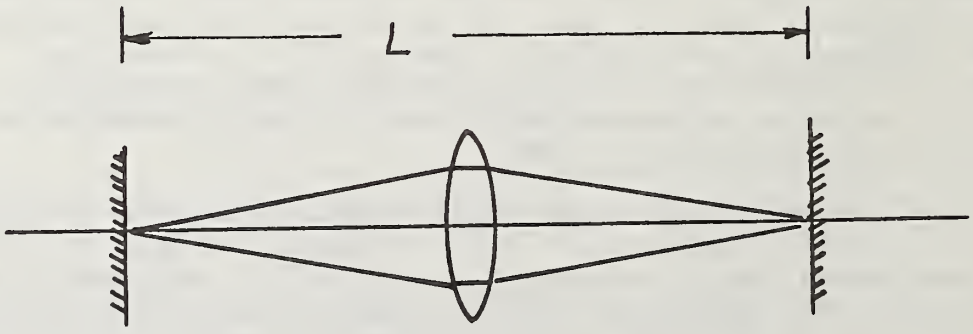

An end mirror can be made using a several cm diameter coil of a few hundred turns carrying a few amperes that produces a maximum field of about B = 0.1 Tesla and gradient of about 1 Tesla/meter. Since the magnetic moment μ_s of a ground state Na atom is $\mu_s \cong \mu_B$, this coil can reflect an axially moving atom having kinetic energy $E = \frac{1}{2} Mv^2 < \mu_B B \cong 10^{-24}$J corresponding to a kinetic temperature of about 0.06°K. These atoms move at about 6 m/s.

It is very curious to note that there is an intimate relation between the depth of a magnetic trap and the ultimate final velocity that can be obtained by laser deceleration of the kind we have achieved at the N.B.S. [10]. This relationship arises because of the heating associated with the random fluorescence of the light absorbed by the atoms from the decelerating laser beam. Although the average impulse transferred to atoms moving with initial velocity v_o by the fluorescence of $n = Mv_o\lambda/h$ quanta is expected to be zero, the rms fluctuations are not zero because of the quantization of momentum in units of h/λ. The rms momentum is thus $\Delta p = \sqrt{n}\, h/\lambda$ and the resulting kinetic energy is $E = \Delta p^2/2M = nh^2/2M\lambda^2 = hv_o/2\lambda = h\nu_D/2$ where $\nu_D = v_o/\lambda$ is the Doppler shift required to bring the laser into resonance with the atom moving at its initial velocity v_o [22]. Therefore $h\nu_D/2$ is the minimum trap depth.

In our experiment this Doppler shift is just compensated by a Zeeman shift produced by an applied magnetic field B, and because the excited state has magnetic moment $\mu_p \cong 2\mu_B$, the optical frequency is shifted by $h\nu_Z \cong \mu_B B$. Therefore $\nu_Z = \nu_D$ and the applied Zeeman field B is just twice as large as it needs to be: the main magnet used in the deceleration process in our experiments can easily serve as one end of the trap [23]. Construction of an appropriate magnet to serve as a mirror for the other end of the trap is straightforward.

Lateral confinement in our trap will be provided by a hexapole electromagnet. These have been described many years ago [19,20] and permanent magnet devices are available commercially [24]. The principle idea is to produce a field that varies quadratically with distance from the axis so that the field gradient (thus the force) varies linearly and produces harmonic motion. Solutions to Laplace's equation for the magnetic potential $\Phi(r,\theta)$ under the boundary condition of six-fold symmetry results in a series with leading term r^3. The field is thus quadratic as desired. An atom moving at some small angle away from the axis will be deflected back towards it in such a way as to produce focussing; these devices have the properties of a lens.

The basic configuration of the magnet is shown perpendicular to the axis [25] below. Although the pole pieces shown here are hyperbolae, the more ideal case of cylindrical boundary conditions at alternating potential 0 and V was solved in Ref. 20 (1959) and the potential is

$$\Phi(r,\theta) = \frac{4V}{\pi} \sum_{n=1}^{\infty} \left(\frac{r}{r_o}\right)^n \frac{\sin(n\theta)}{n} \sin\frac{n\alpha}{2} \sum_{\ell=1}^{N} (-1)^{\ell-1} \sin\left[\frac{n\pi}{2N}(2\ell-1)\right]$$

where N is the number of pole pairs, r_o is the distance to the boundary, and α is the angle subtended by each pole. Then the magnetic field for $N = 3$ and $\alpha = \pi/6$ is

$$B(r,\theta) = B_o \left(\frac{r}{r_o}\right)^2 \left[1 - 2\left(\frac{r}{r_o}\right)^6 \cos 6\theta + \sim \left(\frac{r}{r_o}\right)^{12}\right]^{\frac{1}{2}}$$

The dominant term is the desired quadratic, and the next term is down by an order of magnitude for about 3/5 of the aperture area.

We have designed and built the device shown adjacent to the ideal case. The three independent coils of about 500 turns each of #20 AWG wire, formvar insulated, have a resistance of about 2 ohms each, and stay cool carrying 3 amperes with only ambient air cooling. Careful measurements on a milling machine bed confirmed that the resulting field has the required geometrical symmetry, reaches the design maximum of $B_o \cong 0.2$ Tesla in the gaps, and is very nearly parabolic in the 2 cm diam. central aperture.

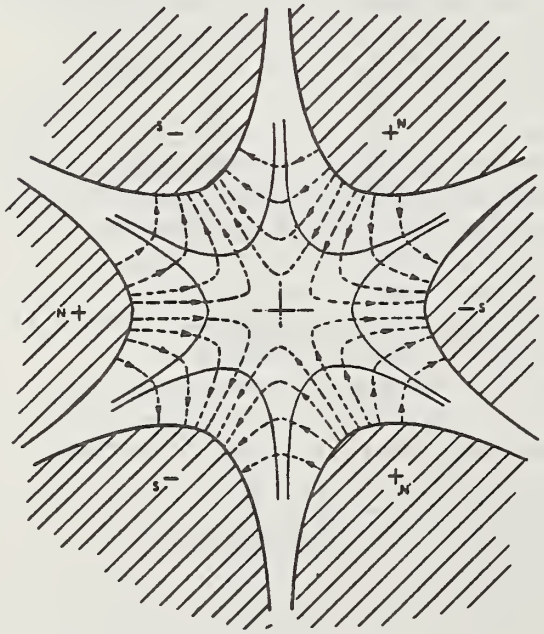

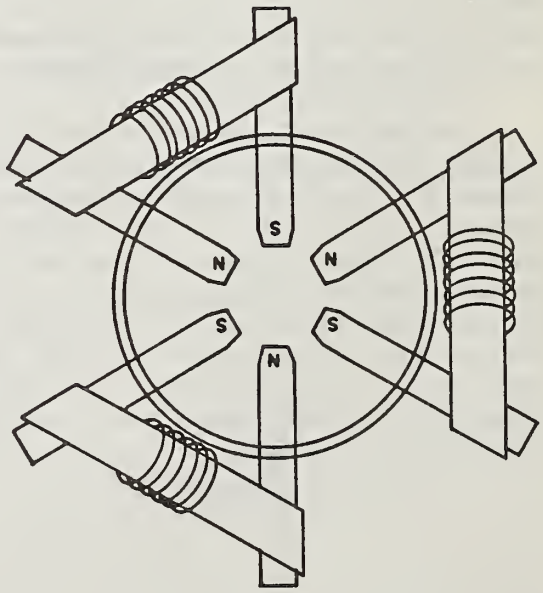

In order to calculate the optical properties of this device, we first note that the oscillation frequency in the harmonic potential is given by $\omega_T^2 = 2\mu_s B_o/Mr_o^2$ and the total phase change of the oscillation for an atom that traverses a magnet of length Z at velocity v is $\Delta\phi = \omega_T Z/v$. Then straightforward geometrical considerations show that atoms diverging from a point on the axis a distance s away from the center of the magnet are bent back to cross the axis again at a distance s' such that $(s + s')/ss' = 1/f$ where $f = v^2/\omega_T^2 Z = (E_{kin}/E_{mag})(r_o^2/Z)$. For thermal atoms it takes a 10 cm long magnet with aperture only 2 mm diam to get f = 20 cm, resulting in a lens of speed f/100. But for atoms decelerated to 40 m/s as we have observed [10], a lens as short as 2.5 cm and as wide as 2 cm diam has a focal length only 13 cm and a speed f/6.5. The collecting power for slow atoms is enhanced by a factor v^2, and hexapole lenses can be tailored for particular needs.

In addition to strongly enhanced collecting power, the use of hexapole lenses for decelerated atoms has another strong advantage over their traditional use with thermal beams. Since the focal length depends on v^2, there are severe aberrations associated with the Maxwellian spread of thermal velocities. This problem is sharply reduced for the compressed velocity distribution of decelerated atoms reported in Ref. 10.

Although we would also like to further cool the atoms in this trap, there is another curious coincidence in Ref. 10 that would seem to make further cooling impossible. The rms velocity $\Delta v = \Delta p/M = v_o/\sqrt{n} \cong 6$ m/s results in an rms Doppler shift $\Delta\nu_D = \Delta v/\lambda \cong 10$ MHz which is almost exactly the natural width of the transition. It would seem that the natural width would present a limit to further deceleration because atoms could also be accelerated in the laser beam. Fortunately this view is too naive, and further cooling can be achieved by weaker, slightly off-resonant light. Of course, the hexapole lens of the trap would have the right focal length only for atoms of a particular speed, but we can compensate for this difficulty by properly tapering the field of the end mirrors. If their field increased linearly with distance along the axis, the position of the turning point would move away from the center of the lens quadratically with velocity and would just compensate the changing focal length of the lens [26].

Loading atoms into this kind of trap presents the usual problems: there must be some way to extract energy from the atoms while they are inside. Our deceleration process does this by its very nature, and therefore provides an ideal damping or velocity-dependent force. Some other methods have been described in the literature cited, and still others appear in these proceedings.

In order for this proposed scheme to work at all, the atomic magnetic moments must be oriented so that they are repelled from regions of strong field. This is certainly the orientation produced by the optical pumping process that occurs during cooling, but it must be preserved while the atom is in the trap, even though the trap fields change directions in a very complicated way. As long as the atom is moving slowly enough, the magnetic

field changes sufficiently slowly that the magnetic moment precesses about the field and follows it adiabatically. The condition is violated, however, if the atom sees a field change with strong enough Fourier component at the frequency of magnetic resonance that would cause a transition to a state of different orientation. That frequency is simply $\omega_L \cong \frac{1}{2}\mu_B B/\hbar$. The transition moment is approximately $\frac{1}{2}\mu_B$, and therefore transitions occur at the rate $\omega_R = \frac{1}{2}\mu_B \Delta B/\hbar$ where $\Delta B = v\nabla B\tau$ is the field change seen by an atom during the time $\tau = \pi/2\omega_L$. Then $\omega_R = (\nabla B/B)(\pi v/2) = \pi v/r = \pi\omega_T$ for motion in the lens, and it appears that an atom cannot survive against Majorana transitions for more than a few oscillations in the trap.

Fortunately, this is not the case. An atom oscillating perpendicular to the trap axis sees an oscillating magnetic field having dB/dt parallel to B, the equivalent of z-polarization, which does not produce the $\Delta m = \pm 1$ transitions required to re-orient the magnetic moment. An atom moving parallel to the lens' axis sees dB/dt = 0 and no transitions occur. Only orbital motion produces the necessary rotating magnetic field, but the atomic moment can precess about the field resulting in a substantially decreased transition rate. More careful considerations of the problem of a magnetic moment in a hexapole trap have been worked out by Matora [27], and suggest that the trap is indeed very nearly stable against this problem. Similar considerations hold for the end mirrors. In fact, the effect of the anisotropy of the gravitational force on the atoms may provide the ultimate limit of the trapping time.

Another consideration for traps of this kind is the vacuum required. Although a trapped ion at thermal energies can survive a few collisions, and even a cooled trapped ion that is struck by residual gas atom having thermal energy can still stay in a typical ion trap, a cooled neutral can not. Since the neutral's trap is so shallow, and since these atoms are 'sitting ducks' for thermal energy background gas, the vacuum requirements are more stringent. The mean free time between collisions must exceed the trapping time. Estimating the cross section for destructive collisions is very difficult because even a very gentle collision (i.e., large impact parameter b) can impart enough energy to eject the atom from the trap. Nevertheless, a mean free time of 1 sec demands $P \cong 10^{-7}$ Torr for b ≅ few Bohr radii, and the required pressure decreases as $1/b^2$.

3. Other Magnetic Traps

There are two other kinds of magnetic traps for sufficiently slow, neutral objects. To illustrate one of these, consider a hexapole field made from six parallel, straight conductors arranged so that they cross a perpendicular plane at the vertices of a hexagon [19,28]. If they each carry constant currents of the same magnitude but alternating directions, then the field produced will be the same hexapole field shown earlier. Adequately strong fields can be made by using very high currents in superconducting wires. A very long, thin structure of this type can be used as a guide to transport slow neutral particles much like a graded-index optical fiber. We can imagine a long structure of this type bent around into a torus as shown below. The particles are guided around the circle in a very similar way to those in very high energy storage rings. As recently as 1977 [29] it was not clear whether or not such a storage ring would work, but one has been built for ultracold neutrons by Paul and coworkers [30].

The other kind of magnetic trap, also a hexapole field and closely related to this one, is shown below. The field configuration is imagined by rotating the hexapole field shown earlier about a vertical line in the

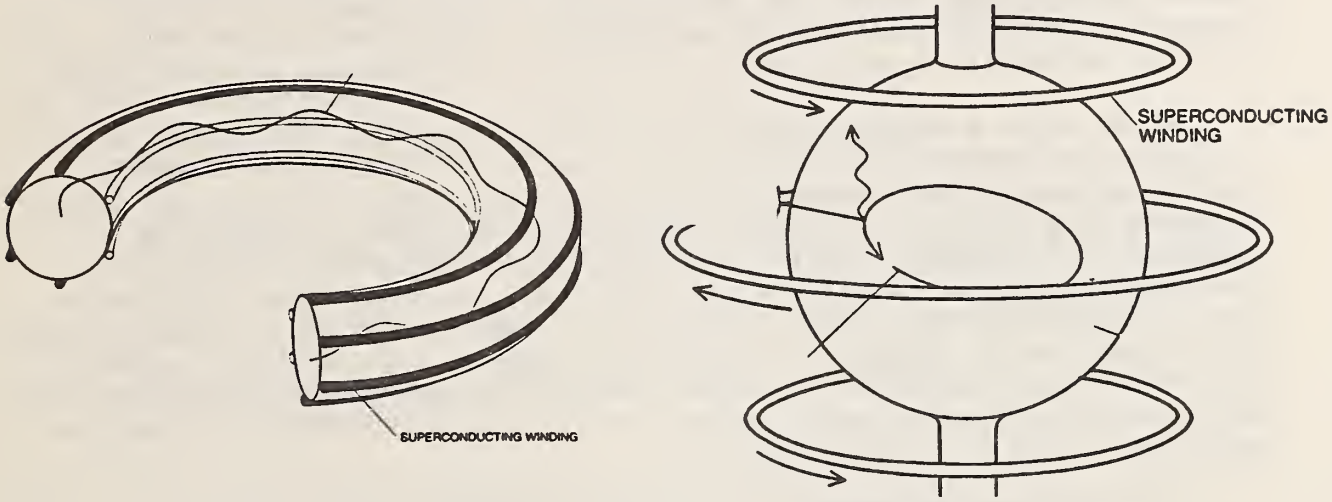

plane of the paper. The magnet is constructed from three superconducting rings of wire carrying appropriate currents. Such a trap has also been built and is being tested in Paul's laboratory [31] with sodium atoms. Although this trap has the desired hexapole field configuration in any vertical plane, it does not have the appropriate symmetry in the horizontal plane and it is not known if the trap will be stable.

4. Future Plans for the N.B.S. Experiment

The atom deceleration experiment of Ref. 10 has not reported atoms slower than about 40 m/s because the signal disappears rapidly at low velocities. We believe that this is an observation problem and not any limit to the particular deceleration process. Most of the difficulties are believed to arise from the unavoidable space between the end of the solenoid and the observation region. This drift region cannot be eliminated because the stray magnetic fields from the solenoid will necessarily cause difficulties in the observation region. We have been concerned with collisions with background gas, with beam divergence from both transverse heating and residual imperfect collimation [32], and with the effect of the laser light in this drift space. Various incomplete solutions to these problems have been partially successful [10].

Much of the signal loss is believed to originate from beam divergence produced by various effects and our first experiment with the new hexapole will therefore be to focus the diverging beam into the interaction region. We hope to produce much higher atomic densities at velocities near 40 m/s, and to observe much slower atoms.

One of the principal characteristics of our hexapole is the relative magnetic independence of the pole pairs. By using different currents in the separate yoke coils, we will be able to move the magnetic center off the axis, and therefore deflect as well as focus our atomic beam. This combination of capabilities should result in a sample of high density, very slow atoms off the optical axis (out of the laser beam).

The next step is to place a small aperture in the off-axis focal plane that will admit the focussed atoms to a differentially pumped, ultra-high vacuum region where we will try to trap them. Many schemes for optical traps have been mentioned above, and others are described in this volume. If we build an optical trap, it will surely be closely related to one of these.

If we build a magnetic trap of the kind described above, we will have to deal with two important problems. First, we do not know if it is stable against magnetic dipole transitions that would re-orient the atom and cause ejection from the trap. Although the toroidal hexapole has worked for neutrons, our proposed trap is complicated by the end mirrors and by the additional possible transitions associated with the hfs of the sodium atom. The second problem we face is detection. Although detection of trapped atoms by fluorescence of light from a weak probe beam is a possibility, we would have to be very careful not to eject the atoms by momentum transfer from the probe and not to heat them by too much recoil momentum. We do not know the solution to either of these problems.

This work was supported by the N.B.S. and the O.N.R.

References

1. R. Frisch, Z. Phys. 86, 42 (1933).

2. J.L. Picqué and J.L. Vialle, Opt. Commun. 5, 402, (1972).

3. R. Schieder, H. Walther, and L. Woste, Opt. Commun. 5, 337 (1972).

4. A. Ashkin, Phys. Rev. Lett. 24, 156 (1970).

5. A. Ashkin, Phys. Rev. Lett. 25, 1321 (1970).

6. A. Ashkin, Phys. Rev. Lett. 40, 729 (1978); A. Ashkin and J.P. Gordon, Opt. Lett. 4, 161 (1979).

7. V. Letokhov, V. Minogin, and B. Pavlik, Soviet Physics J.E.T.P. 45, 698 (1977); V. Letokhov and V. Minogin, J. Opt. Soc. Am. 69, 413 (1979).

8. J.E. Bjorkholm et al., Phys. Rev. Lett. 41, 1361 (1978).

9. S.V. Andreev et al., J.E.T.P. Lett. 34, 442 (1981).

10. W. Phillips and H. Metcalf, Phys. Rev. Lett. 48, 596 (1982); J. Prodan, W. Phillips, and H. Metcalf, Phys. Rev. Lett. 49, 1149 (1982).

11. V. Letokhov and V. Minogin, Physics Repts. 73, 3 (1981). This extensive review contains very many excellent references.

12. J.P. Gordon and A. Ashkin, Phys. Rev. A21, 1606 (1980); also see Ref's. 4 and 6.

13. M. Mittleman et al., Phys. Rev. A16, 583 (1977).

14. W.H. Wing, Phys. Rev. Lett. 45, 631 (1980).

15. V. Minogin and J. Javanainen, Opt. Commun. 43, 119 (1982).

16. R.J. Cook and R.K. Hill, Opt. Commun. 43, 258 (1982); also see several other papers by Cook referenced therein.

17. T. Breeden and H. Metcalf, Phys. Rev. Lett. 47, 1726 (1981).

18. W. Stern and O. Gerlach, Z. Phys. 8, 110 (1921).

19. H. Friedberg and W. Paul, Naturwiss. 38, 159 (1951).

20. A. Lemonick, F. Pipkin, and D.R. Hamilton, Rev. Sci. Inst. 26, 1112 (1955); R. Christensen and D.R. Hamilton, Rev. Sci. Inst. 30, 356 (1959).

21. K.J. Kugler, W. Paul, and U. Trinks, Phys. Lett. 72B, 422 (1978).

22. In our experiments $v_o \cong 10^3$m/s, $n \cong 3\times10^4$, $\lambda \cong 590$ nm, M = 23 a.m.u., and B ≅ 0.1 Tesla.

23. For our experiments there are two other considerations. First, this calculation assumes that the atoms have been completely decelerated to $v_o/\sqrt{n}$. Although we haven't observed these yet, we believe this has been accomplished. Second, the bias field may adequately compensate for any residual velocity.

24. Frequency and Time Systems, Danvers, Massachusetts.

25. N.F. Ramsey, Molecular Beams, Oxford Univ. Press, 1956.

26. Of course we would have to be careful of the effect of the 'mirror' on the lens and vice versa. This scheme may only work in a limited region of space and velocities.

27. I.M. Matora, Sov. J. Nucl. Phys. 16, 349 (1973).

28. See illustration in R. Golub et al., Scientific American 240, 134, June 1979.

29. V.I. Luschikov, Physics Today, 30, 42, June 1977.

30. K.-J. Kugler, W. Paul, and U. Trinks, Phys. Lett. 72B, 422 (1978).

31. N. Niehues, Thesis, Univ. Bonn Physikalishes Institut, A Study of Loading Sodium Atoms Into a Magnetic Bottle (German).

32. Because the transverse velocity component of the diverging beam is not reduced in the deceleration, a beam originally collimated to 0.01 at thermal velocity will diverge at an angle 0.3 when decelerated to $v_o/30$. Focussing the laser light helps reduce this effect.

Laser-Cooled and Trapped Atoms, (Proceedings of the Workshop on Spectroscopic Applications of Slow Atomic Beams, held at NBS, Gaithersburg, MD, 14-15 April 1983) Ed. by W. D. Phillips, Natl. Bur. Stand. (U. S.) Spec. Publ. 653 (1983).

The Motion of Neutral Atoms in a Radiative Trap

J. P. Gordon

Bell Laboratories
Holmdel, New Jersey 07733

A number of proposals have been made in recent years for the cooling and/or trapping of neutral atoms in a near-resonance optical radiation field [1-6]. As we have heard in this workshop, substantial slowing and cooling of an atomic beam has already been achieved. Making a trap is a more difficult problem; so far the only neutral atom traps are on paper. The possibility of success of such a trap depends on two factors; first, the creation of the necessary force field, and second, the ability to cool the atoms sufficiently that they stay contained. Our overall conclusions [7] are that a harmonic oscillator model atom can be trapped successfully, whereas a two-level atom cannot. In the case of a real atom such as sodium, a successful trap must involve at least three levels and three radiation fields of different frequencies.

Let $\vec{f}$ be the ponderomotive force exerted by the radiation field on an atom. We assume that the trapping radiation field is stationary, and the the atom-field interaction is electric dipole. The force field for the trap is the mean value of $\vec{f}$ considering the atom to be motionless (note that the atom can have appreciable momentum without much motion if it is heavy enough). The first order dependence of $\vec{f}$ on the atom's velocity provides the damping mechanism, while the quantum fluctuations of $\vec{f}$ add an inescapable heating mechanism.

If the electric field of the radiation and the electric dipole of the atom are expressed respectively as $\vec{E} + \vec{E}^{\dagger}$ and $\vec{\mu} + \vec{\mu}^{\dagger}$, then the jth Cartesian component of the force on the atom is

$$f_j = \vec{\mu}^{\dagger} \cdot (\partial \vec{E}/\partial x_j) + (\partial \vec{E}/\partial x_j) \cdot \vec{\mu} \qquad (1)$$

Here $\vec{E}$ and $\vec{\mu}$ are the "positive frequency" ($\alpha \exp(-i\omega t)$) parts of the field and dipole; $\vec{E}^{\dagger}$ and $\vec{\mu}^{\dagger}$ are their Hermetian conjugates. Classically (1) is the Lorentz force (including both the electric and magnetic components). Quantum mechanically it is the Heisenberg equation for the time derivative of the momentum if one uses the $-\mu \cdot E$ form of the interaction Hamiltonian. We have also used the rotating wave approximation.

Consider first the trapping force field. For this we need the mean value of (1) for a stational atom. If the trapping field is coherent and monochromatic, its mean is a classical field E. If we express the mean dipole by $\langle \mu \rangle = (\chi' + i\chi'')E$, then the mean of (1) becomes

$$\langle f_j \rangle = (\chi' - i\chi'')\vec{E}^{\,*} \cdot \partial\vec{E}/\partial x_j + \textit{complex conjugate} \tag{2}$$

If we now define the real vectors $\vec{\alpha}$ and $\vec{\beta}$ by

$$\vec{E}^{\,*} \cdot \partial\vec{E}/\partial x_j = (\alpha_j + i\beta_j)|E|^2 \tag{3}$$

then (2) becomes

$$\langle \vec{f} \rangle = 2(\chi'\vec{\alpha} + \chi''\vec{\beta})|E|^2 \tag{4}$$

The two terms of (4) have been called the dipole force and the scattering force.

The real part of (3) is

$$2\vec{\alpha}|E|^2 = \textit{grad}(|E|^2) \tag{5}$$

The dipole force can evidently be used to trap atoms at either a field intensity maximum or minimum, depending on the sign of χ'. In some common cases the dipole force trap can be described in terms of a trapping potential $\bigcup$, such that the dipole is the negative gradient of $\bigcup$. In particular, if χ' saturates with increasing field strength according to $\chi'(E) = \chi'(0)/(1+p)$, where $p = |E|^2/E_s^2$, then the trap potential is

$$\bigcup = -\chi'(0)E_s^2 \ln(1+p) \tag{6}$$

Here $\chi(0)$ is the linear susceptibility of the atom at low field strength, E_s is the saturation field strength, and p is the saturation parameter. Deeper traps can be made by going farther off resonance, so increasing $\chi(0)E_s^2$.

From the imaginary part of (3) and the wave equation $\nabla^2\vec{E}+k^2\vec{E}=0$, one can easily show that

$$div(\beta|\vec{E}|^2)=0 \tag{7}$$

It is therefore clear that the scattering force alone cannot be used to form a trap, since this force cannot point inward everywhere on a closed surface.

For a simple harmonic oscillator or a two level atom the mean force can be expressed as

$$\langle f\rangle = h\langle n\rangle[-2\Omega\vec{\alpha}+\Gamma\vec{\beta}] \tag{8}$$

Here Ω is the detuning ω-ω_o of the field frequency from the atomic resonance, Γ is the radiative decay rate of the atom, and $\langle n\rangle$ is either the mean excitation of the oscillator in units of $h\omega_o$, or the mean upper level population of the atom. The difference between the two is that $\langle n\rangle$ for the atom is $p/2(1+p)$ and so cannot be larger than 1/2. The dipole force potential in the two cases is $U=h\Omega\langle n\rangle$ for the SHO or $(h\Omega/2)\ln(1+p)$ for the two level atom. The next problem is damping. This is determined by the first order velocity dependence of $\langle f\rangle$. If we ignore the polarization anisotropy caused by the atom's motion, then the relation

$$\vec{E}^*\cdot d\vec{E}/dt=\vec{E}^*\cdot(-i\omega\vec{E}+(\vec{v}\cdot\nabla)\vec{E})=[-i\omega+\vec{v}\cdot(\vec{\alpha}+i\vec{\beta})]|\vec{E}|^2 \tag{9}$$

(where $\vec{v}$ is the atom's velocity, and we have used (3)) implies that the motion of the atom results in an effective change in frequency detuning to Ω-$\vec{v}\cdot\vec{\beta}$, and an effective change in damping to $\Gamma+2\vec{v}\cdot\vec{\alpha}$. These changes alter the atom's susceptibility and so alter $\langle f\rangle$. Because the trapping field must be tuned far from resonance to increase the trap depth, it follows that the change in

$\langle f \rangle$ due to these perturbations is quite small, and in fact is too small to be useful. The implication is that one must use a separate radiation field tuned closer to resonance for damping, but here the SHO and the two level atom react quite differently. In the SHO case, the susceptibility χ remains linear, and the mean forces due to two separate beams of rather different frequencies are independent and simply add together. In the case of the two level atom, the dynamic level shifts caused by the intense trapping beam make it impossible to keep the damping beam close to resonance throughout the trap, and its effectiveness is lost. It is fruitful to evaluate the damping for the SHO case, however. If the damping beam is effectively a plane wave in the region of the trap, then it has $\alpha = 0$, $\beta = k$, and its force is therefore $\langle f_d \rangle = \Gamma \langle n_d \rangle \hbar k$, where $\langle n_d \rangle$ is the oscillator excitation due to the damping beam alone. Since $\langle n_d \rangle \propto [\Omega_d^2 + (\Gamma/2)^2]^{-1}$, the first order velocity change in $\langle n_d \rangle$ is $\delta \langle n_d \rangle / \langle n_d \rangle = 2 v \cdot k \, \Omega_d / [\Omega_d^2 + (\Gamma/2)^2]$, so if $\Omega_d = -\Gamma/2$ (for maximum effect), then

$$\delta \langle \vec{f}_d \rangle = [\delta \langle n_d \rangle / \langle n_d \rangle] \langle \vec{f}_d \rangle = -2 \langle n_d \rangle \hbar (\vec{v} \cdot \vec{k}) \vec{k} \qquad (10)$$

This velocity dependent force properly opposes the velocity component along the direction of the damping beam, and as we shall see it is large enough to keep the atoms in the trap cold. Three separate damping beams could be used to provide damping for all velocity components.

The final and most difficult problem is finding the momentum diffusion constant. The contribution from spontaneous emission recoil is relatively easy to understand, but the contribution from induced emission is more complicated. Finding the momentum diffusion constant involves the calculation of the two time autocorrelation function $\langle f(t) \cdot f(0) \rangle$. This can be found exactly [7,8], if velocity effects are ignored, by methods similar to those used to find the spectrum of resonance fluorescence[9,10]. In fact these two problems are interrelated. For the SHO the result is (here P is the momentum)

$$2D_p = \frac{d}{dt}[\langle P^2 \rangle - \langle P \rangle^2] = \hbar^2 \Gamma \langle n \rangle (k^2 + \alpha^2 + \beta^2) \qquad (11)$$

The k^2 term can alternatively be regarded as the cumulative effect of spontaneous emission recoils, or as the effect of the mean dipole interacting with the zero-point fluctuations of the field gradient. The $\alpha^2 + \beta^2$ term can be regarded as due to fluctuations of induced absorption and emission processes, or as the effect of the zero-point fluctuations of the dipole interacting with the mean field gradient. For a two level atom the k^2 term is unaltered, but the α^2 and β^2 terms become more

complicated functions of the saturation parameter, and an $\alpha \cdot \beta$ term appears. There is one particularly important term in the two level atom diffusion constant which effectively limits the trap to small values of the saturation parameter. It is an α^2 term of the form

$$\frac{h^2\alpha^2 p^4(4\Omega^2+\Gamma^2)}{2\Gamma(1+p)^3} \tag{12}$$

It is the only term that does not saturate with increasing field intensity. It is also the only term which increases with the detuning Ω at fixed p. For high saturation it can be explained nicely as the result of the random walk the atom undergoes via spontaneous emission relaxation into one or the other of its two quasi-stationary "dressed states". One can see by comparison with (12), which is otherwise applicable for small $<n> = p/2(1+p)$, that this term can become dominant even for small values of p because $|\Omega/\Gamma| >> 1$ for the trapping beam.

Finally we will show that the SHO can be trapped and cooled to a very low temperature, and comment on the way this might be accomplished for a real atom. The mean translational energy W of the atom in the trap is increased by momentum diffusion and decreased by the average damping δ according to

$$dW/dt = D_p/M - \delta W \tag{13}$$

where M is the mass of the atom. In equilibrium then $W_{eq} = D_p/M\delta$. For the SHO, according to (11) we obtain $\delta W = 2<n_d>h(v\cdot k)^2$. Roughly then because the damping works only on one velocity component, and the kinetic energy is about half of the total energy, we obtain the relation $\gamma M \approx <n_d>hk^2/3$ and therefore

$$W_{eq} \approx 3h\Gamma<n_t>/<n_d> \tag{14}$$

where we have assumed that for the trapping beam $\alpha^2+\beta^2 \approx k^2$, and $<n_t>$ and $<n_d>$ are respectively the mean oscillator excitations by the trapping beam and damping beam as though they acted alone. There seems to be no obstacle in this case to cooling to an energy of the order of $h\Gamma$ or

less, corresponding to a temperature of $h\Gamma/k$, or about one millidegree K if $\Gamma = 10^8 sec^{-1}$.

For a real atom; e.g. sodium, we have calculated [7] that even without an effective damping mechanism the atom can remain in the trap for a time of the order of 1 sec. But of course it would be preferable to have a stable trap. For this one must make the atom look more like an SHO. In particular, by using a double resonance, with three levels and two superimposed trapping beams, one can envisage canceling out the dynamic "light shift" of the lower resonance so that a damping beam can stay near resonance with it. I see no reason why such a scheme should not work in principle, although it yet lacks proof.

References

[1] G. A. Askar'yan, Zh. Eksp. Teor. Fiz. *42*, 1567 (1962) [Sov. Phys. JETP *15*, 1088 (1962)].

[2] A. Ashkin Phys. Rev. Lett. *24*, 156; *25*, 1321 (1970); *40*, 729 (1978).

[3] T. W. Hansch and A. L. Schawlow, Opt. Commun. *13*, 68 (1975).

[4] D. J. Wineland and H. Dehmelt, Bull. Am. Phys. Soc. *20*, 637 (1975).

[5] V. S. Letokhov, V. G. Mingolin, and B. D. Pavlik, Zh. Eksp. Teor. Fiz *72*, 1328 (1977) [Sov. Phys. JETP *45*, 698 (1977); V. S. Letokhov and V. G. Mingolin, Appl. Phys. *17*, 99 (1978).

[6] A. Ashkin and J. P. Gordon, Opt. Lett. *4*, 161 (1979).

[7] J. P. Gordon and A. Ashkin, Phys. Rev. *A21*, 1606 (1980). The arguments above are essentially a resume of this paper, which gives the complete expression for the diffusion constant of the two level atom.

[8] R. J. Cook, Phys. Rev. *A22* 1078 (1980).

[9] M. Lax, Phys. Rev. *129*, 2343 (1963).

[10] B. R. Mollow, Phys. Rev. *188*, 1969 (1969).

Laser-Cooled and Trapped Atoms, (Proceedings of the Workshop on Spectroscopic Applications of Slow Atomic Beams, held at NBS, Gaithersburg, MD, 14-15 April 1983) Ed. by W. D. Phillips, Natl. Bur. Stand. (U.S.) Spec. Publ. 653 (1983).

Some Problems and Possibilities for Quasistatic Neutral Particle Trapping

William H. Wing

Physics Department, Optical Sciences Center, and
Arizona Research Laboratories, University of Arizona
Tucson, Arizona 85721

Some basic considerations regarding the confinement of bound neutral systems of particles in limited regions of space by slowly varying electromagnetic fields are reviewed. Electrostatic traps are described, spectroscopic linewidth is discussed, and several specific cases are described briefly. Use of a light field to lengthen the trapping time of decaying states is proposed. A universal refrigeration system utilizing trapped ions is presented, and its utility for cooling neutrals as well as other charged particles is discussed.

Keywords: atomic hydrogen, cooling, electric and magnetic fields, high-resolution spectroscopy, neutral atoms, polar molecules, positronium, Rydberg atoms, trapping.

1. Introduction

This paper will present and elaborate on several ideas regarding the trapping and confinement of small neutral objects by slowly varying electromagnetic fields, with the particular aim of producing circumstances amenable to high resolution spectroscopy: the approximation of Professor Dehmelt's "single atomic particle at rest in space" and isolated from disturbances. In keeping with the nature of this forum and with the fact that the subject has enjoyed only limited experimental success up to the present, no attempt at completeness will be made, some of the ideas will be both prospective and speculative.

I shall first describe the general principles quasistatic traps employ and discuss the questions of stability and of spectroscopic resolution. Much of this discussion will be applicable to static magnetic field traps as well. Next I shall discuss the specific cases of trapping bulk dielectrics, Rydberg atoms, metastable atoms such as atomic hydrogen and positronium in the 2S state, and polar molecules. Following that, I shall discuss the idea of lengthening trapping times by coherent reexcitation of the trapping internal state and shall present a possible universal means of refrigerating trapped particles by collisions with laser-cooled trapped ions or conceivably other neutrals. A conclusion which may be drawn is that neutral particle traps seem unlikely to replace ion traps as high precision atomic clocks unless a neutral atomic system is found which possesses overwhelming advantages for this purpose compared to trappable atomic or molecular ions.

The effects of gravity on particle traps are discussed in a brief separate note elsewhere in this volume [1].

2. Principles

2.1. The Quasistatic Regime

In quasistatic traps the characteristic frequencies of field oscillation and of particle motion are much smaller than the internal resonance frequencies of the trapped particles. Consequently, transitions between stationary states are unlikely, except for Majorana transitions which may be induced if an accidental degeneracy or near-degeneracy occurs at some point in the particle's orbit. By contrast, in the high-frequency or "optical" traps discussed elsewhere in this volume, the field oscillates at frequencies close to the particle's resonance frequencies and transitions are frequent. Direct momentum transfer between particle and field (as contrasted with momentum transfer between

particle and trap structure mediated by the field) is negligible in the quasistatic regime. This eliminates the radiative recoil method of applying trapping force to the particle and damping (cooling) its motion. At the same time, it eliminates the momentum fluctuations inherent in that force. Therefore the minimum temperature of kinetic motion should be less in a quasistatic trap than in an optical trap, provided that a powerful non-optical method of cooling can be found.* Another point of contrast between quasistatic and optical traps is the field strength that can be applied: It is much higher in the quasistatic case, if equipment of modest cost and complexity is to be used; and in addition, the high fields achievable at the focus of powerful laser beams are likely to induce ionization or dissociation of the particle to be trapped. Thus the potential wells of some proposed quasistatic traps [2-4] are deeper than those of optical traps proposed thus far [5,6]. The differing characteristics, advantages, and disadvantages of the two types suggest that both should be investigated. Ultimately, mixed-regime traps using, for example, quasistatic fields for trapping and optical fields for cooling, as is done in ion traps, may prove to be the best choice.

2.2. Basic Ideas and Constraints

2.2.1. Interaction potential energy

The interaction energy U of a stationary charge or current distribution with an electric or magnetic field can be expanded in multiple moments:

$$U(\vec{R}) = e\phi(\vec{R}) - \vec{p}\cdot\vec{E}(\vec{R}) - 1/6\sum_{j,k} q_{jk}\frac{\partial E_j(\vec{R})}{\partial x_k} + \cdots , \tag{1}$$

where, of course, e≡0 for a current distribution. $\vec{R}$ is the coordinate of the particle and $\vec{E}$ denotes, for the present, either an electric or magnetic field, as appropriate. The dipole moment can further be expanded as

$$\vec{p} = \vec{p}_1 + \frac{1}{2}\vec{p}_2(\vec{E}) \simeq \vec{p}_1 + \frac{1}{2}\,p_2\vec{E} , \tag{2}$$

the second expression applying when the particle is spherically symmetric and the field is not too strong. In the electric case, the orders of magnitude of the trapping energies given by the three terms in Eq. (1) are

$$\begin{aligned} &\text{monopole:} && e\phi_o \\ &\text{dipole:} && e\phi_o\, P_o(a_o/r_o) \\ &\text{quadrupole:} && e\phi_o\, Q_o(a_o/r_o)^2 , \end{aligned} \tag{3}$$

where e is now the electron charge, ϕ_o is the range of variation of $\phi(\vec{R})$, a_o is the Bohr radius, r_o is the range of motion of the trapped particle, and P_o and Q_o are the dipole and quadrupole moments in atomic units. Since $a_o = 5\times10^{-9}$ cm and r_o is at least 10^{-2} to 10^{-3} cm, and since P_o and Q_o are of order unity for atomic-scale particles,** the successive interactions decrease rapidly in size, and the first one not identically zero will dominate. Usually the permanent dipole moment, if not identically zero, will also dominate the induced moment. Ion traps can be rather strong on the atomic scale (a few eV in depth), whereas neutral dipole-moment traps are rather weak (a few μeV to a few meV in depth). Neutral quadrupole-moment traps are so weak that none has, to my knowledge, been considered seriously.

It is instructive to compare the depths of magnetic and electric dipole traps. Writing an atomic magnetic moment μ as $(e\hbar/2mc)\,M_o$ where m, c, and ħ are the electron mass, speed of light, and angular Planck's constant, and M_o is the moment in atomic units, we find

---

*No such scheme appears to exist at the present.

**Or at most 10^2 to 10^4, in Rydberg states.

$$\frac{\mu B}{pE} = \frac{(e\hbar/2mc)}{ea_o}\left(\frac{M_o}{E}\right)\left(\frac{B}{E}\right) = \alpha\left(\frac{M_o}{2P_o}\right)\left(\frac{B}{E}\right), \tag{4}$$

where $\alpha = e^2/\hbar c \simeq 1/137$ and $a_o = \hbar/mc\alpha$. Relation (4) suggests that when the magnetic and electric moments are comparable, for example, an atom bearing an unpaired electron or a polar molecule, the magnetic interaction energy should be about 10^2 times smaller than the electric. This would be true except for the fact that readily achievable laboratory magnetic fields are somewhat over 10^2 times larger than readily achievable laboratory electric fields ($\simeq$140,000 G vs. 500 sV/cm).* Thus, in fact, the maximum magnetic and electric interactions are about equal in this example. In Rydberg states, $P_o \simeq n^2$ whereas $M_o \simeq g_\ell \ell \leq n$. Thus the electric interaction grows with increasing n more rapidly than the magnetic as long as E_{max} and B_{max} are both limited by field technology. Ultimately, however, an n is reached at which a level crossing occurs before the technological field limit is encountered. Now the maximum interaction energy is approximately $\alpha^2 mc^2/2n^3$, half the distance between Rydberg levels [2]. The limit applies in both the electric and magnetic cases, albeit at different n. Figure 1 is a sketch of the maximum interaction strength W_{max} versus n based on these qualitative considerations.

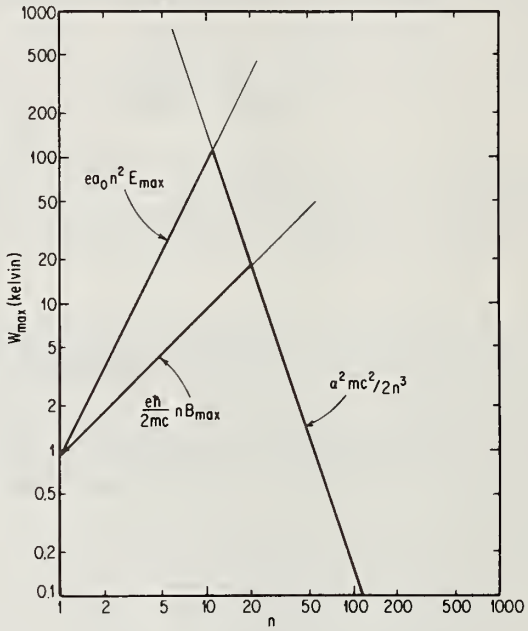

Figure 1. Maximum interaction strength vs. principal quantum number for Rydberg atoms.

2.2.2. Static stability

The starting point in discussing the stability of a particle in a quasistatic electromagnetic field is Earnshaw's Theorem, which states:

> A charged body placed in an electric field of force cannot rest in stable equilibrium under the influence of the electric forces alone [7].

The proof follows immediately from Laplace's Equation

$$\nabla^2\phi = \frac{\partial^2\phi}{\partial x^2} + \frac{\partial^2\phi}{\partial y^2} + \frac{\partial^2\phi}{\partial z^2} = 0 \tag{5}$$

*Considering the complex nature of superconductors and of dielectric breakdown phenomena, this fact may be coincidental, but it is interesting to speculate that its origin is the existence of a mechanism-independent limit on the interaction energy of a material's valence electrons with the field it can stably support, which, again considering Eq. (4), would yield $B_{max}/E_{max} \simeq 1/\alpha$.

and the relation $U = e\phi$, which show that in at least one direction of excursion away from a suspected minimum in U, U cannot increase, so that the equilibrium is unstable or at best neutral. Any combination of potential energies mathematically similar to ϕ will obey the same rule, so that, in particular, no combination of electric charges, permanent magnetic multipoles (regarded as assemblages of magnetic charges) and masses located in a region of constant electric, magnetic, and gravitational fields can rest in stable equilibrium, since each field is derivable from a potential obeying Laplace's equation.

The observed stability of ordinary matter despite the above argument "suggests, with a probability approximating to certainty, that the electrons in an atom or molecule must be in rapid orbital motion. Thus the problem of the structure of the molecule is removed from the province of Earnshaw's Theorem," as Sir James Jeans put it so elegantly [7]. Nonetheless, if we wish to approach the ideal of a particle at rest in an electromagnetic trap, we must try not to invade Earnshaw's territory in a serious way. Thus some form of motion or time variation of the trapping force must contribute significantly to the particle's positional stability.

In the simplest case - that the fields are constant in time and the particle is stationary - we must employ the latter's internal motion. The dipole energy term in Eq. (1), when incorporated into the particle's Hamiltonian, yields field-dependent energy levels W which will also be position-dependent, and hence will lead to external forces, when the field is nonuniform. The force $\vec{F} = -\vec{\nabla}_R W_\alpha(\vec{R})$ on a particle in state α will push it toward the region of lowest W. For ground-state particles, increasing the field strength will always reduce the energy. For a permanent dipole $\vec{p}_1$ this follows from the first-order perturbation energy

$$\delta W_1 = - \langle \vec{p}_1 \cdot \vec{E} \rangle = - \langle \vec{p}_1 \cdot \vec{J} \rangle \frac{M_J E}{J(J+1)} \tag{6}$$

and the fact that M_J ranges from -J to J. Here $\hbar\vec{J}$ is the particle's total angular momentum operator. For an induced dipole $\vec{p}_2(\vec{E})$ the same result follows from the second-order perturbation expression

$$\delta W_2 = \sum_i \frac{|\langle i|\vec{p}\cdot\vec{E}|o\rangle|^2}{W_o - W_i} \equiv \frac{1}{2}\vec{p}_2(\vec{E})\cdot\vec{E} \, , \tag{7}$$

where since state o is the ground state, all $W_o - W_i$ are negative.

Now, unfortunately for static trapping, the following theorem regarding field strength maxima and minima is also true:

> In a region devoid of charges and currents, the strength of a quasistatic electric or magnetic field can have local minima but not local maxima.

The theorem holds for quasistatic gravitational fields as well. The proof, which requires a few lines of vector algebra, is given in Appendix A. Consequently, particles attracted toward strong field regions, such as those in their ground states, will eventually encounter the source of the field. Although they might orbit about it if given sufficient kinetic energy, they will ultimately stick to it if cooled toward stasis.* Places isolated from the field source can exist, however, at which field strength minima occur. The regions of minima can be isolated points, lines, surfaces, and conceivably volumes, and the minimum field strength can be either zero [2] or nonzero [3]. Thus stable static trapping is possible only in excited states, which is in a sense self-contradictory, since excited states eventually decay; one might call this "Earnshaw's Revenge." Nonetheless, certain situations can be found in which the excited-state lifetime is interestingly long. Electrostatic examples include the upper inversion level of a polar molecule such as NH_3, the metastable $2^2S_{1/2}$ state of the H atom, the metastable 2^3S_1 state of the Ps (positronium) atom, and certain upper Rydberg levels of any atom. Some particulars of hypothetical trapping experiments on these substances are discussed later in this article.

*Since the above theorem does not apply to light fields, points of stability are possible at light field intensity maxima devoid of sources, e.g., on the symmetry axis of a Gaussian laser beam.

Magnetic induced-moment trapping should also be possible. An example might be the ground state of the H atom, whose Zeeman diagram is shown in Fig. 2. Here a difficulty arises, however, which seems to occur inevitably with particles containing permanent magnetic dipoles: at B=0 a degeneracy occurs between a trapping state, such as $|F=1, M_F=1\rangle$ or $|F=1, M_F=0\rangle$, and an antitrapping state, such as $|F=1, M_F=-1\rangle$. This seems to be unavoidable since the magnetic moment is an intrinsic particle property: Thus the field interaction energy is orientation-dependent, and the loss of a preferred quantization axis at B=0 will inevitably lead to degeneracy. The likelihood of Majorana transitions at B=0 then arises, the cure for which will be either to make $B \neq 0$ at the trap center or to erect a centrifugal barrier (hence add motion) to keep the particle away from the trap origin. The latter will prevent cooling of the motion to the ultimate extent, at which the particle's motional wave function would be a Σ state, with nonzero amplitude at the origin; the former introduces a perturbation.

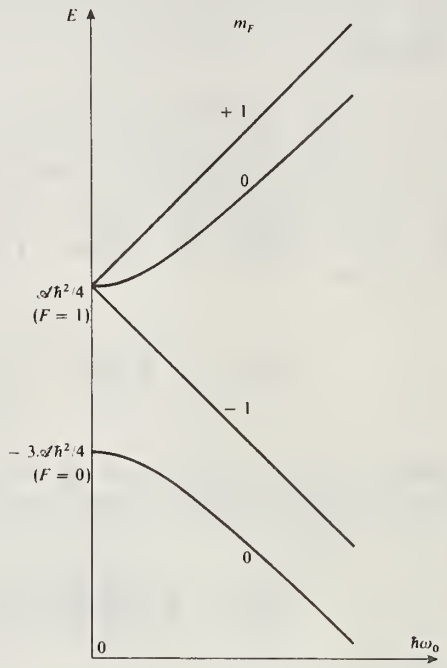

Figure 2. Hyperfine states of $H(1^2S_{1/2})$ in a magnetic field.

Given that we are willing to add a nonzero field at the trap center, we should not neglect the following possibility. Avoided crossings between energy levels may occur at fields other than zero; this happens, for example, between states of the same nonzero M_F when the Breit-Rabi energy level diagram includes $F>1$, which occurs in alkali atom ground states when the nuclear spin I is $>1/2$. These avoided crossings, unlike the one between the $M_F=0$ levels in Fig. 2, are usually nondegenerate, and so the upper one will provide a (meta)stable potential well in a magnetic field.

A polar molecule need not have a Stark level degeneracy at E=0, because its permanent electric dipole moment is not an intrinsic particle property but rather a structural property. For example, in NH_3 the inversion oscillation splits orientation states which would otherwise be degenerate in the absence of an external field.

2.2.3. Dynamical traps

a. Stability induced by motion. Many more possibilities for stability arise when motion or time-varying fields are introduced. Motion, for example, can permit stable trapping near field maxima if the resulting centrifugal effective potential barrier prevents collisions with the source of the field, as is the case for a charged particle orbiting a charged wire (Kingdon trap). However, if damping mechanisms are present, particles trapped this way will ultimately be lost, and if our goal is to cool the particle motion as much as possible, we must look elsewhere for stability. Ultimately, we would like to reduce the kinetic energy to a value approaching the quantum-mechanical minimum, as in an atomic ground state. However, in a trap of dimensions much larger than atomic, this minimum kinetic

energy will be so small that if it alone provides stability,* the system will likely be extremely susceptible to upset by external perturbations, such as vibration, stray background gas collisions, or agitation by thermal radiation, which may, for example, induce Majorana transitions to an antitrapping state. Thus, although ingenious exceptions to this rule may well be found, it seems more profitable to seek trapping situations that exhibit stability in the classical regime, where energies are large and forces are strong, and then ascertain that the stability persists at the quantum limit. Accordingly, I will not consider trapping near static-field-strength maxima further in this paper.

b. Stability induced by time-varying potential energy. I will assume at the outset that the potential energy is quadratic in the coordinates and that its time variation is sinusoidal. Although this is by no means the general case, it lends itself to analytic treatment, and the analytic results exhibit qualitative features which no doubt will persist in at least some of the other useful arrangements. Furthermore, many more complicated potentials and time dependences reduce to the above case when the amplitude of motion is small enough.

We may usefully define an intermediate regime of operation, the "Goldilocks Regime" [2]: the motion is neither too hot nor too cold. At lower temperatures quantum effects in the motion become important; at higher temperatures nonlinearities set in and, ultimately, classical chaos may result. The Goldilocks Regime, however, is nearly classical and is susceptible to analytic treatment. The motion of each particle coordinate obeys Mathieu's differential equation (see Appendix B and Section 4). For stable trapping, the stability regions of each of the coordinate equations must overlap; this generally leads to a lower limit on the field oscillation frequency.

2.3. Spectroscopic Linewidth

If the particle is in a well-defined quantum state of trap motion in both its initial and final internal states, the absorption spectrum of the trap + particle system will consist of a set of extremely sharp lines, which can be resolved using a spectrometer of sufficiently high resolution, such as an extremely high-resolution tunable laser. However, if the resolution is not high enough, or if the coherence time of a trap state is shorter than the reciprocal frequency difference between states, the individual trap resonances will be obscured and the spectral line will be broadened considerably. Defining a "bound" state as one in which the particle and trap momenta are coupled and a "free" state as one in which the momenta are decoupled, we may consider two limiting cases:

(1) initial state free, final state free or bound, uniform external potential, and

(2) both states free, different nonuniform external potentials.

2.3.1. Uniform external potential

I will treat only the energy and momentum conservation aspects, but will do so relativistically. In the initial state we have a free particle $(m,\vec{p})$ of internal energy 0, a trap $(M,\vec{P})$, and several photons $\vec{k}_i$. In the final state the particle and trap have associated to form a state of internal energy W_o and the photons have all been devoured. We may take the potential energy to be zero. Conservation rules state:

$$\text{(momentum)} \quad \Sigma\hbar\vec{k}_i + \vec{p} + \vec{P} = \vec{P}' \tag{8a}$$

$$\text{(energy)} \quad \Sigma h\nu_i + (p^2c^2+m^2c^4)^{1/2} + (P^2c^2+M^2c^4)^{1/2} = (P'^2c^2+(m+M+W_o/c^2)^2c^4)^{1/2} \tag{8b}$$

To make the situation as favorable as possible, let us have the field take care of its own momentum conservation, rather than giving some away to the masses, by setting $\Sigma\vec{k}_i=\vec{0}$ for Doppler-free multiphoton absorption. Let us also simplify the arithmetic by setting $\vec{P}=\vec{0}$. Then $\vec{P}'=\vec{p}$, and when we expand both sides of Eq. (8b) to second order and solve for $\Sigma h\nu_i$, we find

*If the source of the field is small enough and microscopically smooth and if the potential energy increases more slowly than $1/R^2$, a stable lowest motional quantum state may, in principle, exist near it [8].

$$\Sigma h\nu_i = (M+m+W_o/c^2)c^2 + \frac{p^2}{2(M+m+W_o/c^2)} + O(p^4) - mc^2 - \frac{p^2}{2m} + O(p^4) - Mc^2$$

$$\simeq W_o + \frac{p^2}{2}\left[\frac{1}{M+m+W_o/c^2} - \frac{1}{m}\right] . \qquad (9)$$

For atomic systems, $W_o/c^2 << m$. For a free-free transition, M=0 and Eq. (9) reduces to

$$\Sigma h\nu_i = W_o[1-(1/2)(p/mc)^2] , \qquad (10)$$

exhibiting the "second-order Doppler shift," whose origin can be seen from this perspective to be the mass-energy shift accompanying the change of internal state. For a free-bound trap transition, M>>m and Eq. (9) reduces to

$$\Sigma h\nu_i = W_o - p^2/2m . \qquad (11)$$

The p-dependent term is larger by the factor mc^2/W_o in the free-bound case than in the free-free case. If p^2 is statistically distributed, the free-bound case will yield much broader lines than the free-free case and thus will be unsuitable for high-resolution spectroscopy. The range of p^2 which will yield broadening in Eq. (11) will be the lesser of its thermal spread and the mean-square momentum distribution in the bound state; thus a free-bound transition may offer a means of determining the latter.

2.3.2. Different nonuniform potentials

I will treat this case nonrelativistically, assuming for simplicity that we have used the condition $\Sigma\hbar\vec{k}_i=\vec{0}$ to eliminate first-order Doppler broadening. The particle is considered "free" in both the initial and the final states. If the transition occurs over a time Δt and the particle speed is v, the inhomogeneous frequency spread due to variation of the transition frequency $(W_2-W_1)/\hbar \equiv [W_o + U_2(\vec{R}) - U_1(\vec{R})]/\hbar$ is

$$(\delta\omega)_{inhom} = |\vec{v}\cdot\vec{\nabla}_R[U_2(\vec{R}) - U_1(\vec{R})]\,\Delta t/\hbar| \qquad (12)$$

and the uncertainty-principle spread is $(\delta\omega)_{hom}=1/\Delta t$. If we assume these add in quadrature, we find the total spread to be

$$\Delta\omega = \left\{(1/\Delta t)^2 + [\vec{v}\cdot\vec{\nabla}(U_2-U_1)\Delta t/\hbar]^2\right\}^{1/2} . \qquad (13)$$

Minimizing with respect to Δt yields the optimum interaction time

$$(\Delta t)_{opt} = \left|\hbar/\vec{v}\cdot\vec{\nabla}(U_2-U_1)\right|^{1/2} \qquad (14)$$

and minimum transition width

$$(\Delta\omega)_{min} = \sqrt{2}/(\Delta t)_{opt} = 1.41\left|\vec{v}\cdot\vec{\nabla}(U_2-U_1)/\hbar\right|^{1/2} . \qquad (15)$$

The value of $(\Delta t)_{opt}$ can be set by, for example, adjusting the width of a laser beam illuminating the portion of the trap on which spectroscopy is being done.

Evidently it is desirable to do the trap spectroscopy near an extremum of U_2-U_1. $(\Delta\omega)_{min}$ is not zero here, however. Expanded to second order, the inhomogeneous frequency spread now becomes

$$(\delta\omega)_{inhom} = \left| \frac{1}{2} \frac{\partial^2}{\partial x^2} (U_2-U_1) \left(\frac{v\Delta t}{2}\right)^2 /\hbar \right| , \tag{16}$$

where the x direction is the direction of $\vec{v}$. Combining with $(\delta\omega)_{hom}$ as before and minimizing, we find

$$(\Delta t)_{opt} = 2(1/2)^{1/6} \left|\hbar/(U_2''-U_1'')v^2\right|^{1/3} \tag{17}$$

and

$$(\Delta\omega)_{min} = 1.54/(\Delta t)_{opt} = 0.87\left|(U_2''-U_1'')v^2/\hbar\right|^{1/3} . \tag{18}$$

These formulae become more transparent physically when applied to a one-dimensional harmonic trap where

$$U_{1,2} = \frac{1}{2} M\Omega_{1,2}^2 X^2 . \tag{19}$$

Then the linewidth expressions, Eqs. (15) and (18), become

$$\text{(in general)} \quad (\delta\omega)_{min} = 1.42\left|Mvx(\Omega_2^2-\Omega_1^2)/\hbar\right|^{1/2} \tag{15'}$$

$$\text{(at extrema)} \quad (\delta\omega)_{min} = 0.87\left|Mv^2(\Omega_2^2-\Omega_1^2)/\hbar\right|^{1/3} . \tag{18'}$$

Using the relation $x=v/\Omega$ for a "typical" value of x in Eq. (15'), averaging inside the absolute value brackets, and substituting $\langle Mv^2\rangle = n\hbar\Omega (n >> 1)$, we find

$$\text{(in general)} \quad (\delta\omega)_{min} = 1.42\left|n_2\Omega_2^2-n_1\Omega_1^2\right|^{1/2} \tag{15''}$$

$$\text{(at extrema)} \quad (\delta\omega)_{min} = 0.87\left|n_2\Omega_2^3-n_1\Omega_1^3\right|^{1/3} , \tag{18''}$$

where $n_{1,2}$ are the approximate quantum states of the trap motion. Since the Franck-Condon principle will be applicable, trap motional energy will be approximately conserved:

$$n_1\Omega_1 \simeq n_2\Omega_2 \equiv \bar{n}\,\bar{\Omega} \simeq kT/\hbar . \tag{20}$$

If we take Ω_1 and Ω_2 quite different, say $\Omega_2=(3/2)\bar{\Omega}$ and $\Omega_1=(1/2)\bar{\Omega}$, we finally obtain

$$\text{(in general)} \quad (\delta\omega)_{min} \simeq \bar{n}^{1/2}\,\bar{\Omega} \simeq (\Omega kT/\hbar)^{1/2} \tag{15'''}$$

$$\text{(at extrema)} \quad (\delta\omega)_{min} \simeq \bar{n}^{1/3}\,\bar{\Omega} = (\Omega^2 kT/\hbar)^{1/3} . \tag{18'''}$$

2.4. Should One Do High-Resolution Neutral-Particle Spectroscopy in a Trap?

Let us note first of all that the inhomogeneous broadening discussed in the previous section is absent in ion traps, since for monopole interactions Ω_2 always equals Ω_1. We could try to achieve this condition in special cases of neutral trapping as well. When we cannot, it will be useful to compare the trap inhomogeneity broadening with the second-order Doppler broadening in a free-particle spectroscopic experiment at the same kinetic temperature. The second-order Doppler broadening becomes,

from Eq. (10) with $\delta(p^2/2m)\simeq kT$,

$$(\delta\omega)_{2d} \simeq \frac{kT}{mc^2}\,\omega_o \,. \tag{21}$$

For a hydrogen atom at 300 K, using $kT/h=6.2\times10^{12}$ Hz, $Mc^2/h=2.2\times10^{23}$ Hz, and $\omega_o(1S\text{-}2S)=2.2\times10^{15}$ Hz, we find

$$(\delta\omega)_{2d} \simeq 6\times10^{4} \text{ Hz} \tag{22}$$

in the same conditions, with a trap of radius $r\simeq1$ cm, so that $\Omega=v/r=(10^5 \text{ cm/s})/(1 \text{ cm})=10^5$ rad/s$=1.6\times10^4$ Hz, Eqs. (15‴) and (18‴) yield inhomogeneous broadenings of at least

$$\begin{aligned} &\text{(in general)} \quad (\delta\omega)_{min} = 3\times10^{8} \text{ Hz} \\ &\text{(at minima)} \quad (\delta\omega)_{min} = 1\times10^{7} \text{ Hz.} \end{aligned} \tag{23}$$

Thus H-atom spectroscopy can be done much better in a beam than in a trap!

How can we bias the situation in the trap's favor? Lowering the temperature would seem to make its case comparatively worse rather than better, since the Doppler broadening will fall off more quickly than will either inhomogeneous broadening. Reducing Ω will eventually eliminate the trap altogether. The only reasonable approach will be to raise Ω until coherent interaction of light with particle can be maintained throughout an entire orbit or, what amounts to the same thing, until we can resolve the inhomogeneously broadened spectral line into discrete transitions between trap + particle quantum states.

This can certainly be done by setting $\Omega\simeq kT/\hbar$ so that only the lowest one or two quantum states are occupied. For lower Ω, as the motional quantum number $n=kT/\hbar\Omega$ grows, the spectrum will become dense and ultimately confused. The limiting value of Ω will be reasonable only if kT is extremely low; for example, if $T\lesssim10^{-3}$K and $n\lesssim100$, Ω can be $\simeq2\times10^5$ Hz. Now advantage could be made of the good features a trap offers, such as elimination of residual first-order Doppler broadening due to laser beam misalignment.

3. Electrostatic Trapping Examples

3.1. Bulk Dielectrics

It is often shown in elementary physics demonstrations that a dielectric slab is always drawn into a parallel-plate capacitor [Fig. 3(a)]. From the atomic point of view, the explanation is that the slab consists of ground-state atoms, whose Stark shifts are inevitably negative, and which therefore are falling downhill into the region of strongest electric field. The polarizability of these atoms is positive, which results in a bulk dielectric constant $\varepsilon>1$. However, as we have seen, the neutral point at the center of the capacitor cannot be a field strength extremum and so cannot give stable equilibrium. We might therefore wish to make a dielectric out of excited atoms having positive Stark energies, and $\varepsilon<1$, so that it would be expelled from the capacitor and could be suspended at a field strength minimum [Fig. 3(b)]. Such a dielectric would not last long; however, we can find an equivalent more permanent arrangement by noting that the energetics of such an object would be similar to those of an object of dielectric constant ε immersed in another medium of $\varepsilon'>\varepsilon$. A nice realization is a small air bubble floating in oil [Fig. 3(c)].

An electrostatic trap for air bubbles in oil is shown in Fig. 4. The quadrupole end caps are made from two tiny (#0-80) stainless-steel machine screw heads, and the ring electrode is a small (#1-72) stainless-steel machine washer. The end caps are connected electrically. The assembly is installed in a glass envelope which is filled with transparent high-voltage transformer oil, with an airspace left, and sealed off. To excite the "atoms" in the trap, the device is shaken vigorously. A potential of about 5 kV is then applied between the end caps and the ring, and a bubble is almost always trapped at the center (one can be seen in the photograph). Once charged, the trap can be disconnected from the

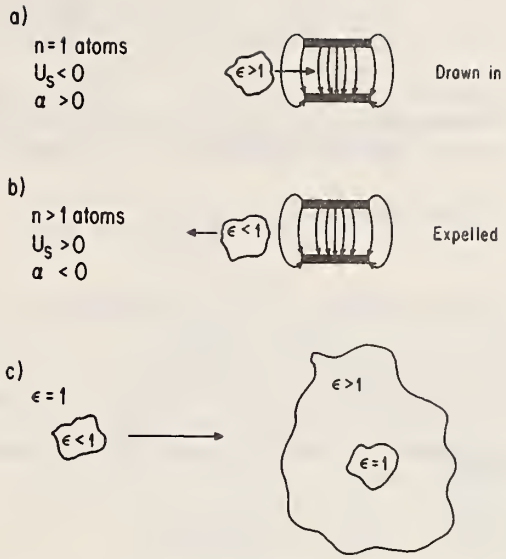

Figure 3. Dielectric particles in electric fields (see text).

voltage source and put on an overhead projector for demonstration before an audience. A small high-voltage capacitor is usually clipped across the trap leads to increase the RC leak-down time of the trap charge, and a short-focal-length lens is placed on top to compensate for the focusing effect of the round oil column.

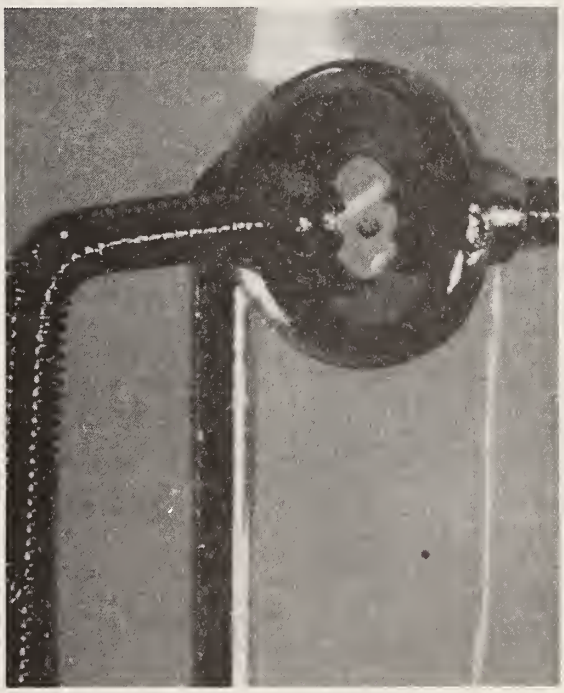

Figure 4. Electrostatic quadrupole trap containing an air bubble in oil.

If the oil viscosity is low enough, a bubble once set in motion will vibrate back and forth across the trap center a few times before damping to rest. This is sufficient to demonstrate the inherent anisotropy in the trap's restoring force: since the electrodes have roughly cylindrical symmetry, the quadrupole potential is of the form

$$\phi = \phi_o(x^2+y^2-2z^2)/2r_o^2 , \qquad (24)$$

which satisfies $\nabla^2=0$. The bubble's potential energy is

$$U = \frac{1}{2}\alpha E^2 = \frac{1}{2}\alpha(-\vec{\nabla}\phi)^2 = \frac{\alpha\Phi_o^2}{2}\,(x^2+y^2+4z^2)/R_o^2\,, \tag{25}$$

where $\alpha(>0)$ is the polarizability of the oil which has been displaced. Writing this in standard harmonic-oscillator form as $U=M(\Omega_x^2x^2+\Omega_y^2y^2+\Omega_z^2z^2)$ shows that

$$\Omega_x:\Omega_y:\Omega_z = 1:1:2\,. \tag{26}$$

Here M is the effective mass of the oil the bubble carries along as it moves.

The coup de grace in this demonstration is to short the capacitor with, for example, the metallic pocket clip of a plastic writing pen. At the crack of the spark, the bubble seems to bestir itself and lazily drifts upward, away from the trap and out of the field of view. The possibility that the lecturer may administer himself a healthy shock in the process (although he never does) heightens the drama and, hence, pedagogical impact of the demonstration.

3.2. Rydberg Atoms

As shown earlier in this article, a Rydberg atom appears to exhibit the deepest trap potential well of any system proposed to date, because its polarizability increases so rapidly with principal quantum number n. The feasibility of trapping sodium atoms in high np states has been discussed elsewhere [2]. To summarize briefly, it was found that a 16p Na atom could be trapped in an electrostatic well of depth 2.1×10^{-3} eV (17 cm^{-1}) and roughly parabolic shape (Fig. 5). The dimensions can be expressed by stating the oscillation frequency, which then determines the restoring force constant. Choosing $\Omega_x=2\pi\times10^7$ rad/s gave a maximum amplitude of oscillation of 2.2 μm, and the end cap separation could be as large as 300 μm before danger of surface breakdown arose. The limit to trapping time is the lifetime of the excited state, which, if it is predominately the zero-field 16p state, is $\tau=24$ μsec. Thus, in the absence of perturbations, x-axis trap motion would evolve through $\Omega_x\tau=1500$ radians, enough to form a well-defined orbit, before 1/e decay.

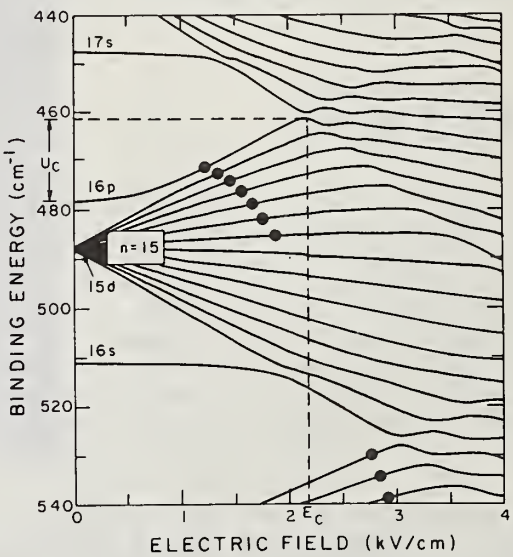

Figure 5. Some excited states of Na ($M_L=0$) about 500 cm^{-1} below the ionization limit; black dots indicate trapping states. (Adapted from M. L. Zimmerman *et al.*, (Ref. 9). U_c and E_c correspond to W_{max} and E_{max} of Fig. 1.

To try out this idea, Dr. Craig Jensen and I built an experiment (Fig. 6) at JILA, Boulder, Colorado in the spring of 1980. The idea was to excite Na atoms on the 2441-Å 3s-16p transition in a trap consisting of three aligned meshes with the outer two biased relative to the center one. A quadrupole trap well would appear in the center of each hole in the middle mesh. Trap oscillations following the

laser pulse would frequency-modulate the 4167-Å fluorescence. A narrowband etalon would convert this to an amplitude modulation, which would be digitized, averaged, and displayed. An estimated 10^3 to 10^4 fluorescent photons from Na(16p) would be detected with each laser shot. Unfortunately, we found that even the highest-purity quartz obtainable fluoresced much more strongly than this, and although the 16p fluorescence could just be detected, no oscillations were seen in the short time our other commitments allowed us to spend on this idea. Nonetheless, the principle appears sound, and accordingly the experiment seems worth describing even though a failure. A different excitation method, and perhaps a different trap design, would enhance the chance of success.

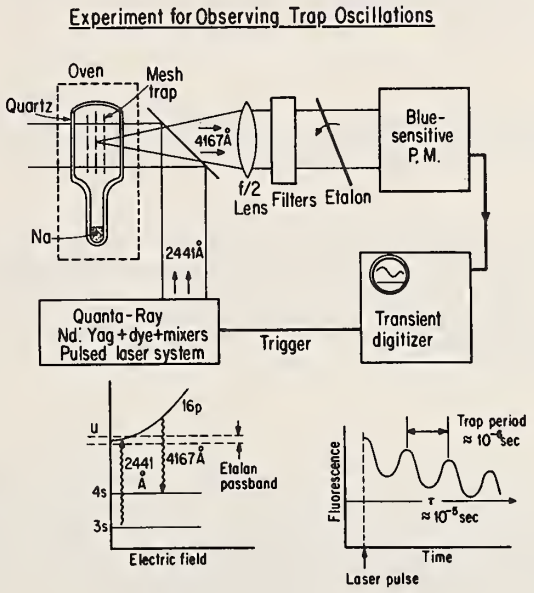

Figure 6. Experiment to detect electrostatically-trapped 16p Na atoms.

3.3. Atomic Hydrogen and Positronium in Their 2S States

Both the $2^2S_{1/2}$ state of atomic hydrogen and the 2^3S_1 state of positronium exhibit positive Stark energies, the former because it is repelled upward more strongly by the nearby $2^2P_{1/2}$ state than downward by the more distant $2^2P_{3/2}$ state, and the latter because it lies above all the other n=2 states. The weak-field Stark levels of H are shown in Fig. 7 and the fine structure of Ps(n=2) in Fig. 8. Since the Stark shift depends on $|M_J|$, atomic hydrogen has only one 2S Stark sublevel ($|M_J|=1/2$), whereas Ps will have two ($|M_J|=0,1$). I will discuss the H case in detail because it is simpler (if hyperfine structure is neglected).

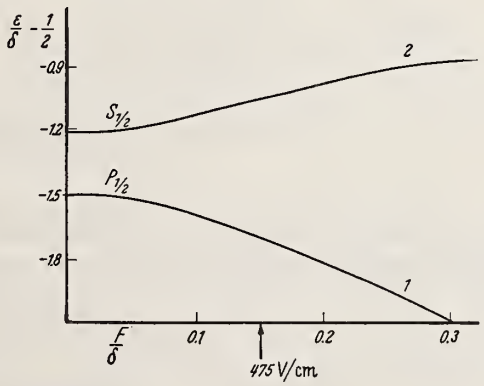

Figure 7. $2^2S_{1/2}$ and $2^2P_{1/2}$ states of H in an electric field, neglecting hyperfine structure (from Ref. 10).

The immediate difficulty would seem to be quenching of the 2S state via coupling to 2P by the trap electric field. However, this is not inevitably severe. Let us neglect the $2^2P_{3/2}$ state, and define a dimensionless field parameter $\xi = (n^2-1)^{1/2}$ nm E/S, where E and S are the electric field and Lamb shift $W(nS_{1/2})-W(nP_{1/2})$, respectively, in atomic units, n=2, and m=$|M_J|$=1/2. The field mixes 2S and 2P, producing a long-lived and a short-lived state. In weak fields, the energy W and decay rate γ of

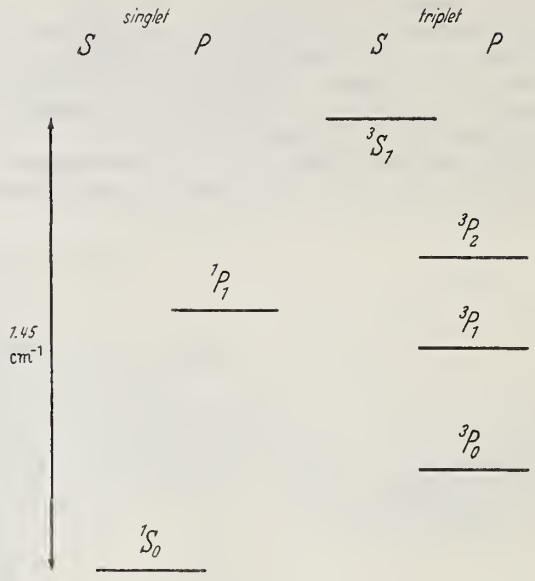

Figure 8. Fine structure of positronium, n=2 (from Ref. 10).

the long-lived state are

$$W = W_{2S} + \xi^2 S \tag{27a}$$

$$\gamma = \gamma_{2S} + \xi^2 \gamma_{2P} \cdot \tag{27b}$$

Numerically, $\gamma_{2S} \simeq 1$ Hz, $\gamma_{2P} \simeq 10^8$ Hz, and $S \simeq 10^9$ Hz. Equation (27a) shows that the trapping potential energy $U \equiv W - W_{2S}$ is harmonic. Eliminating ξ^2 yields

$$\gamma = \gamma_{2S} + (U/S)\gamma_{2P} \cdot \tag{27c}$$

Thus, when averaged over the trap motion, γ will be small for trap states having small average U. If we consider a definite motional quantum state in a quadrupole trap having quantum numbers n_x, n_y, n_z and classical oscillation frequencies Ω_x, Ω_y, Ω_z, the eigenenergy is

$$W(n_x,n_y,n_z) = W_{2S} + (n_x+1/2)\hbar\Omega_x + (n_y+1/2)\hbar\Omega_y + (n_z+1/2)\hbar\Omega_z \ , \tag{28}$$

and since $\langle U\rangle = \langle p^2/2m\rangle = (1/2)[W(n_x,n_y,n_z) - W_{2S}]$ for a harmonic oscillator,

$$\gamma(n_x,n_y,n_z) = \gamma_{2S} + \frac{1}{2}\left[(n_x+1/2)\Omega_x + (n_y+1/2)\Omega_y + (n_z+1/2)\Omega_z\right](\gamma_{2P}/S) \ . \tag{29}$$

We can simplify the spectrum further by using an axially symmetric trap; then $\Omega_x = \Omega_y = \Omega_z/2$ [Eq. (26)] and the trap energies and decay rates become

$$W_N = W_{2S} + (N+2)\ \hbar\Omega_x \tag{30}$$

$$\gamma_N = \gamma_{2S} + (N+2)(\gamma_{2P}/S)(\Omega_x/2) \ , \tag{31}$$

where $N = n_x + n_y + 2n_z$. The energy spectrum consists of a series of equally-spaced levels separated by $\hbar\Omega_x$ that grow progressively broader (Fig. 9) and become confused at $N \simeq 23$. The resolution of adjacent trap levels, if accessed spectroscopically from another bound state of the trap + particle system, is

$$\nu/\delta\nu = 2\Omega_x/(\gamma_N+\gamma_{N+1}) \simeq 4S/(2N+5)\gamma_{2P} \,. \tag{32}$$

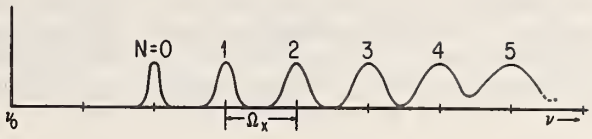

Figure 9. Qualitative sketch of the $H(2^2S_{1/2})$ state energy in an electrostatic trap. ν_0 is the free-atom energy level.

The last form becomes accurate when $\Omega_x >> \gamma_{2S}$, at which the maximum resolution of 8 is achieved for the N=0 to 1 splitting. It should be noted that if the spectrometer responds only to changes in n_z, the resolution will be doubled.

The advantage of spectroscopy in an electrostatic trap rather than in a freely expanding beam is that stray electric fields and their first derivatives become part of the trap field in the former case, and therefore can be accounted for if the individual trap levels can be resolved. However, it should be noted that if the spectroscopic line is a bound-free transition, it will be broadened by the kinetic energy of the absorbers, as shown earlier.

3.4. Polar Molecules

In polar molecules such as NH_3, the Stark levels of the upper inversion state are trapping (positive-energy) levels, whereas those of the lower inversion level are antitrapping levels [11,12]. This fact offers the possibility of stable electrostatic trapping of NH_3, the upper inversion level, with a trap well depth of a few kelvin [cf. Fig. (1)]. We could contemplate using, for example, a quadrupole or hexapole racetrack to store them. The long lifetime against radiative decay of the low-lying rotational states [13] should permit trapping for extended periods of time.* Because many polar molecules can be obtained in bulk, a large trap population should be achievable.

Laser cooling would seem difficult for polar molecules because of the large number of low-lying states: after a few cycles of pumping to an excited state and radiative decay, the population would be spread among many Stark sublevels, some of which would be antitrapping and most of which would be out of resonance with the light field. Thus we must consider alternate methods.

If a racetrack trap were filled at room temperature, only those molecules having velocities predominantly along the track, and transverse kinetic energies of at most a few kelvin, would stay in initially. Collisions would result in further loss of most of the population until the total kinetic energies dropped to a few kelvin, at which point further evaporative cooling would be quite slow. The density would presumably also be low enough that condensation would be unlikely. To cool further, we could store simultaneously a population of ions such as Mg^+ in the trap, and cool them using the optical sideband method. This would require exciting the trap with a radiofrequency voltage rather than a constant voltage, but that change should not affect the stability of the polar molecules' orbits greatly. Ion-molecule collisions would then maintain thermal equilibrium between the two populations, allowing the polar molecules to be laser-cooled indirectly.

A potential problem with this scheme is the reactions or inversion-state flips which might be induced by collisions with both the ions and other polar molecules. The solution for this problem, if there is one, would stem from the temperature dependence of the collision cross sections. At high thermal velocities, the cross sections should fall off as $(1/v)^{2/(s-1)}$, where s=2 to 4 is the inverse power law of the collisional interaction, because of the decreasing collision time. At low thermal velocities the cross sections should also fall off because the frequencies of the main Fourier components of the collisional interaction will be too low to induce a transition at the inversion frequency. In between there will be a "thermal hump" in the collisional loss rate. Whether or not it

*If the apparatus were contained in a high-Q cavity whose dimensions were small compared to the wavelength of the inversion-line radiation, the lifetime might, in principle, be extended beyond the natural lifetime, because there would be no radiation field modes available to receive the emitted photon.

will be possible to cool through the hump without losing all the molecules will depend on whether or not the maximum loss cross section is smaller than the thermalization (momentum transfer) cross section. If so, sufficiently rapid cooling will carry the sample through the loss hump with an acceptable survival rate.

Once the minimum temperature has been reached, the ions can be dumped from the trap by switching back to constant electrode voltages. Now, if the sample is cold enough, the very slow molecule-molecule collisions will be ineffective in causing inversion state flips, and we may anticipate a storage lifetime of at least several seconds, and perhaps much longer. The nature of the collisions in this situation should be quite interesting.

It should be noted finally that a racetrack geometry leads to the possibility of cyclotron acceleration using appropriate alternating field gradients, and that the coherence properties of a beam of molecules emitted by such a device in rather well-defined transverse quantum states should prove quite interesting as well.

4. The Motion of an Atom in a Quasistatic Harmonic Potential Well When Excited by a Light Field

To maintain an excited atom in a trap well beyond its natural lifetime, we may try re-exciting with a light field. This is a complex problem because there are no stationary states. In the full quantum treatment, we must include the wave motion of both the internal coordinates and the center-of-mass coordinates, and no doubt should include momentum fluctuations resulting from the quantum nature of the radiation field as well. Such a treatment is beyond the scope of this paper. It is useful, however, to examine the much simpler case of classical center-of-mass motion in a harmonic potential well under the influence of a classical light field. It seems plausible that when the potential varies little over the deBroglie wavelength of the particle, and also over the distance the particle moves during a light-induced transition, this model will represent the motion of an ensemble of real particles reasonably well, at least for times not too long.

If the particle has two internal states a and b, with external potentials U_a and U_b, which may be different, the wave function for the internal coordinates is

$$|\psi(t)\rangle = C_a(t)|a\rangle + C_b(t)|b\rangle \ . \tag{33}$$

The average force on the particle is

$$\begin{aligned} \langle \vec{F} \rangle &= \langle -\vec{\nabla}_R U \rangle = -\vec{\nabla}_R \langle \psi | U | \psi \rangle \\ &= \vec{\nabla}_R [|C_a(t)|^2 U_a + |C_b(t)|^2 U_b] \ . \end{aligned} \tag{34}$$

If the light field is intense enough and close enough to resonance that saturation occurs [$|C_a(t)|^2 = |C_b(t)|^2 = 1/2$], then whenever the <u>mean curvature</u> of the two external potentials is positive, the force is a restoring force and the particle motion is bounded for small enough kinetic energy. Since the Stark effect generally increases with principal quantum number, the stabilizing propensity of a weak-field-seeking excited-state external potential will tend to outweigh the destabilizing propensity of the strong-field-seeking ground state. Similar cases can be found with the Zeeman effect. The above analysis then offers, in principle, a mechanism for confining a two-level atom at rest in an electrostatic or magnetic trap for times longer than the upper-state decay time.

If the light field is monochromatic, and the initial condition is $|\psi(o)\rangle = |b\rangle$, the probability of finding the particle in state a subsequently is

$$|C_a(t)|^2 = (V/\Omega)^2 \sin^2(\Omega t/2) \ , \tag{35}$$

and that of b is $|C_b(t)|^2 = 1 - |C_a(t)|^2$, where V is the light-atom interaction matrix element and

$$\Omega = [(\nu-\nu_o)^2 + V^2]^{1/2} \tag{36}$$

is the Rabi frequency. Here ν is the light frequency and ν_o is the atomic transition frequency. Now the average potential energy $\langle\psi|U|\psi\rangle$ will be time dependent, as will the force given by Eq. (34). If, for example, $U_b \simeq 0$ and $U_a \simeq M\Omega_x^2(x^2+y^2+4z^2)/2$, which is the case for a high np sodium atom or a 2S hydrogen atom confined in an axially symmetric quadrupole trap, the force will be

$$\vec{F} = -(M\Omega_x^2/2)\,(V/\Omega)^2\,(1-\cos\Omega t)\,(\vec{x}+\vec{y}+4\vec{z})\ . \tag{37}$$

If the amplitude of motion is small enough, we can neglect the variation of Ω with position and velocity.* Appendix B then shows that the motion obeys Mathieu's differential equation with the parameters

$$a_x = a_y = a_z/4 = 2q_x = 2q_y = q_z/2 = 2(V/\Omega)^2(\Omega_x/\Omega)^2\ . \tag{38}$$

The first region of stability ($0<\beta<1$) is shown in Fig. 10. As the Rabi frequency Ω increases, the system moves toward the origin along the operating curve a=2q. Stability occurs when $\Omega > 1.743(V/\Omega)^2\Omega_x$.

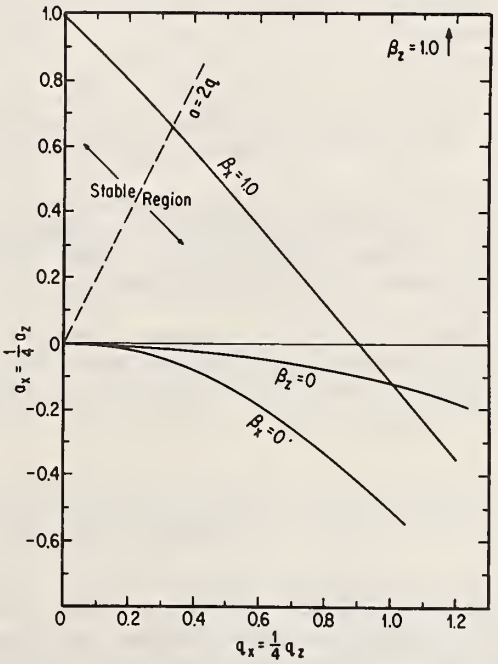

Figure 10. Mathieu stability diagram for an atom in an axially symmetric static-field trap and a light field.

Effects such as spontaneous emission which reduce the coherence between states a and b will reduce the Mathieu q's without altering the a's. The operating curve of the particle will become more and more nearly vertical. A substantial stable region will always exist; in fact, when q=0 [the vertical axis in Fig. 10], all values will give stability, since another stable region extends from β=1 to β=2. However, the stability at (a=1, q=0) is marginal since both stable and unstable regions touch this point. We may anticipate that near here there will be large fluctuations, and it will be wise to turn up the light intensity further.

5. A Universal Trapped-Particle Refrigerator

The optical-sideband cooling method [14-16] has proved very effective for certain kinds of ions, such as Ba^+ or Mg^+, which can be laser-excited readily. For many interesting cases, however, this

*Including these effects will introduce nonlinearities and (positive or negative) damping.

method is impractical. The cases include ions with no convenient energy levels, such as He^+ or high-z ions; ions with too many low-lying levels to allow a simple closed cooling cycle, such as molecular ions; ions with no energy levels, such as elementary paricles; and many neutral atoms and molecules without convenient optically excitable levels. A useful extension of the optical-sideband method would be to trap two species together, A being laser-coolable and B being the subject of interest. Collisions could then, in principle, be used to link A and B together thermally so that both could be cooled. The characteristic optical sideband cooling time is of the order of

$$\frac{1}{\tau_c} \simeq \frac{\gamma h\nu}{K}\left(\frac{v}{c}\right) , \tag{39}$$

where γ is the excitation-fluorescence cycle rate, $h\nu$ is the photon energy, v is the ion mean velocity, and K is the ion mean kinetic energy. The ion-ion thermalization time is of the order of

$$\frac{1}{\tau_{th}} \simeq \left(\frac{v}{b}\right) x^2 \ell n(1 + 1/x^2) , \tag{40}$$

where b is the ion cloud radius, e is the ion charge, and $x = e^2/2Kb$ is the "coupling parameter," the ratio of coulomb interaction energy to relative kinetic energy. In typical ion-trapping conditions, requiring $\tau_{th} \leq \tau_c$ demands $x \gtrsim 10^{-2}$ to 10^{-3}, or $b \lesssim 10^{-3}$ to 10^{-2}, for a hot (500 K) plasma; now thermalization occurs in 10^2 to 10^3 collisions. For a cold (1 K) plasma, $x \gtrsim 1$ is easy to achieve, so that thermalization occurs in one collision. Thus it is easy to keep the ion cloud constituents in thermal equilibrium while they are being cooled. Evidence for the success of this process has been seen in spectroscopy of trapped Mg^+ isotopes [11], but it does not appear to have been widely exploited.

Will it work also for ion-neutral or even neutral-neutral collisions? The interaction is shorter range now, and so the verdict is less certain. However, the coupling between an ion and a polarizable neutral is still quite strong, and my guess is that at least this combination will also work, offering a universal means of trapped-particle refrigeration of considerable usefulness.

In the ion-neutral or neutral-neutral case there is, in principle, a possibility that the collidants will stick together. However, this seems unlikely unless one of them is complex enough, and has a long enough Poincare recurrent time, that an internal vibration can absorb the collision energy and pass it from one internal mode to another until infrared radiation or another collision carries it away.

This work has been supported by the National Bureau of Standards Precision Measurement Grants Program and by the National Science Foundation. The author is also grateful for the hospitality of the Joint Institute for Laboratory Astrophyics, Boulder, the Research Laboratory for Electronics, Massachusetts Institute of Technology, Cambridge, and the Laboratoire de Spectroscopie Hertzienne, École Normal Supérieure, Paris; and for fellowship support from the John Simon Guggenheim Memorial Foundation.

6. References

[1] W. H. Wing, this volume.

[2] W. H. Wing, Phys. Rev. Lett. 45, 631 (1980).

[3] D. E. Pritchard, this volume.

[4] C. V. Heer, Rev. Sci. Instrum. 34, 532 (1963).

[5] A. Ashkin, Phys. Rev. Lett. 40, 729 (1978); A. Ashkin and J. P. Gordon, Opt. Lett. 4, 161 (1979).

[6] V. G. Minogin, Sov. J. Quantum Electron. 12(3), 299 (1982).

[7] Sir James Jeans, The Mathematical Theory of Electricity and Magnetism (Cambridge University Press, Cambridge, U.K., 1925), 5th Ed.

[8] L. D. Landau and E. M. Lifshitz, Quantum Mechanics, Non-Relativistic Theory, Second English Edition (Addison-Wesley, Reading, Mass., 1965), § 35.

[9] M. L. Zimmerman, M. G. Littman, M. M. Kash, and D. Kleppner, Phys. Rev. A 20, 2251 (1979).

[10] H. A. Bethe and E. E. Salpeter, Quantum Mechanics of One- and Two-Electron Atoms (Academic Press, New York, 1957).

[11] J. P. Gordon, H. J. Zeiger, and C. H. Townes, Phys. Rev. 95, 282L (1954).

[12] J. M. Jauch, Phys. Rev. 72, 715 (1947).

[13] J. P. Gordon, personal communication.

[14] D. J. Wineland, R. E. Drullinger, and F. L. Walls, Phys. Rev. Lett. 40, 1639 (1978).

[15] W. Neuhauser, M. Hohenstatt, P. Toschek, and H. G. Dehmelt, Phys. Rev. Lett. 41, 233 (1978).

[16] D. J. Wineland and W. M. Itano, Phys. Rev. A 20, 1521 (1979).

[17] D. J. Wineland, J. C. Bergquist, R. E. Drullinger, H. Hemmati, W. M. Itano, and F. L. Walls, J. de Physique 42, (suppl. au n°12), C8-307 (1981).

[18] J. Green, personal communication.

[19] J. Meixner and F. W. Schäfke, Mathieusche Funktionen und Sphäroidfunctionen, mit Anwerdungen auf physikalische und technische Probleme (Springer, Berlin, 1954).

[20] J. Meixner, F. W. Schäfke, and G. Wolf, Mathieu functions and spheroidal functions and their mathematical foundations, further studies (Springer, New York, 1980).

[21] M. J. O. Strutt, Lamésche-Mathieusche-und verwandte Funktionen in Physik und Technik (Chelsea, New York, 1967).

APPENDIX A: A Theorem on Field Maxima and Minima

The theorem states:

In a region devoid of charges and currents, the strength of a quasistatic electric or magnetic field can have local minima but not local maxima.

a) Maxima (nonexistence: proof by contradiction)

$\vec{E}$ may be either an electric or a magnetic field, and it will be evident that the theorem also holds for gravitational fields. Put the suspected local maximum in $|\vec{E}|$ at the coordinate origin $\vec{o}$. Then at any point $\vec{r}$,

$$\vec{E}(\vec{r}) = \vec{E}(\vec{o}) + \delta\vec{E} \qquad \text{and} \qquad \vec{E}^2(\vec{r}) = \vec{E}^2(\vec{o}) + 2\vec{E}(\vec{o})\cdot\delta\vec{E} + (\delta\vec{E})^2 \ . \tag{A.1}$$

The first and last terms of the rightmost expression are nonnegative. Thus if we have a maximum, $\vec{E}(\vec{o})\cdot\delta\vec{E}$ must be <0 for arbitrary $\vec{r}$ near $\vec{o}$. (Note: $\vec{r}$ need not be an infinitesimal.) If we take the $\hat{z}$ axis along $\vec{E}(\vec{o})$, then $\vec{E}(\vec{o})\cdot\delta\vec{E} = E_z(o)\delta E_z$ and since $E_z(o)>0$, the maximum condition reads

$$\delta E_z(\vec{r}) < 0 \text{ for arbitrary } \vec{r} \text{ near } \vec{o}. \tag{A.2}$$

Is this possible? Recall the vector identity

$$\vec{\nabla} \times (\vec{\nabla}\times\vec{E}) = \vec{\nabla}(\vec{\nabla}\cdot\vec{E}) - \nabla^2\vec{E} \ . \qquad (A.3)$$

For a quasistatic field, with $\rho=0$ and $\vec{j}=\vec{0}$, to a sufficiently good approximation

$$\vec{\nabla}\cdot\vec{E} = 0 \text{ and } \vec{\nabla}\times\vec{E} = \vec{0} \ . \qquad (A.4)$$

The first relation is exact and the second becomes exact as the time derivative of the electromagnetic field goes to zero. Thus (A.3) becomes $\nabla^2\vec{E}=0$, and thus $\nabla^2 E_z=0$, and since $\delta\vec{E}$ is a possible field, $\nabla^2\delta E_z=0$. If we now apply Green's Theorem

$$\int_V (\phi\nabla^2\psi - \psi\nabla^2\phi, d\tau = \int_S (\phi\vec{\nabla}\psi - \psi\vec{\nabla}\phi)\cdot d\vec{s} \ , \qquad (A.6)$$

with $\psi=\delta E_z$ and $\phi=1/r$ $[\nabla^2\phi=-4\pi\delta(r)]$ to a sphere of radius r centered at o, we find easily that the average of δE_z over the surface equals $\delta E_z(\vec{o})\equiv 0$. Thus if $\delta E_z(\vec{r})<0$ in some direction, it must be >0 in some other direction, and condition (A.2) above cannot be true. QED.

b) Minima (existence: proof by demonstration)

If a minimum in $|\vec{E}|$ occurs at $\vec{o}$, then except for the trivial case $\vec{E}$ = const, Eq. (A.1) requires

$$2\vec{E}(\vec{o})\cdot\delta\vec{E} + (\delta\vec{E})^2 > 0 \text{ for arbitrary } \vec{r} \text{ near } \vec{o}. \qquad (A.7)$$

This certainly can be true. The possibilities are:

a) $\vec{E}(\vec{o}) = \vec{0}$. Example: A quadrupole field $\vec{E} = c_x\vec{x} + c_y\vec{y} + c_z\vec{z}$ formed from the potential $\phi = -(c_x x^2 + c_y y^2 + c_z z^2)/2$, where since $\vec{\nabla}\cdot\vec{E} = 0$, $c_x + c_y + c_z = 0$.

b) $\vec{E}(\vec{o})\neq\vec{0}$ but $\vec{E}(\vec{o})\cdot\delta\vec{E}=0$. Example: A linear quadrupole field [$c_z=0$ in a)] plus a uniform field in the $\hat{z}$ direction. To make a true minimum in the middle, the ends of the quadrupole electrodes should be bent together somewhat.

c) $\vec{E}(\vec{o})\cdot\delta\vec{E}>0$ Now if $\delta E_z(z)>0$ for both positive and negative z near o, it must vary as z^2 or a higher even power law. Assuming the power is 2, $\phi(z)-\phi(o)$ varies as z^3 near o [3].

It is clear that several different minimum geometries exist. a), for example, gives a point minimum unless one c_i is zero, in which case it gives a line. b) also gives a line. A combination of a hexapole field and a uniform field gives a surface [18]. Bending a linear multipole field into a closed loop produces a racetrack which has a closed line minimum on the axis. The field can be nonzero there if some current or time-varying magnetic flux links the loop. No doubt ingenuity will reveal a number of other interesting geometries as well.

APPENDIX B: Motion in a Quasistatic Time-Varying Potential

This regime of operation is the "Goldilocks Regime" [2]: the motion is neither too hot nor too cold. If the particle is cooled sufficiently further, quantum wave effects in the motion will become important; if it is heated sufficiently further, classical chaotic motion may result.

We may with sufficient generality write the potential energy as

$$U(xyz) = \frac{1}{2}M(\Omega_x^2 x^2 + \Omega_y^2 y^2 + \Omega_z^2 z^2) \ . \qquad (B.1)$$

If the Ω's were constants, the motion of a particle of mass M would be 3-dimensional simple harmonic oscillation at frequencies Ω_x, Ω_y, Ω_z. Now, however, each Ω_k may include a constant and a time-varying

term:

$$\Omega_k = \Omega_{0k} + \Omega_{1k}\cos\left(\omega_k t + \phi_k\right), \qquad k=x,y, \text{ or } z \ . \tag{B.2}$$

Newton's second law then yields

$$\ddot{x}_k + [\Omega_{0k} + \Omega_{1k}\cos(\omega_k t + \phi_k)]x_k = 0 \ , \qquad k=x,y, \text{ or } z \ . \tag{B.3}$$

This is Mathieu's differential equation, which in standard form reads

$$d^2\eta/d\xi^2 + (a-2q\cos 2\xi)\eta = 0 \ . \tag{B.4}$$

Identifying corresponding variables between (B.3) and (B.4) results in

$$\eta = x_k, \quad \xi = (\omega_k t+\phi_k)/2, \quad a = 4\Omega_{0k}/\omega_k^2, \quad \text{and } q = -2\Omega_{1k}/\omega_k^2 \ . \tag{B.5}$$

The solutions of Eq. (B.4) may be classified by an order index β, whose interpretation is that as $\Omega_1 \to 0$, the βth limiting solution becomes a sinusoidal oscillation at the frequency $\beta\Omega_o$, where β is now an integer. The solutions may be bounded (stable) or unbounded (unstable) as $\xi \to \infty$; the first region of stability lies between $\beta=0$ and $\beta=1$, corresponding to the region in the a-q plane bounded by the curves

$$\begin{aligned} &(\beta=0) \quad a = -q^2/2 + q^4/128 - 29\, q^6/2304 + 68687\, q^8/18874368 + \ldots \\ \text{and} \\ &(\beta=1) \quad a = 1-q - q^2/8 + q^3/64 - q^4/1536 - 11\, q^5/35864 + \ldots \ . \end{aligned} \tag{B.6}$$

The region of three-dimensional stability is then the region of overlap of the three individual stability diagrams. If the six coefficients ($a_x \ldots q_z$) are related to a smaller number of independent physical variables, the stability region can be represented in a space of less than six dimensions; frequently only two dimensions are needed.

References [19-21] are extensive treatments of Mathieu's differential equation.

Laser-Cooled and Trapped Atoms, (Proceedings of the Workshop on Spectroscopic Applications of Slow Atomic Beams, held at NBS, Gaithersburg, MD, 14-15 April 1983) Ed. by W. D. Phillips, Natl. Bur. Stand. (U.S.) Spec. Publ. 653 (1983).

Gravitational Effects in Particle Traps

William H. Wing

Physics Department, Optical Sciences Center, and
Arizona Research Laboratories, Tucson, Arizona 85721

Schiff and Barnhill[1] have shown that an electron (mass m, charge -e) in a cavity within a metal at rest in a gravitational field $-g\hat{z}$ experiences an electric field whose average value -mg/e is just sufficient to cancel the pull of gravity. Similarly, a charged particle (mass M, charge q) in an electromagnetic trap fixed to the earth will feel an average field $E_o = Mg/q$, which amounts to 10^{-7} V/m for a proton. If the trap's vertical restoring force obeys Hooke's Law ($F_z=-k_z z=-M\Omega_z^2 z$, where Ω_z is the vertical oscillation frequency), the gravitational pull will shift the particle's equilibrium position and total energy. The latter shift is equal to the equilibrium-point potential-energy shift $\delta U_o=-M^2g^2/2k_z=-Mg^2/2\Omega_z^2$. This shift is not detectable spectroscopically, however, since it is the same for all states of the trap + particle system. The only detectable effect will be the second-order Stark shift induced by E_o, which is of order $(M/m)(\Omega_z^2/\omega_a\omega)\,\delta U_o$, where ω_a is the Bohr frequency $\simeq 4\times10^{16}$ rad/s and ω is an atomic transition frequency $\gtrsim 10^{10}$ rad/s. For any reasonable value of Ω_z the Stark energy is tiny compared to δU_o and probably is too small to measure.

A neutral particle suspended electromagnetically will also experience a nonzero-average gravitationally induced electromagnetic field. The Schiff-Barnhill field E_o becomes infinite, implying that a higher order treatment is needed, the result of which will depend on the details of the suspension method. However, the case of a harmonic-oscillator effective suspension potential energy (averaged over the micromotion, if any) covers quite a wide variety of situations, including certain permanent[2] and induced[3] dipole traps and laser traps,[4] and so the formula given above for δU_o will still apply. Since the trap stiffness in such traps generally depends on the internal or orientational coordinates of the particle, Ω_z and hence δU_o may change by a large percentage during a spectroscopic transition, and the change may be large enough to measure in a delicate experiment. For example, for a weakly trapped heavy atom for which M=200 amu and $\Omega_z=10^3$ rad/s, $\delta U_o/\hbar=1.6\times10^5$ rad/s. Considering only vertical motion, the spectroscopic transition frequency is $\omega_o-(Mg^2/2\hbar)\Delta(1/\Omega_z^2)+\Delta[(n_z+1/2)\Omega_z]$, where ω_o is the transition frequency of the free particle at rest, n_z is its vertical motional quantum number in the trap, and Δ implies the final-initial state difference. To achieve the necessary resolution, the Doppler effect must be eliminated, i.e., the photon momentum must be delivered either to the trap structure or back to the radiation field. Several tricks can be used to separate out the gravitational term despite our inability to alter g. We may vary the applied trap fields and analyze the nonlinear change in the transition frequency. We may rotate the trap 90° in the yz plane, or equivalently rotate the polarization of the spectrometer, and analyze the frequency shift, most simply when $k_y=k_z$. We may accelerate the trap and make use of the Equivalence Principle to alter the effective g. In all of these it will be desirable to avoid gravitational stress distortions of the trap structure. In certain kinds of traps (e.g., electrical) it may in principle be possible to assure this by employing a charged test particle in the same trap to measure k_y and k_z via its oscillation frequencies, and servoing them to constancy or equality.

Additional signatures of the gravitational effect may be discerned. A shift in the equilibrium point during the transition will result in altered transition probabilities between quantized trap motion states, compared to the g=0 situation. The quenching of a metastable state via a close non-metastable one, e.g., the 2S state of atomic hydrogen via the 2P, will be affected by a gravitationally induced electric field. Finally, if the trap is anharmonic (i.e., the potential energy is quartic or of higher order in the particle height), the analysis will be more complicated, but the observable energy shifts will be of the same order of magnitude as computed here, and still negligible for a charged particle.

A conversation with D. Pritchard valuably clarified these ideas.

[1] L. I. Schiff and M. V. Barnhill, Phys. Rev. 151, 1067 (1966).
[2] C. V. Heer, Rev. Sci. Instrum. 34, 532 (1963).
[3] W. H. Wing, Phys. Rev. Lett. 45, 631 (1980).
[4] A. Ashkin, Phys. Rev. Lett. 40, 729 (1978).

Laser-Cooled and Trapped Atoms, (Proceedings of the Workshop on Spectroscopic Applications of Slow Atomic Beams, held at NBS, Gaithersburg, MD, 14-15 April 1983) Ed. by W. D. Phillips, Natl. Bur. Stand. (U. S.) Spec. Publ. 653 (1983).

A Hybrid Laser-Magnet Trap for Spin-Polarized Atoms

W. C. Stwalley*

University of Iowa
Iowa City, Iowa 52242

This paper presents a brief survey of theoretical issues related to a hybrid laser-magnet trap for neutral spin-polarized atoms. At low densities, such a trap might be used to address a number of fundamental questions, e.g. the interaction of an individual atom with an electromagnetic field, while at high densities it might be used for "containerless" preparation of bulk amounts of a new metastable form of matter, spin-polarized atoms. In particular, a discussion is presented of the feasibility and limitations of a trap based on a near-resonant CW TEM^*_{01} ("doughnut mode") laser beam, which provides trapping in two dimensions, and on a strong homogeneous solenoidal magnetic field (the axis of which is also the laser axis), which provides trapping in the third dimension.

Key words: atom trap; laser; low temperature; magnetic field; neutral atom; spin-polarized atom; trapping

1. Introduction

Among the most exciting developments in atomic and molecular science in the past decade have been the prediction and preparation of bulk quantities of an entirely new (and metastable) form of matter, spin-polarized atoms (discussed in Section 3), and the preparation and detection of very small numbers of various species (even individual ions or atoms) (discussed in Section 2). A new hybrid magnet-laser concept for a low temperature trap for gaseous neutral spin-polarized atoms is proposed here (in Section 4). Such a trap could be used at low density for unique studies of small numbers of atoms and at high density for unique studies of spin-polarized atoms, in each case without confining walls.

2. Preparation and Detection of Very Few Atoms

The detection of very few atoms by laser fluorescence or ionization is now well established [1]. Much effort recently has been devoted to laser cooling [2-4] and laser trapping [3-8] of neutral atoms, inspired by the early work of Ashkin on macroscopic particles [9] and the successful RF quadrupole and Penning traps and laser cooling of atomic ions [10-15]. Related theoretical and experimental studies have also been carried out on atomic beams: deflection [16-19], focusing [20,21] and deceleration (to 70 mK!) [22]. Other 3 dimensional neutral atom traps which have been proposed include a toroidal hexapole magnet [23] for atoms with spin and an electrostatic trap [24] for highly polarizable Rydberg atoms. A new hybrid laser-magnet trap for spin-polarized neutral atoms based initially on the desire for "containerless" confinement of spin-polarized atoms is proposed here.

One of the main motivations for atom and ion traps is to be able to study these species as the temperature approaches zero and as the transition frequency becomes

* Iowa Laser Facility and Depts. of Chemistry and Physics. Supported by NASA and NSF.

increasingly well defined. Also, because a single atom or ion can absorb and emit millions of photons per second (assuming optical pumping effects are avoided), laser fluorescence is easily detected and laser cooling easily achieved, assuming only the resonant or near resonant CW lasers are available.

3. Spin-Polarized Atoms

In the 1950s, it was proposed that a spin-selected sample of H atoms might be stabilized [25,26] and, if stabilized, would be a unique quantum (Bose) gas [27]. Interest was revived in the 1970s by greatly improved calculations of the properties of spin-polarized hydrogen [28-34] and greatly improved cryogenic capabilities, leading to the first successful preparation of $\sim 10^{14}$ spin-polarized H atoms per cm^3 by Silvera and Walraven [35]. Since then, densities exceeding $10^{17}/cm^3$ have been achieved, but nuclear spin relaxation followed by recombination on the relatively inert helium-coated walls seems to be a fundamental limit preventing long time storage of higher densities (see e.g. Reference 36). Such higher densities are of great interest, e.g. a Bose-Einstein condensation (and gaseous superfluidity) is predicted [30,37] in the $10^{19} - 10^{20}/cm^3$ range (depending on temperature) and solidification [38] is predicted at $\sim 10^{22}/cm^3$.

Other spin-polarized atoms are also of considerable interest, e.g. D, Li, N, Na, although only D has yet been prepared. The first accurate calculations of the properties of spin-polarized nitrogen have recently been completed [39]. Although this substance should be a solid at low temperature, it has the highest energy content and also the promise of greater stability than spin-polarized hydrogen or deuterium. The properties of spin-polarized alkali metal atoms are also being examined; they should be non-metallic (rare-gas-like) solids at low temperature. Since the hybrid magnet-laser trap discussed below involves a CW laser near a resonance line of the atom to be trapped, this manuscript will emphasize the Li and Na atoms since appropriate CW lasers are readily available. Vacuum ultraviolet CW lasers for analagous traps for H, D or N atoms are clearly many years away (although pulsed lasers are now available for H and D [40]). Indeed the shortest wavelength CW laser we are aware of is 194 nm [41]. However, the use of magnetic and laser fields for confinement in place of walls is a very intriguing and attractive alternative.

It should be noted that spin-polarized atoms are of interest primarily for fundamental reasons: as a new form of matter, highly metastable, with extreme quantum behavior for H and D. However, possible long-term applications include energy storage, production of polarized beams, and even polarized controlled thermonuclear fusion [42, 43]. The remarkable persistence of spin-polarization in samples at room temperature and above should also be noted in this connection [44].

4. A Hybrid Magnet-Laser Trap for Neutral Spin-Polarized Atoms

As noted above, there are a variety of schemes for "containerless" (i.e. without contact with walls [45]) confinement of neutral atoms, although none have yet been implemented. Of particular interest is "containerless" confinement of spin-polarized atoms [37], especially now that the limit on spin-polarized hydrogen atom density is apparently being determined by the helium-coated walls. The minimal changes (Figure 1) to convert the existing University of Iowa low temperature-high magnetic field ($T \geq 0.012$ K, $B \leq 110$ kilogauss) system [46,47] to a hybrid laser-magnet spin-polarized atom trap would be to introduce a cylindrical laser beam on the magnet axis (defined as z). Some theoretical issues for this trap currently under study are discussed below and given in Table I. It should also be noted that the Iowa Laser Facility, containing both state-of-the-art laser and dilution refrigerator systems, is one of very few labs where such traps could in fact be built with existing equipment once these theoretical issues are resolved.

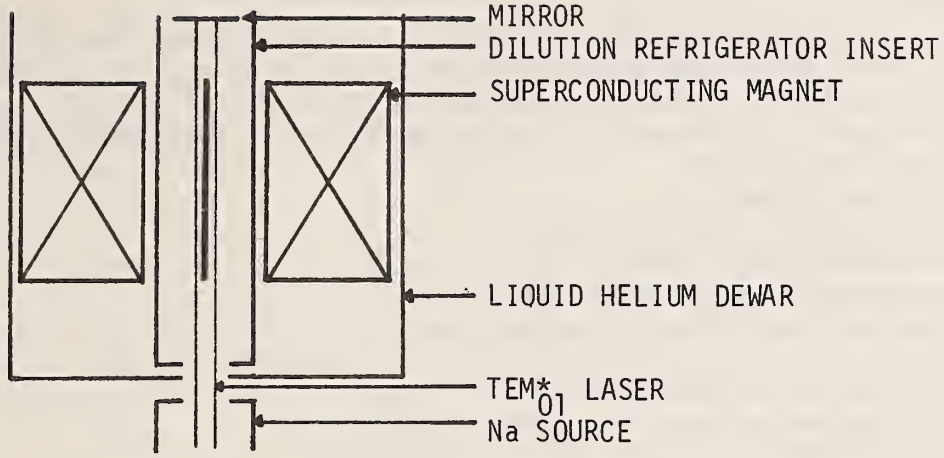

Figure 1. Schematic diagram of the hybrid laser-magnet trap apparatus includes a liquid helium cooled Na beam and coaxial laser directed into an opening in a dilution refrigerator operating below 1 K. The solid line at the center represents the trap region.

Table I. Theoretical Issues for the Hybrid Laser-Magnet Trap

A. The Trap Itself
   1. Determination of optimal laser field
      a. single-mode versus multimode
      b. detuning $\Delta\nu$ (versus laser intensity, magnetic field strength)
      c. extracavity versus intracavity (also ring cavity versus linear cavity)
      d. upper limits on power (multiphoton ionization, four-wave mixing, etc.)
      e. optical pumping concerns
      f. beam parameters (size, focused or not, polarized linear or circular, etc.), cryogenic mirrors (reflectivity, absorption)
      g. "noisy" feedback stabilized high power continuously tunable dye laser versus highly stable medium power line tunable optically pumped dimer lasers (e.g. work in this lab at 5889 Å in $^6Li_2$)
   2. Determination of optimal magnetic field
      a. magnetic field strength (presumably maximum)
      b. field inhomogeneity effects
B. Injection into the Trap
   1. Laser cooling techniques
      a. Doppler profile cooling
      b. cooling by antistokes scattering using Zeeman structure
   2. Collisional cooling
      a. magnitude of low temperature helium cross sections
      b. magnitude of inelastic collisions involving Zeeman levels
   3. Heating sources (black-body absorption, recoil, background gas)
C. Low Density Trap Effects
   1. Radiative destruction of atoms (e.g. multiphoton ionization)

Table I (continued).

2. Atomic manipulations (escape through laser field minima (for single-mode standing wave), steering with a focused laser, periodic array generation, frustrated spontaneous emission, coherent motions, etc.)
3. Tunnelling and other quantum behavior as DeBroglie wavelength approaches trap size, laser wavelength

D. High Density Trap Effects
1. Three-body atomic recombination
   a. spin-allowed to triplet ($^3\Sigma_u^+$)
   b. spin-forbidden to singlet ($^1\Sigma_g^+$)
2. Nucleation on diatomic or polyatomic molecules
3. Possibility of supersaturation by continual photodissociation of diatomic molecules with a different laser
4. Pressure broadening of spin-polarized atoms
5. Light scattering and cavity losses from atoms
6. Quantum fluid effects (e.g. possibility of Bose condensation in super-saturated spin-polarized ^{7}Li or ^{23}Na)
7. Limiting pressure (or density) at a given temperature that can be supported by a given potential well depth
8. Laser-induced radiative collisions

E. Other Issues
1. Implementation of other cooling or trapping ideas given the hybrid laser-magnet trap as an initial condition
2. Frequency standards applications
3. Experimental tests of gauge-invariant and alternative formulations of atom/field interactions
4. Hidden variable tests
5. Ultrahigh sensitivity tunable detector
6. Fundamental temperature limits
7. Multistable devices

In particular, if the laser frequency is slightly to the blue of the atomic resonance frequency, the atom will experience a relatively strong "transverse dipole" force pushing it into the central region of weaker light intensity. This force has been dramatically demonstrated in the Na atom focusing experiments of Bjorkholm and coworkers [20,21,48]. If one employs a TEM^*_{01} ("doughnut mode") laser beam (or, alternatively, a ring of ordinary overlapping TEM_{00} laser beams), one confines the atom in two dimensions (x and y, $\perp$ to the laser and magnetic axis z). They are, of course, already confined along the z direction within the magnet by their spin-polarization [49]; the potential well depth (energy to remove the atom from the magnet) in our system is ~7 K. The depth of the two dimensional laser trap has been estimated to be ~1 K by Ashkin [4] for a typical 1 watt dye laser near the 5890 Å Na resonance line. Commercial dye lasers already exceed this power at 5890 Å and, if an intracavity dye laser is used, much higher powers and much deeper trap potential wells are possible.

In such a case, one need only consider injection of atoms roughly described by a temperature $T \ll 7$ K in order to have an effective trap, i.e. one has a very "robust" trap compared to the others discussed in Section 2. Such cold atoms could possibly be formed by mixing a Na beam with 4 K He. This beam would then be cooled by laser cooling techniques discussed in Section 2 or more simply by cooling with added helium gas (even at 1 K, the vapor pressure of ^{3}He is 8.8 torr [50]). Note the helium gas is very nearly unaffected by the laser and magnetic fields, and the condensed species such as NaHe or Na_2 should also condense on the walls or pass through the system. Even if only a small fraction of the initial Na atoms was trapped, this should be adequate for low density experiments at least. Note also that other impurities (e.g. Li or K) would not be effectively trapped in a Na trap.

In addition to these questions of optimal laser field (and also optimal magnetic field) and of atomic injection, there are many other issues of high interest. For example, considering low densities first, there are obvious problems such as what power of near-resonant photons will produce an unacceptable rate of multiphoton ionization. Recall that gain or loss from the trap is readily monitored by laser fluorescence. The interaction of individual atoms with a single-mode standing wave field or with a "steering" laser field and other sorts of manipulations are of interest. For small numbers of atoms, possibilities such as generation of periodic arrays ("gratings") or of coherent motion of atoms arise. Quantum effects such as tunnelling and diffraction arise as the temperature drops and the de Broglie wavelength approaches first the laser wavelength and second the characteristic trap dimensions.

One interesting issue is the lowest kinetic temperature to which an atom can be cooled in such a trap. Pobell [51], in discussing condensed matter, has alluded to 10 μK as a "brick wall" for refrigeration, although 50 nK has been achieved for nuclear spins (not in full thermal equilibrium) [52]. There are, of course, a great many reasons for being interested in "near zero" [51,53]. In discussing laser cooling, Ashkin [4] has estimated 10^{-3} - 10^{-4} K can be achieved in his 3D laser trap; in ion traps, optical cooling to <36 mK has been achieved in two labs [14,15] and in the later case, a "magnetron temperature" of 1.3 μK has been achieved. Neuhauser et al. [14] feel their technique is capable of achieving a kinetic temperature of 10 nK!

At high densities, additional issues need to be addressed. It is clear that an important loss process will be three-body atomic recombination. Except for recent studies involving low temperature hydrogen atoms [54], atomic recombination has not been studied below 77 K. Even at ~500-620 K, Na atoms still recombine primarily on the walls, not in the gas phase [55]. The dominant recombination of Na or Li should be to form $^3\Sigma_u^+$ dimers by a spin-allowed process; it has been estimated for H that the spin-forbidden process to form $^1\Sigma_g^+$ molecules will be ~5 x 10^{-8} times slower [56]. The $^3\Sigma_u^+$ molecules (in any vibrational-rotational level) could be efficiently photodissociated (to the repulsive $^3\Pi_g$ state) at ~5515 Å for Na [57] or at ~5875 Å for Li_2 [58]. Thus, even though spin-polarized Li or Na might be expected to be a solid at low temperature, it is possible that a supersaturated spin-polarized atomic vapor can be maintained! Depending on the ultimate temperature in fact achievable with this supersaturated vapor, it might even undergo Bose condensation (^{7}Li or ^{23}Na) and other extreme quantum phenomena!

There are a number of other intriguing questions listed in Table I, e.g. questions of experimental tests of predicted line shapes and other observables for one or two photon transitions using gauge-invariant, multipolar-gauge or conventional formalisms [59]. Suffice it to say that the hybrid laser-magnet trap for neutral spin-polarized atoms is an interesting alternative low density trap concept and a quite speculative but promising possibility for a high density spin-polarized atom trap to overcome the wall recombination problem; clearly a great deal of interesting science lies ahead.

5. References

1. V. I. Balykin, G. I. Bekov, V. S. Letokhov and V. I. Mishin, Sov. Phys. Usp. 23, 651 (1980).

2. V. I. Balykin, V. S. Letokhov and V. I. Mishin, JETP Letters 29, 560 (1979).

3. A. Ashkin and J. P. Gordon, Optics Letters 4, 161 (1979).

4. A. Ashkin, Science 210, 1081 (1980).

5. A. Ashkin, Phys. Rev. Letters 40, 721 (1978).

6. V. S. Letokhov and V. G. Minogin, J. Opt. Soc. Am. 69, 413 (1979).

7. J. P. Gordon and A. Ashkin, Phys. Rev. A 21, 1606 (1980).

8. V. G. Minogin, Sov. J. Quantum Electron. 12, 299 (1982).

9. A. Ashkin, Phys. Rev. Letters 24, 156 (1970).

10. H. G. Dehmelt, Advan. At. Mol. Phys. 3, 53 (1967).

11. H. G. Dehmelt, Advan. At. Mol. Phys. 5, 109 (1969).

12. D. J. Wineland, R. E. Drullinger and F. L. Walls, Phys. Rev. Letters 40, 1639 (1978).

13. W. Neuhauser, M. Hohenstatt, P. Toschek and H. Dehmelt, Phys. Rev. Letters 42, 233 (1978).

14. W. Neuhauser, M. Hohenstatt, P. E. Toschek and H. Dehmelt, Phys. Rev. A 22, 1137 (1980).

15. W. M. Itano and D. J. Wineland, Phys. Rev. A 25, 35 (1982).

16. A. Ashkin, Phys. Rev. Letters 25, 1321 (1970).

17. E. Arimondo, H. Lew and T. Oka, Phys. Rev. Letters 43, 753 (1979).

18. A. F. Bernhardt and B. W. Shore, Phys. Rev. A 23, 1290 (1981).

19. J. E. Bjorkholm, R. R. Freeman and D. B. Pearson, Phys. Rev. A 23, 491 (1981).

20. J. E. Bjorkholm, R. R. Freeman, A. Ashkin and D. B. Pearson, Phys. Rev. Letters 41, 1361 (1978).

21. D. B. Pearson, R. R. Freeman, J. E. Bjorkholm and A. Ashkin, Appl. Phys. Letters 36, 99 (1980).

22. J. V. Prodan, W. D. Phillips and H. Metcalf, Phys. Rev. Letters 49, 1149 (1982).

23. V. S. Letokhov and V. G. Minogin, Opt. Commun. 35, 199 (1980).

24. W. H. Wing, Phys. Rev. Letters 45, 631 (1980).

25. J. T. Jones, M. H. Johnson, H. L. Mayer, S. Katz and R. S. Wright, Aeroneutronics Systems, Inc. Publication No. U-218 (1958).

26. M. W. Windsor, in Formation and Trapping of Free Radicals, edited by A. M. Bass and H. P. Broida (Academic Press, New York, 1960), page 400f.

27. C. E. Hecht, Physica 25, 1159 (1959).

28. J. V. Dugan and R. D. Etters, J. Chem. Phys. 59, 6171 (1973).

29. R. D. Etters, J. V. Dugan and R. W. Palmer, J. Chem. Phys. 62, 313 (1975).

30. W. C. Stwalley and L. H. Nosanow, Phys. Rev. Letters 36, 910 (1976).

31. M. D. Miller and L. H. Nosanow, Phys. Rev. B 15, 4376 (1977).

32. R. D. Etters, R. L. Danilowicz and R. W. Palmer, J. Low Temp. Phys. 33, 305 (1978).

33. L. J. Lantto and R. M. Nieminen, J. Low Temp. Phys. 37, 1 (1979).

34. Y. H. Uang and W. C. Stwalley, J. de Physique 51, C7-33 (1980).

35. I. F. Silvera and J. T. M. Walraven, Phys. Rev. Letters 44, 164 (1980).

36. I. F. Silvera, Physica 109 and 110B, 1499 (1982).

37. W. C. Stwalley, Y. H. Uang, R. F. Ferrante and R. W. H. Webeler, J. de Physique 41, C7-27 (1980).

38. L. H. Nosanow, J. de Physique 41, C7-1 (1980).

39. R. F. Ferrante and W. C. Stwalley, J. Chem. Phys. 78, 3107 (1983).

40. K. H. Welge and H. Zacharias, Proc. Lasers '81 Conference (1980), p. 1129

41. H. Hemmati, J. C. Bergquist and W. M. Itano, Proc. Topical Meeting on Laser Techniques for Extreme Ultraviolet Spectroscopy (Boulder, Colorado, March 1982).

42. R. M. Kulsrud, H. P. Furth, E. J. Valeo and M. Goldhaber, Phys. Rev. Letters 49, 1248 (1982).

43. D. Kleppner and T. J. Greytak, Proc. 5th Internatl. High Energy Spin Symposium (Brookhaven National Laboratory, September 1982).

44. N. D. Bhaskar, W. Happer and T. McClelland, Phys. Rev. Letters 49, 25 (1982).

45. Containerless processing, in Materials Processing in Space (National Academy of Sciences, Washington, D. C., 1978), p. 27.

46. W. C. Stwalley, J. de Physique 39, C6-108 (1978).

47. R. W. H. Webeler, R. F. Ferrante and W. C. Stwalley, J. de Physique 41, C7-161 (1980).

48. J. E. Bjorkholm, R. R. Freeman, A. Ashkin and D. B. Pearson, Phys. Rev. Letters 5, 111 (1980).

49. R. W. Cline, T. J. Greytak, D. Kleppner and D. A. Smith, J. de Physique 41, C7-151 (1980).

50. J. Wilks, Properties of Liquid and Solid Helium (Clarendon Press, Oxford, 1967).

51. F. Pobell, Physica 109 and 110B, 1485 (1982).

52. O. V. Lounasmaa, Physica 109 and 110B, 1880 (1982).

53. W. M. Fairbank, Physica 109 and 110B, 1404 (1982).

54. W. N. Hardy, M. Morrow, R. Jochemsen, B. W. Statt, P. R. Kubik, R. M. Marsolais, A. J. Berlinsky and A. Landesman, J. de Physique 41, C7-157 (1980).

55. J. P. Woerdman, S. S. Eskildsen and W. J. J. Rey, ACS Symp. Series 179, 61 (1982).

56. J. M. Yuan and T. K. Lim, J. de Physique 41, C7-39 (1980).

57. J. P. Woerdman and J. J. deGroot, ACS Symp. Series 179, 33 (1982).

58. M. E. Koch, W. C. Stwalley and C. B. Collins, Phys. Rev. Letters 42, 1052 (1979).

59. K.-H. Yang, Phys. Lett. A 94, 259 (1983).

Laser-Cooled and Trapped Atoms, (Proceedings of the Workshop on Spectroscopic Applications of Slow Atomic Beams, held at NBS, Gaithersburg, MD, 14-15 April 1983) Ed. by W. D. Phillips, Natl. Bur. Stand. (U. S.) Spec. Publ. 653 (1983).

Good and Bad Aspects of Traps for Neutral Particles

David E. Pritchard

Department of Physics and
Research Laboratory of Electronics
Massachusetts Institute of Technology
Cambridge, Massachusetts 02139

We exhibit a configuration of magnetic fields which has a field minimum at its center and is therefore suitable for trapping paramagnetic neutral atoms or molecules. The trap has a large field component along the $\hat{z}$ axis and is therefore conducive to high resolution spectroscopy. We propose an RF-laser cooling cycle which appears to be capable of attaining ultimate temperatures of $\sim 10^{-6}$K. Limits to the attainable resolution due to this temperature are discussed.

In order to label the properties of traps for neutral particles as "good" or "bad" it is necessary to have some value system. Mine is that good properties enhance the utility of these traps for studies of properties of the trapped atoms: precise spectroscopy of their levels, collision studies using a dense cold target, and possibly the "solid state" physics of their mutual interaction at high density. (From the contrasting perspective of interesting and/or challenging physics relating to slow atoms, the labels good and bad may well be reversed!)

The Trap Itself

The main requirement for achieving the objectives listed above is the ability to trap atoms in a particular quantum state with a long

(minutes) lifetime; in most cases this means atoms in their ground electronic state. We could build the trap of electric and/or magnetic fields, so it is natural to look at the strength of the relevant magnetic and electric interactions: $\mu_B B$ and $\frac{1}{2}\alpha E^2$. For my favorite atom, Na, these have strength 5 cm^{-1} and 0.02 cm^{-1} respectively at large but readily achievable laboratory fields (10^5 gauss and 10^5 V/cm respectively). From this it seems that magnetic fields are preferable, but if you consider polar diatomic molecules (eg. NaCl with dipole moment $\sim ea_0$) the energy of interaction will be $\sim$4 cm^{-1} for the lowest rotational levels (where j is no longer a good quantum number at this field). These numbers are good news: they are considerably larger than the depths of proposed optical traps (ASH78), moreover, recent experiments show that atoms whose kinetic energy is less than the above limit can be produced either by laser slowing in a beam (PPM82) or cryogenic techniques (CSG80) (note that 1 cm^{-1} = 1.4 Kelvin = $3x10^{10}$ Hz).

The second piece of good news is that traps for neutral particles can be made from static E and/or B fields. The most obvious such trap for neutrals is a long hexapole or quadrupole magnet which is bent into a circle; it would confine weak field seekers to a ring on its axis. The addition of a solenoidal field around the quadrupole would not alter the property that the weakest field was at the center: the solenoidal field would have no components in the transverse direction and the multipole field would have components only in this direction so there would

be no cross terms in $|B|^2 = |\overline{B}_{mp} + \overline{B}_s|^2$. If the solenoidal field were not quite uniform, then there would be confinement at any point(s) along the ring where the field was minimum - i.e. the solenoidal field would become a weak magnetic bottle, $\vec{B}_s \sim [(1 + \frac{1}{2}(kz)^2 - \frac{1}{4}(k\rho)^2]\vec{z} -$ $1/2(kz)(k\rho)\hat{\rho}$ where $\hat{z}$ is along the ring of confinement, confining the weak field seekers along $\hat{z}$ while expelling them along $\hat{\rho}$. However, if the quadrupole field (whose magnitude also increases linearly in ρ) is sufficiently strong, it will overcome the outward instability of the bottle. Clearly a ring-shaped region of stability is not necessary: a straight (and relatively weak) bottle plus a co-axial quadrupole field should create a trap for weak field seekers with non-zero field at the center. If the uniform B-field along $\hat{z}$ is large, the angular variation of the quantization axis will be small and Majorana flops will not occur.

Even in a trap which has zero field at its center the trapped particles will be displaced from this center by gravity (WIN83). For Na (again), the gravitational potential is $\sim$5 MHz per cm, which can obviously be quite significant in a precision spectroscopy experiment where a fairly uniform field is desired.

Trapping Potential Depends on the Quantum Level

In thinking about particle traps for neutrals, one must realize that the interaction of the trap fields with the particle, and hence the particle's motion, depends strongly on the internal quantum numbers of

the particle. Confining the particle requires a spatial variation of the potential energy of the particle; this results from the spatial variation of the field strength. If the particle makes a transition to a different quantum state with a different relationship between potential energy and field, the force and the potential energy will be different. This introduces new possibilities for cooling or heating the atoms (good), but it also introduces inhomogeneous line broadening (bad) as well as difficulties with coherent superpositions of two different states (bad). This is not true of experiments on trapped ions where, to an excellent approximation, the motion depends on only the charge and is therefore independent of the quantum state.

Let us first consider the effects of transitions between two quantum levels 1 & 2 which have different field-independent magnetic moments, μ_1 and μ_2.

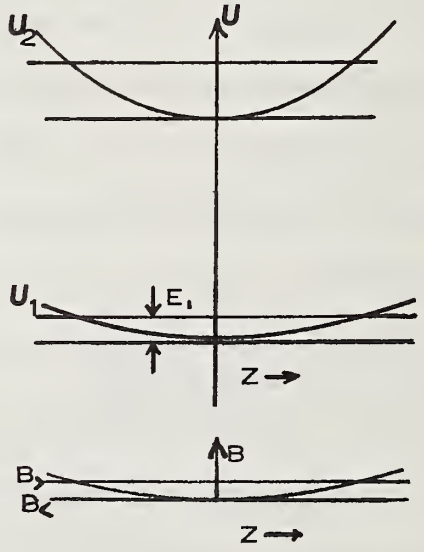

Fig. 1

Assume that the field strength varies as a function of z between $B_<$ and $B_>$ as shown in the lower part of Fig. 1; then the potentials for motion in states 1 and 2 are $U_{1,2} = \mu_{1,2}B$. If the particle is initially in state 1 with total mechanical energy (Kinetic plus Potential) E_1, then it will oscillate in z out to where $U_1 = E_1$. Since we took $\mu_2 > \mu_1$ in this example, the separation between U_2 and U_1 is not constant, leading to a broadening of the transition by the amount $h\Delta\omega = (B_>-B_<)(\mu_2-\mu_1) = E_1(\mu_2-\mu_1)/\mu_1$. This is an inhomogeneous broadening which depends on the position of the particle. It is noteworthy that a superposition of states ψ_1 and ψ_2 (produced, for example, by a very short pulse of radiation at t = 0) will decay in a time $\sim 1/\Delta\omega$. If μ_1 or μ_2 is < 0, then the particle will be bound in that state, causing an even more rapid decay of any superposition than the above limit. These considerations make us pessimistic about some proposed spectroscopy experiments on atoms trapped in E-field traps (WIN80 but see WIN83 for a possible way out). The above situation bears considerable similarity to molecular spectroscopy; in particular the last case is analogous to transitions from a bound to a repulsive potential curve, and the inhomogeneous broadening discussed previously results from the population of many vibrational levels.

Efficient Cooling

The fact that the potential energy depends on the state can be used to generate very efficient cooling, essentially because the

inhomogeneous broadening allows one to make a transition at a selected point in space. We consider now a three state system in a trap whose energy levels vary as shown in Fig. 2.

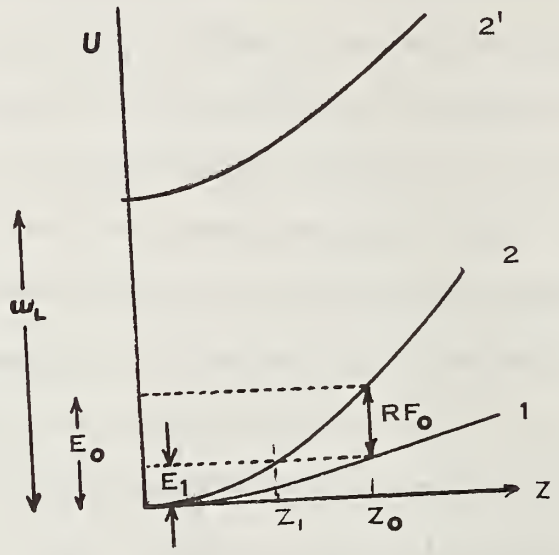

Fig. 2

Imagine that the objective is to produce cold atoms in state 2, and that initially the particles have total mechanical energy E_o. Their maximum excursion is to z_o. If radio frequency radiation is now applied at frequency RF_o it will equalize the populations in levels 1 and 2. On account of the classical Franck-Condon principle, the kinetic energy at z_o will be the same in state 1 and 2 (nearly zero as shown) but the total energy of the particles in state 1 will be reduced to E_1 due to the fact that $U_1(z_o) \ll U_2(z_o)$. If the atoms are now irradiated by

laser tuned to ω_L, atoms in level 1 will undergo transitions to 2' which may decay spontaneously back to 2 in time T_N. Neutral particle traps frequently operate in the regime where T_N << the period of oscillation in states 1 and 2 - under these conditions there will be little change of kinetic energy in the laser-induced cycle except from the momentum transferred by the light. Thus the combined RF-laser cycle has reduced the mechanical energy of the atoms in state 2 by a factor of ∿2, which restricts their motion to $|z|<z_1$. If the RF frequency is now lowered slowly, it will eventually come into resonance with the atoms a second time, cooling them again. This type of cooling cycle is very efficient, and has an ultimate lower momentum limit of a few $h\omega_L/c$ in contrast to Doppler schemes for trapped ions where the limit is $[mh/T_N]^{1/2}$ which is typically ∿x10 larger. For Na atoms the velocity corresponding to 3 photons is 9 cm/sec, and the corresponding kinetic energy is $8x10^{-6}$ cm^{-1} (0.2 MHz).

High Resolution Spectroscopy?

Use of neutral particle traps for high resolution spectroscopy requires a method of eliminating the inhomogeneous broadening which arises when $\mu_2 \neq \mu_1$. A straightforward way to do this is to bias the trap so that $\mu_2^{eff} = \mu_1^{eff}$ at the bias field, B_o [the effective moment is $\mu(B)^{eff} = \frac{-\partial U(B)}{\partial B}$ so at this field the transition frequency field is field-independent (see Fig. 3).]

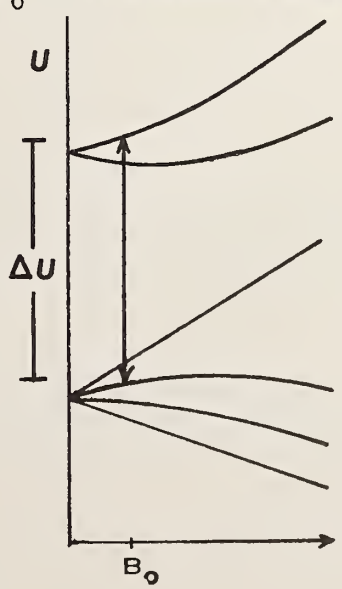

Fig. 3

If we now assume that some of the trapped particles have mechanical energy kT, it is clear that they will make excursions to regions of the trap where the field exceeds B_o by the amount $\Delta B = kT/\mu^{eff}$, shifting the transition energy by the amount $\frac{1}{2}(\Delta B)^2 \left[\frac{d^2}{dB^2}(U_2-U_1)\right]$, and causing broadening of the transition by the order $(kT)^2/\Delta U$. Taking kT to be the cooling limit obtained previously and ΔU to be $\sim$1 GHz (a typical h.f.s. separation) gives a broadening $\sim$40 Hz. This is obviously bad from the standpoint of precise hyperfine spectroscopy.

In order not to end our discussion on such a bad note, we observe that an $S \rightarrow S$ transition in an $^2S_{1/2}$ atomic ground state has the property that the two moments μ_1 and μ_2 are exactly equal at high magnetic fields where the hyperfine interaction is completely decoupled.

These speculations were supported by NSF, and the main ideas presented here were conceived and abandoned in 1977 because I could not see how to get any atoms in the trap! Recent work on both slow (PPM82) and cold (CSG80) atoms promises to overcome the filling problem, and has rekindled my interest. However, this workshop provided the real impetus for me to write them down in a coherent form.

References

ASH 78 A. Ashkin, Trapping of Atoms by Resonance Radiation Pressure, Phys. Rev. Lett. 40, 729 (1978).

CSG 80 R. Cline, D. Smith, T.J. Greytak and D. Kleppner, Confinement of Spin Polarized Atomic Hydrogen, Phys. Rev. Lett. 45, 2117 (1980).

PPM 82 John V. Prodan, William D. Phillips, Harold Metcalf, Laser Production of Very Slow Monoenergetic Atomic Beams, Phys. Rev. Lett. 49, 1149 (1982).

WIN 80 W. Wing, Electrostatic Trapping of Neutral Atomic Particles, Phys. Rev. Lett. 45, 631 (1980).

WIN 83 W. Wing, see proceedings of this conference.

Laser-Cooled and Trapped Atoms, Proceedings of the Workshop on Spectroscopic Applications of Slow Atomic Beams, held at NBS, Gaithersburg, MD, 14-15 April 1983) Ed. by W. D. Phillips, Natl. Bur. Stand. (U.S.) Spec. Publ. 653 (1983).

Cooling of Vapors Using Collisionally Aided Radiative Excitation*

E. Giacobino and P.R. Berman

Physics Department, New York University, New York, N.Y. 10003

Collisionally aided radiative excitation (CARE) is proposed as a mechanism for cooling an atomic vapor. With a CW laser power of 1.0 W/cm^2 and the resonant dipole-dipole interaction providing the collision mechanism, we estimate that temperature gradients of tens of degrees per cm can be achieved at vapor densities of order 10^{16} atoms/cm^3.

Key words: cooling, collisions, resonant broadening, laser assisted collisions.

1. Introduction

Over the past several years, there has been considerable interest in collisional processes that occur in the presence of radiation fields such as reactions of the form

$$A_1 + B_1 + \hbar\Omega \rightarrow A_2 + B_1$$

(A_i, atom A in state i; B_i, atom B in state i), which are commonly referred to as collisionally aided radiative excitation (CARE) [1]. Most experimental studies to date have concentrated on measurements of either the CARE cross sections or the frequency distribution of the reemitted light. However, it can easily be seen that CARE also produces a change in the atoms' translational energy and, as such may have potential use as a method for heating or cooling an atomic vapor [2].

*Supported in part by NSF Grant INT 7921530 and by the U.S. Office of Naval Research.

Let us consider radiation of amplitude E and frequency Ω acting on a two-level atomic system whose Bohr frequency is $\omega = \Omega - \Delta$ ($|\Delta| >>$ Doppler width). As a result of the interaction with the field, the atom may scatter a Rayleigh photon or be excited to its upper state. The latter process, although possible without collisions in strong fields, is greatly enhanced by collisions [1]. Since the final energy level of the atom is different from the energy of the absorbed photon, the energy difference must be compensated by a change in the translational energy of the colliding atoms. As pointed out previously [2] the net result is a cooling or a heating of the vapor. Tuning with $\Omega > \omega$ produces heating and that with $\Omega < \omega$ produces cooling.

2. Expected Cooling

The magnitude of the effect depends strongly on the detuning $\Delta = \Omega - \omega$: each time an atom interacts with a photon the energy $\hbar\Delta$ is removed or added to the vapor. One may choose $\hbar\Delta$ to be an appreciable fraction of kT (at 500°K kT corresponds to a frequency of 10^4 GHz or a wave number of 3×10^2 cm^{-1}), so that velocity changes are large compared with those of order 1.0 cm/sec which occur as a result of photon-recoil processes.

Of course, the process considered here involves a non-resonant atom-field interaction and the rate of excitation is reduced compared to a resonant excitation by a factor Γ^2/Δ^2 where Γ is the collision rate. (For the sake of simplicity we use expressions calculated using the impact limit of line broadening). We shall consider the case of resonant broadening; i.e. the resonant dipole-dipole interaction between two atoms of the species gives rise to the rate Γ.

The rate of excitation to level 2 from level 1, is given by

$$\dot{n}_2 = \frac{2\chi^2\Gamma}{\Delta^2}(n_1 - n_2) \tag{1}$$

where n_i is the population of state i, χ is the Rabi frequency defined by

$$\chi = \frac{\mu E}{2\hbar} \quad , \tag{2}$$

and μ is the dipole matrix element for the transition. If $n_1 >> n_2$, the steady-state upper population of state 2 is

$$n_2 = \frac{2\chi^2\Gamma}{\gamma\Delta^2} \quad , \tag{3}$$

where γ is the decay rate of the upper level. For cooling to actually occur, the atom must decay back to the ground state via spontaneous emission rather than via stimulated emission (stimulated emission would "heat" the atom if absorption cools it). This means that it is advisable to restrict the laser power such that

$$\frac{2\chi^2\Gamma}{\Delta^2} < \gamma \ . \tag{4}$$

Beyond this limit, any additional laser power is useless since there is as much stimulated emission as absorption.

For an atomic density N and cylindrical interaction volume of length L and cross-sectional area A, the power dH/dt removed from the sample is

$$\frac{dH}{dt} = \hbar\Delta \, \frac{2\chi^2\Gamma}{\Delta^2} \, NAL, \tag{5}$$

which may be rewritten as

$$\frac{dH}{dt} = \frac{\hbar\Delta}{1/\gamma} \, \frac{P}{P_m} \, NAL, \quad (P < P_m) \tag{6}$$

where P is the laser power and P_m is the maximum laser power consistent with condition (4). This result suggest a potentially large heating or cooling effect. Taking

$$\hbar\Delta/kT = 0.1 \quad (\Delta/2\pi = 10^3 \text{ GHz}) \ ; \quad \gamma/2\pi = 10 \text{ MHz};$$
$$P/P_m \simeq 10^{-7} \qquad (P \simeq 5.0 \text{ W/cm}^2 \ ; \ N \simeq 10^{15} \text{ cm}^{-3}),$$

one finds

$$\frac{1}{NAL} \, \frac{dH}{dt} \simeq 6 \ \hbar\Delta \text{ sec}^{-1} \tag{7}$$

Under such conditions, the time scale at which the energy is removed or doubled is

1.0 sec. In calculating dH/dt, we assumed the medium to be optically thin.

The above calculation has to be modified when effects of radiation trapping are taken into account. Equation (4) must be replaced by

$$\frac{2\chi^2\Gamma}{\Delta^2} < \gamma' \quad , \tag{8}$$

where γ' is the effective upper state decay rate in the presence of radiation trapping. Typically, one finds [3]

$$\gamma' \simeq \gamma/[KL\ (\pi\ \ell n\ KL)^{1/2}], \quad (KL >> 1) \tag{9}$$

where

$$K = N\sigma_o\ (\gamma/\omega_D) \tag{10}$$

is the absorption coefficient for <u>resonant</u> radiation in a Doppler broadened medium (ω_D = Doppler width). The cross section σ_o is given by

$$\sigma_o = \frac{2\Omega}{\varepsilon_o c}\frac{\mu^2}{\hbar\gamma} \simeq \lambda^2/2 \ , \tag{11}$$

where μ is the dipole matrix element and λ the wavelength for the transition.

The rate of energy loss for the sample is now given by

$$\frac{dH}{dt} = \frac{\hbar\Delta}{1/\gamma'}\frac{P}{P_m'}\,NAL, \quad (P < P_m') \tag{12}$$

where P_m' is the maximum laser power consistent with condition (8). Note that P_m' may be considerably less than P_m. However, since $P_m'/\gamma' = P_m/\gamma$, Eq. (12) may be recast in the form

$$\frac{dH}{dt} = \frac{\hbar\Delta}{1/\gamma}\frac{P}{P_m}\,NAL \ . \quad [P < P_m' = P_m(\gamma'/\gamma)] \tag{13}$$

Equation (13) is identical to the result (6) which we found in the absence of radiation trapping, except that P is limited to a smaller value.

Even though P is limited to a value equal to P'_m, significant cooling can still be achieved. For example, for the parameters chosen above, one can use Eqs. (9-11) to estimate $P'_m/P_m = \gamma'/\gamma \simeq 10^{-6}$, assuming a cell length on the order of 5cm. Since P/P_m was taken equal to 10^{-7}, one finds $P \simeq 10^{-1} P'_m$ which does not violate the condition $P < P'_m$. Thus, the expected cooling is the same as that found in Eq. (7).

3. Temperature Gradient

We can now estimate the temperature gradient in a cell created by this cooling. Considering that the atoms are perfectly thermalized on the wall of the cell, the amount of energy we must remove per second, to keep a temperature gradient dT/dr between the laser interaction region and walls is

$$\frac{1}{S}\frac{dH}{dt} = \kappa \frac{dT}{dr} \quad , \tag{14}$$

where S is the surface of the laser beam [$S = 2\sqrt{\pi AL} = \ell L$; beam circumference $= \ell$] and κ is the thermal conductivity of the gas approximately given by

$$\kappa \simeq ku/\sigma_c \tag{15}$$

where k is the Boltzmann constant, u a mean speed, and σ_c a collision cross section.

Combining Eqs. (14) and (13) and dividing by the wall temperature T_W we obtain

$$\frac{\ell}{T_W}\frac{dT}{dr} = \frac{\sigma_c}{(u/\gamma)L}\left(\frac{\hbar\Delta}{kT_W}\right)\left(\frac{P}{P_m}\right) \text{ NAL} \, . \; (P < P'_m) \tag{16}$$

We may also note that the limiting value P_m determined from condition [4] is given by

$$P_m = 2\frac{\hbar\Delta^2\Omega}{\Gamma\sigma_o} A \quad . \tag{17}$$

To optimize the temperature gradient which can be obtained, we proceed as follows: (1) We choose a density N such that the optical depth for the <u>laser radiation</u> is

equal to unity. That is, we set

$$K_L L = 1 = \frac{N\sigma_o \Gamma\gamma}{2\Delta^2} L \quad ;$$

$$N = 2\Delta^2/(\sigma_o L\Gamma\gamma) \tag{18}$$

For L ≃ 5cm, and Γ determined from theories of resonance broadening [4] (i.e. $\Gamma = 0.023\ N\ \lambda^3\gamma$), λ ≃ 600 nm, and the values of Δ and γ used above, one finds $N \simeq 2 \times 10^{16}$ atoms/cm^3. By choosing an optical depth of unity, we ensure that each photon "does its duty" in removing energy from the sample. (2) For this value of N, Eq. (9) yields a value $\gamma'/\gamma = P'_m/P_m \simeq 10^{-7}$ (3) Using Eq. (17), we estimate the maximum allowed value P'_m for P to be

$$\frac{P'_m}{A} \simeq 1 \times 10^{-7} \frac{P_m}{A} \simeq 0.2\ W/cm^2 \ .$$

(4) Since this value of P'_m/A is readily obtainable with a CW laser for A < 5 cm^2 we set P/P_m equal to its maximum allowed value (P'_m/P_m) in Eq. (16). Moreover, we take $N\sigma_c \simeq 0.1\ \Gamma/u^*$ to finally obtain

$$\frac{\ell}{T_W}\frac{dT}{dr} = 0.1 \left(\frac{\hbar\Delta}{kT_W}\right) \frac{\Gamma\gamma A}{u^2} \cdot (1 \times 10^{-7}) \ . \tag{19}$$

For A ≃ 4.0 cm^2, $\Gamma = 0.6 \times 10^{10}$ sec^{-1}, $u^2 \simeq 10^{10}$ cm/sec, $(\hbar\Delta/kT) = 0.1$,

$$\frac{\ell}{T_W}\frac{dT}{dr} \simeq 0.1 \tag{20}$$

The temperature gradients predicted by Eq. (19) (of order 10 degrees/cm) may be somewhat optimistic. However, this order of magnitude calculation does seem to indicate that significant cooling can be achieved using collisionally aided radiative excitation.

One of us (E.G.) would like to thank Dr. F. Laloe for stimulating discussions on this subject.

*We assume that the excited state population is close enough to saturation to ensure that it is resonant collisions that provide the major contribution to the thermal conductivity.

4. References

[1] See, for example, the review article by P.R. Berman and E.J. Robinson in Photon-Assisted Collisions and Related Topics edited by N.K. Rahman and C. Guidotti, (Harwood Academic Pub., Chur, Switz., 1982) pp.15-34 and other articles in this book.

[2] P.R. Berman and S. Stenholm, Opt. Comm. 24, 155 (1978).

[3] M.I. Dyakonov and V.I. Perel, Sov. Phys. - JETP 20, 997 (1965).

[4] A recent review is given by E.L. Lewis [E.L. Lewis, Phys. Rep. 58, 3 (1980)].

Laser-Cooled and Trapped Atoms, (Proceedings of the Workshop on Spectroscopic Applications of Slow Atomic Beams, held at NBS, Gaithersburg, MD, 14-15 April 1983) Ed. by W. D. Phillips, Natl. Bur. Stand. (U. S.) Spec. Publ. 653 (1983).

A Proposed Study of Photon Statistics in Fluorescence Through High Resolution Measurements of the Transverse Deflection of an Atomic Beam

K. Rubin and M. S. Lubell*

Department of Physics, The City College of C.U.N.Y., New York, NY 10031

Information about the photon statistics in fluorescence can be obtained from the study of the variance in the angular deflection of a beam of atoms interacting with a transverse laser beam. The quantity of interest, $Q = (\overline{\Delta n^2} - \bar{n})/\bar{n}$, is a measure of the departure of the photon statistics from a Poisson distribution, where $\bar{n}$ is the mean and $\overline{\Delta n^2}$ is the variance of the number of photons emitted by a "two-level" atom. We demonstrate in this paper that our existing apparatus has sufficient resolution to make a statistically significant measurement of Q.

1. Introduction

The photon statistics associated with resonance fluorescence are of considerable fundamental interest and have been the subject of several recent papers.[1-7] In particular Mandel[1] has shown that it is possible for the statistics to be Poisson, sub-Poisson, or super-Poisson according to whether the variance, $\overline{\Delta n^2}$, of the number of emitted photons is respectively equal to, less than, or greater than $\bar{n}$, the mean of the number of photons emitted. For a two-level system, Mandel defined a parameter Q, given by

$$Q = \frac{\overline{\Delta n^2} - \bar{n}}{\bar{n}} \tag{1}$$

(which is a measure of the deviation of the statistics from a Poisson distribution) and showed, for example, that at resonance the value of Q should be -3/4. It is

*Alfred P. Sloan fellow.

important that a measurement of Q be made to verify Mandel's predictions. A possible method of measuring Q, first suggested by Cook,[6] is the study of the deflection of a beam of atoms interacting with a transverse laser beam. To make a meaningful measurement of Q, however, requires a high resolution atomic beam apparatus. We propose to use such an apparatus already in existence to perform the measurement, and we will show in this paper that the apparatus has sufficient resolution to accomplish the task.

2. Proposed Experiment

The atom-laser beam geometry is shown in Figure 1. The deflection of the beam is due to absorption and a subsequent spontaneous re-emission of photons. As the

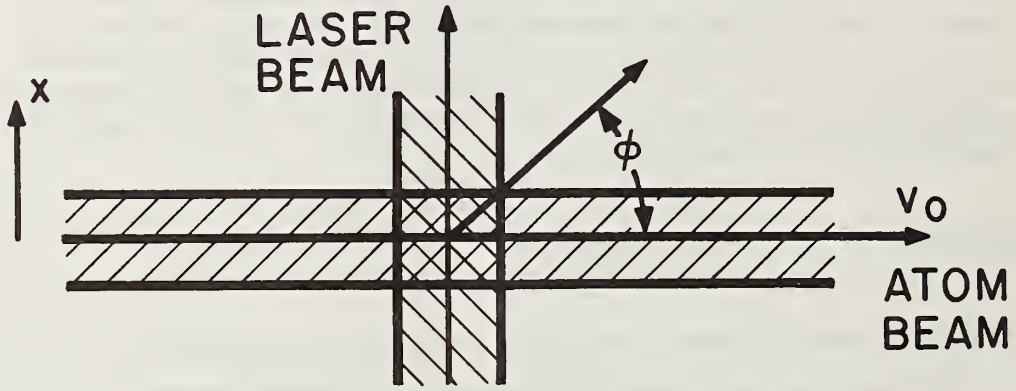

Figure 1. Atom-laser beam geometry.

atom travels through the laser field it absorbs photons and consequently recoils in the +x direction. If, in the time it takes to travel through the laser field the atom absorbs n photons it will acquire a transverse momentum equal to $(nh\nu/c)$, where h is Planck's constant, ν is the near-resonant laser frequency, and c is the speed of light. The n photons will be reradiated in a random direction, within the dipole distribution, adding a random component to the atom's momentum in the +x direction. The average angular deflection $\bar{\phi}$ of an atom of mass m initially travelling with a velocity v_0 is then given by

$$\bar{\phi} = \frac{nh\nu}{cmv_0} \tag{2}$$

for small $\bar{\phi}$. The variance in ϕ is due to both the statistical fluctuations in n and the randomness of the spontaneous decays. Thus for a monoenergetic beam of zero initial angular spread, the variance of the beam after interaction with the laser takes the form

$$\overline{\Delta\phi^2} = \left(\frac{h\nu}{cmv_0}\right)^2 \left(\overline{\Delta n^2} + \frac{2}{5}\bar{n}\right), \tag{3}$$

in which case Q can be expressed in terms of $\overline{\Delta\phi^2}$ and $\bar{\phi}$. However, in unfolding the experimental data, the initial angular dispersion and velocity distribution of the atom beam must be taken into account. Both of these quantities produce additional variances in ϕ. Consequently Q can be expressed as

$$Q = \left(\frac{cmv_0}{h\nu}\right)\left(\frac{\overline{\Delta\phi^2} - \overline{\Delta\phi_0^2} - S^2\bar{\phi}^2}{\phi}\right) - \frac{7}{5}, \tag{4}$$

where $\overline{\Delta\phi_0^2}$ is the angular dispersion in the initial beam and $S^2\bar{\phi}^2$ is due to the velocity distribution in the beam. If the velocity spread is small, S can be written as $S \approx 2\Delta v/v_0$. For an accurate measurement of Q both $\overline{\Delta\phi_0^2}$ and $S^2\bar{\phi}^2$ must be small compared to $\overline{\Delta\phi^2}$. These conditions will be satisfied if

$$\overline{\Delta\phi_0^2} < \left(\frac{h\nu}{mcv_0}\right)^2 \bar{n} \tag{5}$$

and

$$\frac{\Delta v}{v_0} < \frac{1}{2\bar{n}^{\frac{1}{2}}}. \tag{6}$$

For example, if n = 100, Eqs. (5) and (6) yield the requirements

$\overline{(\Delta\phi_0^2)}^{1/2} < 3 \times 10^{-4}$ rad and $v/v_0 < 1/20$. Both of these requirements can be satisfied with our present apparatus.

In addition to satisfying the requirements expressed by Eqs. (5) and (6), the atom beam must be prepared as a two-state system. For sodium, all the experimental conditions can be met in a spatially narrow, velocity-selected beam prepared in the F = 2, m_F = 2 hyperfine ground state. If the state-selected sodium beam intersects a circularly polarized laser beam tuned to the transition $3^2S_{1/2}$(F=2, m_F=2) to $3^2P_{3/2}$(F=3, m_F=3), a two-state approximation can be used since the laser field will cause the atom to oscillate between the (F=2, m_F=2) and (F=3, m_F=3) states until a spontaneous decay occurs with such a decay returning the atom to the initial (F=2, m_F=2) ground state.

The velocity and state selection can be accomplished as shown in Figure 2. The offset source together with the inhomogeneous magnetic field and system of slits serve as a velocity selector.[9] It can be shown that for the given dimensions and with the magnet operating in the high-field region, the range of velocities in the beam exiting from slit S_3 will be given by $(\Delta v/v_0) \approx (s_0/d)$, where s_0 is the width of the source slit and d is the displacement of the source slit from the beam axis. A ratio of 1/50 is easily attainable. The state selection is accomplished by the use of the E-H gradient magnet.[8] This magnet, operated in the low-field region, is adjusted such that the state of interest (F=2, m_F=2) passes through undeflected. For this state the magnetic force is balanced by the electric force while for other hyperfine states angular deflections will occur that will prevent them from passing through slits S_2 and S_3. The arrangement shown in Figure 2 therefore will provide a beam in the (F=2, m_F=2) hyperfine state with the required range of velocities. The angular divergence of the beam at the interaction region for the given dimensions will be less than 4×10^{-5} rad, well within the required range of values.

A scale drawing of the apparatus is shown in Figure 3, with a surface-barrier (hot-wire) atom detector (labeled I) located 130 cm downstream from the interaction region (labeled G). For the given geometry the intensity of the beam arriving at the detector can be estimated easily. Assuming that the source is operated at a vapor pressure of 10^{-1} Torr and that the dimensions of all slits are 25 μm x 2.5 mm, $\sim 10^8$ atoms/cm^{2}s will arrive on the beam axis at the plane of the detector with the desired velocity distribution and state selection. This corresponds to $\sim 2 \times 10^{-14}$ A leaving the hot-wire detector. With the use of an electron multiplier having a gain of 10^5, the final detector current will be $\sim 2 \times 10^{-9}$ A, about ten times greater than the background noise. Furthermore, if the laser beam is modulated and phase sensitive detection, employed, recoil currents

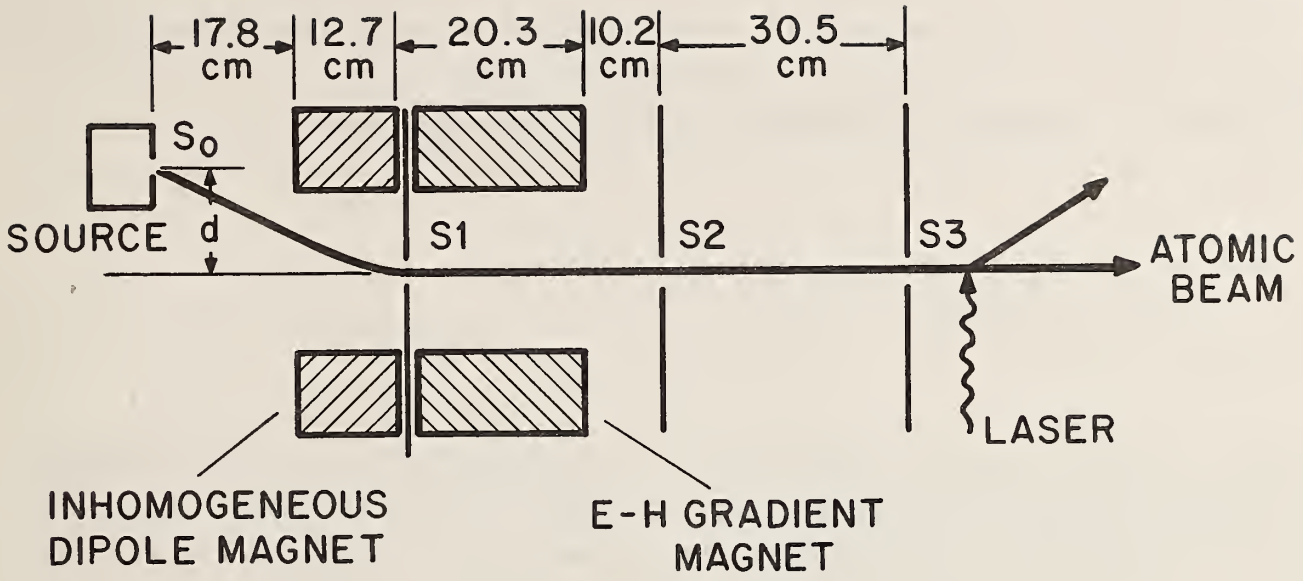

Figure 2. Schematic diagram of experiment showing the inhomogeneous dipole-magnet velocity selector and the E-H gradient magnet[8] state selector. The slits, S_0, S_1, S_2, and S_3 are all taken to have dimensions 25 μm x 2.5 mm.

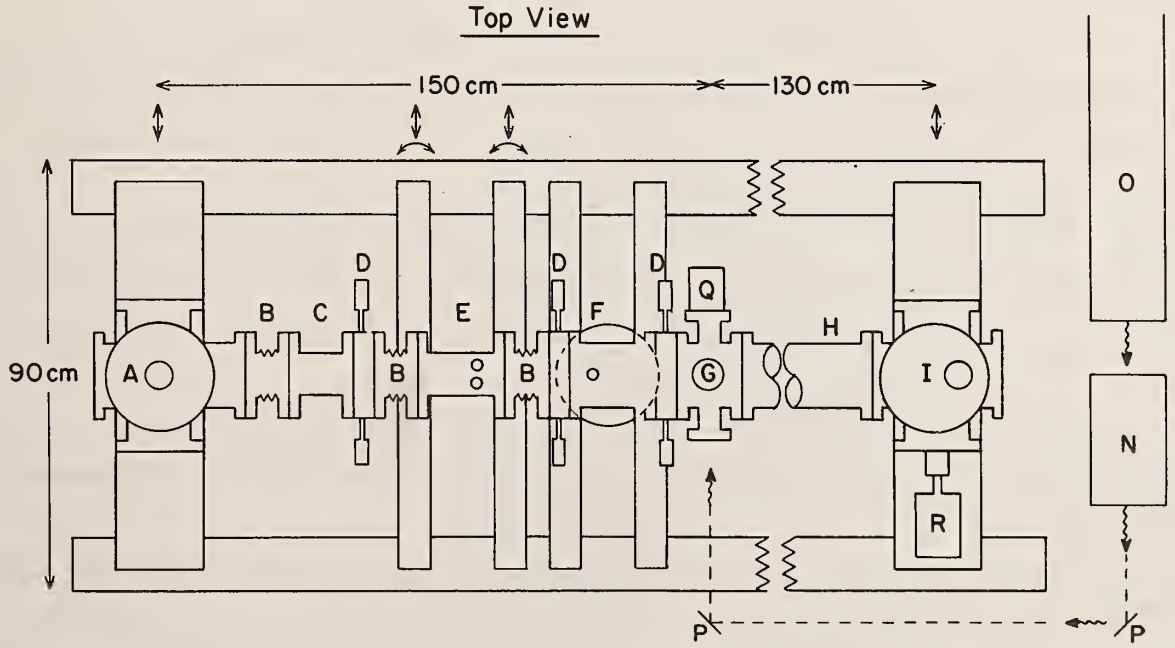

Figure 3. Scale drawing of apparatus showing atom source, A; bellows, B; velocity selector, C; adjustable slits, D; E-H gradient magnet, E; beam flag, F; interaction region, G; drift space, H; surface barrier atom detector, I; dye laser, N; argon ion laser, O; mirror, P; power metter, Q; and stepping motor, R.

that are less than 1/100 of the initial beam can be measured. Thus the beam intensity should be quite sufficient for the proposed measurements.

If the atom beam detector has a transverse resolution of 25 μm, the measurements can be carried out with an angular resolution of 2×10^{-5} rad. Now if the distribution is Poisson, the angular variance will be given by

$$\Delta\phi^2 = \left(\frac{h\nu}{cmv_0}\right)^2 \left(\frac{7}{5}\bar{n}\right) . \tag{7}$$

Assuming a laser operating single mode with a power output of ∿50 mW (more than sufficient to saturate the transition) and a beam width of ∿2.5 mm, an atom will scatter ∿100 photons in passing through the laser beam. Therefore from Eqs. 2, 3 and 6, for a Poisson distribution, $\bar{\phi}$ will be $\sim 10^{-3}$ rad and $(\overline{\Delta\phi^2})^{1/2}$ will be $\sim 4 \times 10^{-4}$ rad. Both of these quantities should be readily observable. Thus deviations from the Poisson character should be measurable, and Mandel's formulation should be eminently amenable to test.

3. References

[1] L. Mandel, Opt. Lett. 4, 205 (1979).

[2] D. Stoler, Phys. Rev. Lett. 33, 1397 (1974).

[3] H. J. Carmichael and D. F. Walls, J. Phys. B 9, L43, 1199 (1976).

[4] H. J. Kimble, M. Dagenais, and L. Mandel, Phys. Rev. Lett. 39, 691 (1977).

[5] L. Mandel, J. Optics (Paris) 10, 51 (1979).

[6] R. J. Cook, Opt. Commun. 35, 347 (1981).

[7] D. F. Walls and P. Zoller, Phys. Rev. Lett. 47, 709 (1981) and references therein.

[8] B. Bederson, J. Eisinger, K. Rubin, and A. Salop, Rev. Sci. Instr. 31, 852 (1960).

[9] K. Rubin, J. Perel, and B. Bederson, Phys. Rev. 117, 151 (1960).

Laser-Cooled and Trapped Atoms, (Proceedings of the Workshop on Spectroscopic Applications of Slow Atomic Beams, held at NBS, Gaithersburg, MD, 14-15 April 1983) Ed. by W. D. Phillips, Natl. Bur. Stand. (U. S.) Spec. Publ. 653 (1983).

Velocity Compression and Cooling of a Sodium Atomic Beam Using a Frequency Modulated Ring Laser*

M. S. Lubell† and K. Rubin

Department of Physics, The City College of C.U.N.Y., New York, NY 10031

A thorough understanding of the effects associated with velocity compression and cooling of atomic beams through laser-atom interactions requires a detailed study of the dipole radiation force. Such a study can be carried out with the use of a high-resolution atomic beam apparatus and a frequency-swept ring laser employed in a counter-propagating colinear laser-atom beam geometry. The principles of the proposed experimental program are discussed as well as directions for future research.

Keywords: Laser-cooling; atomic beams; dipole radiation force.

1. Introduction

The study of resonance radiation pressure on atoms is an old field dating back to Einstein's theoretical analysis in 1917 of the motion of an atom in an electromagnetic wave[1] and Frisch's experimental observations in 1933 of the deflection of an atomic beam by a transverse beam of incoherent resonance light.[2] The development of high power tunable lasers during the last two decades has sparked a new interest in the field,[3] with emphasis being placed both on the fundamental physics of dressed atoms and on the applications of radiation pressure to atom beam cooling,[4-7] focusing,[8-12] deflection,[13-25] and velocity analysis[13] as precursors to the development of isotope separators,[24] neutral atom storage rings, and neutral atom[6,7,25-27] and ion[28-32] traps. Of the various applications there is no doubt that the potential development of neutral atom traps has generated the greatest excitement. That such a fascination for atom trapping should exist is no surprise, given the wide range of applications which atom traps would have. Since the confined atoms could be cooled continually, their velocities would be maintained

*Research supported in part by the National Science Foundation under Grant No. PHY83028868.

†Alfred P. Sloan fellow.

substantially below 10^3 cm/s. Thus high resolution spectroscopy, free from both first and second order Doppler effects as well as motional field effects, could be carried out on a limited ensemble of atoms over long periods of time. The implications for the precision measurement of fundamental constants and the maintenance of time standards are obvious.

While the various applications of atom traps and radiation pressure in general can engender almost endless speculation, the realization of useful devices requires a fundamental understanding of the problem of an atom in strong inhomogeneous radiation fields. The understanding must be experimental as well as theoretical, in the sense that the practical limitations of laser-atom beam configurations must be determined, particularly since most proposed neutral-atom trapping schemes have well-depths ($< 10^{-2}$ eV) that are quite shallow,[33] judged both absolutely and in comparison with ion traps.

Radiation forces on atoms fall into two categories--a recoil or scattering force due to the absorption and spontaneous emission of a photon and a dipole force due to the interaction of an induced dipole moment with spatial inhomogeneities either in the impinging radiation field or in externally applied dc electric or magnetic fields. In a colinear, counter-propagating laser-atom beam geometry the recoil force can be employed to alter the velocity distribution of a beam. Specifically, the distribution can be compressed, with the mean velocity of the beam shifted toward extremely low values of the order of 10^3 cm/s. In a transverse laser-atom beam geometry, the recoil force can be used to deflect an atomic beam, with deflection angles of the order of 1 mrad easily obtained in a single interaction region.

The dipole force, likewise, can be used to induce deflections of atomic beams. However, in addition to this, it can be employed to produce strong focusing and defocusing effects which are central to the various trapping schemes. While the theoretical analysis of the recoil force is relatively simple, needing only a semi-classical treatment, the corresponding analysis of the dipole force is considerably more complex, requiring a quantized field theory or dressed atom approach if, as is often the case, the pumping of the excited state of the atom is fast compared to the natural lifetime of the excited state and the laser line is narrow compared to the natural linewidth of the atomic transition. The quantum mechanical fluctuations[27,34,35] and photon statistics[36-42] associated with such resonance-fluorescence processes are of considerable fundamental interest and have been the subject of several recent papers. Also of interest are the effective polarizabilities and magnetic moments which are needed to characterize the dressed states when external dc electric or magnetic fields are present[20].

2. Experimental Approach

2.1 Laser Cooling and Velocity Analysis

Recent work at the National Bureau of Standards (NBS) has demonstrated that a colinear counter-propagating laser-atom beam geometry can yield substantial atom beam cooling.[7] In contrast to the NBS approach we propose a frequency sweeping scheme rather than a Zeeman sweeping scheme to tune the appropriate atomic transitions. The frequency sweeping procedure, while technically somewhat complex, can be adapted more easily to the high-resolution atomic beam apparatus required for detailed studies of the radiation force and moreover with such an apparatus can produce sizable velocity compression as well as cooling.

For simplicity we consider the case of a sodium atomic beam and a ring dye laser beam in a counter-streaming configuration. Then, atoms whose Doppler-shifted absorption frequencies lie well within the laser line will have a high probability of absorbing a photon. If the laser intensity is far below the saturation limit, the lifetime of the excited atom will be determined by the spontaneous decay rate, which is approximately $6 \times 10^7\ s^{-1}$. Since the spontaneous-decay photons are emitted in random directions determined by the dipole radiation law, while the absorbed photons are always traveling opposite to the atomic beam directions, a net transfer of momentum occurs from the radiation field to the atoms in the beam, with the consequence that the beam velocity is decreased.

In the case where n photons have been absorbed and spontaneously reemitted, the average velocity decrease is $nh\nu/mc$ where ν is the frequency of the photon, m is the mass of the atom, and h and c are respectively Planck's constant and the speed of light. The stochastic nature of the spontaneous emission produces, in addition, a random distribution of velocities each with a magnitude $\sqrt{n}h\nu/mc$, as expected in a random walk problem with n encounters. Thus a spreading of the beam occurs as its longitudinal velocity decreases, with the spreading proportional to $\sqrt{n}$ and the mean decrease of the beam velocity proportional to n. In effect, the atomic beam is cooled. For a fixed laser frequency and the colinear counter-streaming geometry considered, the cooling process ceases when the reduction in the beam velocity Doppler shifts the resonant absorption frequency out of the laser line.

Consider the case of a sodium atom exposed to 3S-3P resonance radiation from a single moded laser with a linewidth of 2 MHz. The Doppler shifted frequency, ν', is given in terms of the unshifted frequency, by the expression $\nu' = \nu\gamma(1 - \beta)$, where $\gamma = (1 - \beta^2)^{-1/2}$ and $\beta = v/c$ with v the speed of the atom. For atomic velocities $v \sim 10^7$ cm/s, ν' can be approximated by $\nu' \approx \nu(1 - v/c)$, so that a

change in velocity Δv produces a change in frequency given by $\Delta\nu' = -(\nu/c)\Delta v = -(1/\lambda)\Delta v$. If an atom undergoes spontaneous emission n times, Δv in turn is given by $\Delta v \approx nh\nu/mc$. Since λ = 5890.6 A for the case considered and $h\nu/mc \sim 3$ cm/s, the spontaneous emission of about 40 photons reduces the velocity by 120 cm/s, an amount sufficient to shift the absorption frequency out of the laser line. Thus the velocity profile of the atomic beam will have a gap in it of width 120 cm/s centered at a value determined by the mean Doppler-shifted laser frequency. If the 3S-3P transition is saturated, spontaneous emission will take place at the rate of 3×10^7 photons/s. Therefore a sodium beam travelling at a mean velocity of $\sim 10^5$ cm/s will have a hole of width 120 cm/s burned into its velocity distribution after it has travelled a distance of only 0.13 cm.

If the laser providing the Doppler shifted resonance radiation is operated multi-mode rather than single-mode, a series of holes will be burned into the velocity distribution separated by a distance $\delta v = \lambda\delta\nu$, where $\delta\nu$ is the mode-spacing. Evidence of such holes has been found in exploratory studies at CCNY, where a multi-mode dye laser with 500 MHz mode-spacing and a 20 MHz linewidth was used, yielding the expected hole separation of $\sim 3 \times 10^4$ cm/s.

From the foregoing description it is clear that for the purpose of slowing down an atomic beam and compressing its velocity distribution, some means must be devised to keep the atoms in resonance with the incident radiation as their velocities are reduced. Added to this problem are the difficulties introduced by the hyperfine structure which can cause populations to build up in states which are completely out of resonance with the incident radiation. In order to overcome these complications we will consider a cooling scheme which utilizes circularly polarized light from a frequency swept single-moded dye laser.

The energy levels, and transitions, pertinent to the cooling scheme are shown in Figure 1. As can be seen, the ground state hyperfine splitting is 1771 MHz, considerably larger than an achievable single-mode laser linewidth of ~ 2 MHz. In general, the sodium atomic beam will have populations in both the F = 1 and F = 2 hyperfine levels of the $3^2S_{1/2}$ ground state. The v^3-Maxwellian velocity profiles for this situation are illustrated in Figure 2(b) for effusive flow of sodium from an oven at a temperature of 750 K.

Suppose at the outset the laser is tuned to a frequency which drives the T_{12} transition (shown in Figure 1) for atoms at the lower end ($\sim 10^4$ cm/s) of the velocity distribution. If $M_F = +1$ circularly polarized light is employed, only the $M_{F'} = 0, +1, +2$ sublevels of the F' = 2 hyperfine state will be excited as indicated in Figure 1. No other transitions will be driven initially because of the level spacings, the laser linewidth, and the low-velocity Doppler tuning condition.

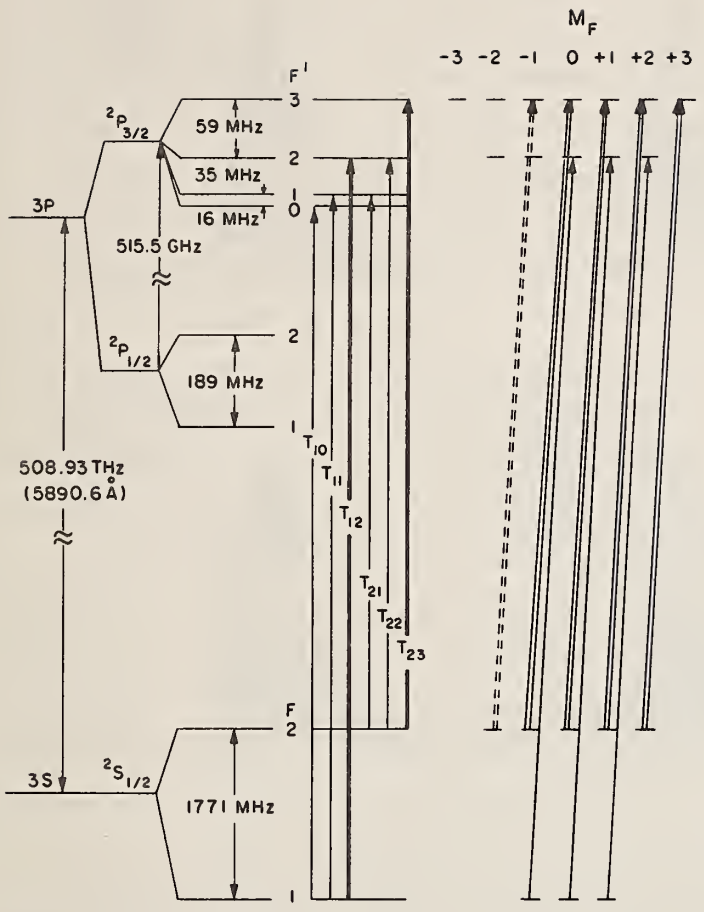

Figure 1. Energy level diagram of sodium. Shown at the left are the frequency spacings of the hyperfine levels of the 3S and 3P states together with the allowed optical transitions from the 3S to 3P manifold. The T_{12} and T_{23} transitions (indicated in bold) are the transitions to be used for the beam cooling process. Shown at the right are the relevant transitions between hyperfine magnetic substates for the circularly polarized light used in the cooling process. Single lines are used for transitions from the $3^2S_{1/2}$, F = 1 sublevels and double lines, for transition from the $3^2S_{1/2}$, F = 2 sublevels. The dashed double line indicates an allowed transition from a sublevel which has no available population during the cooling process.

Consequently, the F = 2 hyperfine level of the ground state will be optically pumped, with the M_F = -1, 0, +1, +2 substates all represented.

If the laser frequency now is swept downward as shown in Figure 2(a), the depletion of the F = 1 velocity profile will be swept upward in velocity. For a frequency sweep rate of 1.5 GHz/ms, a regime which is now technically accessible,[43] and a laser linewidth of 2 MHz any atom will remain in resonance for 1.3 μs, long enough under saturation conditions for 40 spontaneous decays to occur. Thus substantial pumping of the F = 2 hyperfine state will take place. This situation is illustrated in Figure 2(b) at a time t_1 = 0.28 ms after the start of the frequency sweep. As the sweep proceeds, the frequency of the laser will eventually come into resonance with the low-velocity Doppler-shifted T_{23} transition. This situation is illustrated in Figure 2(c) at a time t_2 = 0.13 ms after the start of the sweep. The T_{23} ΔM_F = +1 resonance absorption light optically pumps the M_F = +2 sublevel of the F = 2 hyperfine state, as shown in Figure 2(d) at a time t_3 = 2.0 ms after the start of the sweep.

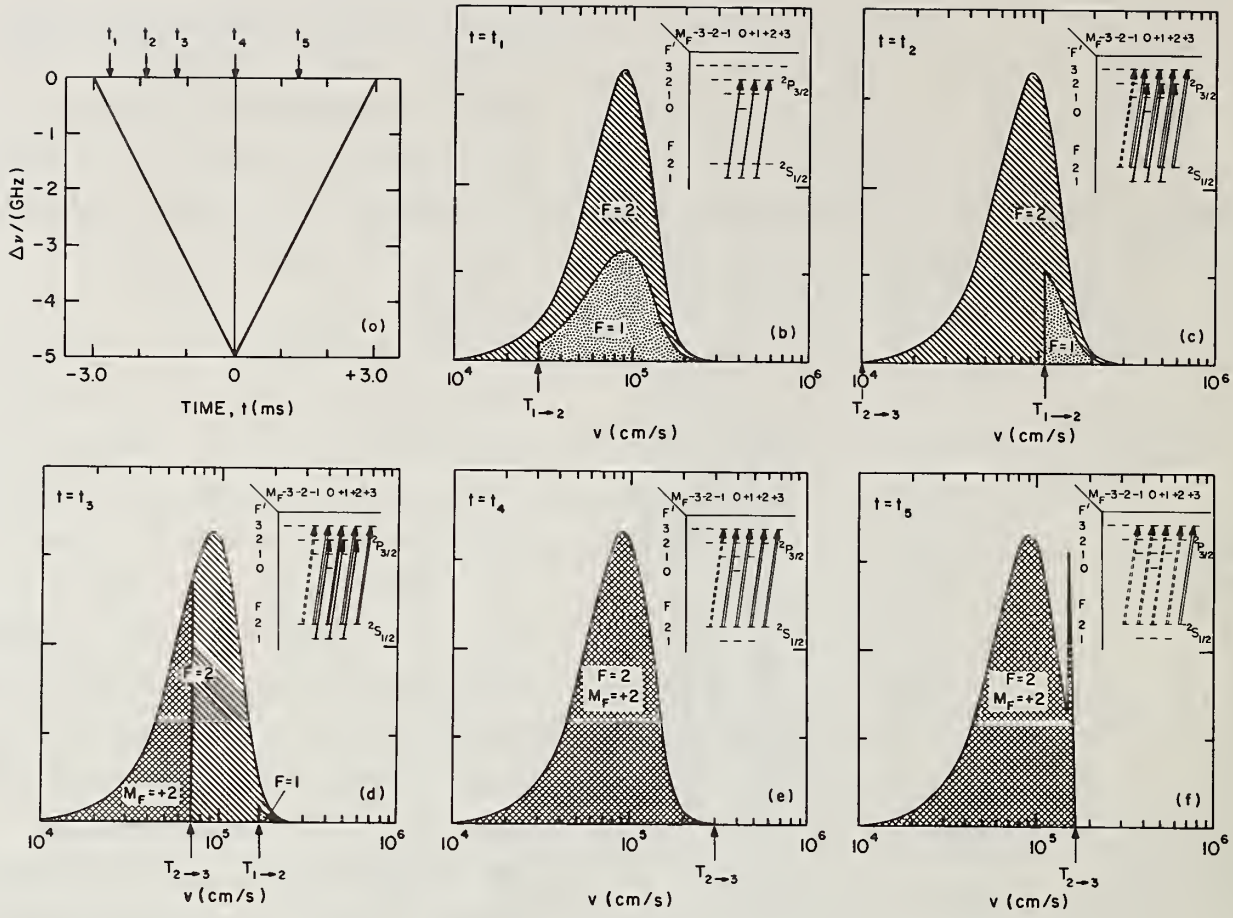

Figure 2. Illustration of the laser cooling process. Shown in the upper left figure is a plot of the swept laser frequency as a function of time. Shown in the remaining five figures are plots of the velocity profile of the sodium atomic beam at the five times, t_1 through t_5, indicated in the upper left figure. A temperature of 750 K is assumed for the sodium oven. The insets in each of the five velocity profile figures display the relevant transitions induced by the circularly polarized light. The notation follows that of Figure 1. The locations of the Doppler tuned resonance for the T_{12} and T_{23} transitions are indicated by arrows on the velocity axis. Profiles for the F = 1 and F = 2 manifolds of the $3^2S_{1/2}$ ground state are indicated respectively by dots and hatches. The cross hatching in the lower figures, representing the profile of the F = 2, M_F = +2 magnetic substate, shows the buildup of the population in this state and, in the figure at the extreme right, the onset of velocity compression and cooling.

By the time the laser is swept into resonance with the low-velocity Doppler-shifted T_{22} transition only the M_F = +2 sublevel will be populated, thereby precluding any excitation to the F' = 2 hyperfine state with ΔM_F = +1 circularly polarized radiation. Thus after 3 ms the entire population of the

velocity profile will be contained in the $M_F = +2$ sublevel of the $3^2S_{1/2}$ F=2 hyperfine state, and only T_{23} transitions, upward or downward, between the $M_F = +2$ and $M_{F'} = +3$ sublevels will be possible under the influence of $\Delta M_F = +1$ circularly polarized radiation. This condition, shown in Figure 2(e), will be achieved within a beam path length of 665 cm.

Now suppose the laser frequency is swept upward as shown in Figure 2(a). Both cooling and velocity compression will take place if the sweep rate is sufficiently low to stay in step with the cooling rate. Since the atoms are slowed down at the rate of 3 cm/s per spontaneously emitted photon, then at saturation, where spontaneous emission takes place at the rate of 3×10^7 photons/s, the atoms will be slowed down at a rate $dv/dt = 0.9 \times 10^8$ cm/sec^2. With the frequency sweep rate given by $d\nu'/dt = -(1/\lambda)(dv/dt)$, a rate of 1.5 GHz/ms will suffice for $\lambda = 5890.6$ A. The cooling and compression are illustrated in Figure 2(f) at a time $t_5 = 1.45$ ms after the onset of the upward sweep. Assuming that atoms initially travelling at velocities of up to 2×10^5 cm/s are to be brought essentially to rest, a beam path length of approximately 225 cm will be required. Thus in order to accommodate both the pumping and the cooling a beam path length of 890 cm must be provided. A scale drawing of the required apparatus is shown in Figure 3, with a number of beam-forming and beam-diagnostic devices included.

In the foregoing discussion we have assumed perfect circular polarization for the exciting radiation. In actuality, with the use of a polarizing beam splitter and a Soleil-Babinet compensator, a circular polarization of 0.995 can be obtained. This deviation from unity, combined with the finite laser linewidth, will cause some atoms during the cooling process to undergo transitions (labelled T_{22} in Figure 1) to the F' = 2 excited hyperfine state from which a fraction will be lost by eventual decay to the F = 1 ground hyperfine state. However, for a laser linewidth of 2 MHz, a hyperfine separation of 59 MHz between the F' = 3 and F' = 2 excited states, and the required number of transitions of 10^5 during the cooling process, fewer than 10 percent of the atoms should be so lost, assuming a laser power of $\sim$10 mW.

In undergoing the cooling process, the beam will acquire transverse velocities lying in the range of 5×10^2 cm/s, corresponding to a temperature of 0.02 K. Under reasonable experimental conditions, the longitudinal velocity will probably be at least an order of magnitude larger. The actual determination of the longitudinal velocity of the cooled beam can be accomplished by a technique employed in the CCNY exploratory studies; namely, deflection in an inhomogeneous magnetic field. In order to avoid pumping effects, however, the laser beam must be blocked during the velocity measurement. This task could be most easily accomplished with a Pockels cell shutter.

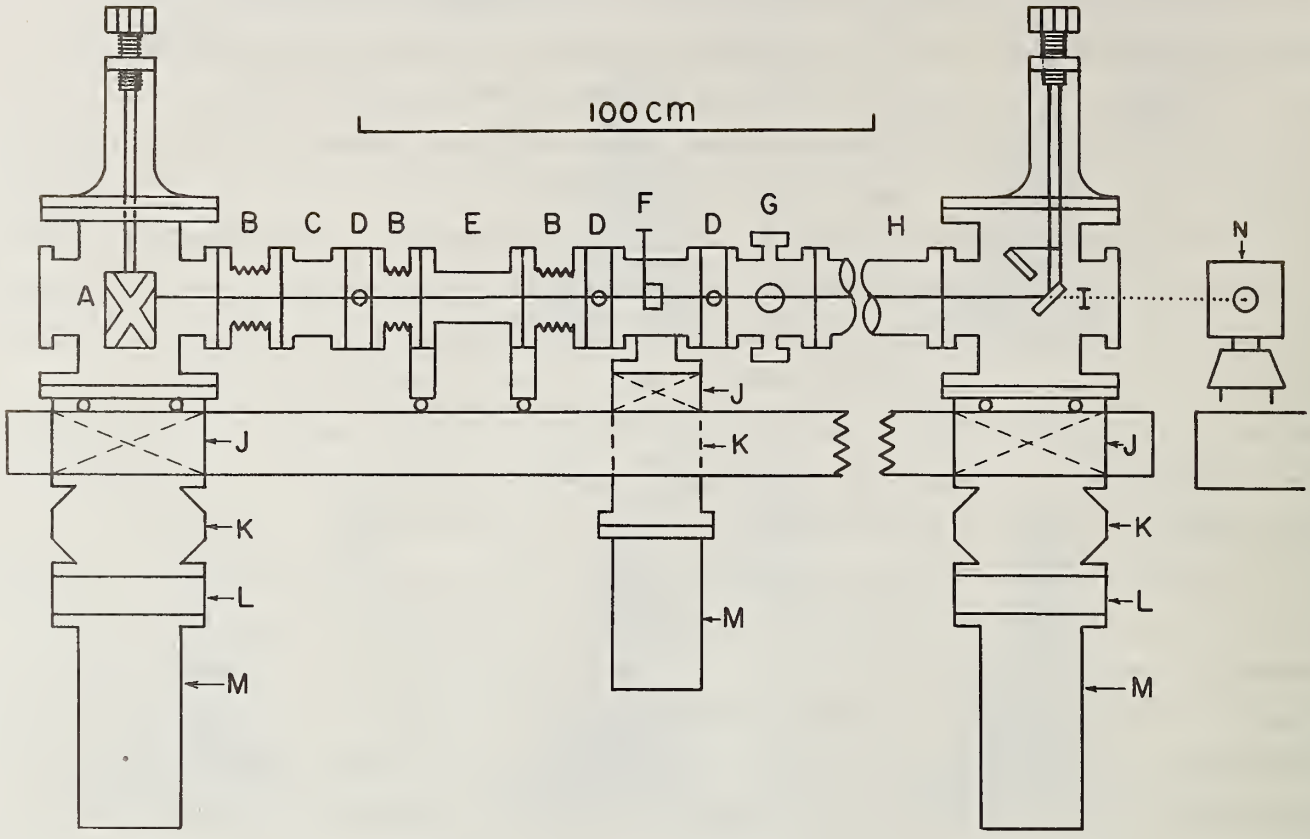

Figure 3. Scale drawing of existing atomic beam apparatus with drift region H added. components shown are A, sodium source; B, bellows; C, velocity selector; D, adjustable slits; E, E-H gradient magnet[44] for state selection; F, beam flag; G, test chamber; H, drift region with deflector magnet at downstream end; I, atom beam detector; J, gate valve; K, LN_2 traps; L, water baffles; M, diffusion pumps; and N, laser.

2.2 Dipole Force Studies

The use of the atomic beam apparatus illustrated in Figure 3 will also permit the dipole force[20] to be studied in detail. Since all optical trapping methods rely on the effects of this force, a thorough experimental investigation of its properties in a realistic situation must be regarded as a prudent course of action. In order to permit treatment of the atom as a two-level system, the atomic beam must be prepared with a narrow velocity spread in the F = 2, M_F = +2 hyperfine level, characteristics readily achieved with the use of the velocity selector and E-H gradient magnet[44] shown in Figure 3. With collimating aperatures having dimensions of 25 μm x 2.5 mm and with the alkali oven operated for a source pressure

of 0.1 Torr, both standard running conditions, a beam flux of $\sim 10^{8}$ atoms/cm^{2}s with a divergence of $< 4 \times 10^{-5}$ rad can be obtained. If this narrow, well collimated beam now intersects at right angles in chamber G of Figure 3 a circularly polarized laser beam chosen for $M_F = \pm 1$ transitions, an effective two-state system results. By adjusting the width, w, of the laser beam, the time which an atom spends in the radiation field can be varied, and by adjusting the laser power, I, and the detuning factor, $\Delta\omega$, the rate of spontaneous emission can be varied. Therefore from measurements of the beam deflection, the magnitude of the centroid and variance of the dipole force can be examined as functions of w, I, and $\Delta\omega$, parameters crucial for the design of optical traps.

Without too much effort it can be shown that in the absence of spontaneous emission, the values of w, I, and $\Delta\omega$ can be chosen so that a thermal atom passing through the laser will suffer an impulse giving rise to an angular displacement of $\sim 10^{-4}$ rad with respect to the incident direction. Such a deflection is just resolvable with the experimental conditions assumed. Cooling of the beam prior to the interaction with the transverse laser will obviously enhance the effect. From a dressed-state[45] analysis it can further be shown that for a judicious choice of laser parameters, the effect of spontaneous emission on the centroid of the dipole force can be neglected. The variance in the force, however, will be dominated by recoil effects associated with spontaneous emission, resulting in a beam spreading angle of $\sim 10^{-4}$. Thus, any effects associated with predicted fluctuations of dressed atom states induced by spontaneous emission[46] will be masked. Conceivably, they could be uncovered through the presence of interference phenomena, but the theoretical understanding of these phenomena is too imperfect to predict the size of their effect.

3. Visions of the Future

While much attention of future applications of cooled beams has rightfully been devoted to their use as injectors for neutral atom traps, several other possible applications should be mentioned. Low atom beam velocities, for example, will make neutral atom storage rings based upon dipole magnetic deflectors and hexapole magnetic focusers a distinct possibility. With the high atom densities which might be achieved with such devices, low rate processes particularly those related to rare isotopic species, could be studied effectively. Applications to efficient isotope separation and the study of collective effects[47,48] in strong radiation fields also deserve to be mentioned as prospects for the future. Doubtless, as compressd, cooled beams become a reality many other uses will become self evident.

4. References

[1] A. Einstein, Phys. Z 18, 121 (1917).

[2] O. Frisch, Z. Phys. 86, 42 (1933).

[3] See for example review articles by A. Ashkin, Science 210, 1081 (1980) and A.P. Kazantsev, Usp. Fiz. Nauk. 124, 113 (1978) [Sov. Phys. Usp. 21, 58 (1978)] and references therein.

[4] T.W. Hansch and A.L. Schawlow, Opt. Commun. 13, 68 (1975).

[5] V.I. Balikin, V.S. Letokhov, and V.I. Mishin, Pis'ma Zh. Eksp. Teor. Fiz. 29, 614 (1979) [Sov. Phys. JETP Lett. 29, 560 (1979)]; Zh. Eksp. Teor. Fiz. 78, 376 (1980) [Sov. Phys. JETP 51, 692 (1980)].

[6] V.S. Letokhov, V.G. Minogin, and B.D. Pavlik, Opt. Commun. 19, 72 (1976); V.S. Letokhov, V.G. Minogin, and B.D. Pavlik, Zh. Eksp. Teor. Fiz. 72, 1328 (1977) [Sov. Phys. JETP 45, 698 (1977)] .

[7] W. D. Phillips and H. Metcalf, Phys. Rev. Lett. 48, 596 (1982); J.V. Prodan, W.D. Phillips, and H. Metcalf, Phys. Rev. Lett. 49, 1149 (1982).

[8] J.E. Bjorkholm, R.R. Freeman, A. Ashkin, and S.B. Pearson, Phys. Rev. Lett. 41, 1361 (1978).

[9] D.B. Pearson, R.R. Freeman, J.E. Bjorkholm, and A. Ashkin, Appl. Phys. Lett. 36, 99 (1980).

[10] G.A. Askar'yan, Zh. Eksp. Teor. Fiz. 42, 1567 (1962) [Sov. Phys. JETP 15, 1088 (1962)] .

[11] D. Grischkowsky, Phys. Rev. Lett. 24, 866 (1970).

[12] J.E. Bjorkholm and A. Ashkin, Phys. Rev. Lett. 32, 129 (1974).

[13] A. Ashkin, Phys. Rev. Lett. 25, 1321 (1970).

[14] R. Schieder, H. Walther, and L. Woste, Opt. Commun. 5, 337 (1972).

[15] J.L. Picque and J.L. Vialle, Opt. Commun. 5, 402 (1972).

[16] J.E. Bjorkholm, R.R. Freeman, and D.B. Pearson, Phys. Rev. A 23, 491 (1981).

[17] R.J. Cook and A.F. Bernhardt, Phys. Rev. A 18, 2533 (1978).

[18] R.M. Hill and T.F. Gallagher, Phys. Rev. A 12, 451 (1975).

[19] B. Jaduszliwer, R. Dang, P. Weiss, and B. Bederson, Phys. Rev. A 21, 808 (1980).

[20] M.H. Mittleman, K. Rubin, R.H. Callender, and J.I. Gersten, Phys. Rev. A 16, 583 (1977).

[21] A.C. Tam and W. Happer, Phys. Rev. Lett. 38, 278 (1977).

[22] A.F. Bernhardt, Appl. Phys. 9, 19 (1976).

[23] P. Jacquinot, S. Liberman, J.L. Picque, and J. Pinard, Opt. Commun. 8, 163 (1973).

[24] A.F. Bernhardt, D.E. Duerre, J.R. Simpson, and L.L. Wood, Appl. Phys. Lett. 25, 617 (1974).

[25] A. Ashkin, Phys. Rev. Lett. 24, 156 (1970).

[26] A. Ashkin, Phys. Rev. Lett. 40, 729 (1978).

[27] J.P. Gordon and A. Ashkin, Phys. Rev. A 21, 1606 (1980).

[28] D.J. Wineland and H. Dehmelt, Bull. Am. Phys. Soc. 20, 637 (1975).

[29] D.J. Wineland, R.E. Drullinger, and F.L. Walls, Phys. Rev. Lett. 40, 1639 (1978).

[30] W. Neushauser, M. Hahenstatt, P. Toeschek, and H. Dehmelt, Phys. Rev. Lett. 41, 233 (1978).

[31] W. Neushauser, M. Hohenstatt, P. Toeschek, and H. Dehmelt, Appl. Phys. 17, 123 (1978).

[32] D.J. Wineland and W.M. Itano, Phys. Rev. A 20, 1521 (1979).

[33] See for example W.H. Wing, Phys. Rev. Lett. 45, 631 (1980).

[34] J.E. Bjorkholm, R.R. Freeman, A. Ashkin, and D.B. Pearson, Opt. Lett. 5, 111 (1980).

[35] R.J. Cook, Phys. Rev. Lett. 44, 976 (1980).

[36] L. Mandel, Opt. Lett. 4, 205 (1979).

[37] D. Stoler, Phys. Rev. Lett. 33, 1397 (1974).

[38] H.J. Carmichael and D.F. Walls, J. Phys. B 9, L43, 1199 (1976).

[39] H.J. Kimble, M. Dagenais, and L. Mandel, Phys. Rev. Lett. 39, 691 (1977).

[40] L. Mandel, J. Optics (Paris) 10, 51 (1979).

[41] R.J. Cook, Opt. Commun. 35, 347 (1981).

[42] D. F. Walls and P. Zoller, Phys. Rev. Lett. 47, 709 (1981) and references therein.

[43] W. D. Phillips, "Rapid Frequency Scanning of Ring Dye Lasers", to be published.

[44] B. Bederson, J. Eisinger, K. Rubin, and A. Salop, Rev. Sci. Instrum. 31, 852 (1960).

[45] C. Cohen-Tannoudji and S. Reynaud, J.Phys. 13 10, 345 (1977).

[46] Actually fluctuations occur even in the absence of spontaneous decays, but these arise from photo fluctuations in the laser field, and their effect is small compared to those produced by spontaneous decays.

[47] N.I. Zhokova, A.P. Kazantsev, E.F. Kazentsev, V.P. Sokolov Zh. Eksp. Teor. Fiz. 76, 896 (1979). [Sov. Phys. JETP 49, 452 (1979)].

[48] B. R. Mollow, Phys. Rev. A 12, 1919 (1975).

Laser-Cooled and Trapped Atoms, (Proceedings of the Workshop on Spectroscopic Applications of Slow Atomic Beams, held at NBS, Gaithersburg, MD, 14-15 April 1983) Ed. by W. D. Phillips, Natl. Bur. Stand. (U.S.) Spec. Publ. 653 (1983).

Chirping the Light -- Fantastic?

Recent NBS Atom Cooling Experiments

Electrical Measurements and Standards Division
John V. Prodan* and William D. Phillips
National Bureau of Standards
Washington, DC 20234

We have successfully decelerated and cooled a neutral atomic sodium beam using a counter-propagating laser beam tuned nearly resonant with the D_2 transition. In order to compensate for the changing Doppler shift as the atoms slow down, the laser frequency was rapidly scanned or "chirped". We have observed final velocities of 6×10^2 m/s, or about 0.5 of the initial velocity. As of yet we have not been able to cool a significant number of atoms to lower velocities.

Key words: atomic beam velocity modification, frequency scanning, high resolution spectroscopy, laser cooling.

Many of the difficulties in studying the spectrum of atoms come from the fact that these atoms are generally in motion. This motion causes the spectral lines to be Doppler broadened which, in turn, limits the information one can get concerning the detailed structure of the atom. In the past several years some very ingenious techniques, the so-called Doppler free spectroscopies, have been developed to drastically reduce 1st order Doppler broadening. Saturation techniques are sensitive to atoms in a very narrow velocity range and hence significantly reduce the problems due to the overall motion of the atoms, while two-photon techniques simply cancel the 1st order Doppler shift.

Another way to deal with the problems imposed by Doppler broadening is to modify the velocity of the atoms themselves. This technique has the advantage of not only reducing 1st order Doppler broadening but also reduces 2nd order Doppler effects. Cooling atoms using near resonant laser light was proposed several years ago [1] and recently we have made significant progress at NBS working with this idea [2,3,7]. A major problem in using laser radiation to slow atoms is that as these atoms slow down, they Doppler shift out of resonance with the laser. Using a changing Zeeman shift produced by a spatially varying magnetic field, we were able to compensate for this change that occurs in the Doppler shift. In this way, the fixed frequency counter-propagating laser remained nearly resonant with the atomic transition as the atom slowed down to near zero (longitudinal) velocity.

An alternate way of compensating for the changing Doppler shift is to quickly frequency scan or "chirp" the cooling laser [4]. For atoms moving at 1000 m/s, corresponding to a Doppler shift of 1.70 GHz, and fully radiatively saturating the D transition (F=2 to F=3 sublevels) in sodium, the deceleration time would be 1.07 ms. This would correspond to a maximum scanning rate for the laser of about 1.6 GHz/ms. The capability of producing such a scan rate and scan width was demonstrated previously by Phillips [5].

One of the motivations for our studying the cooling process using the chirped laser is the ability to look at details of the process not accessible in the spatially varying magnetic field scheme. During our experiments using the magnetic field [3,7], we found that the observed density of slow atoms did not have the velocity dependency that we had predicted. As of yet we do not understand the reasons for this discrepancy. However, with the chirped technique we can investigate this density dependence by varying the rate at which the laser scans as well as the magnitude of that scan. These two parameters would correspond to the spatial rate of change of the magnetic field and the magnitude of the field difference between the high and low field ends of the solenoid, respectively, in our earlier experiments [3,7]. Neither of these two parameters could be easily varied with the solenoid design that was used. The results given below represent the status of our experiments using the chirped laser techniques.

---

*NBS-NRC Research Associate

One final point which needs to be addressed before proceeding with the results of the present experiments is the problem of optical pumping that occurs in sodium. Previously [2,3,7], we dealt with this problem using the same solenoid that provided the changing Zeeman shift. This solenoid was designed so that field created was the sum of a spatially constant "bias" field and spatially changing "taper" field. The bias field was introduced to provide a means of overcoming optical pumping. This field produces sufficient Zeeman splitting and shifts to enable us to make use of certain selection rules that combine to virtually eliminate optical pumping. In the present chirping experiments, this bias field was still used so that we could avoid most problems which might arise due to optical pumping effects.

The experimental set-up is shown in Fig. 1a. The cooling laser is a tunable ring dye laser, modified to scan rapidly and is described in Ref. [5]. It's frequency is modulated with a sinewave drive, Fig. 1b, whose phase is adjusted so that the most linear part of the modulation is centered on the open time of the chopper. During the period when the chopper allows the laser to be transmitted, the frequency is scanned from ν_1 to ν_2. The amplitude and frequency of the sinewave modulation as well as the open time for the laser chopper are all separately adjustable parameters.

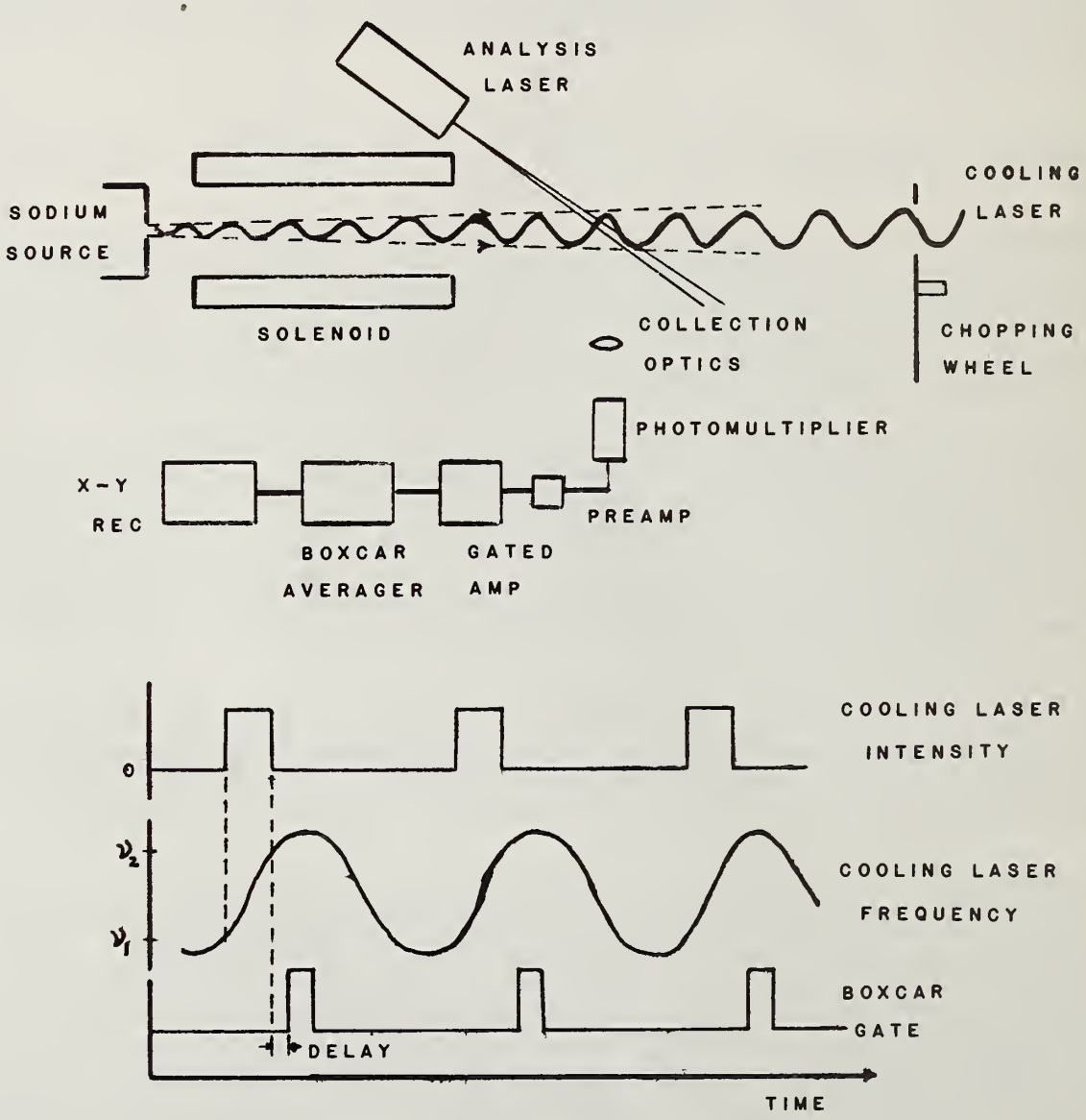

Fig. 1 (a) Block diagram of experimental set up
(b) Timing diagram

The cooling laser is directed in opposition to an atomic sodium beam. The majority of the cooling takes place in a constant magnetic field of 0.064 T in a region about 0.8 meters long. The initial frequency of the cooling laser, ν_1, is such that it is in resonance with atoms moving at a particular velocity in the magnetic field. The velocity distribution of the atomic beam as modified by the cooling laser is analyzed by a second very weak dye laser. This second laser intersects the atomic beam at an angle of 11° from being co-propagating. As this laser is slowly scanned in frequency, the fluorescence that it induces is directed by the collection optics to a photomultiplier tube. The resulting photo-current is processed by a boxcar averager which is set up to observe the current generated after the chopping wheel has shut the cooling laser off. In this manner the modified velocity distribution of the atomic beam is determined.

Some preliminary results of our chirping experiments are shown in Figures 2 and 3. Figure 2 shows a

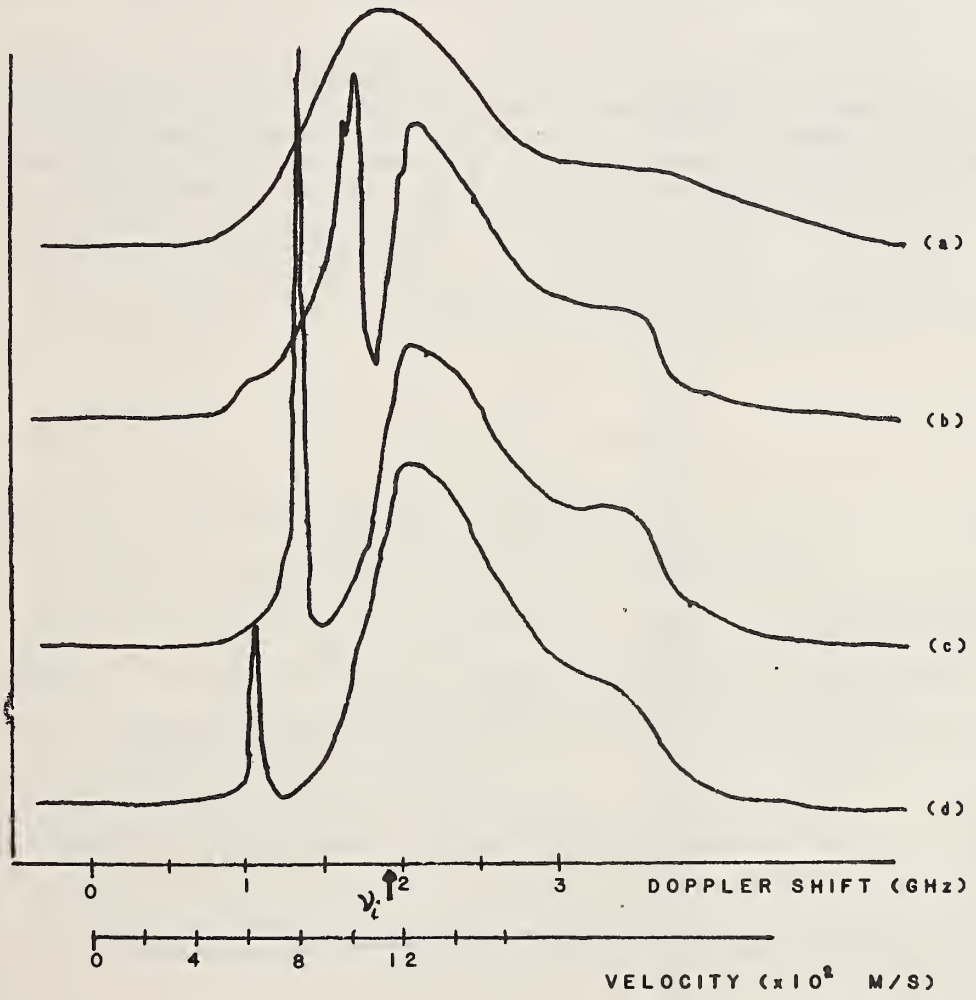

Fig. 2 Velocity distribution of the atomic beam for the case of (a) cooling laser blocked, (b) cooling laser on but not scanned, (c) cooling laser scanned for 480 MHz, and (d) cooling laser scanned for 750 MHz.

sequence of velocity distributions which clearly demonstrate the effects of scanning the cooling laser. An unmodified distribution is presented in Fig. 2a for comparison. The arrow, designated ν on the abscissa, indicates those atoms in the velocity distribution with which the initial laser frequency would be resonant, within the magnet). This frequency corresponds to an atomic velocity of about

1.1×10^3 m/s. To produce the distribution shown in Fig. 2b, the cooling laser was not scanned. A peak in the distribution was produced at approximately 9.8×10^2 m/s. These atoms represent the ones which were initially in resonance with the cooling laser but Doppler shift themselves out of resonance fairly quickly and hence were lost to the cooling process. Considering the power, amount of focussing, the detuning (the difference between the frequency of the laser and the resonant frequency of the atomic transition in the atom's rest frame) and the length of time that the laser interacted with the atoms, the achieved velocity was not inconsistent with predictions made by Minogin [6].

In Figure 2c, the laser was scanned 480 MHz at a rate of 0.64 GHz/ms, well below maximum rate at which atoms should be able to keep in resonance with the laser. We can see that atoms have been compressed into a narrow velocity spike at 8.3×10^2 m/s with a FWHM of 40 m/s. To produce the distribution shown in Fig. 2d, the scan width was increased to approximately 750 MHz (at a rate of 1 GHz/ms). The peak representing the cooled atoms is at a velocity of 6.2×10^2 m/s with a FWHM of about 40 m/s. For both of these two conditions, the velocity of the spike is close to what one would calculate assuming the atom's velocity had resonantly followed the frequency scan from the initial to the final frequency of the laser. Velocities predicted in this manner would have been 8.5×10^2 m/s and 6.6×10^2 m/s respectively.

There are several differences between the two schemes, mentioned earlier, for cooling atoms. In addition to the ability to easily change the rate of cooling and the amount of cooling, the chirping technique should also produce a different spatial distribution of atomic velocities than does the varying Zeeman shift approach to cooling. For the spatially varying magnetic field situation, there should be a unique maximum velocity associated with a given position in the solenoid for a given laser tuning. However, for the chirping scheme, atoms of a given velocity could exist over a rather large

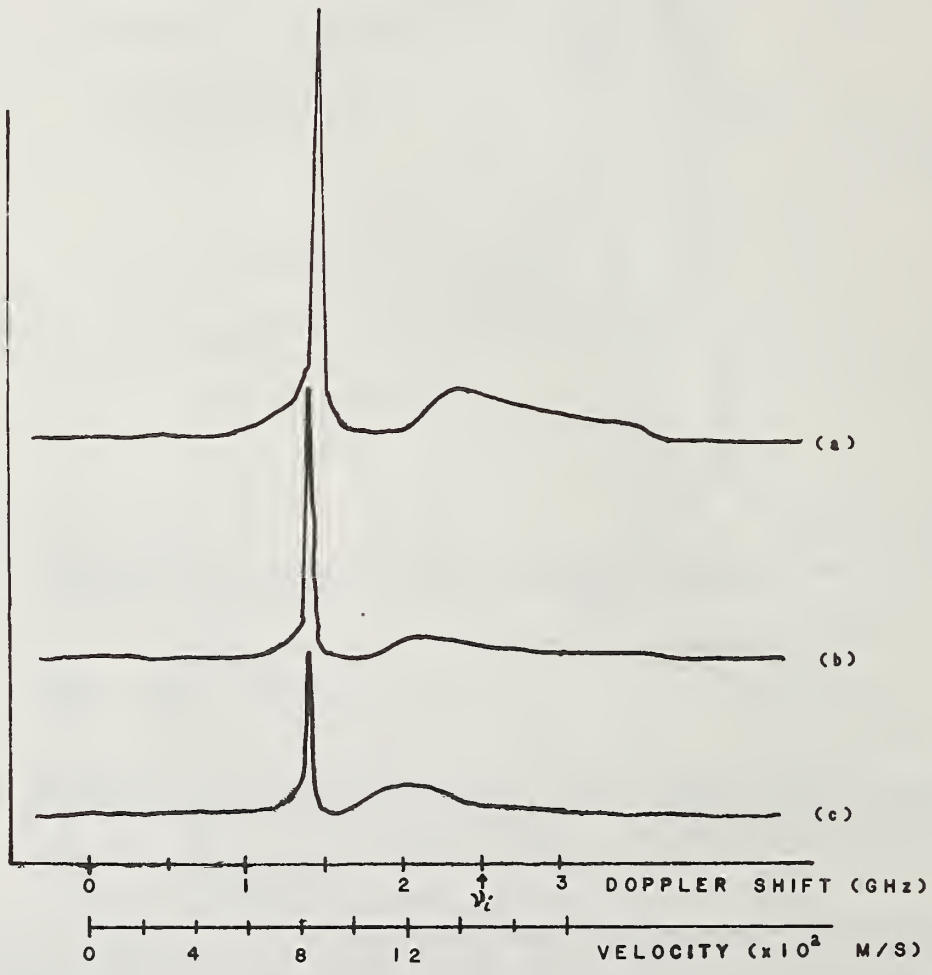

Fig. 3 Velocity distribution of the atomic beam after a delay of (a) 500 μs, (b) 800 μs and (c) 1200 μs. The cooling laser was scanned .87 GHz in 750 μs.

distance, depending primarily on the length of the scan and length of the solenoid. In order to see if such a situation exists, all that we have to do is to change the amount of delay time between when the laser is turned off by the chopping wheel and when the gate of the boxcar is opened. This action allowed us to observe slower and slower atoms originating from from a constant point in space when the spatially varying field was used. However, with the chirping technique we should see atoms at a fixed velocity but originating at different points in space.

The results of a study of the velocity dependence of the detected signal as a function of gate delay are presented in Figure 3. Figure 3a shows the distribution obtained after a delay of 500 μs and we see that there is a narrow group of atoms at a velocity of about 8.5×10^2 m/s. Figures 3b and 3c show velocity distributions after a delay of 800 μs and 1200 μs respectively. One can see that the cooled atoms appear at essentially the same velocity for all three delay times. The atoms that produced the signal shown in Fig. 3a came from a position about 0.5 m from the observation region (5 cm inside the magnet) while the atoms represent in Fig. 3c came from 1.0 m from the observation region (still well within the magnet). These results essentially confirm the predictions stated in the preceeding paragraph.

There are still several items which remain to be done using this scanning technique. As of yet, we have not been able to produce atoms as cold as we were able to achieve using the varying magnetic field scheme [3]. In fact we have not even been able to produce significant numbers of atoms below about 600 m/s. The reasons for this need to be determined. Although we have looked at the velocity distribution produced by a few different scan rates and scan widths, we still have insufficient data to make any statement as to the effects of these parameters. We plan to accumulate more data relating to these two parameters in order to understand their effects. We would also like to investigate the effects of focussing or defocussing the cooling laser as we have some data in this area using the varying magnetic field scheme. In conclusion, while we have made some progress in understanding the details of the cooling process using a chirped laser, there is still much more work that needs to done.

This work was supported in part by the Office of Naval Research

[1] T. W. Hansch and A. Schawlow, Opt. Comm. 13 68 (1975).

[2] W. D. Phillips and H. Metcalf, Phys. Rev. Lett. 48, 596 (1982).

[3] J. V. Prodan, W. D. Phillips and H. Metcalf, Phys. Rev. Lett. 49, 1149 (1982).

[4] V. S. Letokhov, V. G. Minogin and B. D. Pavlik, Opt. Comm. 19, 72 (1976).

[5] W. D. Phillips, Applied Optics 20, 3826 (1981).

[6] V. G. Minogin, Opt. Comm. 34, 265 (1980).

[7] W. D. Phillips, J. V. Prodan and H. Metcalf, these proceedings.

Laser-Cooled and Trapped Atoms, (Proceedings of the Workshop on Spectroscopic Applications of Slow Atomic Beams, held at NBS, Gaithersburg, MD, 14-15 April 1983) Ed. by W. D. Phillips, Natl. Bur. Stand. (U. S.) Spec. Publ. 653 (1983).

Cooling of an Atomic Beam with Frequency-Sweep Techniques

R. Blatt,* W. Ertmer† and J. L. Hall‡

Joint Institute for Laboratory Astrophysics, University of Colorado and National Bureau of Standards, Boulder, Colorado 80309 U.S.A.

We review the ideas of velocity-modifying an atomic beam by resonant scattering of intense light from a frequency-swept laser source. Some of the realistic parasitic effects, particularly fluctuations and residual transverse heating are considered. A computer Monte-Carlo simulation program is described which provides encouragement and insights useful in the design of a real atomic beam apparatus. We describe a new rf/optical modulation method to generate the desired laser optical frequency and intensity profiles versus time. This digital method provides the necessary sweep accuracy and program flexibility in a convenient and powerful way.

Key words: radiative cooling, laser spectroscopy, atomic beam velocity distributions

The possibility of influencing the motion of atoms by resonance laser radiation has received considerable attention for several years now [1]. A particular interest in this field is naturally the reduction of the atomic translational energy because high resolution spectroscopic experiments are ultimately limited by velocity-related effects. Since the pioneering proposals by Hänsch and Schawlow [2] and Wineland and Dehmelt [3] a large amount of theoretical and experimental work has been done. The "cooling" of trapped ions was first demonstrated [4,5] in 1978, while the first experiments on neutral atoms were published by a group in Moscow [6] in 1979 and very recently by a group at NBS Gaithersburg [7,8] in 1982. Trapped ions have been cooled to a residual temperature of a few milli-Kelvins, single ion detection has been demonstrated, and the general advantages of ion trapping techniques for precision measurements have been demonstrated on various ions [4,5,9,10]. All the reported experiments on neutral atoms have been done with Na atoms, the basic scheme being an atomic beam and a counterpropagating cooling laser beam. In order to cool effectively the laser frequency must match the transition frequency of the moving atoms. It has been shown, however, that a laser tuned to the maximum of an atomic beam velocity distribution, but kept fixed in frequency, can change the mean velocity and narrow the width of the distribution [11]. But this scheme is unlikely to be successful in achieving temperatures in the sub-Kelvin regime.

Two methods have been proposed to keep the resonance condition between the cooling laser beam and the moving atoms even as they slow down. The first, reported by Letokhov and Minogin [12], is based on scanning the laser frequency, but no further results using that method have been published yet.

---

*Permanent address: Johannes Gutenberg University, Mainz, West Germany.

†Permanent address: University of Bonn, Bonn, West Germany.

‡Staff Member, Quantum Physics Division, National Bureau of Standards.

The second technique uses the Zeeman shift to keep the resonance condition and led for the first time to very promising cooling results on neutral atoms [8]. However, the application of a strong magnetic field (several hundred gauss) can bring its own problems.

In the following, exploiting the ideas of Letokhov and Minogin, a proposal is made to cool the atoms by rapidly sweeping the laser frequency under precise control. We are optimistic that the absence of magnetic fields coupled with precise time-domain control of the laser frequency will allow clear interpretation of the final velocity distributions. It could well be that, armed with what we hope to learn from these swept frequency experiments, it would be interesting to return to cw beam cooling using electric or magnetic fields with optimized spatial gradients. However, the pulsed cooling method has its own advantages in producing a relatively high density "rod" of essentially-stopped atoms, just freely falling under gravity. The high resolution interactions with these atoms can thus occur away from their cooling experiences. Further, the "falling rod" geometry is attractive for successive excitations with longitudinal (possibly weakly-focused) laser beams (as in the multiple-excitation Ramsey interference fringe method), and for output interrogation using optical heterodyne techniques. Finally, the atomic beam machine may be oriented a bit off the true vertical to produce the "fountain beam" of emotional significance to atomic beamists and of possible utility in filling a weak trap for neutral species.

In order to study the basic properties of the frequency-swept cooling concept and to investigate the features of such a device, a Monte-Carlo simulation of the proposed experiment was performed. The results of that calculation agree with preliminary computations based on a differential equation.

1. Basic Idea of Atomic Beam Cooling with Chirped Lasers

As mentioned above, the main problem in cooling an atomic beam by means of a counter-propagating laser beam is the changing Doppler shift. Once the laser is on resonance with atoms of a certain velocity of the atomic beam, those atoms begin to slow down and clearly walk out of resonance due to their altered velocity. To retain the resonance condition either the frequency of the atomic absorption has to be adjusted [8] or the laser frequency has to be tuned to the new absorption maximum.

The resonance frequency of an atom depending on its velocity is given by the Doppler formula

$$\nu_L(t) = \nu_0\left(1 - \frac{v(t)}{c}\right)$$

where ν_0 is the unshifted transition frequency of the atom, v(t) is the (now time dependent) velocity and c denotes the speed of light. Or, if the time dependent laser frequency $\nu_L(t)$ were given, v(t) then reads

$$v(t) = \left(1 - \frac{\nu_L(t)}{\nu_0}\right) \cdot c$$

with its derivative

$$\dot{v}(t) = -\frac{\dot{\nu}_L}{\nu_0} \cdot c \quad .$$

On the other hand the change in the velocity of an atom due to the momentum transfer by absorbed photons is given by

$$\dot{v}(t) = -\frac{h\,\nu_L(t)}{m \cdot c \cdot 2\tau}$$

provided the laser intensity is high enough to ensure that the transition is well saturated, and assuming a two-level system. Here m is the mass of the atom, h is Planck's constant and τ is the natural lifetime of the excited state. To determine the frequency

dependence $\nu_L(t)$ and the velocity dependence $v(t)$ we solve the resulting differential equation:

$$\dot{\nu}_L(t) - \alpha\nu_L(t) = 0 \quad , \quad \alpha = \frac{h \cdot \nu_0}{mc^2 2\tau} \quad .$$

The solution reads:

$$\nu_L(t) = \nu_s \cdot e^{\alpha t}$$

where ν_s denotes an initially given starting frequency, corresponding to the initial velocity of the atoms. For the velocities this yields

$$v(t) = \left(1 - \frac{\nu_s}{\nu_0} e^{\alpha t}\right) \cdot c \quad .$$

If we take Na atoms as an example, we get the numerical value $\alpha \approx 3 \times 10^{-3}\ s^{-1}$ which gives a time to stop atoms of initially 1000 m/s in $t_{max} \approx 1 \times 10^{-3}$ s. This clearly indicates that the exponential behavior of the frequency sweep is almost entirely determined by the linear approximation of the exponential expression and thus the laser sweep is given by

$$\nu_L(t) = \nu_s(1+\alpha t) \quad ,$$

which is indicated in Fig. 1. Due to the cooling and the corresponding frequency scan all velocities less than the starting velocity ultimately come into resonance with the laser, and will join the group of already-slowed atoms.

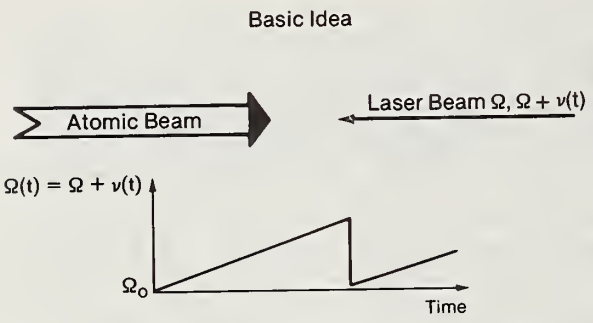

Fig. 1. Basic geometry and scan scheme for atomic beam cooling by a frequency-swept laser.

Assuming a starting velocity for Na atoms of 1000 m/s and a final velocity near zero, we get a sweep constant of $d\nu_L/dt \approx 1.7$ GHz/ms. An atom requires about 33000 cycles of laser absorption and spontaneous emission to be stopped.

2. Computational analysis of the chirped cooling

In spite of its simplicity, this approach indicates the feasibility of a frequency-swept ("chirped") laser atomic beam cooling. A serious calculation, however, has to take into account many additional effects which have been neglected in this first approach.

These are, in particular:

(a) The laser beam intensity. It has been assumed above that the transition is very well saturated. That is not necessarily satisfied because of the gaussian spatial profile of the laser beam and the intensity variation due to the spatial position of the atoms.

(b) Statistical absorption and emission processes. No statistical processes have been included in the differential equation above. Due to the random absorption and emission the position and velocity of the atoms are not determinate, giving some variations in the intensity the atoms see during the cooling process, and of course in the final position and velocity as well.

(c) Optical pumping. These effects have been totally neglected in the first approach. For a real atom, the two-level system approach can hold only approximately, so corrections have to be included.

(d) Experimental scan scheme. In the basic calculation only a simple frequency sweep is taken into account; a more elaborate scanning scheme might be better suited for ultimate cooling and narrowing of the velocity distribution. For example, it might be useful to stop the laser's sweep and reduce its power at the end of the cooling cycle. A general possibility to evaluate these effects should be included.

(e) More dimensional aspects. The approach above finds results only for a one-dimensional problem. More dimensions in velocity and position lead to coupled differential equations and should be properly included.

(f) Dipole forces due to stimulated transitions. Only forces due to spontaneous scattering have up to now been included. Dipole forces that may lead to further cooling are to be entirely included.

In order to obtain reliable results which will provide reasonable values for the design of any atomic beam cooling device based on laser chirping, and in order to understand the basic physics of this process, we have to consider all the mentioned influences.

The scattering force is dependent on the saturation parameter P. Therefore it now reads [13]

$$\frac{\vec{F}_{sp}}{m} = \dot{\vec{v}} = -\frac{\hbar\vec{k}_L}{m \cdot c} \cdot \frac{1}{\tau} \cdot \frac{P}{1+2P}$$

with $\vec{F}_{sp}$ the force induced by the spontaneous scattering processes, P is defined [14] as $P = B \cdot \sigma(\nu)/A$ where B and A denote the Einstein coefficients for the correspondent transition, and $\sigma(\nu)$ is the spectral energy density. The vector notation accounts for the various dimensions and hence for the angle between the velocity $\vec{v}$ and the counterpropagating laser beam ($\vec{k}_L$). The saturation parameter depends on the intensity I and detuning $\Delta\nu$, which are in turn functions of position and velocity. P is given by [14]

$$P(\nu) = \frac{I(r,z)}{I_{sat}} \cdot \frac{1}{1 + \left(\frac{2\Delta\nu}{\gamma_n}\right)^2}$$

with

$$\gamma_n = \frac{1}{2\pi\tau}$$

$$I(r,z) = \frac{2P_0}{\pi w^2} e^{-\frac{2r^2}{w^2}}, \qquad w^2 = w_0^2 + \frac{\lambda^2}{\pi^2 w_0^2} z^2$$

$$I_{sat} = \frac{4\pi^2 \gamma_n \cdot h \cdot \nu}{\lambda^2}$$

where P_0 denotes the applied laser power in watts and w_0 the laser beam waist radius in the focal plane of the gaussian beam.

The experimental scanning scheme can be included by proper calculation of the detuning

$$\Delta\nu = \nu_0(v) - \nu_L(t)$$

as a function of the atomic velocity and the time dependent laser frequency.

The dipole forces are given by [14,15]

$$\vec{F}_{dip} = -\frac{2\pi}{c} \alpha \vec{\nabla} I$$

where α is the polarizability of the corresponding transition.

A full theoretical treatment of the cooling problem leads to a differential equation of the Fokker-Planck type [13].

In order to calculate the cooling process for laser chirping including all experimental requirements, two main approaches were pursued. The first, a Monte-Carlo simulation study is based on a step-by-step calculation and hence requires considerable calculation time. The second approach, based on an integration of a simplified Fokker-Planck equation, is much more involved in accounting for all the experimental details.

A. Monte-Carlo Simulation

This Monte-Carlo program simulates the cooling process of an atomic beam by a counter-propagating, fast scanned laser beam. The basic idea of this program is to take into account each change in velocity or position of the atoms caused by the subsequent absorption or emission of photons.

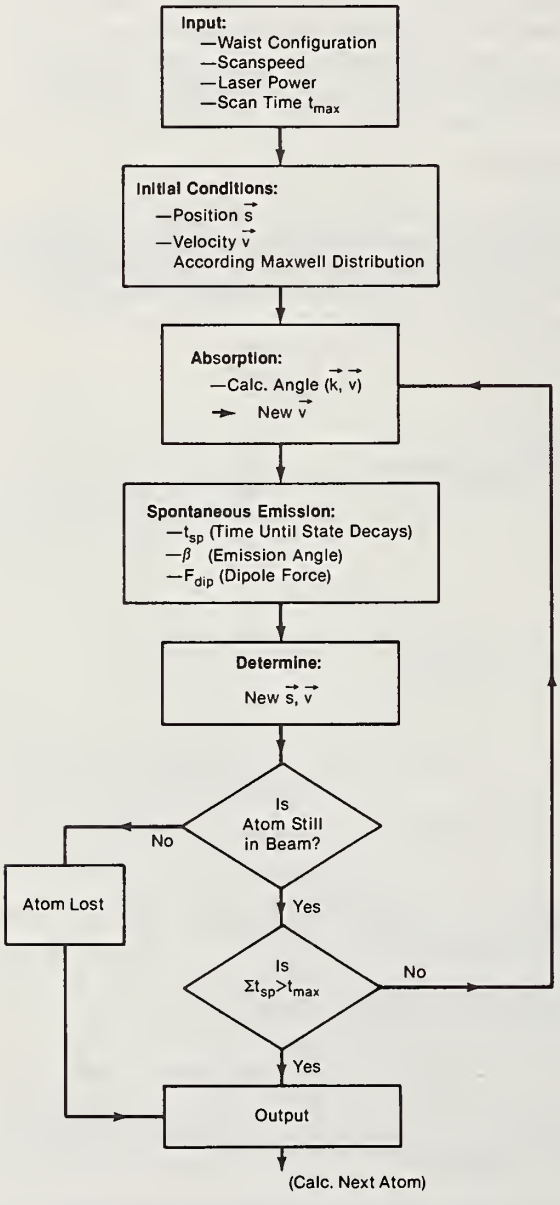

Fig. 2. Flow chart for Monte-Carlo simulation.

According to their nature, all statistical processes are calculated in a random manner, to include all effects which contribute to the residual velocity distribution or density in a given atomic beam.

Another important aspect is the consideration of all experimental details: e.g., atomic beam properties, laser beam configurations, and sweeping of the laser frequency. Thus we are able to learn easily the main influences of experimental parameters on the cooling process and can start our experiment with an optimized experimental setup and sweep-scheme. Moreover, in the future, comparison of these calculations with experimental results will be a versatile tool in interpreting the experiment.

The flow chart of the program is given in Fig. 2. The input parameters are the laser beam properties (waist and waist location, laser power) and the sweep scheme (scan speed, one or more laser frequencies, timing of the frequency scan).

In the beginning the program generates randomly a set of, for example, 100 atoms with the spatial density and velocity distribution of a usual atomic beam. Each atom is then treated separately during the cooling process in the following way: first the atom absorbs a photon and changes its velocity according to the $\vec{k}$-vector at that position. Then the lifetime of the excited state is calculated randomly taking into account the influence of the saturation parameter $P = P(\vec{r},\vec{v},t)$ for the time that the atom spends in the excited state. After calculating randomly the emission-angle of the spontaneously emitted photon, the resulting new position and velocity are calculated including the

influence of the dipole forces. The dipole forces are considered to be constant between the two absorptions. Before the next absorption takes place it is verified that the atom has not walked out of the atomic beam limits and that the end of the sweep time is not reached. Then the atom absorbs the next photon, and so on. Having reached the end of sweep time or the atomic beam limits, the cooling process is finished and the next atom is cooled. The result of each complete cooling process is the end-position and end-velocity of all atoms, in addition to other interesting parameters, such as the saturation parameter at the end.

All computations were done for Na atoms, the atomic beam divergence is assumed (according to the design of the apparatus) to be 3 mrad.

Figure 3 shows the random initial velocities, with the transverse velocity plotted versus the longitudinal velocity according to a Maxwellian distribution in the atomic beam. The cooling process transforms these "initial velocities" into the "final velocities" after one cooling cycle corresponding to one laser sweep. A typical final distribution is given in Fig. 4. The run was taken with t_{max} = 1.140 ms, dv_L/dt = 1.489 GHz/ms, starting at a maximum initial velocity of 1000 m/s.

Laser "compression" of the original longitudinal velocity distribution -- with a maximum at 760 m/s and a width of several hundred m/s -- leads to a final distribution shown in Fig. 5. The width of each bar is 1 m/s thus indicating a residual width of about 3 m/s. The choice of the stopping time controls the final longitudinal velocity.

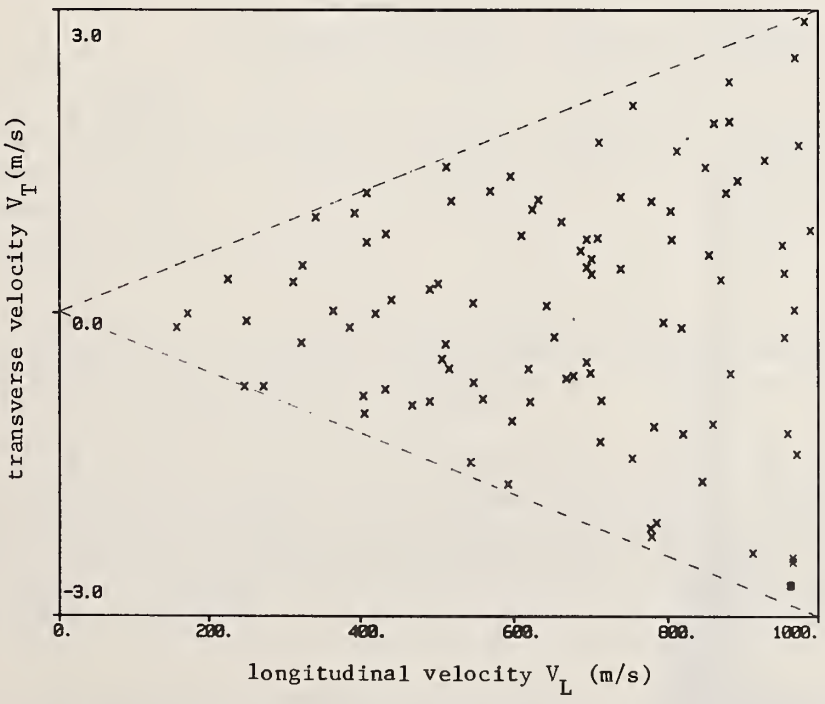

Fig. 3. Initial velocities in the atomic beam according to a beam-Maxwellian distribution (each x represents one atom).

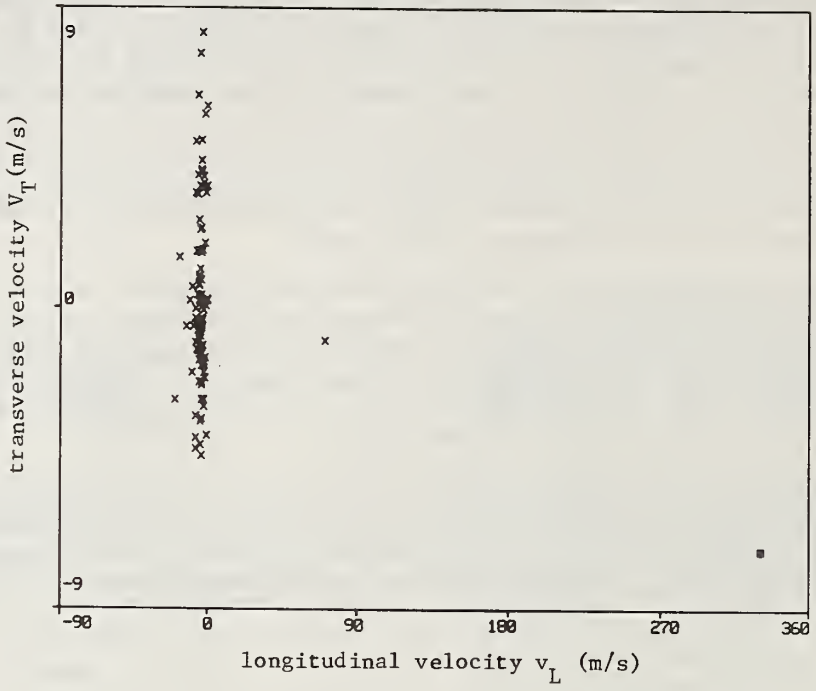

Fig. 4. Final velocities in the atomic beam after one frequency scan (square indicates a lost atom).

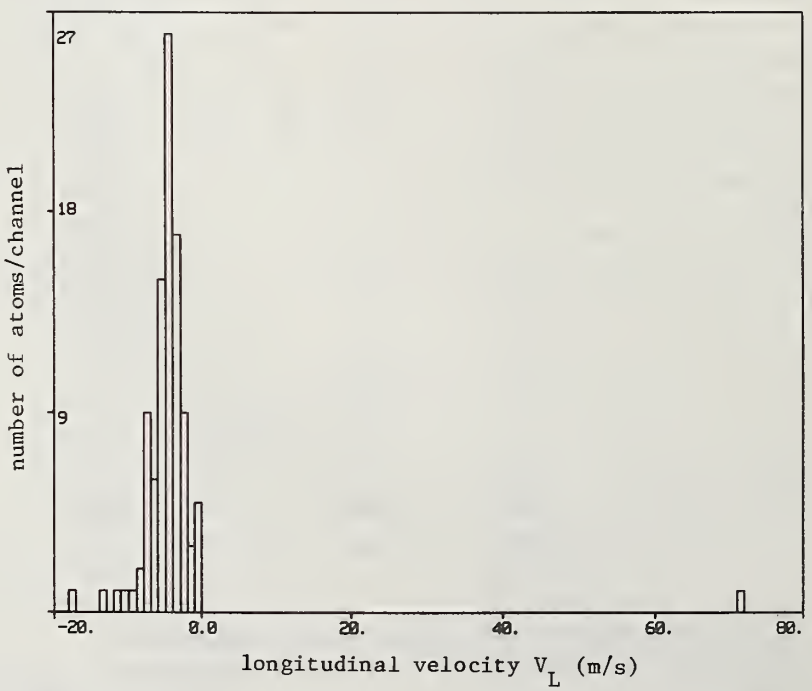

Fig. 5. Histogram of the final longitudinal velocities corresponding to Fig. 4.

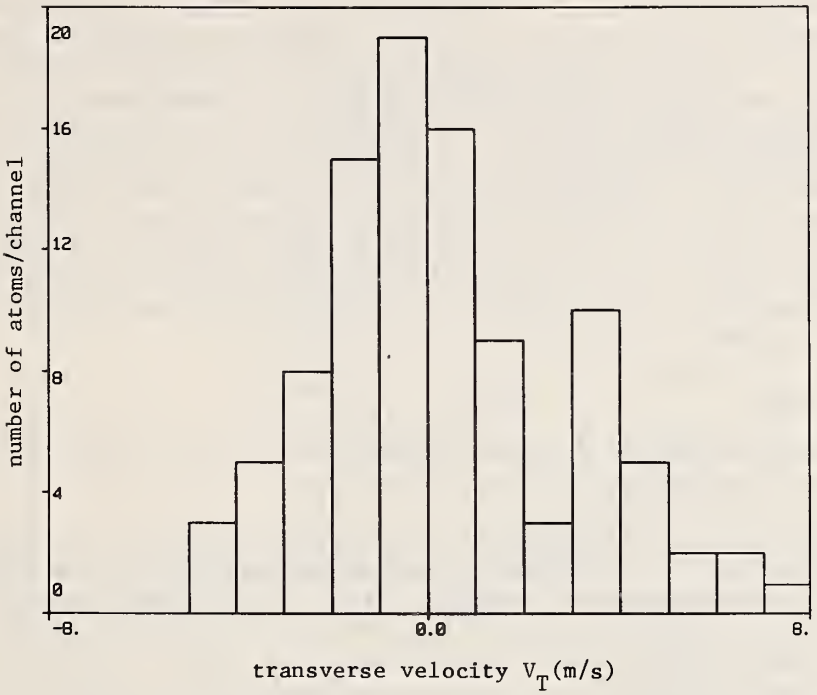

Fig. 6. Histogram of the final transverse velocities corresponding to Fig. 4.

The final transverse velocity distribution also behaves as expected. Initially the transverse velocity width is given by the atomic beam divergence and amounts to about 3 m/s. From Fig. 6 we find a final width of about 5 m/s, which is due to "transverse heating" caused by the emission processes. However, this value is already reduced by the dipole forces which help in focusing the atomic beam. A case was run with the same initial parameters as in Fig. 6 but without dipole forces. The transverse velocity width came out to be about 7 m/s, indicating in the previous case the well-known transverse focusing caused by the dipole forces [16].

The program allows us also to change experimental parameters such as laser-power, -waist, and -frequency sweep during each cooling process. If it is desired, the program can also calculate the induced processes randomly in place of using the average of the population time in the excited state or ground state.

Although quite successful in calculating experimental details, the program is far from being complete. The known limitations of the present program are the assumption of a pure two-level system, isotropic emission of the spontaneous photons and a calculation only in the x, y plane. Therefore, the optical pumping process and the related radiation characteristic for spontaneous emission as well as calculations in three-dimensional space will be included in future. The latter is especially important when gravity is to be taken into account.

When all these effects are included, the program will be well suited to calculate the filling process of neutral atoms into an "optical trap," as well as calculating the long- and short-term behavior of atoms in those traps. The generality of our calculation allows detailed evaluation of any trapping scheme.

B. Integration of Simplified Equation of Motion

To check this program as well as to learn more about diffusion and related effects influencing the cooling process, we are also trying a different approach to calculating this cooling process. It is similar to calculations made by Minogin [13]. In these calculations, kinetic equations are derived which evaluate the distribution functions of two-level atoms interacting with a laser beam. In addition to Minogin's computations, these equations of the Fokker-Planck type also take the laser frequency sweep scheme into consideration. As a consequence, computer solution of these equations has encountered several numerical problems. Due to these difficulties only preliminary results are available at present. However, in cases where the two approaches can be compared, all important features, such as final velocity and velocity width, show good agreement with those provided by the Monte-Carlo method. We are anxious to confront all these calculational "experiments" with laboratory data!

3. Experimental Design

After first calculations, we designed an apparatus to cool an atomic sodium beam by a periodically fast-scanned counter-propagating laser beam.

The hyperfine structure splitting of the cooling transition $^2S_{1/2} \leftrightarrow {}^2P_{3/2}$ is shown in Fig. 7. As can be seen from this figure, optical pumping is one of the main problems in cooling sodium. An elegant way to overcome it is to use two laser frequencies: one laser frequency is tuned to the transition $^2S_{1/2}$ (F=2) $\leftrightarrow$ $^2P_{3/2}$(F=3) (see Fig. 7) with circular polarization, the other one is tuned to the $^2S_{1/2}$ (F=1) $\leftrightarrow$ $^2P_{3/2}$ (F=2) transition. The first realizes a nearly perfect two-level scheme (F=2, m_F=2 $\leftrightarrow$ F=3, m_F=3) whereas the second pumps the atoms in the beginning from the F=1 level into the F=2 level of $^2S_{1/2}$. During the cooling the second field also restores atoms lost due to imperfect polarization etc.

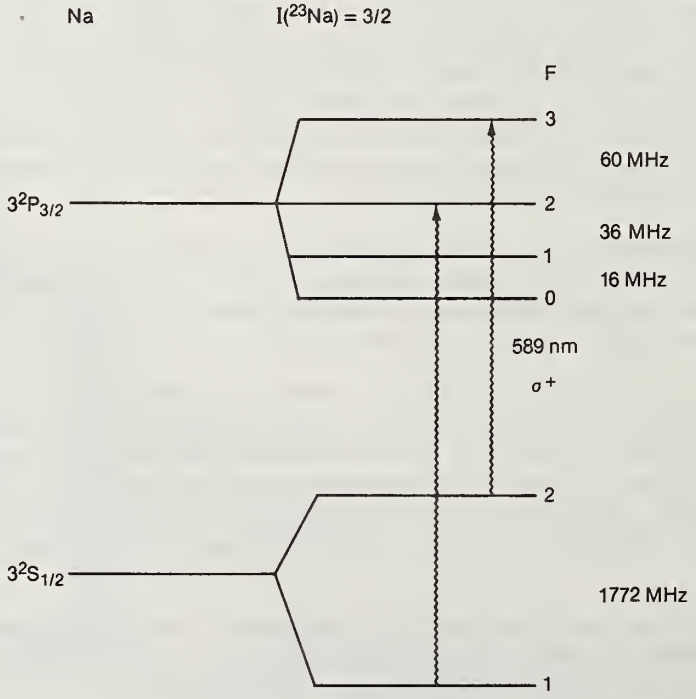

Fig. 7. Level scheme of Na with the cooling transitions.

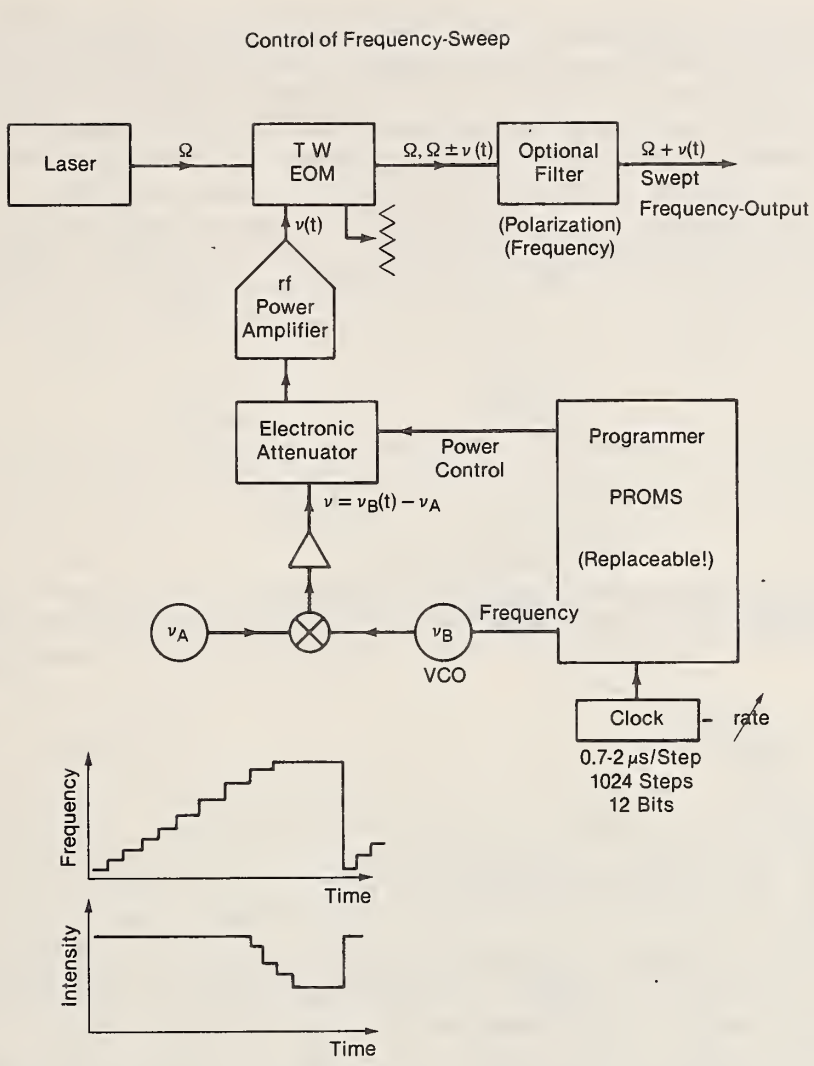

Fig. 8. Control of the frequency sweep using Programmable Read Only Memory.

The necessary second laser frequency can be produced, for example, by an electro-optic modulator, to convert a part of the carrier intensity into the desired side band.

As mentioned above, the laser frequency must be tuned very rapidly (1-2 ms sweep time) over a relatively large scan range (~1.7 GHz) with high precision. This can be achieved, too, by an electro-optic modulator. Figure 8 shows an experimental setup for generating the precise, fast-scanning frequency needed. The main feature is a PROM (Programmable Read Only Memory) controlled rf source, which allows both very fast and precise scanning of the rf and an easy and quick change of the scan scheme. The basic voltage-tunable oscillators shown in Fig. 8 operate for example in the 2.5-3.5 GHz range, tuning this range and settling within a few microseconds. With this setup, which has already been tested for frequencies up to 800 MHz, a power of about 20% of the carrier power in the first sideband should be possible with a 10 W rf power amplifier. Conversion efficiency above 12% has been observed at 2.5 W.

It should be explicitly noted that the cooling radiation will be taken to be the upper sideband produced by the modulation process. This will allow the "unused" laser carrier and lower sideband to provide transverse confinement through the dipole force term. Also the end of the cooling cycle will occur when the modulation frequency is at its maximum value. The predictable high frequency efficiency loss of the modulator will actually be an advantage in reducing the power broadening of the cooled transition, thus leading at the last moment to a further (although perhaps small) velocity narrowing. Finally, we note that the 1772 MHz needed for repumping the F=1 atoms can easily be inserted into the rf power amplifier along with the frequency-swept rf from the heterodyne source. An alternative configuration would be separate power amplifiers combined with an appropriate hybrid coupler.

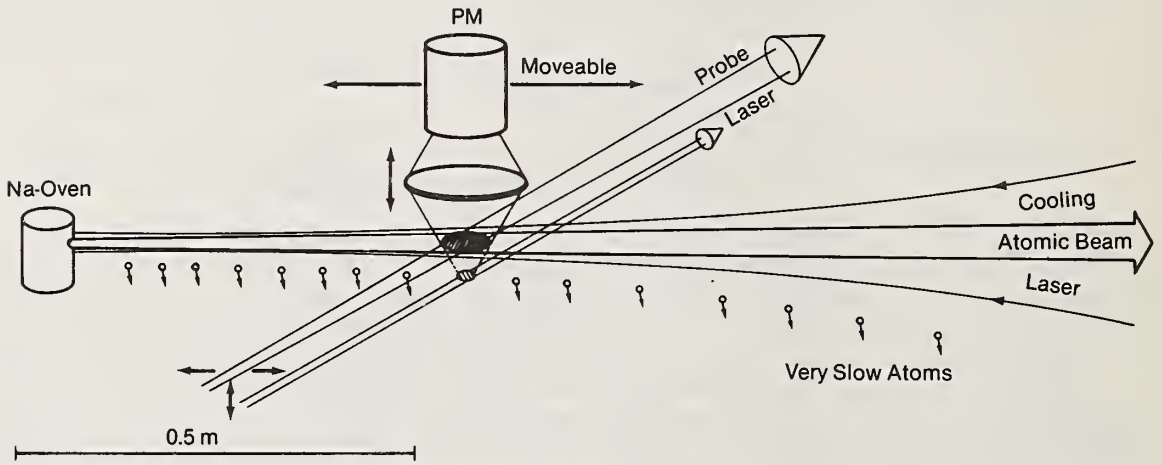

Fig. 9. Scheme of the experimental setup.

The atomic beam experiment is shown schematically in Fig 9. The apparatus consists of three parts: the sodium oven chamber, the main interaction and detection chamber, and a chamber for controlling the laser frequencies by monitoring the fluorescence light from the crosspoint of atomic beam and perpendicular laser beam. The whole atomic beam has a length of about 1.3 m. The apparatus is designed to work equally as well in horizontal as in near vertical positions. The big "middle chamber" has two large side windows for the detection laser, which monitors the density and velocity distribution over a relatively long part of the atomic beam. On top of the chamber is a related large window for detection of the fluorescence light. The chamber is also suited to detect very slow atoms, which "fall out" below the atomic beam. At both ends of this chamber are cold traps, which provide good vacuum and low sodium background.

For the measurement of the momentary velocity distribution, different schemes are possible. One is laser excitation of the $^2P_{3/2}$ atoms into higher s-states, which decay in cascades to the ground state. This allows an easy discrimination of the fluorescence light from the background sources. In order to cool the transverse velocity also, three transverse laser beams can be applied to the atomic beam at several positions.

3. Conclusions

Despite the many proposals and theoretical publications about cooling and trapping of neutral atoms only a few experimental approaches are known today. The most interesting and successful approach is described in Ref. 8. It has the advantage of working with a "fixed" frequency dye laser and of producing a continuous, strong, polarized slow atomic beam in

the $^2S_{1/2}$ (F=2) state. One disadvantage of this scheme is the still-unsolved problem of optical pumping (many of the atoms stay in the $^2S_{1/2}$(F=1) state with their initial velocity distribution) especially at the entrance and exit regions of the magnetic field. Fast beam components may also reduce the density of cool atoms collisionally. A second problem concerns detailed interpretation of the experimental results. In that apparatus, as presently configured, it is not easy to study the cooling process as it evolves inside the magnet.

We are optimistic that the approach described in this paper, which avoids the magnetic field and its related problems, will turn out to be a rather promising alternative. One future advantage of the frequency-swept scheme is that it need not depend strongly on the polarization of the laser light. This may be particularly important for the next step: the optical trap. It is almost impossible in most of the proposed schemes to work in a pure two-level system, if isotopes with nonzero nuclear spin are to be investigated.

The Monte-Carlo simulation of the cooling process as well as of the trapping process appears to be a versatile tool in the preparation and understanding of the whole experiment. This has already been proven by our first calculations of the planned cooling scheme.

Sodium was chosen as the first candidate because of technical reasons and the possibility to compare directly with other experiments. Future candidate atoms of potentially high intrinsic interest are described in Ref. 17.

Acknowledgments

It is a pleasure to acknowledge stimulating discussions with J. Prodan, W. D. Phillips, and P. Zoller. P. Zoller was particularly involved in the calculations concerning the Fokker-Planck equation. Two of the authors (R. B. and W. E.) gratefully acknowledge fellowship support by the Deutsche Forschungsgemeinschaft. This research at JILA is supported in part by the National Science Foundation and the Office of Naval Research, and in part by the National Bureau of Standards through its program of research on topics of potential application to fundamental standards of measurement.

References

1. S. Stenholm, Phys. Rep. 43, 151 (1978).
2. T. W. Hänsch and A. L. Schawlow, Opt. Comm. 13, 68 (1975).
3. D. J. Wineland and H. G. Dehmelt, Bull. Am. Phys. Soc. 20, 637 (1975).
4. W. Neuhauser, M. Hohenstatt, P. Toschek, and H. Dehmelt, Phys. Rev. Lett. 41, 233 (1978).
5. D. J. Wineland, R. E. Drullinger, and F. L. Walls, Phys. Rev. Lett. 40, 1639 (1978).
6. V. I. Balykin, V. S. Letokhov, and V. I. Miskin, Pis'ma Zh. Eksp. Teor. Fiz. 29, 614 (1979).
7. W. D. Phillips and H. Metcalf, Phys. Rev. Lett. 48, 596 (1982).
8. J. V. Prodan, W. D. Phillips, and H. Metcalf, Phys. Rev. Lett. 49, 1149 (1982).
9. D. J. Wineland, J. J. Bollinger, and W. M. Itano, Phys. Rev. Lett. 50, 628 (1983).
10. D. J. Wineland, see contribution to this workshop.
11. S. V. Andreev, V. I. Balykin, V. S. Letokhov, and V. G. Minogin, Sov. Phys. JETP 55, 828 (1982).
12. V. S. Letokhov and V. G. Minogin, Phys. Rep. 73, 1 (1981).
13. V. G. Minogin, Sov. Phys. JETP 52, 1032 (1980).
14. A. Ashkin, Phys. Rev. Lett. 40, 729 (1978).
15. J. P. Gordon, Phys. Rev. A 8, 14 (1973).
16. J. E. Bjorkholm, R. R. Freeman, A. Ashkin, and D. B. Pearson, Phys. Rev. Lett. 41, 1361 (1978).
17. W. Ertmer, R. Blatt and J. L. Hall, see contribution to this workshop.

Laser-Cooled and Trapped Atoms, (Proceedings of the Workshop on Spectroscopic Applications of Slow Atomic Beams, held at NBS, Gaithersburg, MD, 14-15 April 1983) Ed. by W. D. Phillips, Natl. Bur. Stand. (U. S.) Spec. Publ. 653 (1983).

Some Candidate Atoms and Ions for Frequency Standards Research Using Laser Radiative Cooling Techniques

W. Ertmer,* R. Blatt,† and J. L. Hall‡

Joint Institute for Laboratory Astrophysics, National Bureau of Standards and University of Colorado, Boulder, Colorado 80309 U.S.A.

The rapid progress in laser atomic cooling ideas and also in laser spectral coverage and frequency stabilization make it appropriate to re-examine the periodic table for atoms and ions that may be of special interest for radiatively-cooled frequency standards research. We discuss Hg^+, Pb^+, Ba^+, neutral alkalis, Mg, Ca, and Ag. Optical two-photon and weak single-photon transitions are represented, along with microwave hfs and fs transitions.

Key words: radiative cooling, optical frequency standards, laser stabilization

Several years ago we saw the first spectacular, experimental demonstrations of radiative cooling to sub-Kelvin kinetic temperatures of trapped Mg^+ ions by Wineland and his colleagues [1], and of a few, even single Ba^+ ions by Toschek, Dehmelt and their colleagues [2]. The beauty of these experiments was marred only by the relative scarcity of ions and matching laser sources appropriate for this kind of application. However, there have been many improvements of tunable laser performance and tuning range, notably through the use of new laser dyes and color centers for the active lasers, and through the application of nonlinear optical mixing and optical harmonic techniques to extend the range of useful output far into the ultraviolet.

In this report, we note a few transitions in candidate ions and atoms made accessible by these and earlier laser developments. We particularly want to focus attention on those atomic systems which have the super-narrow transitions that will be of interest in connection with atomic frequency standard research, even though many of these very same candidate ions and atoms may pose severe problems for our ingenuity and technological possibilities in achieving effective radiative cooling.

Probably the most exciting ion being considered at present is Hg^+. The relevant energy levels of Hg^+ are shown in Fig. 1. For microwave standards work a high transition frequency is useful to improve the "Q": the 40 GHz hfs transition in $^{199}Hg^+$ and 26 GHz in $^{201}Hg^+$ offer welcome increases in this way over Rb and Cs. These Hg^+ transitions have long been appreciated and studied since the early work by Major and Dehmelt, down through contemporary work at Hewlett Packard, the Laboratoire de l'Horloge Atomique, and now at NBS, Boulder by Bergquist and colleagues. A really new and decisive breakthrough in this work likely will come out of the remarkable recent success of Hemmati, Bergquist and Itano in producing the coherent 194 nm radiation needed to radiatively cool Hg^+. By summing in a

*Permanent address: University of Bonn, West Germany.

†Permanent address: Johannes Gutenberg University, Mainz, West Germany.

‡Staff Member, Quantum Physics Division, National Bureau of Standards.

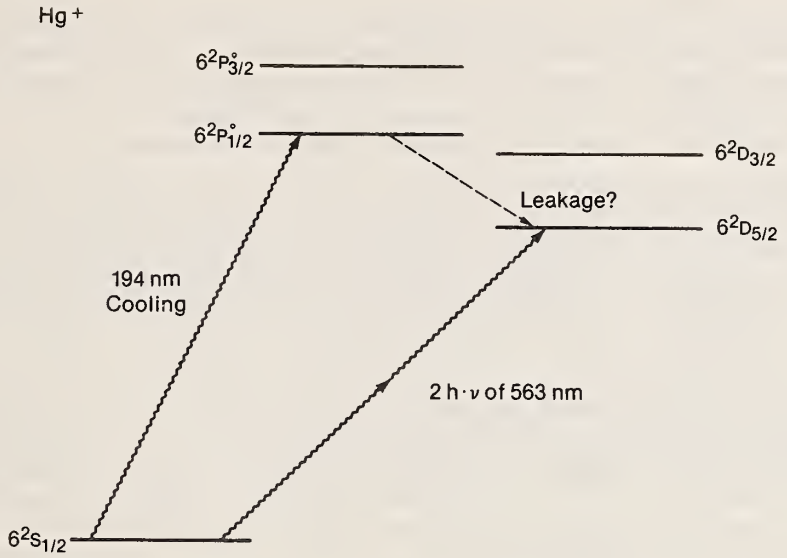

Fig. 1. Partial energy level diagram for Hg^+.

second nonlinear crystal the output of a frequency-doubled Ar^+ laser operating at 514 nm with the output of a dye laser operating at 792 nm, these workers were able to obtain a few μW of coherent UV output at 194 nm [3].

The marvelous thing about appropriate ion trapping techniques is that they are so benign relative to reheating the ions' motion that just a few microwatt optical power level will suffice to achieve good cooling, thus greatly relieving the pressure on coherent UV generation techniques in the sub-200 nm part of the spectrum where the resonance lines of ions are typically found.

Surely other interesting ions will be identified and studied as the laser UV techniques evolve. In some respects the Hg^+ ion may remain unique however, considering the remarkable two-photon optical transition [4] at 563 nm connecting the ground state with the $D_{5/2}$ metastable level. See Fig. 1. The calculated [5] E_2 decay rate of the upper level is 9.5 s^{-1}, leading to an expected potential line Q of this transition of almost 10^{15}! After the ion cloud has been radiatively cooled, one will use a repetitive cycle of excitation of the sharp resonance, followed by checking for population in the excited level. For example, a Ramsey two-pulse excitation sequence will lead to two coherent amplitudes for populating the $6s^2\ ^2D_{5/2}$ metastable level. A subsequent strong pulse laser at 399 nm can transfer this D-state population to $6p\ ^2P^o_{3/2}$ leading to 165 nm fluorescence decay. This operation of testing for excited state population will reveal the Ramsey interference term between the two excitation amplitudes and thus lead to supernarrow resonances. With such a sequential excitation and interrogation scheme one should be able to have both narrow lines and high detection efficiency. Alternatively, with fewer ions and stronger excitation of the "clock" transition, one could test for the decrease in light scattering on the cooling transition $6s\ ^2S_{1/2} \rightarrow 6p\ ^2P^o_{1/2}$ at 194 nm, following the suggestion by Dehmelt [6].

An ion interesting for its clock transition was identified by Strumia [7]: Pb^+. The fine-structure splitting between ground $6p\ ^2P^o_{1/2}$ and excited $6p\ ^2P^o_{3/2}$ states lies at 710 nm and has a calculated lifetime [5] of 38 ms. Such a sharp magnetic dipole transition might be ideal for studying the final phase of the cooling process and, conceivably, could be used to drive the system (slowly!) to a new regime of ultralow kinetic temperatures.

Unfortunately, direct cooling of Pb^+ would require 168 nm radiation for direct P ↔ S cooling, so application of Pb^+ as an optical atomic clock will have to wait for further laser advances even farther into the UV. It may not be impossible to cool ions such as Pb^+ with long-range Coulomb collisions with a good "refrigerator ion" such as the Mg^+ transition used by Wineland et al. [1] in their first experiments.

No discussion of ion trapping candidates would be complete without consideration of Ba^+, the other ion for which dramatic cooling has been demonstrated [2]. The relevant energy levels for Ba^+ are shown in Fig. 2. One has strong cooling on the $6\ ^2S_{1/2} \rightarrow 6\ ^2P^o_{1/2}$ resonance line at 493 nm. Unfortunately, there is an important leakage from $6\ ^2P^o_{1/2}$ down to $5\ ^2D_{3/2}$ with a branching ratio of ≈1:3. The solution adopted by Toschek et al. is to re-excite the ion back to the $^2P_{1/2}$ level with a 650 nm broadband laser. Cooling and stable trapping was only observed in the presence of both laser fields. A variety of interesting three-level effects remain to be studied in this system. In particular, with a narrow laser at 650 nm as well as at 493 nm, one will look for the "population trapping" or "resonance Raman lineshapes" recently discussed by numerous authors [8] and spectacularly demonstrated by Thomas et al. [9]. Such a Raman coherence may well allow study of a sharp transition such as the 2.05 μm quadrupole line indicated in Fig. 2 without a primary laser source operating at that wavelength. We note that this clock transition could also be explored by two-photon spectroscopy using a 4.1 μm source.

Turning now to atomic species of interest for radiative cooling experiments in atomic beams, without doubt the most popular atom for this work is sodium. Certainly the wavelength match with conventional Rh 6G dye lasers and easy atomic beam formation and detection represent important advantages of using Na in the radiative cooling experiments. Unfortunately, the relatively large hyperfine splitting and strong optical pumping effects add difficulty to the design of clear experiments. Since one needs to scatter ~30,000 photons from each atom to cool it, even a small leakage effect (due to slightly defective laser polarization for example) will ultimately cause an important effect. As several of the papers at this workshop deal with these problems in depth, we take this opportunity to consider alternative atoms for atomic beam laser cooling experiments.

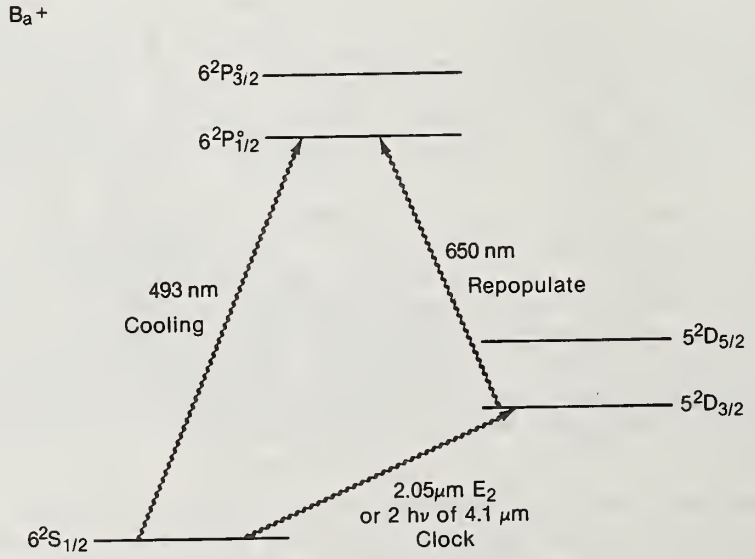

Fig. 2. Partial energy level diagram for Ba^+.

One first approach is to consider other alkali atoms. For example, Li could be cooled with a dye laser operating at 671 nm with the dyes DCM or Rh 101. K (767 nm) could be cooled with LD 700 as the dye. The advantage of these atoms relative to sodium lies in their smaller hyperfine splitting interval (804 MHz and 462 MHz respectively) so that it would be an easier technical task to use electro-optical modulation to produce a frequency-offset laser field for repumping the atoms lost into the "wrong" hfs state. Rb (780 nm) also can be cooled with an LD 700 dye laser. The 3 or 6.8 GHz hfs splittings of Rb (isotopes 85 and 87) are probably too large to address with current bulk EO Modulator technology relative to the repumping problem [10]. However, Rb has the interesting advantage that two-photon transitions to Rydberg states in Rb fall right in the spectral domain ~ 595 nm where sub-100 Hz dye laser stability has been demonstrated [11]. Certainly a good demonstration of laser-cooled Cs would be of interest to the frequency standards community.

Lewis [12] at NBS and Arditi and Picqué [13] in France have explored the use of diode lasers for optically-pumping Cs beams to increase the population in the useful $m_F = 0$ level and for tuning purposes. The recent demonstrations of high diode laser power levels [14] and rapid tuning rates [15] promise an exciting future prospect to strongly slow an ordinary atomic Cs beam with "simple" lasers.

Continuing our discussion of slow beam atomic clock systems based on magnetic dipole transitions between appropriate states, one of the more attractive systems is provided by Mg. See Fig. 3. Here the cooling can be effected in a direct way with 285 nm radiation, probably derived as the doubled frequency output of a Rh 110 dye laser operating at 570 nm. The absence of nuclear spin and an "$^1S_0$" -type ground state means a total absence of problems due to optical pumping effects during the cooling cycle. The penalty for Mg may lie in the difficulty of producing frequency-doubled dye laser output of sufficient intensity,

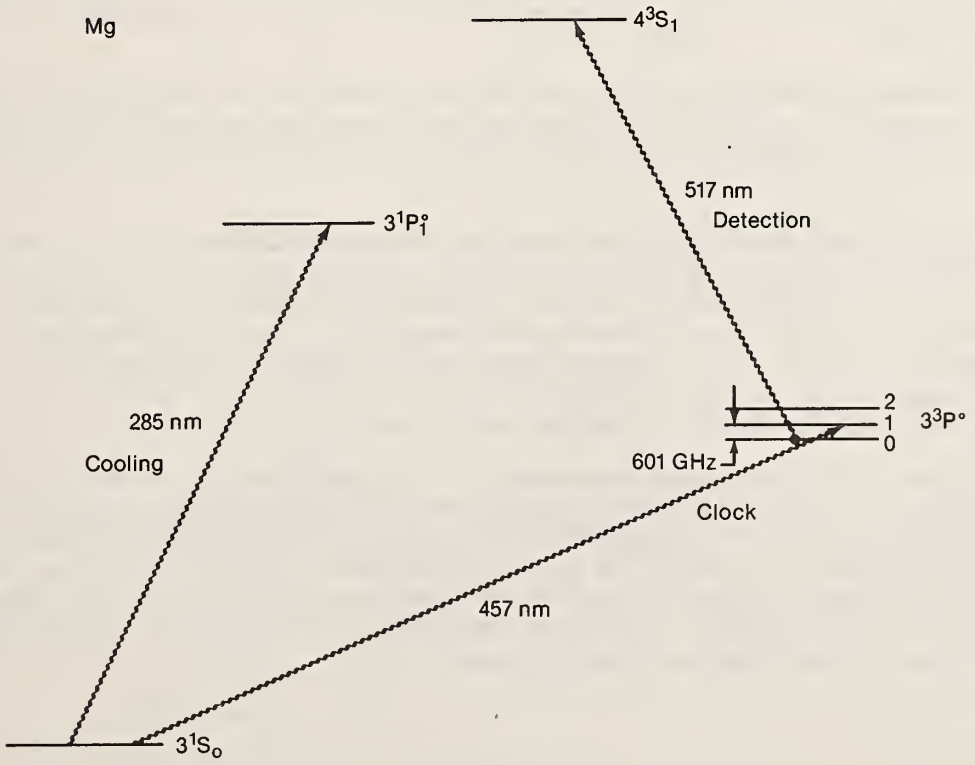

Fig. 3. Partial energy level diagram for Mg.

but it seems certain that this problem can be addressed with "build-up cavity" techniques using a ring cavity topology. Two very attractive clock possibilities are to be found in Mg. In the first, one uses the 601.277 16(5) GHz $3\ ^3P_1^o \rightarrow 3\ ^3P_0^o$ M1 transition which has recently been measured by Bava et al. [16]. Population reaching $3\ ^3P_0^o$ could be detected by magnetic deflection analysis and a hot wire detector. Alternatively, the $^3P_0^o$ atoms could be excited upwards with 517 nm laser pulses to the 4^3S_1 level from which fluorescence could be observed. Pavlik and Letokhov suggested that interesting optical transitions could be provided by the alkaline earth singlet-triplet intercombination lines [17]. For Mg this line falls at 457 nm for which the laser dye Stilbene 3 would be suitable, but it requires an expensive Ar^{2+} laser for pumping the highly stabilized 457 nm laser. The lifetime of the triplet level involved, $3\ ^3P_1^o$, has recently been measured to be (2.4±0.2) ms [18].

Similar schemes can also be discussed in Ca. The cooling transition would be $4\ ^1S_0 - 4\ ^1P_1^o$ at 423 nm. Unfortunately, in Ca and the heavier alkaline earths the ^1D lies below ^1P. In Ca the allowed decay to 3^1D is at 5.5 μm wavelength. The ν^3 density of states factor is more than 2000-fold in favor of the decay to ^1P, but as we need roughly 30,000 scattering events, this leakage problem will have to be addressed. It is perhaps worth noting that a CO laser line is tabulated to be within 1.2 GHz of the frequency needed to repump this line. Alternatively, one might be able to recover many of the captive atoms by pumping upward with 504 nm light to $4s5p\ ^1P^o$ which decays rather strongly to ground. The fine structure transition $^3P_1 \rightarrow {}^3P_0$ in Ca is at 1.565 THz which certainly is beginning to become unreasonably difficult relative to coherent rf/sub mm source technology. Ultimately one expects optically-pumped far IR lasers to fill this need.

The first real metrological interest in slow Ca would be in probing the intercombination line $4\ ^1S_0 - 4\ ^3P_1$ at 657 nm. Barger has already shown Ramsey interference resonances on this line with a ~1 kHz "width" almost totally determined by the atomic beam velocity distributions working through the second-order Doppler shift [19]. The natural width of this transition is thought to be ~300 Hz based on recent lifetime measurements giving (0.55±0.04) ms [18].

Still another interesting clock transition in Ca would be the two-photon line at 915 nm connecting $4\ ^1S_0$ to $3\ ^1D_2$. This stable laser could well be based on the F_2^+ color center in LiF [20]. Presumably this level could also be excited by an E_2 transition at 458 nm.

An attractive and technically less-demanding opportunity exists in Ba for which the primary cooling radiation at 554 nm can be directly obtained from a Rh 101 dye laser. However, as may be seen in Fig. 4, a serious leakage channel to 5^1D will ultimately trap the population after ~20 cycles in the cooling transitions. Thus this system will require a "repopulation" laser at 1.5 μm, perhaps based on F_2^+ centers [20] in NaCl or the remarkable KCl:Tl laser [21]. The resonance Raman three-level coupling process [8,9] discussed previously will be particularly interesting here as well.

We turn now to the last and perhaps most exciting candidate atom in this little list, neutral Ag [Fig. 5]. We know from the epoch of Stern and Gerlach that Ag forms nice atomic beams although the speed of their deposition-type detector does not ideally match our laser servo bandwidth needs. The cooling of Ag in a contemporary experiment would use the resonance lines at 328 nm or 338 nm obtained by frequency doubling a DCM dye laser operating at 656 or 676 nm. Unfortunately, the lower wavelength D2 line falls in a region where no crystal for non-critical phase matching is known.

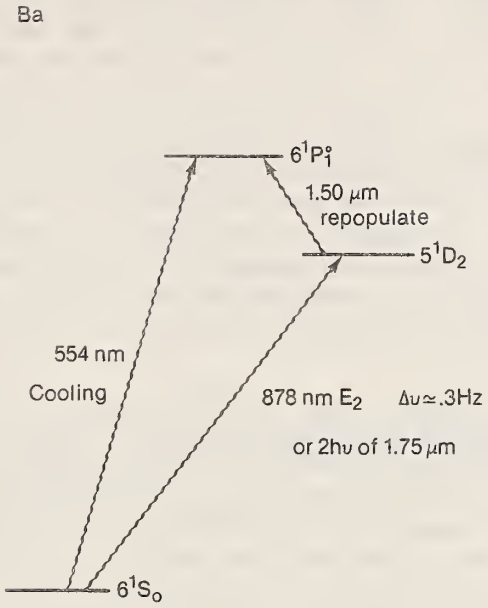

Fig. 4. Partial energy level diagram for Ba.

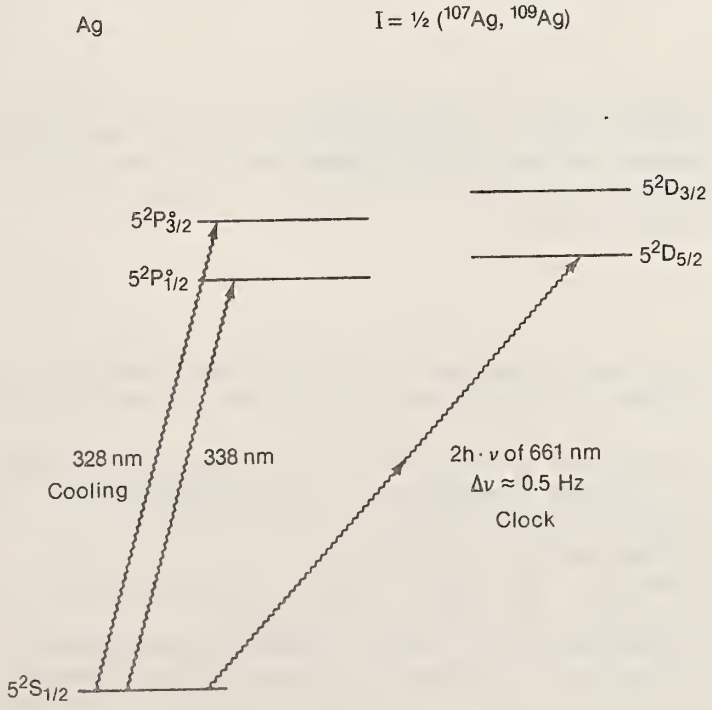

Fig. 5. Partial energy level diagram for Ag.

The D1 line at 338 is very near the limit of cooled RDA. Using the D1 line for cooling will require successful attention to optical pumping effects, but the Ag ground-state hyperfine frequencies (1.7 and 2.0 GHz) are low enough that we can provide the needed optical sidebands by EO modulation. The exciting thing about Ag is its two-photon visible transition [4] at 661 nm, $5\ ^2S_{1/2} \rightarrow 5\ ^2D_{5/2}$. The $D_{5/2}$ level has an estimated lifetime of 0.25 s, leading to a sub-Hz natural width and a line Q of over 1×10^{15}!

Detection of many of these long-lived excited states have been discussed above in the context of radiative excitation followed by fluorescence decay. We should also note the effective detection of metastable atom beam constituents by Auger electron emission from a low work-function surface. Such Auger detectors were pioneered by Lurio and his associates and used successfully in many atomic beam measurements, including the measurement of analogous weak two-photon transitions in an atomic beam of Bi [22]. As may be expected when a monolayer surface film is the active element, such a detector lives a longer life in an ultrahigh vacuum environment.

Dye lasers of spectral width ~ 1 MHz, available commercially, are completely appropriate for the radiative cooling tasks we have discussed. Lasers to explore these ultranarrow lines, with widths measured in Hz, are definitely not available commercially. However, recent cross-stimulation between the stable laser and gravity-wave detector communities has led to some useful progress, basically the reinvention in an optical context of Pound's rf microwave frequency stabilizer. (Interestingly enough, this techique was developed independently and essentially simultaneously by two groups [11,23].) A new paper reports sub-100 Hz dye laser line widths [11] and sub-Hz line widths are expected from contemporary experiments using improved techniques. We cannot claim that the laser technology is really well in hand and ready to explore these incredibly-narrow resonances, but from the above discussion of several atomic systems, it does appear that there will be something interesting to measure when ultraslow atomic beams and ultrastable lasers are available together.

Acknowledgments

Two of the authors (R. B. and W. E.) gratefully acknowledge fellowship support by the Deutsche Forschungsgemeinschaft. This research at JILA is supported in part by the National Science Foundation and the Office of Naval Research, and in part by the National Bureau of Standards through its program of research on topics of potential application to fundamental standards of measurement.

References

1. D. J. Wineland, R. E. Drullinger and F. L. Walls, Phys. Rev. Lett. 40, 1639 (1978).
2. W. Neuhauser, M. Hohenstatt, P. Toschek and H. Dehmelt, Phys. Rev. Lett. 41, 233 (1978).
3. H. Hemmati, J. C. Bergquist and W. M. Itano, Opt. Lett. 8, 73 (1983).
4. P. L. Bender, J. L. Hall, R. H. Garstang, F. M. J. Pichanick, W. W. Smith, R. L. Barger and J. B. West, Bull. Am. Phys. Soc. 21, 599 (1976).
5. R. H. Garstang, J. Res. NBS 68A, 61 (1964).
6. H. Dehmelt, Bull. Am. Phys. Soc. 20, 60 (1975); D. J. Wineland, J. C. Bergquist, W. M. Itano and R. E. Drullinger, Opt. Lett. 5, 245 (1980).
7. F. Strumia, Proc. 32nd Annual Freq. Control Symposium 444 (1978).
8. See, e.g. B. J. Dalton and P. L. Knight, Opt. Comm. 42, 411 (1982) and references therein.
9. J. E. Thomas, P. R. Hemmer, S. Ezekiel, C. C. Leiby, Jr., R. H. Picard and C. R. Willis, Phys. Rev. Lett. 48, 867 (1982).

10. However, some remarkable advances in EO Modulator design have recently given 10% sidebands at 4 GHz. G. C. Bjorklund and N. H. Tran, private communication.
11. R. W. P. Drever, J. L. Hall, F. V. Kowalski, J. Hough, G. M. Ford, A. J. Munley and H. Ward, Appl. Phys. B 31, in press.
12. L. Lewis, private communication.
13. M. Arditi and J. L. Picqué, Opt. Comm. 15, 317 (1975).
14. Remarkable results have recently been obtained with coherently-phased multi-diode laser arrays. See, e.g. D. R. Scifres, R. D. Burnham and W. Streifer, Appl. Phys. Lett. 41, 1030 (1982).
15. P. Pokrowsky, W. Zapka and G. C. Bjorklund, Opt. Comm. 44, 175 (1983).
16. E. Bava, A. de Marchi and A. Godone, presented at conference on sub mm lasers, 1983.
17. V. S. Letokhov and B. D. Pavlik, 1975 Vavilov Conference, Novosibirsk.
18. G. Giusfredi, P. Minguzzi, F. Strumia and M. Tonelli, Z. Physik A274, 279 (1975).
19. R. L. Barger, Opt. Lett. 6, 145 (1981).
20. L. F. Mollenauer, Opt. Lett. 1, 164 (1977).
21. W. Gellerman and F. Lüty, Conference Proceedings: Lasers '81, 364.
22. J. L. Hall, O. Poulsen, S. A. Lee and J. C. Bergquist, J. Opt. Soc. Am. 68, 697 (1978), and references therein.
23. G. C. Bjorklund, Opt. Lett. 5, 15 (1980).

Laser-Cooled and Trapped Atoms, (Proceedings of the Workshop on Spectroscopic Applications of Slow Atomic Beams, held at NBS, Gaithersburg, MD, 14-15 April 1983) Ed. by W. D. Phillips, Natl. Bur. Stand. (U.S.) Spec. Publ. 653 (1983).

Trapping of Low Energy Neutrons

G.L. Greene

Quantum Metrology Group
National Bureau of Standards
Washington, DC 20234

A brief review of recent work concerning the trapping of low energy neutrons is given. Particular emphasis is placed on magnetic confinement schemes which might also be applicable to neutral atoms. Important differences between the neutron and neutral atom cases are mentioned.

Key words: hexapole; trapping; ultra cold neutrons.

In considering the problem of neutral atom trapping, it is highly instructive to examine the effort which has been devoted to the confinement of another neutral particle, the neutron. The neutron is often facetiously described as an atom with Z=0, and indeed atomic physics techniques are often applicable to neutron research. (There is even a chapter devoted to neutron beams in Ramsey's Molecular Beams [1].) There are, however, important differences between neutrons and atoms which should be emphasized. It is therefore appropriate to briefly note the neutron properties which are relevant to the trapping question.

The neutron is a neutral, spin 1/2 particle with a magnetic dipole moment of approximately -1.91 nuclear magnetons [2,3]. (This is of course three orders of magnitude less than typical atomic spin and orbital moments.) The dielectric polarizability of the neutron is conjectured to be very small [4] and may be considered zero for laboratory fields. The combination of neutrality, small magnetic moment and zero polarizability implies a very low neutron-neutron cross section. This in turn implies that a "gas" of neutrons is very nearly non-interacting.

The interaction between other matter and low energy neutrons is usually dominated by nuclear forces. It can be shown [5,6,7] that the coherent scattering of low energy neutrons with matter is well described by assigning an index of refraction to the matter. For most materials [9] this index is less than one, implying the possibility of reflection below some critical angle at the surface of such material. For sufficiently low energy neutrons, the critical angle for reflection can reach 90° and therefore neutrons at all angles will be reflected. Neutrons with such low energy have come to be called Ultra Cold Neutrons. Ultra cold neutrons typically have energies of $\sim 10^{-7}$ eV; this corresponds to a temperature of $\sim$ 1 mK.

Since reflection occurs at all angles, Ultra Cold Neutrons can be trapped in a "bottle" [10]. Such trapping was first observed by Lushikov [11] and has since become the basis for an exciting experimental search for a static neutron electric dipole moment. However as this method of trapping is not appropriate to atoms, the reader is referred to several excellent review articles for further information [9, 12-16].

An important difference between neutrons and atoms arises from the very small neutron-neutron scattering cross section. Since a neutron gas is nearly non-interacting, a thermal beam of neutrons will have the predicted population at the extreme low energy tail of the Maxwellian distribution. Thus, unlike the atomic case where "cooling" is required to obtain nearly stationary particles, very slow neutrons are available by velocity selection alone. This method of producing very low energy neutrons has been the most widely employed to date. Other schemes have been proposed and show great promise.

Because it is neutral and unpolarizable, a purely electromagnetic trap must couple to the neutron magnetic dipole moment. A natural candidate for such a trap is the hexapole field suggested by W. Paul [17, 18]. The possibility of total confinement of neutrons by such a field was suggested by Vladimirski [19]. In recent years this notion has led to an active program in magnetic neutron confinement by W. Paul and his colleagues [20, 21].

Magnets having two geometries have been constructed by Paul and his co-workers. These are shown schematically in Fig. 1. The spherical bottle (1a) is a true trap for neutrons in one spin state. There is a point of zero field at the center of the trap, but it is not anticipated that the loss of particles due to Majorana flips near this point will be significant. Though the use of this bottle has not yet been successfully demonstrated, a program is now in progress in which it will be filled using the superthermal superfluid He phonon source proposed by Golub and Pendelbury [22].

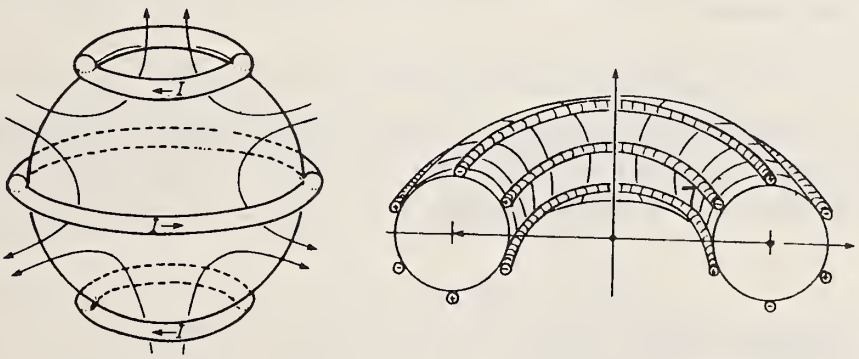

Figure 1. (a) Spherical hexapole trap, and (b) Toroidal hexapole trap (taken from Paul and Trinks, Ref. 20).

The suggestion that neutrons could be stored in a hexapole torus, as shown schematically in Fig. 1b, was first made by Heer [23] and others [24]. This geometry has been successfully used to store neutrons by Paul and his co-workers using the ultra cold neutron source at the Institut Laue Langevin (ILL) in Grenoble [20, 21].

The actual geometry employed at the ILL is somewhat different from that indicated in Fig. 1b. The inner two current loops were omitted "opening" the trap in the direction of the torus center. This effect was compensated for by the centrifugal barrier arising from the circular motion around the torus. A useful effect of this geometry is that it "moves" the zero field point where Majorana transitions may occur out of the volume occupied by the neutrons. As a result, losses due to Majorana transitions are probably negligible. The magnet was superconducting with a maximum usable field of 3.5T. The acceptance velocity of the trap in the azimuthal direction (around the torus) was $\sim$ 7-20 m/s. In the perpendicular direction the acceptance was $\sim \pm$ 4 m/s. This corresponds to energies up to 2×10^{-6} eV. A typical "fill" loaded the ring with $\sim$ 100 neutrons. Neutrons were detected in the trap after times up to 20 minutes. It is interesting to note that this corresponds to approximately two neutron lifetimes [25]. (It is also interesting to note that this experimental tour-de-force was accomplished with only 20 hours of beam time.) The dominant loss mechanism in the trap probably arises from a coupling between azimuthal and perpendicular velocities [13, 20, 21]. This is a problem which must be considered in any "racetrack" trapping scheme.

The successful confinement of neutrons by purely magnetic fields poses both a hope and a challenge to those seeking to trap neutral atoms. Paul, Trinks and Kugler have clearly demonstrated that neutral particles can be trapped by electromagnetic fields. The problems associated with trapping neutral atoms are quite different and will certainly require ingenuity on the same level as that demonstrated in their elegant experiments.

I am indebted to numerous colleagues at the Institut Laue Langevin for many educational discussions. In particular I wish to thank R. Golub and J.M. Pendelbury who have shared with me some of their extensive knowledge of ultra cold neutrons.

References

[1] N.F. Ramsey, Molecular Beams, Oxford U.P. (1956), p. 189.

[2] G.L. Greene et al., Phys. Rev. D 20, 2139 (1979).

[3] G.L. Greene et al., Metrologia 18, 93 (1982).

[4] Aleksandrov et al., JETP Lett. 4, 134 (1966).

[5] E. Fermi, Nuclear Physics, Univ. of Chicago Press (1949), p. 201.

[6] I.I. Gurevich and L.V. Tarasov, Low Energy Neutron Physics, North Holland (1968).

[7] V.F. Turchin, Slow Neutrons, Israel Program for Scientific Translations (1965).

[8] L. Koester, in Neutron Physics, Springer Verlag (1977).

[9] See also R. Golub and J.M. Pendelbury, Rep. Prog. Phys. 42, 439 (1979), p. 443, for a simple explanation of this phenomenon.

[10] Yu. B. Zeldovich, JETP 9, 1389 (1959).

[11] Luschikov et al., JETP Lett. 9, 23 (1969).

[12] A. Steyerl, in Neutron Physics, Springer Verlag (1977).

[13] R. Golub and J.M. Pendelbury, Contemp. Phys. 13, 519 (1972).

[14] R. Golub et al., Scientific American 240, 134 (1979).

[15] W.B. Dress et al., Phys. Rev. D 15, 9 (1977).

[16] I.S. Altarev et al., Nuclear Physics A341, 269 (1980).

[17] H. Friedberg and W. Paul Naturwiss. 38, 159 (1951).

[18] W. Paul, Proc. Intern. Conf. on Nuclear Physics and Physics of Fundamental Particles, Chicago (1951).

[19] V.V. Vladimirski, JETP 12, 740 (1961).

[20] W. Paul and U. Trinks, in Fundamental Physics with Reactor Neutrons and Neutrinos, ed. T. von Egidy, Institut of Physics Conference Series 42 (Bristol) 1977.

[21] K.J. Kugler, W. Paul and U. Trinks, Phys. Lett. 72B, 422 (1978).

[22] R. Golub and J.M. Pendelbury, Phys. Lett. 62A, 337 (1977). See also Ref. 9 for a thorough review.

[23] C.F. Heer, Rev. Sci. Instrum. 34, 532 (1963).

[24] I.M. Matora, Sov. J. Nucl. Phys. 16, 349 (1973).

[25] J. Byrne et al., Phys. Lett. 92B, 274 (1980), and C.J. Christensen et al., Phys. Rev. D 5, 1628 (1972).

LIST OF WORKSHOP PARTICIPANTS

Lloyd Armstrong
National Science Foundation
1800 G St., NW
Washington, DC 20550

Arthur Ashkin
Bell Laboratories
Crawford's Corner Road
Holmdel, NJ 07733

Ted G. Berlincourt
Office of Naval Research
800 N. Quincy St.
Arlington, VA 22217

Paul R. Berman
Physics Dept.
New York University
4 Washington Place
New York, NY 10003

John E. Bjorkholm
Bell Laboratories
Room 4C-318
Holmdel, NJ 07733

R. Blatt
JILA/Univ. of Colorado
Boulder, CO 80309

Donald A. Emmons
Frequency and Time Systems
34 Tozer Road
Beverly, MA 01915

W. Ertmer
JILA/University of Colorado
Boulder, CO 80309

Kenneth Evenson
National Bureau of Standards
Boulder, CO 80303

Shaoul Ezekiel
Massachusetts Institute of Technology
33-113
Cambridge, MA 02139

Elisabeth Giacobino
New York University
Dept. of Physics
New York, NY 10003

James P. Gordon
Bell Telephone Labs
Rm. 4E 410
Holmdel, NJ 07733

G. L. Greene
National Bureau of Standards
Quantum Metrology Group
Washington, DC 20234

J. L. Hall
National Bureau of Standards
JILA
Boulder, CO 80303

Bobby R. Junker
ONR, Code 412
800 N. Quincy St.
Arlington, VA 22217

Karl G. Kessler
National Bureau of Standards
Bldg. 221, Rm. B160
Washington, DC 20234

Daniel J. Larson
University of Virginia
Dept. of Physics
Charlottesville, VA 22901

Howard P. Layer
National Bureau of Standards
Bldg. 221, Rm. B160
Washington, DC 20234

Lindon Lewis
National Bureau of Standards
325 Broadway
Boulder, CO 80303

Michael S. Lubell
The City College of CUNY
Dept. of Physics
Convent Ave. & 138th St.
New York, NY 10031

Harold Metcalf
State Univ. of New York
Physics Dept.
Stony Brook, NY 11790

Marvin Mittleman
City College of CUNY
Physics Department
138th St. at Convent Ave.
New York, NY 10031

William D. Phillips
National Bureau of Standards
Bldg. 220, Rm. B258
Washington, DC 20234

David E. Pritchard
Massachusetts Institute of Technology
Rm. 26-231
Cambridge, MA 02139

John V. Prodan
National Bureau of Standards
Bldg. 220, Rm. B258
Washington, DC 20234

Keeneth Rubin
City College of New York
138th St. & Convent Ave.
New York, NY 10031

James J. Snyder
National Bureau of Standards
Quantum Metrology Group
Washington, DC 20234

Duncan G. Steel
Hughes Research Labs
3011 Malibu Cyn. Road
Malibu, CA 90265

Samuel R. Stein
National Bureau of Standards
Div. 524
325 Broadway
Boulder, CO 80303

William C. Stwalley
Univ. of Iowa
Dept. of Chemistry
Iowa City, IA 52242

Barry N. Taylor
National Bureau of Standards
Bldg. 220, Rm. B258
Washington, DC 20234

Harry T. M. Wang
Hughes Research Labs.
3011 Malibu Canyon Road
Malibu, CA 90265

David Wineland
National Bureau of Standards
Div. 524
Boulder, CO 80303

W. H. Wing
Univ. of Arizona
Physics Dept.
Tucson, AZ 85721

NBS-114A (REV. 2-8C)

U.S. DEPT. OF COMM. BIBLIOGRAPHIC DATA SHEET (See instructions)	1. PUBLICATION OR REPORT NO. NBS SP 653	2. Performing Organ. Report No.	3. Publication Date June 1983

4. TITLE AND SUBTITLE

Laser-Cooled and Trapped Atoms
Proceedings of the Workshop on Spectroscopic Applications of Slow Atomic Beams, held at the National Bureau of Standards, Gaithersburg, MD, on 14-15 April 1983.

5. AUTHOR(S)

William D. Phillips, Editor

6. PERFORMING ORGANIZATION (If joint or other than NBS, see instructions)

NATIONAL BUREAU OF STANDARDS
DEPARTMENT OF COMMERCE
WASHINGTON, D.C. 20234

7. Contract/Grant No.

8. Type of Report & Period Covered
Final

9. SPONSORING ORGANIZATION NAME AND COMPLETE ADDRESS (Street, City, State, ZIP)

National Bureau of Standards
Department of Commerce
Washington, DC 20234

Office of Naval Research
Physics Program Code 412
Arlington, VA 22217

10. SUPPLEMENTARY NOTES

Library of Congress Catalog Card Number: 83-600541

☐ Document describes a computer program; SF-185, FIPS Software Summary, is attached.

11. ABSTRACT (A 200-word or less factual summary of most significant information. If document includes a significant bibliography or literature survey, mention it here)

The proceedings of the Workshop on Spectroscopic Applications of Slow Atomic Beams contain papers on laser cooling of atomic beams, gases, and trapped particles and papers on trapping of neutral atoms in laser, electric, and magnetic fields. These and other papers discuss possible applications of cooled atoms to spectroscopy and to time and frequency standards. The present status and directions of research in time and frequency standards is also discussed.

12. KEY WORDS (Six to twelve entries; alphabetical order; capitalize only proper names; and separate key words by semicolons)

atom traps; clocks; cooled atoms; frequency standards; high resolution spectroscopy; ion traps; laser cooling; laser deceleration; laser traps; optical frequency standards; slow atomic beams.

13. AVAILABILITY

☒ Unlimited

☐ For Official Distribution. Do Not Release to NTIS

☒ Order From Superintendent of Documents, U.S. Government Printing Office, Washington, D.C. 20402.

☐ Order From National Technical Information Service (NTIS), Springfield, VA. 22161

14. NO. OF PRINTED PAGES
172

15. Price

USCOMM-DC 6043-P80

★ U.S. GOVERNMENT PRINTING OFFICE: 1983-380-997:5092

NBS TECHNICAL PUBLICATIONS

PERIODICALS

JOURNAL OF RESEARCH—The Journal of Research of the National Bureau of Standards reports NBS research and development in those disciplines of the physical and engineering sciences in which the Bureau is active. These include physics, chemistry, engineering, mathematics, and computer sciences. Papers cover a broad range of subjects, with major emphasis on measurement methodology and the basic technology underlying standardization. Also included from time to time are survey articles on topics closely related to the Bureau's technical and scientific programs. As a special service to subscribers each issue contains complete citations to all recent Bureau publications in both NBS and non-NBS media. Issued six times a year. Annual subscription: domestic $18; foreign $22.50. Single copy, $5.50 domestic; $6.90 foreign.

NONPERIODICALS

Monographs—Major contributions to the technical literature on various subjects related to the Bureau's scientific and technical activities.

Handbooks—Recommended codes of engineering and industrial practice (including safety codes) developed in cooperation with interested industries, professional organizations, and regulatory bodies.

Special Publications—Include proceedings of conferences sponsored by NBS, NBS annual reports, and other special publications appropriate to this grouping such as wall charts, pocket cards, and bibliographies.

Applied Mathematics Series—Mathematical tables, manuals, and studies of special interest to physicists, engineers, chemists, biologists, mathematicians, computer programmers, and others engaged in scientific and technical work.

National Standard Reference Data Series—Provides quantitative data on the physical and chemical properties of materials, compiled from the world's literature and critically evaluated. Developed under a worldwide program coordinated by NBS under the authority of the National Standard Data Act (Public Law 90-396).

NOTE: The principal publication outlet for the foregoing data is the Journal of Physical and Chemical Reference Data (JPCRD) published quarterly for NBS by the American Chemical Society (ACS) and the American Institute of Physics (AIP). Subscriptions, reprints, and supplements available from ACS, 1155 Sixteenth St., NW, Washington, DC 20056.

Building Science Series—Disseminates technical information developed at the Bureau on building materials, components, systems, and whole structures. The series presents research results, test methods, and performance criteria related to the structural and environmental functions and the durability and safety characteristics of building elements and systems.

Technical Notes—Studies or reports which are complete in themselves but restrictive in their treatment of a subject. Analogous to monographs but not so comprehensive in scope or definitive in treatment of the subject area. Often serve as a vehicle for final reports of work performed at NBS under the sponsorship of other government agencies.

Voluntary Product Standards—Developed under procedures published by the Department of Commerce in Part 10, Title 15, of the Code of Federal Regulations. The standards establish nationally recognized requirements for products, and provide all concerned interests with a basis for common understanding of the characteristics of the products. NBS administers this program as a supplement to the activities of the private sector standardizing organizations.

Consumer Information Series—Practical information, based on NBS research and experience, covering areas of interest to the consumer. Easily understandable language and illustrations provide useful background knowledge for shopping in today's technological marketplace.

Order the **above** *NBS publications from: Superintendent of Documents, Government Printing Office, Washington, DC 20402.*

Order the **following** *NBS publications—FIPS and NBSIR's—from the National Technical Information Service, Springfield, VA 22161.*

Federal Information Processing Standards Publications (FIPS PUB)—Publications in this series collectively constitute the Federal Information Processing Standards Register. The Register serves as the official source of information in the Federal Government regarding standards issued by NBS pursuant to the Federal Property and Administrative Services Act of 1949 as amended, Public Law 89-306 (79 Stat. 1127), and as implemented by Executive Order 11717 (38 FR 12315, dated May 11, 1973) and Part 6 of Title 15 CFR (Code of Federal Regulations).

NBS Interagency Reports (NBSIR)—A special series of interim or final reports on work performed by NBS for outside sponsors (both government and non-government). In general, initial distribution is handled by the sponsor; public distribution is by the National Technical Information Service , Springfield, VA 22161, in paper copy or microfiche form.

U.S. Department of Commerce
National Bureau of Standards

Washington, D.C. 20234
Official Business
Penalty for Private Use $300

POSTAGE AND FEES PAID
U.S. DEPARTMENT OF COMMERCE
COM-215

THIRD CLASS
BULK RATE